Host immune response in immunodeficient mice against infection with *Cryptosporidium parvum*

Dissertation

zur Erlangung des Grades

"Doktor der Naturwissenschaften"

am Fachbereich Biologie

der Johannes Gutenberg-Universität Mainz

Tesfaye Sisay Tessema

geb. am 14.03.1974 in Dessie, Äthiopien

Mainz, 2008

Tag der mündlichen Prüfung:10.12.2008

Table of contents

Abbreviations

AIDS	Acquired immunodeficiency syndrome
bp	base pair
CD	Cluster of differentiation
cDNA	Complementary DNA
DNA	Deoxyribonucleic acid
dNTP	Deoxynucleotide triphosphate
GAPDH	Glyceraldehyde-3-phosphate dehydrogenase
GKO	IFN-γ knock out
ELISA	Enzyme linked immunosorbent assay
FACS	Fluorescence activated cell sorting
FITC	Fluorescein isothiocyanate
HIV	Human immunodeficiency virus
IEC	Intestinal epithelial cell
IEL	Intraepithelial lymphocyte
IFN	Interferon
Ig	immunoglobulin
IL	Interleukin
KO	Knock out
M	mole
MACS	Magnetic activated cell sorting
MHC	Major histocompatibility complex
MLN	Mesenteric lymph node
mRNA	messenger ribonucleic acid
NK	Natural killer
i.p.	intraperitoneal
i.v.	intravenous
PCR	Polymerase chain reaction
PE	Phycoerythrin
PPs	Peyer's patches
RNA	Ribonucleic acid
RT-PCR	Reverse transcription polymerase chain reaction
SCID	Severe combined immunodeficiency syndrome

SPF	Specified pathogen free
TCR	T-cell receptor
Th	T helper
TNF	Tumor necrosis factor
UV	Ultra violet
V/V	volume per volume
W/V	weight per volume

I. INTRODUCTION

1. Pathobiology of *Cryptosporidium parvum*

1.1. *Cryptosporidium* species

1.1.1. Brief history

The credit for the discovery of *Cryptosporidium* spp dates back to Ernest Edward Tyzzer who successively identified the oocysts of the organism from mice as well as has named two important species: *Cryptosporidium muris* and *Cryptosporidium parvum*. He provided the name '*Cryptosporidium*' because of the uncertain taxonomic status of the oocysts (reviewed in Fayer et al., 1997). However, the association of the organism with disease was first described after 48 years in turkeys (Slavin, 1955) and subsequently in cattle (Panciera et al., 1971). The organism ignited public interest after the report of association of *Cryptosporidium* with immunosuppression due to steroidal drugs (Meisel et al., 1976) and AIDS (anonymous, 1982) and as a cause of massive waterborne outbreak in Milwaukee, WI, USA (Mac Kenzie et al., 1994).

1.1.2. Taxonomy

C. parvum belongs to the Phylum Apicomplexa (possessing apical complex of secretory organelles), Class Sporozoasida (reproduce by asexual and sexual cycles, with oocyst formation), Subclass Coccidiasina (life cycle involving merogony, gametogony and sporogony), Order Eucoccidiida (schizogony occurs), Suborder Eimeriina (independent micro and macrogamy develop), Family Cryptosporiidae (4 naked sporozoites within oocysts- no sporocyst) (Tzipori and Widmer, 2000).

Cryptosporidium affects a wide range of vertebrates. Multiple parameters such as morphology, developmental biology, host specificity, histopathology and also molecular biology have been utilized to classify *Cryptosporidium* into 14 valid species:
C. andersoni (cattle), *C. baileyi* (chicken and some other birds), *C. canis* (dogs), *C. felis* (cats). *C. galli* (birds), *C. hominis* (humans), *C. meleagridis* (birds and humans), *C. molnari* (fish), *C. muris* (rodents and some other mammals), *C. parvum* (ruminants and humans), *C. wrairi*

(guinea pigs), *C. saurophilium* (lizards and snakes), and *C. serpentis* (snakes and lizards) (rewiewed in Xiao et al., 2004). Among the human-pathogenic *Cryptosporidium* spp, *C. hominis* and *C. parvum* are responsible for most human cases of infection with some geographical differences (Xiao and Fayer, 2008).

1.1.3. Life cycle

All species of *Cryptosporidium* are obligate intracellular parasites. Unlike other coccidia, Cryptosporidia do not require a period of maturation (sporulation) outside the host to become infectious. *Cryptosporidium* oocysts are fully sporulated and infectious when excreted in the gut lumen (Smith et al., 2005).

The life cycle begins with the ingestion of oocysts by the host; the four naked sporozoites are then released in the gut and infect intestinal epithelial cells (enterocytes). Sporozoites become enveloped by the host apical cell membrane, reside in a resulting parasitophorous vacuole that contains membrane components from both the host and *C. parvum*, and differentiate into the spherical trophozoites (Figure 1). *C. parvum* resides intracellularly but outside of the cytoplasm, which contrasts with other related intracellular pathogens (e.g. *Toxoplasma*) that reside in parasitophorous vacuoles within the cytoplasm (Laurent et al., 1999). They undergo asexual development through two successive generations of merogony, releasing 8 and 4 merozoites, respectively. The four merozoites released from the second merogony give rise to the sexual developmental stages, the micro- and macrogamonts. The release of microgametes, and their fusion with macrogametes give rise to the zygote which, after two asexual divisions, forms the environmental resistant oocyst containing 4 sporozoites (O'Donoghue, 1995; Tzipori and Griffiths, 1998; Smith et al., 2005) (Figure 1).

1.2. Human and animal cryptosporidiosis

1.2.1. Epidemiology

Important aspects pertinent to the epidemiology of the disease in man are briefly described as follows.

1.2.1.1. Target population of cryptosporidiosis

Cryptosporidiosis affects all age groups, but the young population of 1-to-2-year old age seems to be the most affected. In addition, in developing countries, cryptosporidiosis is associated with children under malnutrition (Nichols, 2008). The immunocompromised population also shows high prevalence of the disease. These include untreated HIV/AIDS patients, people with congenital genetic immune deficiencies such as X-linked hyperimmunoglobulin M syndrome, CD40 ligand deficiency, severe IgA and *Saccharomyces* opsonin deficiency, and gamma interferon deficiency (Warren and Guerrant, 2008). People with malignancies, including those with hematological malignancies (such as leukemia) undergoing chemotherapy or bone marrow transplantation, patients with solid-organ transplants, and patients on hemodialysis, also have a high prevalence of cryptosporidiosis (Nichols, 2008).

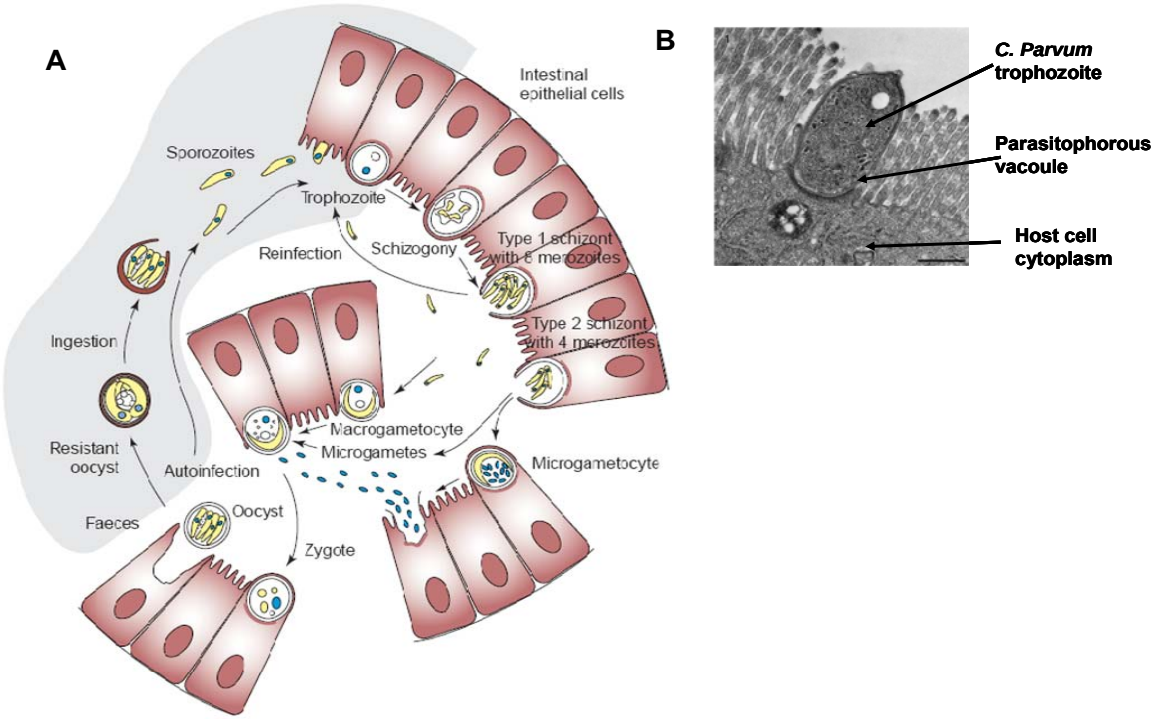

Figure 1. (A) Life cycle of *Cryptosporidium parvum*. The sporozoites invade enterocytes to initiate the asexual cycle within a parasitophorous vacuole (B) that is intracellular but extracytoplasmic. Refer to the text for the details of the subsequent developmental steps of the pathogen (Smith et al., 2005). (B) Electron micrographs of gut section from a piglet experimentally infected with *C. parvum* genotype 1 showing ultrastructural view of the parasitophorous vacuole (Tzipori and Ward, 2002).

Young animals are more susceptible to infection, while infections in adult animals are often asymptomatic or do not occur. Calves are susceptible to infection shortly after birth, within 8 to

15 days of age, and remain so for several months. Lambs and goat kids are commonly affected under the age of 1 month old (Ramirez et al., 2004).

1.2.1.2. The transmission stage: Oocyst

Oocysts of *Cryptosporidium* spp are small (from 3.8 by 4.6 µm to 6.3 by 8.4 µm) containing 4 naked sporozoites. Their ubiquitous, durability coupled to their small size, resistance to many disinfectants as well as evading filtration lend transmission of the oocysts by municipal drinking water, with a potential to cause community-wide outbreaks of infection (Robertson and Gjerde, 2007). The WHO's guideline for drinking water (WHO, 2006) classifies *Cryptosporidium* as a pathogen of significant public health importance, contributed in part by the organism's low infective dose (ID), ID_{50} of 9 – 1042 oocysts (Okhuysen et al., 1999; Smith et al., 2005), and resistance to conventional water treatment such as chlorination.

1.2.1.3. Transmission of infection

The disease is transmitted through person-to-person contact with infected patients (family members, health care workers, users of communal swimming pools, travelers), human-animal contact (zoonotic) (veterinarians, farmers), or via indirect transmission through the environment (particularly by water) (Chen et al., 2002).

1.2.1.4. Zoonosis

According to molecular epidemiological studies, geographic differences in the distribution of *C. parvum* and *C. hominis* infections within a country support the likelihood of zoonotic cryptosporidiosis in the industrialized world. The role of zoonotic infections in human cryptosporidiosis in developing countries appears much less important than in industrialized world since 70 – 90 % of human infections in developing countries result from *C. hominis*. (Xiao and Fayer, 2008). Cattle have been considered to be an important source of zoonotic cryptosporidiosis since the 1980s whereas the role of companion animals is less important (Xiao and Feng, 2008). Mixed *Cryptosporidium* infections have also been reported in HIV-infected patients (Cama et al., 2006), indicating multiple sources of infection.

1.2.2. Clinical features and pathogenesis

The natural history of the illness differs in immunocompetent and immunocompromized individuals. In the immunocompetent individual, *Cryptosporidium* commonly causes acute self-limiting gastroenteritis. Oocyst excretion occurs from less than 3 to 30 days, coinciding with symptoms. In immunocompromized patients such as those with HIV/AIDS, acquired abnormalities of T-lymphocytes, congenital hypogammaglobulinaemia, severe combined immunodeficiency syndrome (SCID), immunosuppressive drug recipients and severely malnourished ones, symptoms include frequent episodes of watery diarrhea, cramping, upper abdominal pain, profound weight loss, weakness, malaise, anorexia and low grade fever (Smith and Corcoran, 2004).
Domestic animals exhibit the same prominent clinical sign of infection as humans, watery diarrhea (Fayer, 2004).

The molecular basis for pathogenicity is not understood and no specific virulence factors have been unequivocally shown to cause direct or indirect damage to host tissues. Diarrhea in cryptosporidiosis could result from a combination of the following factors:

1) loss of absorptive epithelium due to apoptosis and villus atrophy results in malabsorption, and release of inflammatory cell mediators stimulate electrolyte secretion and diarrhea.

2) increased intestinal secretion which may be partly mediated by enterotoxin-like activity produced by *C. parvum* itself or as shown in a piglet model as a result of endogenous secretory mediators such as prostaglandins which alter NaCl transport primarily by stimulating the enteric nervous system (Sears and Guerrant, 1994; Fayer, 2004).

3) Cytokines induced by infection may directly involve in the pathogenesis of diarrhea as reviewed by Lean *et al.* (2002). TNF-α stimulates chloride secretion in the intestine via a prostaglandin mediator (Clark and Sears, 1996). Interferon (IFN)-γ, besides conferring resistance to the parasite, has a well documented role in secretory diarrhea. Exogenous IFN-γ inhibits both of the Na/H ion exchanger (Rocha et al., 2001) and Na/K exchanger (Sugi et al., 2001) resulting in increase in intracellular Na concentration which leads to an increase in cell volume, which in turn has been implicated in the decreased expression of a number of transport

and barrier proteins (Sugi et al., 2001). These events ultimately lead to a leaky and dysfunctional epithelium, manifested by diarrhea.

1.2.3. Diagnosis

Laboratory techniques that are applied for identification of *Cryptosporidium* have been reviewed by Petry (2000). The need to identify the organism in diarrheal patients is useful to avoid misuse of antibiotics, to reduce the spread of the disease in a community; as well as to follow the epidemiology of the disease in an area and further stress for the need of control and preventive measures.
Detection of *C. parvum* oocysts has been performed using: histological sections of small intestine or rectum (Nime et al., 1976; Meisel et al., 1976); staining techniques to identify the oocysts in the feces (Petry, 2000); oocyst antigen detection via immunofluorescence, enzyme-linked and agglutination assays (Petry, 2000); PCR amplification of *C. parvum* specific DNA targets (Widmer, 1998; Morgan and Thompson, 1998; Sulaiman et al., 1999). There are pros and cons of each of these approaches; however, it is beyond the limit of this work to discuss them in detail.

Serological diagnosis of *C. parvum* specific antibodies has also been applied to detect wide range of time span post infection and also can be used as a marker for epidemiological surveys (Petry, 2000).

1.2.4. Control and prevention of cryptosporidiosis

The approach to control and prevent cryptosporidiosis has been threefold: treatment of symptomatic cases, immune reconstitution, and risk reduction by the avoidance of exposure to the organism.

1.2.4.1. Chemotherapy

To date there is no approved effective anti-cryptosporidial drug available, although studies reported variable results on the drugs tested so far (reviewed in Smith and Corcoran, 2004). Similarly, a recent review could not find any evidence to support the role of chemotherapeutic agents in the management of cryptosporidiosis among immunocompromized individuals. Some

evidence of effectiveness for nitazoxanide in a combined population of immunocompetent and immunocompromized individuals was identified but has to be supported with a large scale randomized trial among immunocompromized individuals (Abubakar et al., 2007a; Abubakar et al., 2007b).

Some researchers suggest the closer relation of *Cryptosporidium* to the Gregarinidae than the classical coccidia, based on the biological behavior of *Cryptosporidium* in cell-free culture systems (Hijjawi et al., 2004) and continuing phylogenetic analysis (Morrison et al., 2004). Their atypical responses to traditional anticoccidial medications may be due to their uncertain taxonomic place (Stockdale et al., 2008).

1.2.4.2. Passive immunotherapy

Passive immunotherapy using oral bovine serum concentrate improved symptoms and reduced oocyst shedding in calves with experimental cryptosporidiosis (Hunt et al., 2002), but colostrum from cows hyperimmunized with *C. parvum* oocysts achieved limited success in both human and non-human hosts (Gomez Morales and Pozio, 2002). A monoclonal antibody responsible for the circumsporozoite precipitate-like reaction reduced, but did not eliminate, persistent murine *C. parvum* infection (Riggs, 2002). *Cryptosporidium* genome has been completed (Abrahamsen et al., 2004); therefore, further database mining is expected to contribute in the discovery of additional protective antigens and virulence factors.

1.2.4.3. Immune reconstitution

In immunocompromized patients with HIV-related disease, the treatment of choice is immune reconstitution using highly active antiretroviral therapy (HAART). This acts prophylactically, but is also useful as a treatment and secondary prophylaxis when cryptosporidiosis is established (Miller, 1998; Chen et al., 2002). With HAART therapy, the number of $CD4^+$ T-cells in the gastrointestinal mucosa, where their number is required, increases faster and to a higher level than in blood (Schmidt et al., 2001). In addition, HAART inhibits viral replication using a combination of nucleoside and non-nucleoside reverse transcriptase inhibitors (NNRTIs) and HIV protease inhibitors (Caccio and Pozio, 2006). Hommer *et. al*. (2003) reported that protease inhinitors used in HAART inhibited *C. parvum* development in vitro; the

inhibitory effect is significant when the protease inhibitors were used in combination with the aminoglycoside paromomycin.
In non-AIDS related immunosuppression, such as in a post-renal transplantation (Abdo et al., 2003), reduction in immunosuppression was associated with oocyst clearance and resolution of the disease.

1.2.4.4. Prevention

Cryptosporidial oocysts potentially contaminate all sources of recreational and drinking water (even disinfected and filtered water sources) (reviewed in Smith and Corcoran, 2004). Reducing oocyst contamination of public water sources, are thought to offer the best protection from waterborne disease (Rose et al., 2002; Smith and Corcoran, 2004). Removal of the oocysts from drinking water by either boiling or by filtering the water through a filter with a pore size of <1 µm is also recommended for AIDS patients (Leav et al., 2003).

To date, there are no approved prophylactic means of preventing cryptosporidiosis formulated for either human or animal use. Therefore, proper understanding of the immune response to the parasite is required to design appropriate therapeutic as well as preventive measures.

1.2.5. Animal models of *C. parvum* infection

Experimental studies of *C. parvum*, especially studies addressing the immune response to the pathogen, are hindered by the lack of a suitable animal model, as most mammalian host species are susceptible to infection only as neonates (Tzipori, 1988). This has forced researchers to use newborn animals for *in vivo* studies of the parasite in the immunocompetent host (Heine et al., 1984b; Fayer et al., 1989; Bjorneby et al., 1991).

The problem of using neonates could be the immature immune system of neonates; therefore, the resulting infection pattern as well as the immune components involved could not be fully characterized. In some cases neonate models succumb to death because of infection. This forced people to look for alternative ways of rendering adult animals susceptible to infection. Different approaches were used to compromise the adult immune system so that adult animals become infectable. Consequently, adult athymic nude and severe combined immunodeficiency (SCID) mice have been extensively used (Heine et al., 1984a; Brasseur et al., 1988; Gardner et al.,

1991; Mead et al., 1991b). Additionally, animals immunosuppressed with drug therapy (Rehg et al., 1987; Rasmussen et al., 1991; Petry et al., 1995); as well as transgenically-immunodeficient animals (Ungar et al., 1990; Taghi-Kilani et al., 1990; Mead and You, 1998; Campbell et al., 2002) have been highly valuable to address certain questions of host resistance to the parasite.

1.3. Host immune response to *C. parvum*

1.3.1. Innate immunity

1.3.1.1. Interferon-γ (IFN-γ) and natural killer (NK) cell in innate immunity

IFN-γ is a significant player in the innate immune response against *C. parvum* as shown in nude mice (lacking thymus and T-cells) and SCID mice (lacking both T and B-cells). Production of IFN-γ by a non-T-cell was shown in a study done on adult mice where anti-CD4 treated animals given anti-IFN-γ treatment have an increase infection compared to anti-CD4 treated ones (Ungar et al., 1991). This was further supported by experiments done on adult SCID mice, although deficient in T and B-lymphocytes, are relatively resistant to *C. parvum* infection. The resistance of these mice to *C. parvum* infection is IFN-γ-dependent, as shown by IFN-γ-neutralization (Chen et al., 1993b; McDonald and Bancroft, 1994).

In vitro cryptosporidial sporozoites activated splenic NK cells from SCID mice in the presence of macrophages to produce IFN-γ through IL-12 and TNF-α (McDonald and Bancroft, 1998). NK cells from the peripheral blood of humans were activated through IL-15, which is up regulated during *C. parvum* infection (Dann et al., 2005). A T-cell independent source of IFN-γ has also been shown in infections of other intracellular pathogens; the source of IFN-γ in such conditions is NK cells (Bancroft et al., 1991; Hunter et al., 1994).

Nevertheless, evidence that NK cells in the intestine are the source of IFN-γ in T-cell-independent mechanism of immunity is lacking. No effect on reproduction of *C. parvum* in SCID mice treated with anti-asialo-GM1 antibodies, which effectively deplete NK cell numbers *in vivo*, has been observed (Rohlman et al., 1993). In addition stimulation of NK activity by injection of IL-2 did not affect the pattern of infection in SCID mice (McDonald and Bancroft, 1994). It is possible that, in these studies, anti-asialo-GM1 antibodies or exogenous IL-2 was less effective in the gastrointestinal tract than in other organs. Alternatively, another cell type in

addition to T-cells and NK cells in the mucosa can produce IFN-γ. SCID mice retain elements of innate immune system including NK cells and phagocytes were shown to activate macrophages through NK cell secreted IFN-γ in response to a variety of pathogens including *C. parvum* (Bancroft and Kelly, 1994).

Further work by Urban *et al*. (1996) showed that IL-12 confers resistance to *C. parvum* in SCID mice through IFN-γ production since the role of IL-12 was blocked by administration of anti-IFN-γ. Studies in other models strengthen this idea in that IFN-γ was induced in the ileum of infected mice within 24 hrs p.i. in wild type mice (Leav et al., 2005).

1.3.1.2. The action of phagocytes against *C. parvum*

Free radicals of nitric oxide (NO) produced during intestinal inflammation induced by infection play protective role against invading microorganisms (Nathan and Shiloh, 2000). Bactericidal properties of such radicals have been shown to aid in the killing mechanisms of macrophages and neutrophils (MacMicking et al., 1997; Nathan and Shiloh, 2000).

NO synthesis is significantly increased in *C. parvum* infection and it arises from the induced expression of inducible nitric oxide synthase (iNOS) by the infected epithelium (Leitch and He, 1999; Gookin et al., 2004). In the absence or inhibition of iNOS, epithelial infection and oocyst shedding are significantly exacerbated (Leitch and He, 1994; Leitch and He, 1999; Gookin et al., 2006). Furthermore, administration of antioxidants has been consistently shown to exacerbate *C. parvum* infection (Leitch and He, 1999; Yassien et al., 2001; Huang and Yang, 2002).

In addition, it has been shown in neonatal piglets that neutrophils have minimal impact in mediating the pathological sequelae of *C. parvum* infection. Although neutrophils were recruited into the gut lamina propria, neutrophil depletion did not ameliorate formation of free radicals, suggesting that these cells are not a significant source of free radicals in *C. parvum*-infected mucosa. Finally, barrier function of *C. parvum*-infected mucosa was significantly worsened, rather than improved, in the absence of neutrophils. These observations suggest that in non-invasive infection of intestinal epithelium, influx of neutrophils promotes physiological rather than pathological effects *in vivo* (Zadrozny et al., 2006).

Additional NO substrate in the form of L-arginine incites prostaglandin-dependent secretory diarrhea and does not promote epithelial defense or barrier function of *C parvum*–infected neonatal ileum (Gookin et al., 2008).

Recently, in a study using mice lacking T-cells and NK cells (SCIDbg mice) and SCIDbg mice additionally lacking macrophages and neutrophils (SCIDbgMN mice), it has been shown that acute *C. parvum* infection with a high mortality rate was developed in SCIDbgMN mice but not in SCIDbg mice. Macrophages and neutrophils are thus assumed to be involved in host resistance during acute *C. parvum* infection (Takeuchi et al., 2008).

1.3.1.3. Complement system

The complement system is an important component of the host innate immune system. Complement can be activated via three pathways, *i.e.*, the classical, the alternative, and the lectin pathway. The classical pathway is initiated by the C1q molecule, which by binding to IgM and IgG bearing immune complexes, bridging the innate and the adaptive immunity (Loos and Clas, 1987; Petry and Loos, 1998). The alternative pathway is initiated by binding of an activation product, C3b, of the third component of complement to the surface of pathogens. The lectin pathway is activated by binding of the mannan-binding lectin (MBL) (or members of the ficolin family) to microbes. A correlation of MBL deficiency and cryptosporidiosis was reported, in AIDS patients with homozygous MBL gene mutations (Kelly et al., 2000) and in children with serum MBL deficiency (Kirkpatrick et al., 2006a). Recently, we showed that *C. parvum* can activate both the classical and lectin pathways, leading to the deposition of C3b on the parasite. Besides, parasite development could be demonstrated in adult mice lacking mannan-binding lectin (MBL-A/C KO) but not in mice lacking complement factor C1q (C1qA KO) or in wild type mice (Petry et al., 2008).

In addition to the above discussed anti-Cryptosporidial innate immune mechanisms, the intestinal epithelial cells themselves, which are infected by the parasite, contribute to the innate defense system against infection. This important part of the host cell response is discussed as part of the gut mucosal immune system on section 1.3.3.

1.3.2. Adaptive immunity

1.3.2.1. Cell-medated immunity

i. T-Lymphocytes

The importance of T-cells for recovery from *Cryptosporidium* infection was studied in congenitally athymic (nude) mice (lacking T-cells) by Heine *et al* (1984a). Subsequently, adoptive transfer of cells from thymus, spleen and bone marrow of wild type mice to SCID mice resulted in functional immunologic reconstitution followed by complete eradication of infection (Mead et al., 1991a). SCID mice die of chronic infection compared to wild type mice (Kuhls et al., 1992). A subsequent study showed the importance of T-lymphocytes but not that of B-lymphocytes in this process using *C. muris*. This was done by McDonald *et al*. (1992) who described that SCID mice injected intraperitoneally with spleen or mesenteric lymph node cells from uninfected wild type mice were able to recover from the *C. muris* infection. Moreover, in this study the protective effect of donor spleen cells was not reduced by depletion of the B-cell population but was significantly reduced by depletion of Thy.1 cells, or $CD4^+$ T-cells.

ii. $CD4^+$ T-cells are predominant against *C. parvum*

The immune reconstitution of SCID mice by transferring splenocytes from immunocompetent donors was reduced or eliminated by anti-CD4 treatment (Chen et al., 1993a), but not by treatment with anti-CD8 or anti-asialo-GM1 antibodies. This indicates that $CD4^+$ T-cells are crucial for the resolution of established *C. parvum* infection in SCID mice.

Aguirre *et al* (1994) showed that MHC-II (important for $CD4^+$ T-cells) deficient mice are more susceptible to *C. parvum* infection than MHC-I deficient mice (important for function of $CD8^+$ T-cells). Additionally, Harp *et al* (1994) demonstrated proliferative responses of $CD4^+$ T-cells purified from spleen of *C. parvum* infected mice on *in vitro* stimulation with the parasite antigen. In contrast, $CD8^+$ T-cells were unresponsive to the parasite antigen. Spleen $CD4^+$ T-cells, depleted of $CD8^+$ T-cells, gave profound reduction of infection in SCID mice with persistent *C. parvum* infection; the effect was less for $CD8^+$ T-cells (McDonald and Bancroft, 1994; Perryman et al., 1994).

Data from humans also support the requirement of $CD4^+$ T-cells in resistance in that HIV/AIDS patients with the lowest $CD4^+$ T-cell counts are the most severely affected ones (Flanigan et al., 1992). However, the study done by Abrahamsen *et al*. (1997) in calves showed the importance of $CD8^+$ T-cells during *C. parvum* infection since the number of $CD8^+$ T-cells were increased after challenge infection of recovered calves. There is no study showing the direct cytotoxic activity of $CD8^+$ T-cells yet as was shown in the immune response of the related pathogen, *Toxoplasma gondii* (Chardes et al., 1994).

Therefore, the immune effector functions that resolve *C. parvum* infection in animal or human hosts is still a challenging question. The lack of evidence for cytotoxic removal of infected cells like any intracellular pathogens, but only the prominent involvement of $CD4^+$ T-cells in almost all infected hosts points to questions which are very difficult to explain under the current knowledge. Are $CD4^+$ T-cells capable of killing *C. parvum* infected cells, where as the general knowledge is that $CD4^+$ T-cells are helper cells for $CD8^+$ T-cell-mediated killing or B-cell mediated antibody production? The scientific knowledge that has been accumulating on $CD4^+$ T-cells is discussed in detail in the following section.

iii. Immune effector functions of $CD4^+$ T-cells

A. The dogma of Th1/Th2 hypothesis

Mosmann *et al*. (1986) formulated a central hypothesis in immunology 20 years ago. Based on functional bioassays and protein expression studies, helper T-cells were categorized as Th1 and Th2 cells. Th1 cells secrete the cytokines interferon (IFN)-γ, and tumor necrosis factor (TNF)-α, which allow these cells to be particularly effective in protecting against intracellular infections by viruses and bacteria and micro-organisms that grow in macrophages, as well as eliminating cancerous cells. Th2 cells secrete interleukin (IL-4), -5, -10 and -13, which activate B-cells to up-regulate antibody production and target parasitic organisms. In addition, Th2 cells involve in allergy such as asthma. (Steinman, 2007; Reiner, 2007; Kaiko et al., 2008) (Figure 2).

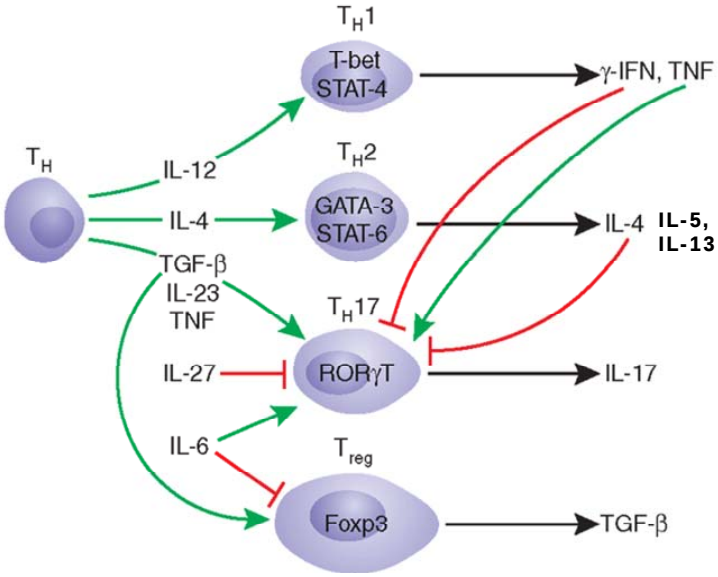

Figure 2. The helper (Th) cell ($CD4^+$ T-cell) differentiation and regulation. Naive Th cells differentiate into Th1 and Th2 cells based on their cytokine secretion pattern as well as the transcription factors regulating the particular cell lineage. Recently, two more Th subsets, termed as Th17 and T reg are described based on their cytokine and transcriptional factor requirements. Cytokines from one Th subset regulates the differentiation of other subsets as indicated by the arrows. Green arrows indicate upregulation, while red lines indicate inhibition. Transcription factors for particular lineages are placed in the nucleus. (Steinman, 2007)

B. Th1/Th2 paradigm

The discovery of two further T-cell subsets to explain some of the pathological phenomena is on the verge of changing the original Th1/Th2 hypothesis (Figure 2). Th17 cells that produce interleukin-17 and mediate delayed type hypersensitivity (DTH), a function that has been ascribed to Th1 cells, is the first challenge (Ivanov et al., 2006). The second subset is termed as regulatory T-cell (Treg). With increasing understanding of the cellular and molecular nature of $CD4^+$ T-cells and their functions there may be further emergence of different subsets of $CD4^+$ T-cells. In line with this, quite recently a distinct $CD4^+$ T-cell lineage termed as T follicular helper (Tfh) cell was described (Nurieva et al., 2008). Mouse Tfh cells are shown to have a divergent gene expression profile from Th1, Th2, and Th17 cells and developed *in vivo* independently of these lineages.

Therefore, the helper T-cell ($CD4^+$) population heterogeneity is not as simple as it was thought.

C. Th1/Th2 cytokines in *C. parvum* infection

Th1 cytokine response is a dominant player

In addition to the involvement of IFN-γ during the innate immune response to the parasite, the cytokine is also a key player during adaptive immune response. Whereas a non-T-cell is the source of the cytokine during early period, the T-cells which are important components of the adaptive immunity are the dominant source.

Harp *et al* (1994) used cultures of $CD4^+$ T-cells purified from immunized mice incubated with *C. parvum* antigen and detected the production of IFN-γ from the supernatant. Furthermore, IFN-γ was required to prevent initiation as well as to limit the extent of infection (Ungar et al., 1991). This is supported by studies using IFN-γ gene targeted (GKO) mice which are significantly susceptible to infection in a strain dependent manner (Mead and You, 1998; Smith et al., 2000). An increased intestinal IFN-γ expression was associated with recovery of immunocompetent neonatal mice (Kapel et al., 1996), calves (Wyatt et al., 2001) and humans (White, Jr. et al., 2001).

Although IFN-γ has been shown to be an important part of both the innate and adaptive immune responses to *C. parvum*, the mechanisms of resistance mediated by the cytokine alone are not completely understood. In an *in vitro* experiment, exogenous IFN-γ directly inhibited the development of *C. parvum* in cultured enterocytes, where inhibition of parasite invasion and depletion of intracellular iron were identified as possible mechanisms of action (Pollok et al., 2001). The activation of tumour necrosis factor-α (TNF-α) expression via up regulation of its transcription factor NF-κB by IFN-γ has been suggested as one potential mechanism (Shtrichman and Samuel, 2001). However, conflicting results have been obtained by different experimental approaches that address the role of TNF-α in *C. parvum* infection. Neutralization of TNF-α by anti-TNF-α antibodies showed no effect on infection (Chen et al., 1993a; McDonald and Bancroft, 1994). In contrast, increased expression of TNF-α was reported in *C. parvum* infection *in vitro* and *in vivo* experiments (Seydel et al., 1998; Maillot et al., 2000; Lacroix et al., 2001; Robinson et al., 2001a). Lean *et al*. (2006) showed a parasite development in a murine enterocyte cell line potentially through inhibition of parasite invasion. However,

TNF-α might have only a redundant role in resistance to *C. parvum* since TNF-α deficient mice controlled infection as effectively as wild type mice.

Interleukin-12 is an additional important Th1 cytokine that involves in *C. parvum* infection. IL-12, as an important regulator of IFN-γ prevented *C. parvum* infection through an IFN-γ-dependent mechanism, and also limited *C. parvum* infection *in vivo* (Urban, Jr. et al., 1996). IL-12KO mice were also susceptible to infection (Campbell et al., 2002). However, IFN-γ is induced in infected IL-12KO mice (Ehigiator et al., 2005; Jakobi and Petry, 2008), showing that there are other additional factors that regulate the secretion of IFN-γ in *C. parvum* infection. In contrast, in neonatal calves administered with recombinant IL-12, strong gut immune response was stimulated but the response was not able to provide protection from challenge inoculation with *C. parvum* oocysts (Pasquali et al., 2006).

Interleukin-18 is another Th1 cytokine that has been shown to involve during *C. parvum* infection. IL-18 was up regulated in response to *C. parvum* infection (Ehigiator et al., 2005); exogenous IL-18 decreased *C. parvum* load markedly and also IL-18 KO mice were susceptible to infection (Ehigiator et al., 2007). McDonald *et al*. (2006) also detected IL-18 mRNA and protein up regulation *in vitro* in a human intestinal epithelial cell line, where they also showed that one potential protective role of IL-18 could be through inhibition of intracellular development of the parasite through IL-18 mediated expression of antimicrobial peptides. However, IL-18 is a pluripotent cytokine involving in different innate and adaptive immune mechanisms (reviewed in Nakanishi et al., 2001). Therefore, it is possible that the cytokine participates through different effector immune mechanisms during *C. parvum* infection. Interleukin-18, otherwise termed as IFN-γ–inducing factor, has been shown as an important IFN-γ regulator in the presence or absence of IL-12 (Okamura et al., 1995b), but there is no study that addresses the role of IL-18 as IFN-γ inducer cytokine during *C. parvum* infection yet.

Th2 cytokines

Enriquez and Sterling (1993) applied cytokine depletion experiments, by injecting adult mice with monoclonal antibodies, to find out the importance of the Th2 cytokines, IL-4 and IL-5, for controlling cryptosporidiosis. Reports of different outcome of infection in different IFN-γ KO mice strains (Mead and You, 1998) indicated an IFN-γ-independent immune mechanism. BALB/c mice which are genetically biased to mount a Th2 response resolve the infection

whereas the C57BL/6 mice, which are biased to mount a Th1 response, die of chronic infection. In contrast, results from our lab indicated the recovery of C57BL/6 IFN-γ-KO mice within 2 weeks (Jakobi and Petry, 2008).

Aguirre *et al*. (1998) strengthened this idea by showing the role of IL-4 especially at later stage of *C. parvum* infection, suggesting the involvement of both Th1 and Th2 responses, the Th1 being critical during early stages of infection but the Th2 cooperates with Th1 for parasite clearance at later stages of infection (McDonald, 2000). Further reports from different groups indicated that both Th1 and Th2 cytokines may act in a well-controlled fashion for an effective control of *C. parvum* infection (Huang et al., 1996; Smith et al., 2000; Smith et al., 2001; Ehigiator et al., 2005; Singh et al., 2005).

D. Unknown effector functions of $CD4^+$ T-cells

In addition to helping other effector immune mechanisms, *i.e*. cell-mediated and antibody-mediated responses, some subsets of $CD4^+$ T-cells, Th17, can mediate effector functions in some immunopathological conditions. Until now, there is no report showing a sole involvement of $CD4^+$ T-cell subset having an effector function to eliminate infection, such as infected cells. This is one of the dilemmas in understanding resistance to *C. parvum* where the dominant immunological role is played by $CD4^+$ T-cells. However, it is difficult to depict $CD4^+$ T-cell-mediated destruction of *C. parvum* infected cells *in vivo* with the current scientific knowledge. The failure of previous studies to demonstrate the role of classically known arms of immune response, *i.e*. cell-mediated and antibody-mediated, to resolve *C. parvum* infection further complicates the situation.

A detailed investigation of *C. parvum* specific immune responses, as mediated by $CD4^+$ T-cells, using the state of the art methods available to date is highly crucial. Novel immune effector mechanisms of $CD4^+$ T-cells may be identified at the end. There are important methodological gaps that need to be filled to address these questions: such as designing *in vitro* continuous culture systems; identification of novel virulence factors and immune inducing epitopes on the different developmental stages of the parasite; the molecular mechanism of antigen processing and presentation; designing *C. parvum* epitope specific $CD4^+$ T-cells to apply them in studying *in vivo* immune effector functions and possibly to use them for designing cellular prophylactic

approaches. *In vivo* study of *C. parvum* specific effector and memory cells using *C. parvum* peptide loaded T-cells, especially $CD4^+$ T-cells, is a much demanded experimental approach.

1.3.2.2. Humoral immunity

i. *C. parvum* antigens recognized by infected hosts

In order to design active immunization strategies for *C. parvum* prophylaxis, *C. parvum* relevant antigens should be identified and characterized. Difficulties in isolation of auto-infective asexual and sexual stages continue to be a barrier to their immunologic characterization. Therefore, the efforts have been limited to the surface-exposed antigens of the extracellular stages, which are involved in motility, attachment, invasion, and/or intracellular development. Thus, antigens identified on such effort include CSL, GP900, CP47, CP17, p23 and others (reviewed in Riggs, 2002).

ii. Antibody responses to *C. parvum* infection

C. parvum infection is accompanied by an antibody-mediated Th2 response in infected individuals with production of parasite-specific immunoglobulin (Ig) of all major classes (Williams and Burden, 1987; Hill et al., 1990; Peeters et al., 1992). In a recent report from our lab, immunodeficient mice infected with the parasite mounted parasite specific systemic as well as mucosal IgA and IgG responses; moreover, challenge infection led to a booster effect in immunoglobulin response despite the absence of oocyst shedding (Jakobi and Petry, 2008).

However, the protective role of antibodies is questionable by the fact that high titres of parasite-specific IgG/IgA and mucosal IgA can be found in AIDS patients with chronic cryptosporidiosis (Ungar et al., 1986; Reperant et al., 1994; Cozon et al., 1994). Furthermore, studies employing gene-targeted B cell-deficient mice indicate that B-cells are not essential for resistance to and recovery from *C. parvum* infections in mice (Chen et al., 2003).

iii. Prevention strategies based on antibody response

Passive transfer of anti- *C. parvum* antibodies

Polyclonal antibodies against whole *C. parvum* preparations produced inconsistent results in rodent models, neonatal ruminants, and immunocompromised humans (Crabb, 1998). Therefore, attention has been focused on functionally defined antigens for production of polyclonal as well as monoclonal antibodies. In this regard, newborn calves fed with colostrum from cows immunized with P23 antigen of *C. parvum* showed reduced oocyst shedding and diarrhea (Perryman et al., 1999). Cows immunized with CP 15/60 based DNA vaccine transferred protection to immunosuppressed mice where there was a partial protection upon *C. parvum* infection (Jenkins et al., 1999). These results demonstrate that antibody-mediated resistance to the parasite can not confer complete resistance and also stress the need for complete identification of protective antigens from the parasite.

In summary, the antibody response observed during *C. parvum* infection may be of minor importance that is raised only to the exposed antigens of the extracellular stages of the parasite. This questions the relevance of humoral immunity for resistance against infection considering the fact that parasite stages inside infected cells are not accessible to an antibody attack. This remains to be the major obstacle that hinders the use of classical vaccines, with the aim of antibody production, for future application. However, mucosal IgA may assist the cellular immune response by coating surfaces of the infective stages and preventing attachment to the epithelial cells. Therefore, a successful control scheme may involve a combination of both cellular based and some mucosal IgA based strategies.

1.3.3. Gut mucosal (local) immune system

1.3.3.1. Gut associated lymphoid tissues (GALT)

The GALT has been functionally divided into inductive and effector sites (Figure 3). The inductive sites are the places where the antigens of the mucosal lumen are collected and where the immune response is induced. The effector sites are the places where the immune cells differentiate and exert their function, *i.e*. a cellular response being mediated by T-cells and a local humoral response (mainly secretory IgA) by B-cells. The inductive sites include

mesenteric lymph nodes, Peyer's patches in the small intestine, and other lymphoid aggregates. The effector sites include intestinal lamina propria and intestinal epithelium, which contains intraepithelial lymphocytes (IELs). The lamina propria contains a large and heterogeneous group of lymphoid and myeloid cells: lymphocytes, macrophages, dendritic cells, granulocytes and mast cells (Kelsall and Strober, 1999; Magalhaes et al., 2007).

The roles of the intestinal epithelial effector sites, epithelial cells and intraepithelial lymphocytes (IELs), during *C. parvum* infection will be discussed in following sections.

1.3.3.2. Intestinal epithelial cells (IECs)

IECs provide barrier function to invading microbes through various physical and biochemical factors (Shen and Turner, 2006; Magalhaes et al., 2007). In addition, there are numerous reports suggesting that IECs can influence innate and adaptive immune cell function. IECs constitutively express pattern-recognition receptors, including Toll-like receptors (TLRs) and intracellular Nod-like receptors that enable microbial recognition. Ligation of TLRs and Nod-like receptors results in activation of innate immune responses, including induction of the expression of proinflammatory cytokines and chemokines that are essential components of the anti-pathogen response. IECs express a wide range of cytokines and chemokines, including tumor-necrosis factor (TNF), transforming growth factor-β (TGF-β), IL-1, IL-6, IL-7, IL-8, IL-10, monokine induced by interferon gamma (MIG), IFN-inducible T cell-chemoattractant (ITAC), macrophage inflammatory protein (MIP)-3α, CXCL9, IFN-γ-inducible protein 10 (IP-10 or CXCL10), CXCL11, and fracktalkine that can promote the recruitment and / or activation of immune cells (reviewed in (Artis and Grencis, 2008). They also express major histocompatibility complex class I and class II molecules and all the machinery required for antigen processing and presentation (Hershberg and Mayer, 2000).

C. parvum infected epithelial cells respond by upregulating certain C, C–C, and C–X–C class chemokines as shown in neonate mice (Lacroix-Lamande et al., 2002); CXCL10 is highly upregulated in intestinal epithelial cells of AIDS patients with active cryptosporidiosis (Wang et al., 2007). The potential role of intestinal epithelial cells to produce DC-attracting chemokines in response to *C. parvum* infection has been reported (Auray et al., 2007).

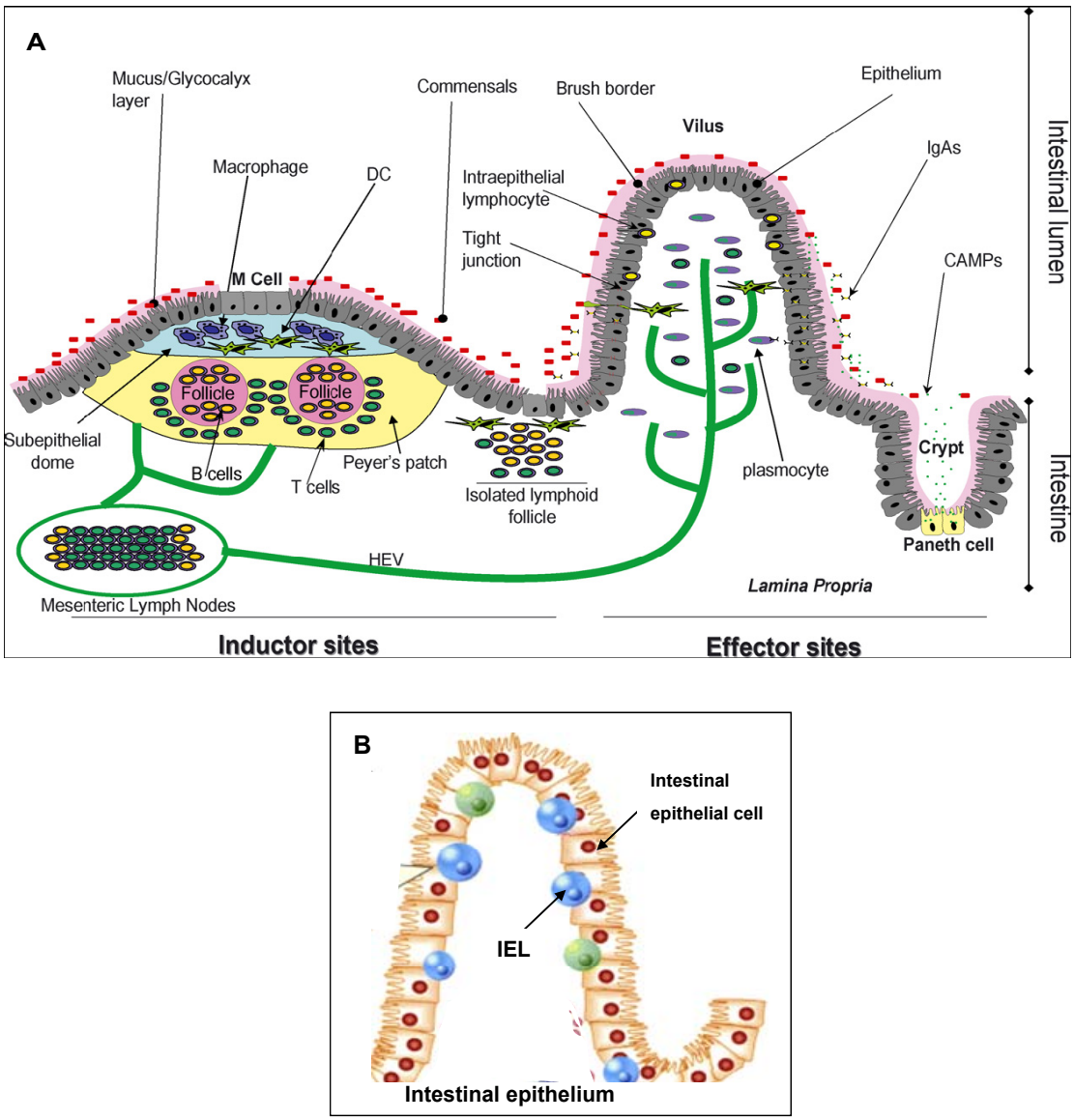

Figure 3. The intestinal (gut) mucosal immune system. (A) The gut flora in the lumen is separated from the lamina propria by a single layer of epithelial cells. The intestinal immune system is divided in two functional compartments: the inductive and effector compartments. Inductive compartments include Peyer's patches, mesenteric lymph nodes, colonic patches and isolated lymphoid follicles. Effector compartments include the lamina propria and the epithelium. In the epithelium, scattered intraepithelial lymphocytes monitor epithelial damage, while the lamina propria contains a large numbers of T-cells, IgA-producing plasmocytes, macrophages and DCs. These DCs sample the lumen compartment by extending their dendrites, migrate to the mesenteric lymph nodes through the lymph and present antigens to T-cells.(Magalhaes et al., 2007) (B) Intestinal intraepithelial lymphocytes (IELs) are located at the base of the intestinal epithelial cells. The figure is modified from that of Kunisawa et al. (Kunisawa et al., 2007).

One of the important roles of intestinal epithelial cells is as a cellular source of interleukin-18 (Takeuchi et al., 1997). IL-18 mRNA and protein were up regulated upon *C. parvum* infection of intestinal epithelial cells (McDonald et al., 2006). IL-18 is a multifunctional Th1 cytokine; the role of IL-18 originated from *C. parvum* infected intestinal epithelial cells in the pathobiology of *C. parvum* infection in the gut is a very interesting mucosal immune mechanism for future investigation.

The intestinal epithelial cells also contribute to the innate defense system through antimicrobial peptide response. *C. parvum* actively modulated epithelial β-defensin expression and function both in human (*in vitro*) and in mouse (*in vivo*), which may allow the parasite to escape early immunosurveillance leading to increased persistence at the intestinal mucosal surface (Zaalouk et al., 2004). Several studies have demonstrated that defensins exhibit killing activity against a wide range of organisms, including enteric pathogens such as *Salmonella* spp. (Wilson et al., 1999), *E. coli* (Ayabe et al., 2000), and *Giardia* spp. (Aley et al., 1994). Although not fully understood, one mechanism of defensin action may be through the formation of pores in the microbial membrane resulting in fatal disruption of integrity and function (Zasloff, 2002).

1.3.3.3. Intestinal intraepithelial lymphocytes (IELs)

IELs are lymphocytes residing as single cells between IECs, near the basement membrane, at a frequency of one IEL for every 4 – 10 IECs in the small intestine (Figure 3). Given the immense surface area of intestinal epithelia, resident IELs can comprise a substantial fraction of the body's T-cells (Kunisawa et al., 2007).

IELs are different from their systemic counterparts in their subset composition. Systemic (spleen, peripheral blood, lymph node) T-cells readily subdivide into major histocompatibility complex (MHC) class II-restricted $CD4^+$ T-cells and MHC class I-restricted $CD8^+$ T-cells. On the contrary, >70 % of small intestinal IELs comprise $CD8^+$ T-cells. A large fraction of these $CD8^+$ T-cells express a CD8αα homodimer, which is essentially absent from the circulation (Jarry et al., 1990). Likewise, $CD4^-CD8^-$ "double negative" cells, which are rare in the systemic circulation, can account for >10 % of murine small intestinal IELs and the majority of IELs in other compartments. Conversely, $CD4^+$ αβ T-cells are under represented in many IEL compartments and, of the few present in the small intestine, many also express CD8αα. These T-cell antigen receptor–positive (TCR^+) "double positive" cells are also unprecedented in the

systemic circulation. IELs include greater numbers of TCRγδ+ cells than are found in the murine or human circulation. Between 35 – 65 % of murine $CD8^+$ small intestinal IELs express TCRγδ with TCR repertoires specific to particular sites and distinct from those in the blood (reviewed in Hayday et al., 2001).

T cells in the IEL population can be activated specifically by infection with mucosal pathogens such as *Trichinella*, *Listeria*, *Cryptosporidium*, *Toxoplasma* and others (reviewed in (McDonald, 1999). In a study done on murine gastric parasite, *C. muris* which is in the same genus as *C. parvum*, immunity could be adoptively transferred to immunocompromised SCID mice using small intestinal IELs, as donor cells, from animals recovered from infection. The protection obtained was predominantly associated with the donor $CD4^+$ T-cell population, as removal of these cells before transfer abrogated immunity. Significantly, the gut IEL population of reconstituted SCID mice that recovered from infection became populated with the protective $CD4^+$ T-cells (McDonald et al., 1996).

During *C. parvum* infection, there were changes in cytokine expression of IELs as shown by different workers. Increased cytokine mRNA levels were detected in the IEL of *C. parvum* infected mice on *in vitro* mitogen stimulation (Huang et al., 1996). *Cryptosporidium* antigen-specific production of IFN-γ was seen in IELs from mice (Culshaw et al., 1997). Furthermore, Leav *et al* (2005) demonstrated that naive $CD8^+$ αβ T-cells of IEL population express and secrete IFN-γ within early (24 hr) time of *C. parvum* infection in mice. The cytokine pattern expressed by IELs from calves with cryptosporidiosis was different from control calves (Wyatt et al., 1999). Wyatt *et.al* (2002) reported a temporal association between the expression of IL-10 by ileal IELs and the expression of *C. parvum* antigens in infected calf epithelium prior to development of cryptosporidiosis. IELs from infected calves showed increased IL-10 mRNA by 3 days p.i., before the development of diarrhea.

Changes in location and composition of IELs during *C. parvum* infection have been shown by studies done in mice as well as calves. IELs changed their location from the basal area to intermediate and apical areas of villous epithelial cells during the early stage of infection. In three week old conventionally bred immunocompetent mice, IEL phenotypes also changed upon infection; whereas $CD4^+$ T-cells increased temporarily on day 7 p.i., $CD8^+$ T-cells increased significantly on days 16 and 20 p.i. (Chai et al., 1999). Wyatt *et al* (1997) observed significantly larger numbers of intraepithelial $CD8^+$ T-lymphocytes in ileal mucosae from

acutely infected calves compared with those from control animals. In addition, a proportion of intraepithelial $CD4^+$ T-cells from acutely infected calves co-expressed CD25 (IL-2 receptor α chain), whereas there was an absence of co-expressed CD25 on $CD4^+$ T-cells from control calves. *In vitro*, there was a statistically significant increase in the number of $CD8^+$ T-lymphocytes per 100 epithelial cells in oocyst-inoculated tissue compared with uninoculated explants. In addition, there were increased numbers of $CD4^+$ T-cells and activated ($CD25^+$) lymphocytes adjacent to *C. parvum*-infected epithelium. These results show that resident mucosal T-lymphocytes can accumulate at the epithelium during *C. parvum* infection (Wyatt et al., 1999).

1.3.4. Adoptive transfer of immunity and future prospects

1.3.4.1. Immunological memory: memory $CD4^+$ T-cells

When naive $CD4^+$ T-cells are primed with specific antigen peptide:MHC ligand on antigen presenting cells (APCs), $CD4^+$ T-cells undergo many steps of division and differentiation into various subsets distinguished by the production of particular cytokines and effector functions (LaRosa and Orange, 2008) (Figure 4). There are two important effector functions of $CD4^+$ T-cells: Th2 cells 'help' for B-cells, which promotes Th2 immune response (antibody production); and Th1 cells help for naive $CD8^+$ T-cells to promote their optimum differentiation into cytotoxic effectors and memory cells and to support their maintenance (Swain et al., 2006).

The features that typify memory T-cells are the following: (1) persistence of an increased frequency of antigen-specific precursors (100-fold to 1000-fold more than naive host); (2) accelerated responsiveness and rapid effector molecule acquisition on encounter with specific antigen; and (3) antigen-independent steady-state maintenance (homeostatic proliferation) dependent on IL-7 and IL-15 (Kalia et al., 2006; Robertson et al., 2006). As a result, $CD4^+$ memory T-cells are suited to deal quickly with secondary infections.

In addition, $CD4^+$ memory T-cells have surface markers that distinguish them from naive cells. In both humans and mice $CD4^+$ memory T-cells are defined by high expression of CD44 (homing receptor) surface molecule. $CD4^+$ memory T-cells, unlike naive T-cells, can accumulate in extra lymphoid tissues, and this characteristic presumably contributes to their ability to patrol the body (Robertson et al., 2006).

There are two main models of memory T-cell development. The conventional model of linear differentiation states that memory cells are derived from effector cells. Activated naive T-cells undergo dramatic clonal expansion, but after the acute response, this is followed by apoptosis-induced contraction to maintain steady state; those that survive establish memory. The alternative model is a divergent pathway in which memory is established independent of an effector stage (LaRosa and Orange, 2008) (Figure 4).

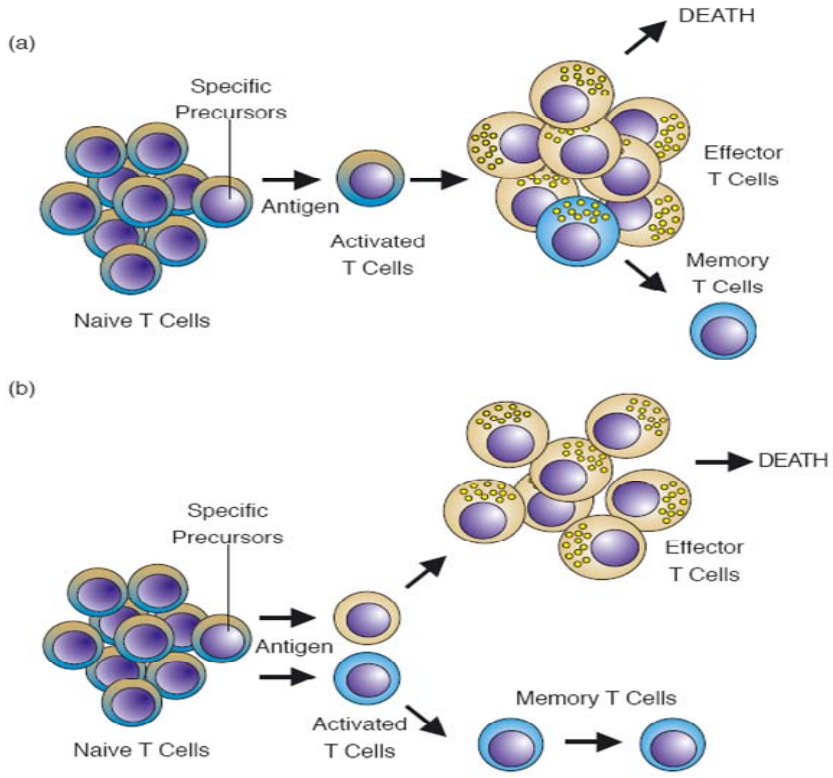

Figure 4. T cell memory differentiation. (a) The linear model of memory generation states that upon activation with antigen, naive T-cells differentiate into effector cells. From this effector population, the majority of the expanded specific cells will undergo apoptosis, but a subset of these cells will survive and become memory T-cells. (b) The divergent differentiation model proposes that after naive T-cells encounter antigen and become activated, two distinct populations arise: the effector T-cell population and the memory T-cell population. After the antigen is cleared, the effector population will die off while the memory T-cell population persists. (Teichgräber, 2004)

The inherent characteristic of T-cells to differentiate into antigen specific memory T-cells that last long with better response upon re-exposure to the same antigen has been utilized to design immune therapeutic and prophylactic approaches, such as vaccination and adoptive immunotherapy. As recently reviewed by Leen *et al*. (2007) adoptive immunotherapy using antigen-specific T-cells, specifically $CD8^+$ T-cells, for the prevention and treatment of virus-associated diseases, such as Epstein Barr virus (EBV)-associated post-transplant

lymphoproliferative disease (PTLD), cytomegalovirus (CMV) and some types of cancer have been shown to be safe, effective, and protective *in vivo*.

1.3.4.2. Adoptive transfer of immunity in *C. parvum* infection

Transfer of immunity from *Cryptosporidium* primed mice to naive mice, mostly SCID mice, was carried out to address certain immunological questions. As mentioned earlier, adoptive transfer was used to show the importance of T-cells and $CD4^+$ T-cells in resistance to the parasite (Mead et al., 1991a; McDonald et al., 1992; Chen et al., 1993a; McDonald and Bancroft, 1994; Perryman et al., 1994). Using *C. muris* McDonald *et al* (1996) showed adoptively transferred small intestinal IELs, as donor cells, from animals recovered from infection to immunocompromised SCID mice. The protection obtained was predominantly associated with the donor $CD4^+$ T-cell population, as removal of these cells before transfer abrogated immunity. Adjei *et al* (2000) showed protection of SCID mice with primed IELs from immunocompetent BALB/cJ mice compared to recipients of unprimed IELs.

1.4. Objectives of the thesis work

Previous workers have addressed some aspects of host's immune response to *C. parvum* using various approaches; there is general agreement that $CD4^+$ T-cells and IFN-γ play dominant roles against infection. However, effector mechanisms that lead to resistance are poorly understood. Consequently, the proper understanding of the immune response to the pathogen has been far from complete due to basic problems attributed to the organism as well as other factors. These factors include: absence of methods for long-term *in vitro* propagation of the pathogen, the lack of adult immunocompetent animal infection models, and differences in the experimental setup such as the mouse strains and parasite isolates used by different workers leading to variation in the interpretation of the data. The present study attempted to address these problems by using two adult immunodeficient mouse models, i.e., C57BL/6 GKO and C57BL/6 IL-12KO mice in parallel as well as adult immunocompetent mice thus results from one model may complement those deficient in the other.

Furthermore, *C. parvum* is a gut mucosal pathogen infecting and developing in the gut mucosal surface epithelium; to date, there is no report indicating the crossing of any of the pathogen's developmental stages through the epithelial layer to the blood circulation. Therefore, the

involvement of different immunological compartments during infection is an important factor to be addressed. This may help in designing immunological control and preventive strategies to combat the disease. The traditional way of producing systemic vaccines simply aimed at inducing systemic antibody production has failed repeatedly at least because of the difficulty of systemic antibodies to get access to the intracellularly located pathogen, which resides only in the gut mucosal surface.

Therefore, this thesis work is designed to investigate two important questions on the host's immunological response to *C. parvum*:

1) To indentify the factors that contribute to resistance against infection. These factors considered in this study will be Th1 and Th2 cytokines as well as $CD4^+$ T-cells.

2) To study if the resistance established during or after infection is transferrable from infected to naive animals through immune cells, i.e. IELs and $CD4^+$ T-cells.

I. The role of Th1 and Th2 cytokines in host resistance to *C. parvum* infection

The contribution of Th1 and Th2 cytokines in resistance to *C. parvum* infection will be carried out in three different experimental setups.

1. Studying the dynamics of Th1 and Th2 cytokine gene expression induced *in vivo* at key time points during a patent *C. parvum* infection.

In order to address this objective, animals will be infected with the pathogen and tissue samples will be collected at different time points post infection, i.e. before the start of oocyst shedding, at the start of oocyst shedding, at the peak of oocyst shedding and the resolution of oocyst shedding. The tissue samples to be studied represent the site of infection, i.e. gut mucosa (distal ileum), the lymph nodes draining the site of infection (mesenteric lymph nodes (MLNs)), and the systemic immune tissue (spleen). Total mRNA will be isolated from the tissues and analysed using qualitative RT-PCR as well as quantitative real-time RT-PCR.

This experiment will help us to identify the presence of any differential expression of Th1 and Th2 cytokines in the time course of infection, as well as between local (mucosal) and systemic immune tissues.

2. Studying the Th1 and Th2 cytokine gene expression pattern after challenge infection.

We have recently reported that after resolution of the primary infection, both GKO and IL-12 KO mice were resistant to challenge infection since there was no discharge of oocysts. This

gives the possibility to study the cytokines induced *in vivo* in recovered animals upon challenge infection so as to understand the differences in the immune mechanisms involved during primary and challenge infection. This objective will be addressed using the same protocols applied for the primary infection except the time points of tissue collection. Because there is no detectable oocyst shedding post challenge infection, tissues will be collected at arbitrary chosen days post challenge infection.

3. Studying the contribution of interleukin-18 in host resistance to *C. parvum* infection.

Although IFN-γ plays a major role in *C. parvum* resistance, the mechanisms involved in regulation of its induction during infection require further study. IL-12 prevented *C. parvum* infection through an IFN-γ-induction in vivo. However, IFN-γ is induced by the parasite even in IL-12KO mice, indicating the presence of IL-12 independent factors that regulate the production of IFN-γ in *C. parvum* infection. IL-18 was first discovered as IFN-γ-inducing factor, and has been shown to induce IFN-γ during many bacterial and fungal infections. Therefore, the possibility of IFN-γ induction by IL-18 during *C. parvum* infection will be addressed in this study. This will be carried out by studying the changes in gene expression of IL-18 in parallel to that of IFN-γ during infection, in vivo neutralizating IL-18 protein using a monoclonal anti-IL-18 antibody, and analyzing the changes in gene expression of Th1 and Th2 cytokines during anti-IL-18 treatment and *C. parvum* infection. Therefore, the possible role of IL-18 in regulating cytokines other than IFN-γ will be studied additionally.

II. Adoptive transfer of cellular immunity from infected to naive animals

In order to answer the question if there is transferrable resistance (or immunity) from infected to naive animals, the methodology of adoptive transfer will be applied. So far, adoptive transfer experiments in *C. parvum* infection have been used as a tool to examine the roles of T-cells and their subsets in resistance to the pathogen. These experiments applied mice lacking lymphocytes, notably SCID mice, as recipients. These studies show the importance of both primed and naive donor cells, although primed cells were much more protective than naive cells. The relevance of transferring primed $CD4^+$ T-cells in animal models having $CD4^+$ T-cells, i.e., intact cellular immunity, is not known. The present work aims to study the possibility of transferring protective cellular immunity to naive animals with intact cellular immunity, except lacking IFN-γ or IL-12. Besides, the time of development of this transferrable cellular immunity in reference to the patent *C. parvum* infection will be investigated. The relative contribution of

T cells of the gut mucosal (IELs) versus systemic immune compartments in resistance to *C. parvum* will also be studied. By comparing the significance of protection provided by donor cells from GKO and IL-12KO mice, the study will help to infer the requirement of IFN-γ in IELs versus in spleen and MLN $CD4^+$ T-cells for the transferred resistance. The importance of priming donors with infection for the success of transferring immunity will be addressed.

These objectives will be achieved by isolating IELs from the small intestine and $CD4^+$ T-cells from MLN and spleen of mice post peak and resolution of *C. parvum* infection, followed by transferring these primed cells to naive recipients and follow protection from infection. Moreover, pan T-cells ($CD4^+$ and $CD8^+$ T-cells) will also be transferred in parallel to that of $CD4^+$ T-cells to examine the effect on the efficiency of transferred protection by incorporating $CD8^+$ T-cells. In addition, cells from naive as well as wild type mice will be used to assess the importance of priming for success of transferring cellular immunity.

Addressing these questions will likely forward our understanding of the host immune response to the pathogen, point out further questions to be addressed and, therefore, paves the way for immunological approaches to control and prevent infection in susceptible hosts. Identifying the role of primed $CD4^+$ T-cell donors in *C. parvum* infection in animals having $CD4^+$ T-cells will further strengthen the prominent role of pathogen specific $CD4^+$ T-cells as a major factor in resistance to the parasite.

II. Materials and Methods

2. Materials

2.1. Parasites

The isolate of *Cryptosporidium parvum* used in this experiment is the IOWA strain. *C. parvum* oocysts were obtained from a commercial source (Bunch Grass Farm, Deary, Idaho, USA). This animal and human pathogenic strain has passaged through Holstein-Friesian new born calves. According to the supplier, oocysts were purified from calf faeces by sucrose density centrifugation, washed and suspended in PBS. Parasites were stored at 4°C in the presence of 1000 U/ml penicillin and 1000 µg/ml streptomycin (Coulliette et al., 2006). In our laboratory the oocyts are stored up to 6 months at 4^{o}C with occasional controlling of the infectivity of the parasites.

2.2. Bacterial strain

Organism: *Escherichia coli* Strain: JM109 (Fermentas, St. Leon-Rot, Germany)
Genotype: *endA*1, *recA*1, *gyr*A96, *thi*-1, *hsdR*17 (r_K-, m_K+), *relA*1, *supE*44, Δ (*lac-proAB*), [F', *traD*36, *proAB*, *lac*I^qZΔM15]

2.3. Mouse strains

Breeding pairs of IL-12p40 deficient mice (IL-12KO) (Magram et al., 1996) and interferon-γ deficient mice (GKO) (Dalton et al., 1993), both with genetic background of the C57BL/6 strain, were generously supplied by Prof. Dr. E. Schmitt (Institute of Immunology, Mainz). All mouse strains including C57BL/6 wild-type mice were further bred at the central animal facilities of the University of Mainz under specified pathogen free (SPF) conditions. Regular microbiological screening for specified pathogens was performed. Animals were fed sterile food and water *ad libitum*, kept in filter top cages and handled under a laminar flow. Genotyping of the breeding colonies was performed using specific primers for the neomycin gene (oIMR0128 and oIMR0129), IL-12p40- (oIMR0457 and oIMR0458) and IFN-γ-gene (oIMR0126 and oIMR0127) and PCR conditions according to the genotyping protocols of The

Jackson Laboratory <http://jaxmice.jax.org/>. All animal experimentation was licensed by the regional health authorities.

2.4. Nucleic acids

DNA ladder (100 bp)	Invitrogen (Karlsruhe)
dNTPs	Invitrogen (Karlsruhe)
Oligo-dT primers	Invitrogen (Karlsruhe)

Oligonucleotide PCR primers were designed using the Primer3 software (Rozen and Skaletsky, 2000) or derived from published sequences. Custom primer synthesis was done at Invitrogen (Karlsruhe, Germany).

Table 1. List of PCR primers used for RT-PCR and quantitative real-time RT-PCR.

Target	Sequence 5'→3'	Amplicon length (bp)	Annealing temp (^{o}C)	Accession number/ reference
	Mouse cytokines			
IFN-γ	FW GAACTGGCAAAAGGATGGTGA RV TGTGGGTTGTTGACCTCAAAC	210	60.5	NM_0083337
TNF-α	FW CCCCAGTCTGTGTCCTTCTAAC RV TATCCAGCCTCATTCTGAGACA	248	60	NM_013693
IL-12p35	FW CTGTGCCTTGGTAGCATCTATG RV GCAGAGTCTCGCCATTATGATTC	169	61	NM_008351
IL-12p40	FW CCTCAGAAGCTAACCATCTCC RV TTTGGTGCTTCACACTTCAGG	389	62	NM_008352
IL-23p19	FW CATGGGGCTATCAGGGAGTA RV AATAATGTGCCCCGTATCCA	167	50	NM_031252.1
IL-27 EBI3	FW CGGTGCCCTACATGCTAAAT RV GCGGAGTCGGTACTTGAGAG	206	52	NM_015766.2
IL-18	FW ACAACTTTGGCCGACTTCAC RV CTTCACAGAGAGGGTCACAGC	200	63	NM_008360

IL-4	FW GAGATCATCGGCATTTTGAA RV GCAGCTTATCGATGAATCCAG	249	60	NM_021283
IL-5	FW CTCTGTTGACAAGCAATGAGACG RV TGCCCACTCTGTACTCATCACA	269	63	NM_010558
IL-10	FW GGTTGCCAAGCCTTATCGGA RV ACCTGCTCCACTGCCTTGCT	191	56	NM_010548
IL-13	FW CAGCCCACAGTTCTACAGCTC RV AATCCAGGGCTACACAGAACC	263	62	NM_008355
	Other mouse genes			
GAPDH	FW GCAGTGGCAAAGTGGAGATT RV TCTCCATGGTGGTGAAGACA	249	60	BC096440
tdy gene	FW TGG GAC TGG TGA CAA TTG TC RV GAG TAC AGG TGT GCA GCT CT	402	63	(Petry et al., 2001)

FW, forward; RV, reverse; IFN-γ, interferon-gamma; TNF-α, tumor necrosis factor-α; IL-, interleukin; GAPDH, glyceraldehyde-3-phosphate dehydrogenase.

2.5. Equipment and Instruments

Axiovert 25	Zeiss (Oberkochen, Germany)
Axioskop 2 with HBO 100	Zeiss (Oberkochen, Germany)
Fluorescence unit, Axiocam HRc, Axiovision	
Fluorescence filter	
EX BP 510-560, BS FT 580, EM LP 590	
EX BP 450-490, BS FT 510, EM LP 515	
EX BP 365/12, BS FT 395, EM LP 397	
COULTER®EPICS®XL™ flow cytometer	Beckman CoulterTM (Krefeld, Germany)
Digital camera DC 120 Zoom	Kodak
Gel electrophoresis apparatus (agarose gel)	Pharmacia (Sweden) BIO-RAD Sub-Cell® GT
Electrophoresis power supply	RENNER (Dannstadt, Germany)
ELISA Photometer (Sunrise™)	TECAN (Crailsheim, Germany)
Heating block	Bioblock Scientific (USA)

Hemocytometer		Blaubrand (Germany)
Incubator 37^{o}C		Labotec (Wiesbaden, Germany)
Incubator with shaker 37^{o}C		WTB binder (Tuttlingen, Germany)
Infrared lamp (150W/220V) Type 808		Schott (Langenhagen, Germany)
Light microscope		Zeiss (Germany)
Liquid Nitrogen cylinders (transportable)		KGW Isotherm (Germany)
MACS separators (MiniMACS, MidiMACS)		Miltenyi biotec (Bergisch Gladbach, Germany)
Magnetic stir plates		Heidolph (Germany)
Mouse restrainer		(Leybold, Germany)
Multichannel micropipettes		Thermo Laborsystems (Finnland)
NanoDrop® ND-1000 Spectrophotometer		Wilmington (USA)
PCR Thermocycler		Eppendorf® AG (Hamburg, Germany)
pH-Meter (pH 315i)		WTW (Weilheim, Germany)
Pipettes		Thermo Laborsystems (Finnland)
		Gilson (France)
Refrigerators (4^{o}C, -20^{o}C)		Liebherr
Refrigerator -70^{o}C		Heraeus (Hanau, Germany)
Refrigerated centrifuges	Minifuge GL	Heraeus (Hanau, Germany)
	RC5C	Sorvall(Bad Nauheim, Germany)
	GPKR	Beckman (UK)
Roche LightCycler version 1.5		Roche (Mannheim, Germany)
Shaker (Rocky)		Labotec (Wiesbaden, Germany)
Table top Centrifuge 5415 C		Eppendorf (Hamburg, Germany)
Biofuge fresco		Heraeus (Hanau, Germany)
TissueLyser (50/60 Hz) & accessories		Qiagen (Hilden, Germany)
UV-Transilluminator (302 nm)		Bachofer (Reutlingen, Germany)
Waterbath		Labotec (Wiesbaden, Germany)
Weighting balance		Sartorius AG (Göttingen, Germany)
Vortex-2 Gene		Scientific Industries (Bohemia, USA)
Ring stand & clamps (for nylon wool)		VWR (Darmstadt, Germany)

2.6. Consumables

Cell strainer (40 µM Nylon)	BD FalconTM, VWR (Darmstadt, Germany)

Conical centrifuge tubes (Falcon) (15 & 50 ml)	Cellstar® Frickenhausen, Germany
Culture tubes (15 ml)	Falcon (France)
Cryovials	Nalgene (USA)
Glass articles	Schott (Mainz, Germany)
Glass capillaries	Roche (Mannheim, Germany)
Glass tubes (15 ml, for FACS)	Greiner Labortechnik (Frickenhausen, Germany)
Eppendeorf tubes (DNase-free, RNase-free)	Roth (Karlsruhe, Germany)
Erlenmeyer flasks (50 ml)	Roth (Karlsruhe, Germany)
Filter (Cellulose acetate) (0.2 µM)	Schleicher & Schuell Microscience (Dassel, Germany)
Infusion canula (1.20×50-60)	P&W (Berlin, Germany)
Injection cannula (oral gavage)	Roth (Karlsruhe, Germany)
Iris scissors; forceps	Roth (Karlsruhe, Germany)
MACS Columns (MS, LS) & plungers	Miltenyi biotec (Bergisch Gladbach, Germany)
Magnetic stirring bars (20×6 mm)	VWR (Darmstadt, Germany)
Microwell plates (96-well)	Nunc (Wiesbaden, Germany)
Nylon wool fiber	Polysciences (Eppelheim, Germany)
Needles (sterile)	Braun (Melsungen, Germany)
PCR tubes (200 µl) (DNase-free, RNase-free)	Roth (Karlsruhe, Germany)
Pipette tips (with filters) (DNase-free, RNase-free)	Roth (Karlsruhe, Germany)
Plastic Transfer-pipettes	Sarstedt (Nümbrecht, Germany)
Scissors	Roth (Karlsruhe, Germany)
Sterilization filters (0.45 µm, 0.2 µm)	Millipore (Eschborn, Germany)
Stop cock (mini three-way)	neoLab (Heidelberg, Germany)
Surgical disposable scalpels	Braun (Tuttlingen, Germany)
Syringes	Braun (Melsungen, Germany)

2.7. Chemicals and Reagents

2.7.1. Chemicals

All chemical were analytical grade and purchased from Sigma (Deisenhofen, Germany) except the following ones.

Acetic Acid	Fluka (Neu Ulm, Germany)

Agar	BD GmbH (Heidelberg, Germany)
Agarose	Biozym (Hess. Oldendorf, Germany)
Ampicillin	ICN (Eschwege, Germany)
Ammonium chloride	Roth (Karlsruhe, Germany)
Ammonium Sulphate	Roth (Karlsruhe, Germany)
Clorax (commercial bleaching agent)	FLOREAL Haagen (Saarbrücken, Germany)
Dimethyldichlorsilan	Merck (Darmstadt, Germany)
Disodium EDTA	Roth (Karlsruhe, Germany)
Disodium hydrogen phosphate	Roth (Karlsruhe, Germany)
Disodium hydrogen phosphate dihydrate	Roth (Karlsruhe, Germany)
Ethanol (Absolute, 70 %)	Alkopharm (Heilbronn, Germany)
Ethylendiamin-N,N,N',N'-tetra-acid (EDTA)	GERBU (Gaiberg, Germany)
Fetal calf serum (FCS)	Invitrogen (Karlsruhe, Germany)
Formaldehyde (ca. 36 %)	Roth (Karlsruhe, Germany)
Formamide	Fluka (Neu Ulm, Germany)
(D-) Glucose	Merck (Darmstadt, Germany)
L-Glutamine	Invitrogen (Karlsruhe, Germany)
Glycerol	Roth (Karlsruhe, Germany)
Glycerin (for Fluoresence microscopy)	Merck (Darmstadt, Germany)
Hanks balanced salt solution (HBSS), Ca^{2+}- and Mg^{2+}-free	Invitrogen (Karlsruhe, Germany)
Histofix	Roth (Karlsruhe, Germany)
Hydrochloric acid (HCl)	Roth (Karlsruhe, Germany)
N-2-Hydroxyethylpiperazin-N'-2-ethansulfonic acid (HEPES)	Invitrogen (Karlsruhe, Germany)
Isopropanol	Fluka (Neu Ulm, Germany)
2-Mercaptoethanol	Roth (Karlsruhe, Germany)
Methanol	Roth (Karlsruhe, Germany)
Penicillin/Streptomycin	Invitrogen (Karlsruhe, Germany)
Peptone	BD GmbH (Heidelberg, Germany)
Percoll™	Amersham Biosciences (Sweden)
Potassium bicarbonate	Merck (Darmstadt, Germany)
Potassium chloride	Fluka (Neu Ulm, Germany)
Potassium dihydrogen phosphate	Merck (Darmstadt, Germany)
RNAlater	Qiagen (Hilden, Germany)

Resins (AG 501-X8 Molecular biology grade)	Bio-Rad (CA, USA)
RPMI-1640 medium	Invitrogen (Karlsruhe, Germany)
Sodium bicarbonate	Merck (Darmstadt, Germany)
Sodium chloride	Fluka (Neu Ulm, Germany)
Sodium dihydrogen phosphate	Roth (Karlsruhe, Germany)
Sodium pyruvate	Invitrogen (Karlsruhe, Germany)
Sulphuric acid (H_2SO_4)	Merck (Darmstadt, Germany)
Trichlorethan	Merck (Darmstadt, Germany)
Tris	Roth (Karlsruhe, Germany)
Trypan blue	Serva (Heidelberg, Germany)
Trypton	BD GmbH (Heidelberg, Germany)
Yeast extract	BD GmbH (Heidelberg, Germany)

2.7.2. Antibodies

Table 2. Antibodies used in this work.

Name of antibody	Antigen	Application	Source
Rat anti-mouse CD4 FITC labeled; Clone: GK 1.5	Mouse CD4	FACS	BD Pharminogen TM (Germany)
Rat anti-mouse CD8α (Ly-2, Lyt-2), PE labeled Clone: 53-6.7	Mouse CD8α	FACS	BD Pharminogen TM (Germany)
Rat IgG2a, k isotype control PE labeled; Clone: R35-95	Mouse pooled Ig	FACS	BD Pharminogen TM (Germany)
Rat IgG2b, k isotype control FITC labeled; Clone: A95-1	Trinitrophenal (TNP)	FACS	BD Pharminogen TM (Germany)
Rabbit anti-*C parvum* Clone: rb115	*C .parvum* oocyst lysate	IFAT	(Jakobi and Petry, 2006)
Anti-rabbit IgG AlexaFluor488 labeled	Rabbit IgG	IFAT	Molecular probes (USA)
Anti-mouse IFN-γ Clone: XMG1.2	Mouse IFN-γ	*In vivo* Neutralization	(Cherwinski et al., 1987)
Mouse-anti-mouse IL-18	Mouse IL-18	*In vivo*	(Lochner et al.,

Clone: SK113AE-4		Neutralization	2002)

2.7.3. Enzymes

DNase I with buffer (RNase-free)	Qiagen (Hilden, Germany)
HotStar Taq DNA polymerase	Qiagen (Hilden, Germany)
Omniscript Reverse Transcriptase	Qiagen (Hilden, Germany)
Peqlab Taq DNA Polymerase	PeqLab (Erlangen, Germany)
Proteinase K	Qiagen (Hilden, Germany)
Ribobloc Ribonuclease inhibitor	Fermentas (St. Leon-Rot, Germany)
Restriction endonucleases	NEB (Frankfurt, Germany)
BamH I; EcoR I; Hind III; Pst I; Rsa I; Sau3A1; Sty I	
RNase A	Qiagen (Hilden, Germany)

2.8. Media, Buffers and Solutions

2.8.1. Media for bacterial culture

LB (Luria-Bertani)-Medium	1 % (w/v) Trypton, 0.5 % (w/v) yeast extract, 0.5 % – 1 % (w/v) NaCl, pH 7.3 – 7.4

2.8.2. Agarose gel electrophoresis buffer

TBE (10x)	0.89 M Tris, 0.89 M Boric acid, 0.02 M EDTA, pH 8.3
DNA sample buffer (6x)	0.25 % (w/v) Bromophenolblue, 0.25 % (w/v) Xylenecyanol, 30 % (v/v) Glycerin in TE; pH 8.0
MOPS buffer (10x)	200 nM MOPS, 50 mM Sodium acetate (Stock solution: 3 M, pH 6.0), 10 mM EDTA (Stock solution: 0.5 M, pH 8.0)

Sodium phosphate buffer (0.5 M)	0.5 M disodium hydrogen phosphate dehydrate, 0.5 M Sodium dihydrogen phosphate dehydrate, pH 7.0 (1 M HCl/ 1 M Tris)
Glyoxal mix (RNA sample buffer)	56 µl 40 % deionized glyoxal solution, 200 µl DMSO, 8 µl 10 % SDS, 8 µl 0.5 M Sodium phosphate buffer
0.2 M Sodium acetate	Sodium acetate trihydrate, pH 5.15 adjusted with 0.2 M Acetic acid
RNA-sample buffer	7.2 ml Formamide, 1.6 ml MOPS buffer (10x), 2.6 ml Formaldehyde (37 %), 1 ml Glycerin (80 %), 0.8 ml Bromophenolblue (saturated solution), 1.8 ml RNase-free H_2O

2.8.3. Buffers and solutions used for cell isolation

CMF Solution	100 ml 10× Hanks balanced salt solution (HBSS), Ca^{2+}- and Mg^{2+}-free,100 ml 10× HEPES-bicarbonate buffer, 20 ml FCS (2 % FCS), H_2O added to 1 liter and filter sterilized
HEPES-bicarbonate buffer (10×)	23.8 g HEPES (100 mM final), 21 g sodium bicarbonate (250 mM final), H_2O to 1 liter, pH adjusted to 7.2 with HCl
Complete RPMI (10 % FCS)	RPMI-1640 medium, 15 mM (final conc.) HEPES, 2 mM L-glutamine, 100 Units/ml Penicillin, 100 µg/ml Streptomcin, 10 % FCS
Supplemented RPMI 2 % FCS	RPMI-1640 medium, 15 mM (final conc.) HEPES, 2 mM L-glutamine (1 %), 1 % Penicillin-Streptomcin, 2 % FCS
Percoll solutions	
1× stock solution (100 %)	90 ml Percoll and 10 ml of 10× HBSS

44 % Percoll solution	44 ml of 1× stock and 56 ml RPMI 1640
67 % Percoll solution	67 ml of 1× stock and 33 ml RPMI 1640, pH 7.2 with HCl
ACK Erythrocyte lysing buffer	0.15 M Ammonium chloride, 10 mM Potassium bicarbonate, 0.1 mM disodium EDTA, pH 7.2 – 7.4 with 1 N HCl; filter sterilized through 0.2 μm filter

2.8.4. Other buffers and solutions

Phosphate buffered saline (PBS)	10 mM Na_2HPO_4, 10 mM NaH_2PO_4, 150 mM NaCl, pH 7.5; K= 15 mS
PBS-K^+	10 mM Na_2HPO_4, 10 mM KH_2PO_4, 150 mM NaCl, 15 mM KCl, pH 7.5; K= 15 mS
TBS (Tris buffered saline)	50 mM Tris, 150 mM NaCl, pH 7.5
TE (Tris-EDTA buffer)	10 mM Tris pH 8.0, 1 mM EDTA
ELISA buffers	
Coating buffer	8.4 g $NaHCO_3$, 3.56 g Na_2CO_3, deionized water ad to 1L, pH 9.5
Wash buffer	PBS with 0.05 % Tween-20.
Stop solution	2 N H_2SO_4
MACS buffer	PBS, pH 7.2, 0.5 % BSA, 2 mM EDTA
FACS buffer	PBS-K^+ with 0.1 % BSA

3. Methods

3.1. Animal Experiments

3.1.1. Mouse infection protocol with *C. parvum* oocysts

Mice were between 8 and 12 weeks old at the time of primary infection. Age and sex matched groups of 3 – 5 animals were inoculated with 10^6 *C. parvum* oocysts in 100 µL of PBS by oral gavage. A similar number of uninfected mice were used as controls for each set of experiment. The oocyst shedding pattern in both animal models was considered, as previously described (Jakobi and Petry, 2008), in choosing the time points for tissue preparation. Mice were sacrificed on days 1, 3, 8, and 15 post primary infections of GKO mice representing the times of before start, start, peak and resolution of fecal oocyst shedding. For IL-12KO mice the corresponding days were 1, 3, 4, 8, and 15. Day 4 represents the day of peak oocyst shedding in IL-12KO mice. In order to analyze the mechanisms conferring resistance towards infection with *C. parvum*, a secondary challenge was set at 5 weeks (36 days) post primary infection. Mice were sacrificed on arbitrarily selected days, 1, 4, and 15, as no oocyst shedding was detected post challenge infection in both mouse models due to development of resistance (Jakobi and Petry, 2008). Distal ilea, spleen and mesenteric lymph nodes (MLNs) were collected and kept in RNA stabilizing solution (RNAlater, Qiagen, Hilden, Germany) and stored at -70^{o}C until processing for RNA isolation. While collecting ileal segments, Peyer's patches were carefully excised.

For adoptive transfer experiments, the following protocol was applied. About 10 animals to be used as donors were inoculated with 10^6 *C. parvum* oocysts in 100 µl of PBS by oral gavage. Two time points post infection were chosen for each mouse strain to collect cells for adoptive transfer of immunity to naïve recipients: the peak of infection and the resolution of infection. Each experiment, i.e. adoptive transfer from a given time point p.i., was repeated two to four times. A similar number of mice were uninfected and used as control donors.

For each cell type to be transferred, at least four recipient animals were used. Naive recipient mice were injected with a total of 2×10^6 IELs or $CD4^+$ T-cells in a volume of 500 µl at one time at the tail vein. In order to compare the effects of increasing the cell number on the protection of recipients, 4×10^6 IELs were transferred to a group of mice in parallel to mice receiving 2×10^6

IELs. Three days post adoptive cell transfer animals were infected with 10^6 *C. parvum* oocysts in 100 μl of PBS by oral gavage.

3.1.2. Antibody treatments

i) *In vivo* neutralization of mouse-IL-18

The neutralizing mouse anti-mouse IL-18 monoclonal antibody was produced in the hybridoma cell line SK113AE-4 (Lochner et al., 2002) and was purified via protein G affinity chromatography from culture supernatants by FPLC. Groups of 4 age-matched GKO as well as IL-12KO mice were injected intraperitoneally (i.p.) at days -2, 0, 2, 4, and 6 post infection. Two different optimal concentrations were chosen for i.p. injection. IL-12KO mice received 1 mg per injection whereas GKO animals were injected with dose of 2 mg anti-IL-18. *C. parvum* fecal oocyst shedding was monitored as described below. Mice receiving antibody injection as well as untreated animals were sacrificed at day 3, 8, and 15 for GKO and 4, 8, and 15 for IL-12KO mice. An uninfected control group of 4 mice for each strain was sacrificed and cytokine expressions in spleens and distal ilea were analyzed.

ii) *In vivo* neutralization of mouse-IFN-γ

Anti-mouse IFN-γ monoclonal antibody was produced in the hybridoma cell line XMG 1.2 (Cherwinski et al., 1987) and was purified via protein G affinity chromatography from culture supernatants by FPLC. A group of four GKO mice was injected with $CD4^+$ T-cells from wild type mice. One day after cell transfer, recipient GKO mice were treated with anti-IFN-γ antibody (XMG) at days -2, 0, 2, 4, and 6 in reference to the time of infection (day 0); therefore, any IFN-γ secretion by the donor cells would be neutralized and these mice are basically identical to the GKO mice. Another group of four GKO mice was injected with $CD4^+$ T-cells from wild type mice and treated with IgG control at the same days used for XMG to be used as a control group.

3.1.3. Adoptive transfer of immune cells to naive mice

Mice were heated up under laminar flow using an infrared lamp so that the tail veins were engorged with blood and visible to the naked eye. The skin over the vein was disinfected with

alcohol-soaked tissue paper. Cells were well mixed with syringe, and 500 µl (2×10^6 cells) was injected via the tail vein. Mice were fixed in a mouse restrainer for proper handling while injection.

3.1.4. Animal sample collection

3.1.4.1. Tissue samples for RNA isolation

Tissues (intestinal pieces, MLN, spleen) were collected immediately after the mice were euthanized by cervical dislocation under sterile conditions in a laminar flow. The skin was opened and tissues were cut out under sterile conditions using sterile instruments and wearing hand gloves. The intestines were processed by clearing off connective tissue surrounding and by removing the fecal matter from the lumen (by pressing and sliding the tip of forceps over the outer surface of the intestine longitudinally). The connective tissue surrounding the MLN and spleen was also removed before further processing. The fresh tissues were trimmed into pieces using scissors on Petri-plates. The trimmed tissue pieces were immersed into an appropriate volume (approximately 10 µl reagent per 1 mg tissue) of RNA stabilizing solution (RNAlater RNA stabilization reagent, Qiagen, Hilden, Germany) in an Eppendorf tube (2 ml). This solution penetrates tissue pieces by diffusion and stabilizes cellular RNA in freshly harvested samples thus preventing unwanted changes in the gene-expression pattern due to RNA degradation or a new induction of genes. After the completion of tissue collection, stabilized tissues in RNAlater were stored at -70ºC until required for RNA isolation.

3.1.4.2. Tissue samples for genomic DNA isolation

Tissues were removed from mice and processed as described above and immediately frozen in a jar containing liquid nitrogen. Afterwards, they were stored in -70ºC until required for genomic DNA isolation.

3.1.4.3. Fecal sampling

In order to monitor oocyst shedding through feces of infected mice fecal droppings were collected from day 3 to day 10 p.i. daily and in addition on days 12 and 15 p.i. Collected fecal droppings were soaked with Histofix (buffered 4.5 % formaldehyde, Roth) under laminar flow

and stored at 4ºC until further processing. The formaldehyde preserves the oocyts, renders non-infectious limiting the hazard on lab personnel while processing, as well as softens the dried fecal droppings so that they are easily homogenized on later processing.

3.1.4.4. Blood sampling

Blood sample collection was performed at the retro-orbital site as follows. Mice were hand fixed; the skin over the eyeball was pulled away with fingers so that the eyeball is bulging out of the socket. The tip of a glass Pasteur pipette was inserted into the corner of the eye socket underneath the eyeball. Collected blood was transferred to 15 ml tubes and sera were stored at -70°C.

3.2. Microbiological Methods

3.2.1. Culture of *E. coli* cells

Lyophilised *E. coli* cells were reconstituted with 0.5 ml liquid LB medium and well mixed; the mixture was inoculated onto LB agar plate and incubated overnight at 37°C. Fresh colonies were used for transformation with recombinant plasmids. After transformation, *E. coli* cells were grown as above. Sub cloning was done from the overnight culture by transferring single colonies onto separate LB agar plates. The sub clone inoculates were also grown as above.

3.2.2. Long-term storage and recovering of recombinant *E .coli* cells

From an overnight culture in LB broth medium of *E. coli*, 10 ml was centrifuged at 3000 rpm at room temperature for 10 min. The pellet was dissolved with 1 ml of LB broth medium containing 15 % glycerol and dispensed into cryogenic vials. The cryogenic vials were thrown into liquid nitrogen for immediate freezing followed by indefinite storage at -70°C.

When required, *E. coli* were recovered from the glycerol stock by scraping some of the ice with a sterile toothpick and streaking out on LB medium with ampicillin.

3.2.3. Preparation of *C. parvum* oocysts for mouse infection

The stock oocyst suspension was mixed thoroughly by vortexing and the required volume of the suspension was centrifuged at 4000 × g, 4°C for 10 min. The procedure was carried out in a laminar flow and the oocyts were kept on ice to preserve their viability. After centrifugation, the supernatant was discarded to a disinfecting solution, and the oocyst pellet was treated with 1:10 diluted commercial bleach (approx 3.8 % sodium hypochlorite) for 5 min on ice in order to surface sterilize the parasites. Then oocysts were washed three times in sterile PBS, each time by centrifugation for 10 min. Finally, the pellet was dissolved in PBS and a 1:10 dilution was used to determine the number of oocysts in the final preparation, on a differential interference contrast microscope at 400 × magnification. The concentration of oocyst preparation was adjusted to 1×10^6 per 100 µl depending on the total oocyst yield for mice infection. Until required for infection the prepared oocysts were temporarily kept at 4°C.

3.2.4. Determination of *in vitro* oocyst excystation rate (Test for viability)

In vitro excystation to determine the viability of *C. parvum* oocysts was carried out in RPMI medium containing 7.5 % Na-taurocholate, which mimics the *in vivo* gut environment where excystation is achieved by the action of bile salts. After *C. parvum* oocysts were prepared as described above, oocyst pellets were mixed with RPMI medium containing 7.5 % Na-taurocholate in an eppendorf tube and incubated at 37°C in a water bath for 2 h. The tubes were vortexed for proper mixing, and 10 µl of the parasite suspension was used to count in a hemocytometer. Differential counting of excysted oocysts (empty oocyst walls) versus intact oocysts was performed under a differential interference contrast microscope at 400 × magnification. The percent of excystation was calculated as follows:

No of excysted oocysts + partially excysted oocysts / total No of oocysts

Total No of oocysts is the sum of excysted oocysts, partially excysted oocysts and intact oocysts.

Excystation rates of oocysts used for mouse infection were > 80 %.

3.3. Molecular Biological Methods

3.3.1. Preparation and analysis of nucleic acids

3.3.1.1. Total RNA isolation

Total RNA from tissues was isolated according to the procedures outlined in a commercial kit (RNeasy® Protect Mini Kit, Qiagen, Hilden, Germany). The kit applies the selective binding properties of a silica-gel-based membrane with the speed of microspin technology. A high-salt buffer system allows all RNA molecules longer than 200 bases to bind to the RNeasy silica-gel membrane. The procedure provides enrichment for mRNA since most RNAs <200 nucleotides (such as 5.8S rRNA, 5S rRNA, and tRNAs, which together comprise 15 – 20 % of total RNA) are selectively excluded.

About 10 – 15 mg of tissue was weighed and trimmed into very small pieces using sterile blade and plates. Immediately the trimmed tissue pieces were put into lysis buffer (buffer RLT) containing a denaturing guanidine isothiocyanate (GITC) and 1 % β-Mercaptoethanol, which immediately inactivates RNases to ensure isolation of intact RNA. Disruption and homogenization of the tissue in the buffer was carried out using TissueLyser (Qiagen, Hilden, Germany) for 3 min at 24 Hz. The tissue lysate was centrifuged and the supernatant was mixed with equal amount of 70 % ethanol, well mixed, and applied to a mini spin column containing silica-gel-membrane (to facilitate RNA binding). After centrifugation, DNase digestion within the column was carried out using RNase-free DNase I as described by the manufacturer (Qiagen). The column was washed with washing buffer (buffer RW1) before and after DNase treatment. Contaminants were further washed out by using another washing buffer (buffer RPE).
Elution of RNA was carried out using RNase-free water by centrifuging for 1 min. The concentration of the RNA was determined spectrophotometrically and stored at -70ºC in aliquots until required for further processing.

3.3.1.2. Genomic DNA isolation from mouse tissues and cells

Genomic DNA from cells and tissues was isolated according to the procedures outlined in a commercial kit (DNeasy® Tissue Kit, Qiagen, Hilden, Germany). Intraepithelial lymphocytes,

prepared as described on section 3.4.3.1, were centrifuged, and the cell pellet was resuspended in PBS. RNA contamination was avoided by incubating the cells with 4 µl RNase A for 2 min at room temperature.

Cell lysis was achieved by addition of proteinase K and lysis buffer at 70ºC as described by the manufacturer (Qiagen). About 10 – 25 mg of tissues used, i.e. spleen, mesenteric lymph nodes (MLNs) and Peyer's patches (PPs) were trimmed into small pieces and lysed with lysis buffer and proteinase K at 55 ºC. 96 % ethanol was added to the sample and loaded to the spin column to facilitate DNA binding to the silica-gel-membrane. Ethanol carry-over was washed out by centrifugation with successive wash buffers provided with the kit. Finally, DNA was eluted with elution buffer provided in the kit, concentration determined and stored at -70ºC.

3.3.1.3. Plasmid DNA preparation

Purification of plasmid DNA was carried out using the procedures described in a commercial kit (QIAprep® Spin Miniprep Kit, Qiagen, Hilden, Germany). The plasmid miniprep procedure was based on alkaline lysis of bacterial cells followed by adsorption of DNA onto silica in the presence of high salt and elution in low-salt buffer (Qiagen).
A single bacterial colony from a fresh LB plate was inoculated into LB broth medium containing ampicillin, and incubated for 12 □ 16 hrs at 37°C with vigorous shaking.
The bacterial cells were harvested by centrifugation and resuspended in lysis buffer containing RNase A to degrade RNA contaminants. After centrifugation, the supernatants were loaded to a spin column, centrifuged and washed with high salt buffer to facilitate binding of DNA to the silica. Salts were removed by a subsequent wash step. DNA elution was achieved using an elution buffer (10 mM Tris.Cl, pH 8.5). The concentration of the plasmid was measured spectrophotometrically, visualized by agarose gel electrophoresis, and stored at -70°C until required.

3.3.1.4. Extraction of DNA from agarose gel

DNA extraction from agarose gel after electrophoresis was performed using the procedures of a commercial kit (QIAquick® Gel Extraction kit, Qiagen, Hilden, Germany). The principle for DNA purification after agarose gel electrophoresis was based on the spin-column technology and the binding properties of silica-gel membrane according to the manufacturer's instructions

(Qiagen). Accordingly, the specific DNA fragment was excised from agarose gel under UV-illumination with a clean sharp scalpel. The gel was dissolved in lysis buffer by incubating at 50°C for 10 min. After the lysis was completed the pH was adjusted with 3 M sodium acetate to facilitate the adsorption of DNA to the silica-gel membrane, which is efficient only at pH ≤ 7.5. Isopropanol was added to the mixture to increase the yield of DNA fragments < 500 bp which was the case for all of the PCR products used for cloning in this work.
The sample was applied to the spin column and centrifuged for 1 min for DNA binding. The column was washed and DNA was eluted from the column with 50 µl elution buffer, concentration measured spectrophotometrically and stored at -20°C until required.

3.3.1.5. Determination of nucleic acid concentration

For all kinds of nucleic acid preparation (RNA, genomic DNA, plasmid DNA, gel extracted DNA), concentration was determined spectrophotometrically (Nanodrop®ND, PeqLab, Erlangen, Germany) at 260 nm. The nucleic acid preparation was well mixed with sterile pipettes. The buffer or water used for eluting a given nucleic acid preparation was used as blank to adjust the spectrophotometer. Then, 2 µl of the nucleic acid was dropped on the lens of the instrument and concentration (in nanogram per µl) as well as the purity of the preparation (as 260/280 nm ratio) was determined by the spectrophotometer.

3.3.2. Primer design

The Primer3 software (Rozen and Skaletsky, 2000) was used to design primers from murine cytokine gene sequences available in the GenBank database. Criteria used for primer design were annealing temperature of 55 – 65 ºC (similar or close Tm of the two primers); GC content of 40 – 60 % (closer values for both primers); primer length of 20 – 22 bp; amplicon length of 100 – 500 bp (optimally 200 – 300 bp); intron-extron spanning primer sequences so as to avoid possible genomic DNA contaminants from interfering gene quantification. Special consideration was given for the 3' end of the primer to avoid the presence of palindromes, runs of 3 or more G/C, 3' end T, complementarity between the primer pairs.
The primers for IL-12p40 and glyceraldehyde-3-phosphate dehydrogenase (GAPDH) were previously described (Jakobi and Petry, 2008). The primers for IL-23p19 and IL-27EBI3 were also described elsewhere (Sonobe et al., 2005). Primer sequences, optimized annealing temperatures, and the sizes of target PCR products are shown in Table 1.

3.3.3. Reverse transcription polymerase chain reaction (RT-PCR)

3.3.3.1. Reverse transcription

Reverse transcription from isolated RNA to cDNA was performed using a commercial kit (Omniscript® Reverse Transcription Kit, Qiagen, Hilden, Germany). According to the manufacturer, synthesis of cDNA was done by the enzyme Omniscript reverse transcriptase from 2 µg of total RNA and oligo dT primers (Invitrogen, Karlsruhe, Germany) in a reaction volume of 20 µl, incubating at 37°C for 90 minutes. RNA samples were denatured by incubating at 65°C for 5 minutes before the reverse transcription reaction. Any potential RNase degradation of RNA was prevented by adding RNase inhibitor (Ribolock Ribonuclease inhibitor, Fermentas) in the reaction mixture. cDNA synthesis was controlled by amplification of the GAPDH transcript.

3.3.3.2. Polymerase chain reaction (PCR)

PCR was performed on different types of templates (cDNA, plasmid DNA, genomic DNA) as required. Amplification of cDNA templates was done using cytokine specific primers to analyze differential gene expression during *C. parvum* infection.

PCR reactions were carried out using 2 µl of cDNA as a template (1 µl equivalent to 100 ng of total RNA). An optimum number of amplification cycles were performed for each gene target in order to compare among different time points post infection, depending on the abundance of the target in a given tissue. The HotStarTaq polymerase (Qiagen) was activated for 15 min at 95°C. PCR programs consisted of a 1 min denaturing step at 94°C, 1 min annealing at a primer specific annealing temperature (table 1) and 1 min elongation at 72°C. After the last cycle a 10 min elongation step at 72°C was added. A negative control without template was included in every PCR.

The reaction mixture components as well as the reaction parameters used to amplify cytokine genes are presented in tables 3 and 4 respectively.

3.3.3.3. Electrophoresis of nucleic acids

i. Agarose gel electrophoresis for analysis of DNA

Ten µl of each DNA sample (originating from PCR, RT-PCR, colony PCR, plasmid PCR, Real-time PCR) was mixed with 2 µl of 6× DNA loading buffer. Agarose gel electrophoresis was performed in 1× TBE buffer at 10 V/cm using 1.5 – 2 % gels. A 100 bp DNA marker was run in parallel with the samples to determine the size of the DNA samples. Amplification products were stained with ethidium bromide (0.5 µg/ml) after electrophoresis for about 30 minutes, detected with a UV-illuminator and recorded with a digital camera (Kodac documentation and analysis system 120). Further processing of agarose gel images suitable for documentation and presentation was carried out using Adobe Photoshop® software (Adobe Systems Inc). Gel photographs were presented as inverted mode for better presentation of results.

Table 3. Reaction composition used for PCR.

Reagent	Amount to be added (µl)	Final concentration
Template (cDNA) 2µl	-	-
10x Qiagen buffer (plus 15 mM $MgCl_2$)	5	1×
dNTPs 10 mM of each	1	200 µM of each dNTP
FW Primer 20 µM	1	0.4 µM
RV Primer 20 µM	1	0.4 µM
Water, autoclaved	ad 50	-
HotstarTaq-DNA-Polymerase (2.5 units)	0.25	2.5 units/reaction
Total volume	50	-

To improve amplification efficiency the $MgCl_2$ concentration was adjusted to 2.5 mM or Q-solution was added in some PCR assays.

Table 4. PCR cycling conditions applied for amplification of genes of interest.

PCR program	Time	Temperature (°C)	No of PCR cycles*
Activation of polymerase	15 min	95	-
3-step cycling Denaturation Annealing Extension	 1 min 1 1 min	 94 X 72	 . 20 – 35
Final Extension	10 min	72	-
Cooling	-	4	-

* No of PCR cycles were optimized for each cytokine gene primer and performed as indicated on the results section. X= annealing temperature is dependent on the primer pairs and is presented on Table1.

ii. Denaturating agarose gel electrophoresis for analysis of RNA

The integrity of mRNA is an important criterion for subsequent analysis especially for gene expression study by quantitative real-time PCR. Agarose gel electrophoresis of RNA requires the inclusion of denaturing agents in the gel to prevent formation of compact secondary structures, which disturb the relationship between molecular weight and mobility. Two alternative standard methods were used to denature RNA during electrophoresis, both of which produced comparable results.

Formaldehyde agarose gel electrophoresis

A 1 % agarose gel was made by dissolving agarose powder in RNAse-free water (DEPC-treated) in RNase-free flask, and cooled to 55ºC in a water bath. A 1:10 volume of 10×MOPS was added to the cooled gel and incubated for 5 min. The gel was transferred to a chemical fume hood to add 5.4 % of 37 % formaldehyde (v/v), well-mixed and poured to a cleaned casting tray. One µg of RNA samples was mixed with 2 µl of sample loading buffer, filled to 10 µl with DEPC-treated water and incubated at 95ºC for 2 min. One µl of 1:10 diluted ethidium bromide stock solution (10 mg/ml) was added to the sample and loaded on the gel to run in RNAse-free water containing 1/10 volume of 10×MOPS (MOPS buffer) at 5 – 10 V/cm.

Glyoxal agarose gel electrophoresis

Denaturation of RNA using glyoxal was done by mixing 10.8 µl of glyoxal mix (sample buffer) with 1 µg of total RNA filled to 5 µl with RNAse-free water and incubating at 50ºC for 1 hr. Then, the samples were kept on ice, mixed with 3 µl loading dye and loaded to a 1 % agarose gel (prepared using 10 mM Na phosphate buffer). The samples were separated using 10 mM Na phosphate running buffer. Due to the poor buffering capacity of the running buffer regular mixing with syringe from one end to the other of the electrodes was required to keep the pH relatively constant. Higher pH may lead to the separation of the glyoxal molecules from RNA minor groves, leading to the formation of secondary structures that prevent proper running of the RNA samples.

After electrophoresis, the gel was sequentially incubated with shaking in 0.1 M NaOH for 15 minutes, and twice in 0.2 M sodium acetate each for 15 minutes. The gel was stained with Ethidium bromide for 15 minutes and examined under UV-illumination to look for the presence and relative thickness of the 28S and 18S ribosomal RNA bands as an indicator of intact RNAs. Gel documentation was done as described before.

3.3.4. Cloning of gene-specific PCR products

3.3.4.1. Generation of primer specific PCR products

Cytokine PCR products were generated by RT-PCR using total RNA from murine spleen and the primer pairs described in table 1. Each of the specific amplicon was visualized on agarose gel and the band of interest was gel-extracted (Gel extraction kit, Qiagen) to be cloned in pJET1/blunt vector.

3.3.4.2. Ligation with pJET1/blunt cloning vector

pJET1/blunt PCR cloning vector

Cloning of PCR products was performed using pJET1/blunt PCR cloning vector provided in a commercial PCR cloning kit (GeneJET^{TM} PCR Cloning kit, Fermentas, St.Leon-Rot, Germany).

The pJET1/blunt is a linearized blunt-end cloning vector, ready for ligation with blunt or blunted PCR products. The 5'-ends of DNA at the vector cloning site contain phosphoryl groups. Therefore, ligation of a blunt PCR product does not require additional phosphorylation of the PCR product or the use of phosphorylated primers during the PCR reaction. PCR products with 3'–dA overhangs generated using *Taq* DNA polymerase or other non-proofreading thermostable DNA polymerases are blunted with a thermostable DNA bunting enzyme prior to ligation.

Additionally, pJET1/blunt is a positive selection vector. The vector contains the gene for a restriction endonuclease which is lethal for all *E. coli* strains commonly used for cloning. Ligation of a DNA fragment into the cloning site disrupts this lethal gene. As a result, only cells with recombinant plasmids are able to propagate.

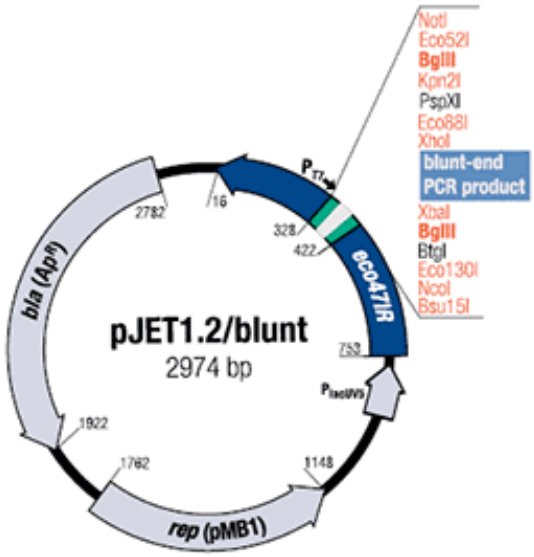

Figure 5. pJET1/blunt cloning vector map. It is a linearized blunt-end cloning vector. It is a positive selection vector; recircularized vector molecules lacking the insert express a lethal restriction endonuclease after transformation, thus *E. coli* cells lacking the insert are not propagated. Unique restriction sites within the multiple cloning site are indicated.

Blunting sticky-end PCR products

PCR products were generated using HotStar Taq DNA polymerase resulting with 3' –dA overhangs. The sticky ends were removed by incubating with DNA blunting enzyme as described by the manufacturer of the kit (Fermentas).

Ligation

Ligation was done in a 20 µl reaction volume by adding 1 µl of vector and 1 µl of T4 DNA ligase to the blunting reaction mixture. The ligation mixture was vortexed briefly and centrifuged for 3 – 5s, then incubated at room temperature (22ºC) for 30 min. Afterwards, the ligation mixture was used directly to transform competent *E. coli* cells.

3.3.4.3. Preparation of competent *E. coli* cells

Competent JM109 *E. coli* cells were prepared based on the procedures outlined by the manufacturer (TansformAidTM Bacterial Transformation kit, Fermentas, St.Leon-Rot, Germany). The bacteria were taken out of storage and inoculated on LB culture plate at 37ºC overnight. Culture tubes containing the TransformAidTM C-medium were pre-warmed at 37ºC. About 4 mm diameter of bacterial culture was inoculated into the C-medium from the overnight LB plate. The tubes were suspended by gently mixing and incubated in a shaker at 37ºC for 2 hrs.

3.3.4.4. Transformation of competent *E. coli* cells

Transformation of the recombinant *E. coli* cells was based on the protocols of the manufacturer (TansformAidTM Bacterial Transformation kit, Fermentas). LB-ampicillin agar plates were pre-warmed in a 37ºC incubator for 20 min. 1.5 ml of fresh culture was spun in a microcentrifuge at maximum speed for 1 min at room temperature. The pelleted cells were resuspended in T-solution, and the tubes were incubated on ice for 5 min. Then, the cells were spinned down for 1 min at room temperature. The pellets were resuspended in T-solution and incubated on ice for 5 min.
For transformation, 2.5 µl of the ligation mixture was mixed with 50 µl of competent *E. coli* cells. The cells were immediately inoculated on pre-warmed LB-ampicillin agar plates, and incubated overnight at 37ºC.

3.3.4.5. Analysis of transformed (recombinant) colonies

i. Colony PCR

The template used for colony PCR was prepared by resuspending a single colony from an agar plate in a 1.5 ml eppendorf tube containing 50 µl of water. The pellet was incubated at 95^{o}C on

a heating block for 10 minutes to lyse the cells, and centrifuged at 12,000 g (~ 9000 rpm) for 1 minute. 5 µl of supernatant was used as a template for PCR, as described in section 3.3.3.2.

ii. Plasmid PCR

The presence of the desired insert in the recombinant plasmid was confirmed by amplification of the insert using specific primer pairs as well as pJET1 vector specific primers (Fermentas, St.Leon-Rot, Germany); FW GCCTGAACACCATATCCATCC; RV, GCAGCTGAGAATATTGTAGGAGATC. When insert specific primes were used, the PCR protocols applied were the same as described in section 3.3.3.2.

iii. Restriction digestion analysis

A single or double enzyme digestion was performed depending on restriction sites available on the insert and availability of the enzymes in the lab. A single enzyme digestion was achieved in a 50 µl reaction volume using 1 Unit restriction enzyme, 1 µg plasmid DNA, 5 µl 10× NEB buffer (1× final concentration) and water. When an enzyme requires BSA for digestion it was added to the buffer at a final concentration of 100 µg/ml for optimal activity from a stock of 10 mg/ml. A double digestion was performed in a 100 µl reaction volume using 1 Unit of each restriction enzyme, 2 µg plasmid DNA, 10 µl NEBuffer and water.

The reaction mix was thoroughly but gently mixed and incubated at 37ºC for 1hr. The digestion was analyzed on 1 – 2 % agarose gel depending on the size of the expected digestion products. Restriction sites available on the insert were identified using the online software NEBcutter V2.0 (tools.neb.com/NEBcutter2/index.php). The compatible enzymes and the appropriate reaction buffers required in a double digestion were determined by NEB double digest finder (www.neb.com/nebecomm/DoubleDigestCalculator.asp). Accordingly, IL-4, IL-12p40, IL-12p35, IL-27EBI3 inserts were digested with RsaI. IFN-γ, IL-23p19, IL-5, TNF-α, IL-10 and GAPDH inserts were digested with PstI, BamHI, StyI, EcoRI, EcoRI and HindIII respectively. Double digestion of the IL-18 insert in the plasmid vector was performed with Sau3A1 and Rsa1.

3.3.5. Designing external standard curves

The procedures applied in preparing standard curves for quantitative PCR are as described in the technical notes of Roche LightCycler (Roche, 2003). External standards are amplified during the same run as the unknowns, but in separate reaction glass capillaries. Data obtained from the standards are used to plot a standard curve of crossing point (Cp) versus log concentration. The standard curve is the linear regression line through the data points on a plot of cycle number (crossing point or Cp) versus logarithm of standard sample concentration.
Based on the recombinant plasmid concentrations determined spectrophotometrically the corresponding copy numbers were calculated using the formula:
No. of copies/µl = 6×10^{23} (copies/mol) × plasmid concentration (g/µl) ÷ no. of base pairs (plasmid + insert) × 660 g/mol.

Ten-fold serial dilutions of the plasmid constructs were used as external standards to design standard curves. The LightCycler software provides two analysis algorithms for generating a standard curve. The automatic Second Derivative Maximum method was chosen for all quantifications in this work. The software performs all calculation steps necessary for generation of a standard curve; determines the crossing points of unknown samples and displays the concentrations of the unknowns (calculated from the curve). The determined concentrations of the unknown samples is the absolute amount of cytokine mRNA copy numbers in RNA preparations and expressed as number of RNA copies per 100 or 200 ng of RNA. Based on the performance of the cDNA synthesis kit, 1 µl of cDNA template is equivalent to 100 ng of total RNA.

3.3.6. Quantitative Real-time PCR

3.3.6.1. Assay design

Quantitative PCR of cytokine mRNAs was performed on LightCycler version 1.5 (Roche) by using LightCycler FastStart DNA Master and Master^{PLUS} SYBR Green I master mixes (Roche, Mannheim, Germany) and murine cytokine primer pairs (Table 1). Both kinds of SYBR Green I mixes are ready-to-use reaction mixes designed for real-time PCR assays using the SYBR Green I detection format on LightCycler systems. They are used to perform hot-start PCR in 20 µl glass capillaries using FastStart Taq DNA Polymerase which is a chemically modified form

of thermostable recombinant Taq DNA polymerase that shows no activity up to 75°C. Hot-start PCR has been shown to significantly improve the specificity and sensitivity of PCR (Chou et al., 1992; Kellogg et al., 1994; Birch, 1996) by minimizing the formation of non-specific amplification products at the beginning of the reaction. The enzyme is active only at high temperatures, where primers no longer bind non-specifically, and becomes completely activated in a single pre-incubation step (95°C, 10 minutes) before cycling begins.

Generation of PCR products was detected by measurement of the SYBR Green I fluorescence signal (at 530 nm). SYBR Green I is a DNA double helix-intercalating dye which has an enhanced fluorescence upon DNA binding. In a PCR reaction, the increase in fluorescence is directly proportional to the amount of double-stranded DNA generated. During elongation step of PCR dye molecules bind to the newly synthesized DNA; fluorescence measurement at the end of the elongation step of every PCR cycle is performed to monitor the increasing amount of amplified DNA.

When Master^{PLUS} SYBR Green I was used, reactions were set up in microcapillary tubes with a total volume of 20 µl using the following final concentrations: 0.5 µM of each primer, 4 µl of 5× SYBR Green mix (SYBR Green I dye, reaction buffer, dNTP mix, $MgCl_2$), and 2 µl of cDNA. For some primer pairs Master SYBR Green I was used to optimize further the $MgCl_2$ concentration; the reaction mixture was prepared from final concentrations of 0.5 µM of each primer, 2 µl of 1× SYBR Green mix (SYBR Green I dye, reaction buffer, dNTP mix, 10mM $MgCl_2$), 4 mM of $MgCl_2$, and 2 µl of cDNA. The capillaries were sealed with stoppers. The capillaries, contained in centrifuge adapters were centrifuged in a bench top microcentrifuge rotor (Biofuge) briefly at 700 × g (3000 rpm) for 5s; then the samples were cycled in LightCycler 1.5.

3.3.6.2. Standard PCR protocol

The enzyme mixes were applied to design a hot-start PCR protocol composed of 4 cycle programs as shown on table 5A: pre-incubation for activation of the polymerase and denaturation of the template; amplification of the target template; a melting curve for PCR product identification and cooling the rotor and thermal chamber.
After an initial denaturation step (95°C for 10 min), cycling conditions were as follows: denaturing (95°C for 10 s), annealing (at primer specific temperature for 4 s) and elongation

(72°C for 15 – 20 s). Amplification was repeated 40 times with a single fluorescence measurement at the end of the 72°C step. At the end of amplification a melting curve was generated (65°C with a heating rate of 0.1°C/s and a continuous fluorescence measurement) and a cooling step to 40°C was carried out.

3.3.6.3. Modified PCR protocol

In some assays, a modified PCR protocol was applied, where a product specific melting temperature was included immediately after extension and before fluorescence acquisition (Table 5B) so as to avoid the effect of primer dimer formation which may interfere with the fluorescence acquisition from the specific product. Such quantification strategy has been described by Ball *et al*. (2003).

Table 5A. Standard PCR protocol.

Cycle program	Analysis mode	Segment	Target Temp. (°C)	Incubation time	Fluorescence acquisition mode
1. Pre-incubation Cycles:1	None		95	10 min	None
2 Amplification Cycles:35-40	Quantification	Denaturation Annealing Extension	95 **60** 72	10s **4s** **20s**	None None **Single**
3. Melting Curve	Melting curve	Denaturation Annealing Melting	95 65 95	0s 15s 0s	None None **Continuous**
4 Cooling	none	Cooling	40	30s	none

Table 5B. Modified PCR protocol.

2 Amplification Cycles:35-40	Quantification	Denaturation	95 °C	10s	None
		Annealing	60 °C	4s	None
		Extension	72 °C	20s	None
		Melting of primer dimers	X °C	5s	**Single**

X= the temperature used for melting of primer dimers depends on the specific gene PCR product and experimentally determined from the melting curve analysis. The value of x equals 85°C for IL-4; 83°C IL-5; 84°C IL-10; 89°C IL-13; 81°C IL-18; 82°C IFN-γ.

3.3.6.4. Quantification analysis

Fluorescence data acquisitions and data analyses were performed with LightCycler Data Analysis Software version 3.5 (Roche). At the end of every reaction the software displayed amplification curves represented by fluorescence values versus cycle number. Additionally, the standard curve and its parameters (Cp, slope and error) used for quantification were displayed. The calculated value of the standard curve as well as that of the unknown samples was displayed both as Cp values as well as number of copies. Using the applications of the software, all the relevant data were exported to a Microsoft EXCEL sheet to calculate mean of copies, SD and also to present the data as bar graphs if necessary.

When a standard curve designed in one experiment was used to quantify successive cDNA samples in separate runs, the software provides the possibility of using one reference sample quantified together with the standard curve and included during the later reactions. The original standard curve was imported to the desired experiment as external standard curve and used to quantify the unknown samples.

All samples were assayed in duplicates, and the mean of the quantifications was expressed as number of mRNA copies per 100 or 200 ng RNA.

3.3.6.5. Melting curve analysis

Specificity of the amplified PCR product was assessed by performing a melting curve analysis provided by the software. For this, the reaction mixture was slowly heated to 95°C, which causes melting of double-stranded DNA and a corresponding decrease of SYBR Green I fluorescence. The fluorescence decrease was continuously monitored and displayed by the

instrument as melting peaks. Each melting peak represents the characteristic melting temperature (TM) of a particular DNA product. These melting peaks were used to discriminate between primer-dimers or non-specific products and specific product; the specific product melted at a higher temperature than the primer-dimers. Additionally, this method was applied to exclude the interference of non-specific products with lower melting temperatures than the specific products. The melting curve analysis procedure was also applied to identify the melting points of specific products in order to perform the modified PCR protocol.

3.4. Immunological Methods

3.4.1. Oocyst detection by immunofluorescence test (IFT)

The fecal droppings soaked in formaldehyde solution were homogenized using plastic Pasteur pipette and a vortexer in a laminar flow. After centrifugation for 10 min at 16 000 × g, 4°C on a table top centrifuge, the supernatants were discarded (and disinfected); the pellets were mixed with an equal volume of 1×PBS and stored at 4 – 8°C or processed immediately. Fecal suspensions were homogenized with pipette tips further diluted 1:5 in PBS and 5 µl aliquots were placed in duplicates on poly L-lysine coated slides (Adcell, Roth, Karlsruhe, Germany) to facilitate adherence of the oocysts to the glass slides. After air-drying (for about 1 hr in laminar flow) and methanol fixation (by placing in a chemical fume hood for 10 min) slides were incubated for 1 h with a 1:500 dilution of anti-*C. parvum*-oocyst rabbit serum (rb115) (primary antibody) at room temperature, which has been generated in the lab using standard immunization protocols (Jakobi, 2006). During antibody incubation, drying of the slides was prevented by placing in a rack containing moistened tissue paper and covered. After two washes, each for 5 min, in PBS with shaking, the slides were incubated with a 1:250 dilution (with PBS having 1 % BSA) of the secondary antibody (goat-anti-rabbit IgG-AlexaFluor 488; Molecular Probes, Invitrogen) for 1 h in a wet and dark rack. This was followed by two washes as above, but in a dark condition to prevent bleaching of the labelling dye.

The slides were then covered with drops of glycerol, and with 24×60 mm cover slips. Air bubbles formed between the cover slide and the slide were removed using forceps. The slides were placed in dark till the cover slip is well-adhered to the slide and the edges of the slides were sealed with nail varnish to prevent drying out of the glycerol. The slides were dried in dark and examined under fluorescence microscope for oocyst detection using the oil immersion

objective. Oocyst counting was performed by screening 50 optical fields (×1000) from each of the duplicate spots and expressed as number of oocysts in 100 high power optical fields.

3.4.2. Enzyme Linked Immunosorbent Assay (ELISA)

Serum protein concentrations of the cytokines IL-18 and IFN-γ were quantified using commercial ELISA kits, mouse IL-18 ELISA kit was from MBL (Kyoto, Japan) and mouse IFN-γ ELISA kit was from Biolegend (San Diego, CA, USA). The detection limits of the kits were 25 pg/ml for IL-18 and 30 pg/ml for IFN-γ.
Three to 5 mice of both strains were bled at days -3, 4, 7, and 14 p.i. and sera were stored at -70°C. Each serum sample was diluted with assay diluent.

The mouse IL-18 ELISA kit measures mouse IL-18 by sandwich ELISA using two monoclonal antibodies against two different epitopes of mouse IL-18. Samples were added to mouse IL-18 antibody coated micro-wells and incubated for 60 min at room temperature. The well contents were discarded, and washed with wash solution 4 times. The wells were incubated with the conjugate solution (Peroxidase conjugate anti-mouse IL-18 monoclonal antibody) for 1 hr at room temperature, followed by washing with washing buffer. The wells were incubated with the substrate reagent (TMB/H_2O_2) for 30 min at room temperature. The reaction was stopped by adding stop solution (2 N H_2SO_4), and the absorbance of wells was read at 450 nm. The mean absorbance of each standard was calculated to construct a standard curve. The IL-18 concentration of samples was calculated by multiplying the value read from the standard curve by the dilution factor. Serial dilutions of recombinant proteins served as standard curves. Initial screening was performed with serum pools from 3 to 5 mice. From positive pools individual sera were tested.

IFN-γ ELISA was done using the same principle following the manufacturer's instructions. The mouse IFN-γ kit (ELISA MAX^{TM} Set Standard) (Biolegend, San Diego, CA, USA) contains mouse IFN-γ specific capture antibody; biotinnylated detection antibody; recombinant mouse IFN-γ standard; avidin horseradish peroxidase (Av-HRP).

3.4.3. Separation of mouse lymphocytes for adoptive transfer

This methodology was applied in order to address the possibility of protecting naive mice using T-lymphocytes isolated from mice at different time points post *C. parvum* infection. We hypothesized that T-lymphocytes from mice recovered from primary infection, i.e. at day 15 in our experimental models, should transfer protective immunity to naive mice recipients. Additionally, we selected the peak of infection in both mice models, i.e. day 5 in IL-12KO and day 8 in GKO mice, as a possible time point when resistance could be transferred through T-lymphocytes. Therefore, we isolated T-lymphocytes at the peak of infection as well as after resolution of the primary infection in both mice models.

Total T-lymphocyte population ($CD4^+$ and $CD8^+$) as well as only the $CD4^+$ T-lymphocyte population were isolated from the site of infection (intestine), the local lymph nodes draining the intestine (Mesenteric lymph nodes, MLN) and also the systemic immune tissue (spleen).

3.4.3.1. Isolation of mouse intestinal intraepithelial lymphocytes (IELs)

The methodology applied for isolation of lymphocytes located between intestinal epithelial cells is based on Davies *et al*. (1981) and Lefrancois and Lycke (2003). Accordingly, the procedure was carried out as follows:

i. Removal and cleaning of mouse small intestine

Mice were euthanized; the small intestines were removed (0.5 cm below stomach) and placed in Petri dishes containing cold (4^oC) RPMI 1640. The guts were washed twice with cold (4^oC) CMF (See 2.8.3) using a 20 ml syringe fitted with a short infusion cannula. About 40 ml cold CMF was used to clean the intestine from one mouse. The cleaned intestine was placed on CMF-moistened Petri dishes. Fat, connective tissue, blood vessels and Peyer's patches were removed carefully and as completely as possible from the surface of the intestine. Then, the intestine was opened longitudinally and cut laterally into ~0.5 cm pieces.

ii. Preparation of cell suspensions

The intestinal pieces were washed by placing in 50 ml conical tubes with 40 ml 4°C CMF. The tubes were inverted several times so as to facilitate removal of mucus and associated fecal

matter. The intestinal pieces were allowed to settle and the supernatant was poured off or aspirated with plastic Pasteur pipette. The procedure was repeated three or more times until the supernatants were relatively clear.
The washed gut pieces were poured into a sterilized 50 ml siliconised flask with 20 ml supplemented RPMI/2 % FCS (See 2.8.3). (Flasks were treated with 2 % solution of dimethyldichlorsilan in Trichlorethan (v/v) under a chemical fume hood; a Teflon-coated magnetic stir-bar was inserted into each flask; the flasks were covered with aluminium foil and autoclaved before the day of IEL isolation).

The flask was covered with aluminium foil and incubated on magnetic stirrer at a speed of 350 rpm for 30 minutes at 37°C. Afterwards, the gut pieces with the solution were transferred to 50 ml centrifuge tubes and shaken vigorously with vortex for 15 sec at maximum setting. The gut pieces were allowed to settle and the supernatant was transferred to another 50 ml conical tube. The tube with the supernatant was kept on ice. Another 20 ml RPMI/2 % FCS was added to the remaining intestinal pieces; the above procedures were repeated three times and the supernatants obtained by these three collections were combined.

The combined supernatant was filtered through sterile pieces of gauze; the filtered debris was discarded; whereas the filtrate (cell suspension) containing the IEL and some epithelial cells were kept on ice.

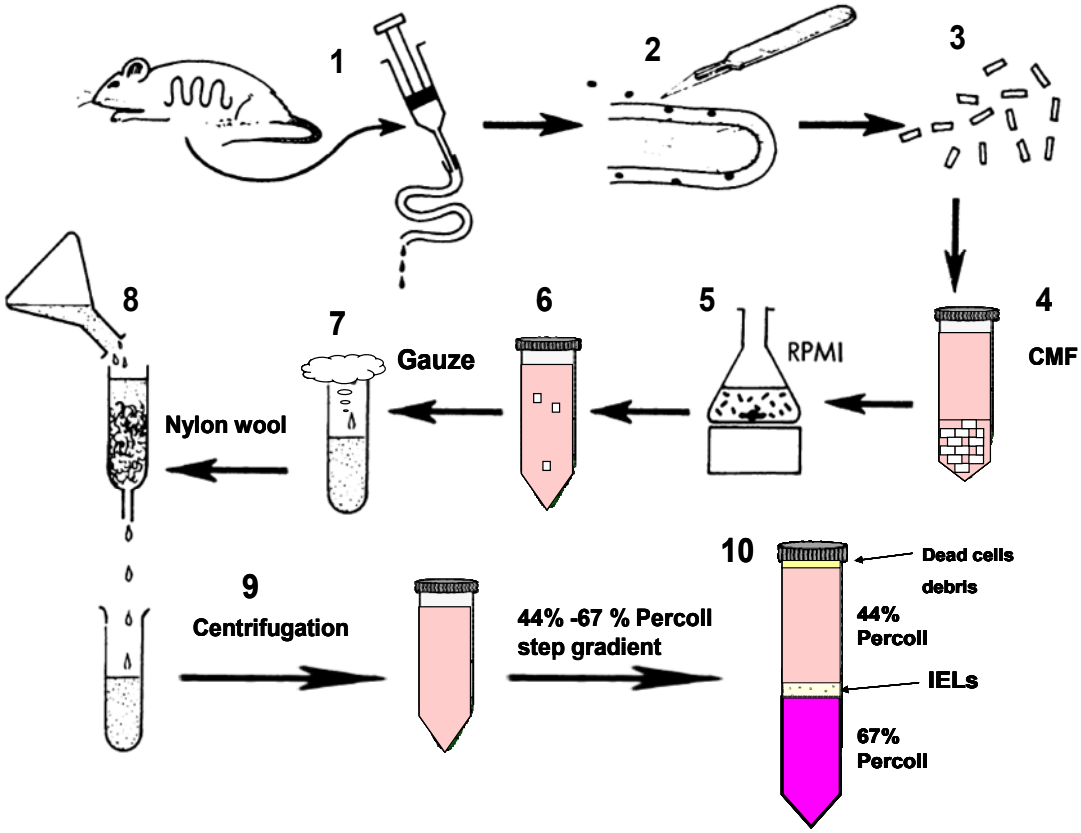

Figure 6. Isolation of intestinal intraepithelial lymphocytes (IELs) from mouse small intestine. Modified from Davies et al. (1981) (1) Small intestines were removed from animals; thoroughly washed with cold CMF (4°C) using a 20 ml syringe fitted with a short cannula. (2) All Peyer's patches, blood vessels, fat, and mesentery were completely removed. (3) The intestines were opened longitudinally; cut laterally into small pieces (0.5 – 1 cm). (4) The pieces were well washed in CMF in a 50 ml flask. (5) The pieces were incubated in RPMI/2 % FCS with magnetic stirring (at 350 rpm) for 30 minues at 37°C to release IELs mechanically. (6) The supernatants from three times stirring were combined together and put on ice. (7) The supernatant was filtered over gauze. (8) The filtrate was further filtered through Nylon wool column clamped to a ring stand. (9) The IEL enriched eluate from the Nylon wool was centrifuged for 5 min at 400 × g. (10) The cell pellets were resuspended in 44 % Percoll and centrifuged in 44 % – 67 % Percoll step gradients; the IELs were aspirated from the interface between 44 % and 67 % Percoll layers. The figure is modified from Davies et al. (1981).

iii. Nylon wool filtration (T-cell enrichment)

This step was applied for T-cell enrichment of the gauze-filtered supernatant while adherent cells (such as B-cells adhere to the nylon wool), as well as for removal of dead cells or debris from the suspension. Nylon wool column was prepared as follows. About 300 mg of nylon wool fiber was weighed in a chemical fume hood; the fibers were straightened and loosened with gloved hand and packed into a 10 ml sterile syringe from which the plunger was removed.

Then, nylon wool syringe columns were put in a glass beaker, covered with aluminium foil and sterilized by autoclaving.

A sterilized nylon wool column (in a 10 ml syringe) was clamped to a ring stand. A stopcock (or, 0.45×12 mm sterile needle) was placed on Luer tip of the syringe. This step and all subsequent steps were performed in a laminar flow to maintain sterility.

The column was equilibrated by running 10 to 20 ml of 4°C (or, ice cold) RPMI/10 % FCS (See 2.8.3) through the column. Trapped air bubbles were removed by firmly tapping on the sides of the column until no white (dry) areas were visible. Finally, the nylon wool was tamped down with a sterile pipette to compact the nylon and extrude any additional trapped air. The stopcock was opened (or needle was removed) to drain the medium from the column.

The gauze-filtered cell suspension was passed through the nylon wool column and allowed to drain completely. Immediately, the column was washed with an additional 20 ml 4°C RPMI 1640/10 % FCS to ensure that all cells penetrate the column. The entire volume of eluate was collected in a 50 ml conical centrifuge tube.

The eluate from the nylon wool was centrifuged for 5 min at 400 × *g* (Minifuge GL Heraeus), 4°C. The cell pellets were resuspended in 24 ml room temperature 44 % Percoll.

iv. Isolation of IEL by Percoll gradient centrifugation

IELs were isolated from the interface of 44 % – 67 % Percoll gradients assembled as follows.
Three 15 ml falcon tubes were precoated with FCS. 5 ml of 67 % Percoll was added to each gradient tube. Then, 8 ml of the 44 % Percoll/cell suspension from the above step was slowly filled on the side of each tube taking care not to mix the two gradient solutions. When performed correctly, one can easily distinguish the lower 67 % Percoll from the 44 % Percoll layer that floats above.
The gradients were centrifuged for 20 min at 600 × *g* (~1600 rpm in Beckman centrifuge) at room temperature. The top half of gradient was aspirated to within <2 cm of the interface. The interface (IELs) between the bottom and upper Percoll layers was harvested with a plastic Pasteur pipet. The harvested cells were diluted 1:3 with 4°C RPMI 1640/10 % FCS and centrifuged for 5 min at 400 × *g*, 4°C.

v. Assessment of purified IELs

The viability of cells was measured by trypan blue exclusion; cell numbers were estimated by counting in a hemocytometer. The purity of IELs was assessed by staining preparations of cells with FITC-coupled-anti-CD4, and PE-coupled-anti-CD8, in parallel with their isotype controls; the proportion of $CD4^+$ and $CD8^+$ T-cells is measured by FACS to determine indirectly the approximate percentage of T-cells in the IEL preparation.

3.4.3.2. Separation of mouse spleen and MLN lymphocytes

i. Preparation of spleen and MLN cell suspensions

Freshly isolated spleen and MLNs were placed in Petri dish containing (4^oC) RPMI 1640. Splenocytes were flushed out of the covering capsule with the medium through a syringe fitted to a sterile needle. MLNs were pressed through a 40 μm Nylon cell strainer in a circular motion with the plunger of a 5 ml syringe until mostly fibrous tissue remained. The cell suspension was centrifuged for 10 min in Sorvall H-1000B rotor at 960 rpm (200 × *g*). MLN cell pellets were resuspended in 20 ml RPMI 1640/10 % FCS, centrifuged again, and resuspended in a volume suitable for counting. Spleen cell pellets were continued with red blood cells (RBC) lysis.

ii. Removal of red blood cells (RBCs) from spleen cell suspensions

Spleen cell pellets were resuspended in ~5 ml ACK RBC lysing buffer (See 2.8.4) per spleen in a 12 ml test tube and incubated 5 min at room temperature with occasional shaking.
The cells were washed by adding medium to fill the tube and spinning for 10 min at 200 × *g* in a low-speed centrifuge. The supernatant was discarded. The cell pellets were washed twice by adding RPMI 1640/10 % FCS and spinning for 10 min at 200 × *g*. Cell clumps formed after RBC lysis were filtered by passing the cell suspension through a 40 μm Nylon cell strainer. The pellet was resuspended in appropriate volume of the medium to determine cell number.

3.4.3.3. Magnetic-activated cell sorting (MACS) of mouse lymphocytes

Isolation of $CD4^+$ T-lymphocytes and total (pan) T-lymphocytes from spleen and MLN cell suspensions by MACS technology was carried out using the reagents and equipment as described by the manufacturer (Miltenyi Biotec, Bergisch Gladbach, Germany)

i. Separation of spleen and MLN $CD4^+$ T-lymphocytes

The principle of $CD4^+$ T-lymphocyte isolation using MACS procedure was as follows. $CD4^+$ T-cells are magnetically labeled with anti-CD4 (L3T4) microbeads (extremely small, supermagnetic particles). Then, the cell suspension was loaded onto a MACS® column which was placed in the magnetic field of a MACS Separator. The magnetically labeled $CD4^+$ T-cells are retained on the column which contains a matrix that generates a strong magnetic field when placed in a MACS separator. The unlabeled cell fraction (depleted of $CD4^+$ T-cells) runs through. After removal of the column from the magnetic field, the magnetically retained $CD4^+$ T-cells can be eluted as the positively selected cell fraction (Figure 7 and 8).

A. Magnetic labeling

The cell suspension prepared as above was centrifuged at 300 × g for 10 minutes, and the supernatant was pipetted off completely. The cell pellet was resuspended in 90 µl of buffer per 10^7 total cells; 10 µl of CD4 (L3T4) microbeads [anti-mouse-CD4 antibodies (L3T4, clone GK1.5] conjugated to microbeads was added per 10^7 total cells. It was mixed well and incubated for 15 minutes at 4 – 8°C.

Afterwards, the cells were washed by adding 1 – 2 ml of buffer per 10^7 cells and centrifuged at 300 × g for 10 minutes. The supernatant was pipetted off completely. Up to 10^8 cells were resuspended in 500 µl of buffer.

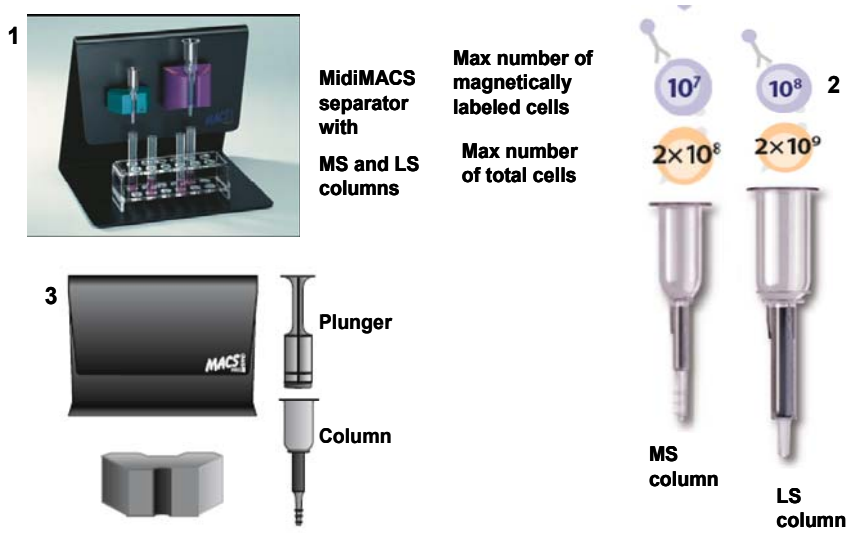

Figure 7. The apparatus applied in MACS technology: MACS columns and separators used for MACS separation of lymphocytes. (1) Magnets attached to MS and LS columns placed on a MidiMACS separator. Effluents from the columns were collected in the test tubes placed on the rack. (2) MS and LS columns contain a magnetic matrix (grey) to bind magnetically labeled cells. (3) Cells bound to the magnetic matrix of the column are flushed out by applying a plunger through the column.

B. Magnetic separation

An appropriate MACS column (MS or LS) and MACS separator (MiniMACS, MidiMACS) was chosen according to the number of total cells used and the number of $CD4^+$ T-cells required (Figure 7). Magnetic separation with MS or LS columns was done as follows:

The capacity of MS column is 10^7 labeled cells and was used by placing the column in the magnetic field of MiniMACS separator. The capacity of the LS column is 10^8 labeled cells and was used by placing the column in the magnetic field of MidiMACS separator.In both cases, the column was prepared by rinsing with the appropriate amount of buffer. The cell suspension was applied to the column. Unlabeled cells which pass through were collected and the column was washed three times with appropriate amount of buffer. The column was removed from the separator and placed on a suitable collection tube. Appropriate amount of buffer was pipetted onto the column; the magnetically labeled cells were flushed out immediately by firmly applying the plunger supplied with the column. To increase the purity of the magnetically labeled fraction ($CD4^+$ T-cells), the fraction from the first column was passed over a second, freshly prepared column.

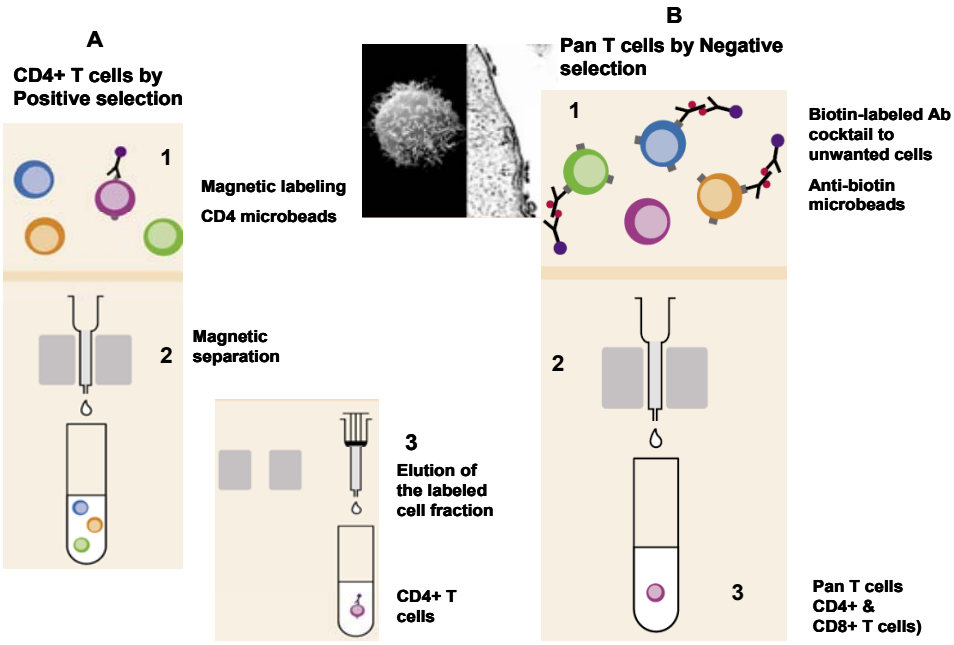

Figure 8. The principles of lymphocyte separation in a MACS technology.

(A) Positive selection of $CD4^+$ T-cells. Cells are labeled with CD4 microbeads (1), passed through a MACS separation column (2) which traps $CD4^+$ T-cells selectively while the non $CD4^+$ T-cells pass through. $CD4^+$ T-cells are eluted by forcing with plunger (3). (B) Negative selection of pan T-cells. Cells are incubated with antibody (Ab) cocktails to label non T-cells (1), passed through a MACS separation column (2) which traps non T cells. Pan T-cells are collected as flow through (3).

ii. Isolation of spleen and MLN pan T-lymphocytes

The principle of Pan T-cell separation was based on negative selection (depletion of non T-cells) using the procedures of the manufacturer (Pan T-Cell Isolation kit, Miltenyi biotec, Bergisch Gladbach, Germany). Non T-cells are indirectly magnetically labeled with a cocktail of biotin-conjugated monoclonal antibodies, as primary labeling agent, and anti-biotin monoclonal antibodies conjugated to microbeads, as secondary labeling agent. The magnetically labeled non T-cells are depleted by retaining them on a MACS column in the magnetic field of a MACS separator, while the unlabeled T-cells pass through the column.

The cell suspension prepared as described earlier was counted and spun down by centrifugation at 300 × g for 10 minutes.

A. Magnetic labeling

The cell pellet was resuspended in 40 µl of buffer per 10^7 total cells. 10 µl of biotin-antibody cocktail [(biotin-conjugated anti-CD11b (Mac-19 (rat IgG2b), CD45R (B220) (rat igG21), DX5 (rat IgM) and Ter-119 (rat IGG2b)] was added per 10^7 total cells, well mixed and incubated for 10 minutes at 4 – 8ºC. 30 µl of buffer and 20 µl of anti-biotin microbeads (microbeads conjugated to anti-biotin antibody, clone Bio3-18E7.2 mouse IgG1) were added per 10^7 total cells. It was well mixed and incubated for additional 15 minutes at 4 – 8 ºC. Cells were washed with buffer by adding 10 – 20 × labeling volume and centrifuged at 300 × g for 10 minutes. The supernatant was pipetted off completely. The cell pellet was resuspended in 500 µl of buffer per 10^8 total cells.

B. Magnetic separation with MS and LS columns

A column was placed in the magnetic field of a suitable MACS separator, MS column for up to 10^7 magnetically labeled cells. The column was prepared by rinsing with the buffer. The cell suspension was applied in a suitable amount of buffer onto the column. The cells were allowed to pass through and the effluent collected as fraction with unlabeled cells, representing the enriched T-cell fraction. The entire effluent was collected in the same tube as effluent of T-cells.

3.4.3.4. Flow Cytometry (FACS)

About 2 $\times 10^5$ cells (IELs, spleen or MLN lymphocytes) were resuspended in 100 µl PBS K^+ buffer with 0.1 % BSA. IELs were incubated with 5 µl of FITC-rat anti mouse-CD4 and 5 µl of PE-rat anti mouse-CD8 antibodies. In parallel, the isotype control antibodies, FITC-Rat IgG2b and PE-Rat IgG2a, were mixed with a similar amount of cells to control the non-specific fluorescence from the FITC and PE dyes. The mixture of cells and antibodies, in a glass tube, was incubated at 4ºC for 20 min. Then, 100 µl PBS with 0.1 % BSA was added to the mixture, centrifuged for 5 min at 1100 rpm in a Beckman centrifuge. Afterwards, the supernatant was decanted and the remaining small pellet (invisible to naked eye) was vortexed. 500 µl PBS was added to the pellet; the tube was wrapped in aluminium foil and used for FACS analysis or incubated at 4ºC overnight. Identical results were obtained even after three days incubation at 4 ºC.

The phenotypic population of CD4+ and CD8+ T-cells in IEL preparation was determined by acquiring 10,000 events on a Beckmann Coulter Epics XL-MCLTM flow cytometer version 3.0 (Beckman Coulter, Krefeld, Germany) and analyzed using EXPO 32 ADC software version 1.1.C (Beckman Coulter, Krefeld, Germany).

3.4.3.5. Homing of transferred lymphocytes to recipient mouse tissues

In order to determine the time required for transferred cells to home to immunologically relevant tissues (gut, MLN, PPs and spleen), with respect to *C. parvum* infection, a PCR assay was developed. This was achieved by using male mice as donors and female mice as recipients so that the male chromosome (Y) specific gene *tdy* was amplified from the recipient mice tissues by PCR. 2×10^6 cells from male donor mice were transferred via i.v. to female mice recipients; after three days genomic DNA was prepared from IELs, PP, MLN and spleen of recipient mice. Ten fold serial dilutions of a PCR product amplified from Chromosome Y was used to compare the relative abundance of homed male cells in the different tissues of female mice by comparing the band intensity of the PCR product after agarose gel electrophoresis.

3.5. Software, data banks and web-based programs

Adobe Photoshop®CS2 Version 9.0.2	Adobe Systems Inc (California, USA)
ExpoTM32 ADC Software	Beckman CoulterTM (Krefeld, Germany)
Kodak Digital Science 1D software	Kodak
Lightcycler®software version 3.5	Roche (Mannheim, Germany)

NCBI: http://www.ncbi.nlm.nih.gov/blast/ (Online public)
NEBcutter V2.0 (online) (tools.neb.com/NEBcutter2/index.php)
NEB double digest finder (online) (www.neb.com/nebecomm/DoubleDigestCalculator.asp
Primer3 software (Online) (Rozen and Skaletsky, 2000)

3.6. Statistical Analysis

For comparison of the oocyst shedding and the antibody titers statistical analyses were performed by using a paired Student's test. $P < 0.05$ was regarded significant.

III. RESULTS

4. Dynamics of Th1/Th2 cytokines in interferon-gamma and interleukin-12p40 KO mice during primary and challenge *Cryptosporidium parvum* infections

The complete understanding of the immune response to *C. parvum* has been generally hindered by the lack of adult immunocompetent animal infection model, forcing researchers to use neonatal or immunocompromised mice. It is further complicated by the differences in the experimental setup such as the mouse strains and parasite isolates used by different workers leading to variation in the interpretation of the data. The present study attempted to address these problems by using two adult mouse immunodeficient models, i.e., C57BL/6 interferon-γ KO (GKO) and C57BL/6 interleukin-12 KO (IL-12KO) mice in parallel as well as adult immunocompetent mice (C57BL/6 wild type) thus results from one model may complement those deficient in the other. Thus, the involvement of IFN-γ independent factors in the resolution of infection could be addressed in adult GKO mice.

These mouse models have been established in the laboratory (Jakobi and Petry, 2008) (Figure 9A). Both mice were susceptible to *C. parvum* infection as shown by shedding of *C. parvum* oocysts in the feces starting from day 3 p.i.; however, they have different patterns of infection though both of them resolve the infection within two weeks p.i. On the contrary, the immunocompetent wild type mice were not susceptible to infection as indicated by very few or negligible oocyst shed upon infection.

The difference in susceptibility between these three mouse models with different phenotypes of immunocompetence was appealing to study the factors for differences in susceptibility, as well as the factors that resolve the infection from the host immune response point of view. Therefore, the first objective of the work was to study the cytokines induced in vivo at key time points during the patent infection of *C. parvum* in the gut mucosal (intestine and mesenteric lymph nodes, MLN) as well as in systemic (spleen) immune compartments.

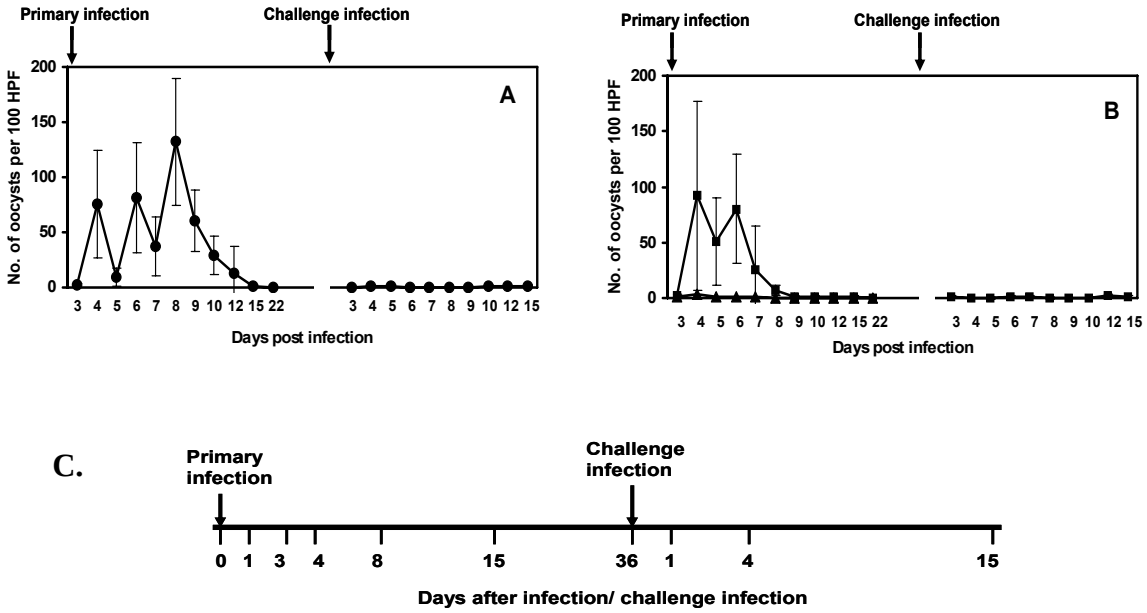

Figure 9. Experimental animal models (A and B) and infection protocol (C) applied to study gene expression of cytokines during *C. parvum* infection.

Parasite shedding from mice after infection with 10^6 *C. parvum* oocysts. Mice were re-challenged 5 weeks (36 days) after primary infection. GKO mice (A, ●); IL-12KO (B, ■) and C57BL/6 wild-type mice (B, ▲). Error bars represent SDs of the means of six (GKO) and four (IL-12KO) different experiments (Jakobi and Petry, 2008). (C) After primary infection of mice with 10^6 *C. parvum* oocysts, tissue samples (ileum, MLN and spleen) were collected at days 1, 3, 4, 8, 15 and 36 p.i.; as well as, at days 1, 4 and 15 post challenge infection.

4.1. Gene expression of Th1 and Th2 cytokines in the gut mucosa during a patent primary *C. parvum* infection

We studied the expression of Th1 (IFN-γ, TNF-α, IL-18, IL-12p40, IL-12p35, IL-27EBI3, and IL-23p19) and Th2 (IL-4, IL-5, IL-10 and IL-13) cytokine mRNA species during primary *C. parvum* infection. As indicated on figure 9, the following important time points of the patent infection were considered in order to analyze changes of gene expression patterns: day 3 (start of oocyst shedding), day 4/5 (peak of oocyst shedding in IL-12KO mice), day 8 (peak of oocyst shedding in GKO mice), day 15 (resolution of oocyst shedding), and day 36 (time before challenge infection). We applied conventional RT-PCR to study the mRNA expression pattern across time points during infection. The results from infected mice were compared with uninfected control mice.

Accordingly, we showed that the expression patterns of both Th1 and Th2 cytokines follow the oocyst shedding pattern in GKO mice as shown in figure 10A. As shown by band

intensities on the agarose gel, the mRNA levels of IL-4, IL-10, TNFα, and IL-18 did not differ from the uninfected controls at the start of oocyst shedding (day 3); however, the expression of IL-13 was slightly lower on day 3 compared to uninfected controls. Maximum levels were reached at the peak of infection (day 8), and finally fall down to basal levels after resolution of oocyst shedding (day 15). There were no differences in the gene expression of GAPDH between uninfected control mice and infected mice, demonstrating equal quality of the RNA preparation and efficiency of cDNA synthesis.

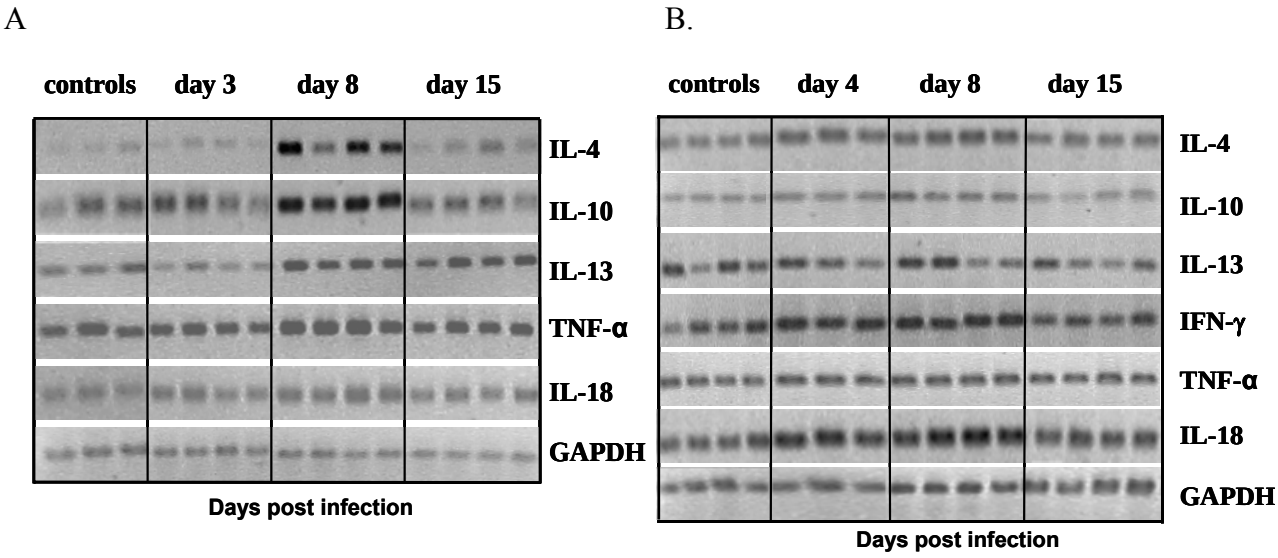

Figure 10. RT-PCR amplification of Th1 and Th2 cytokine mRNA species in the distal ilea of *C. parvum* infected GKO (A) and IL-12KO (B) mice.

Total RNA was extracted from the distal ilea of mice sacrificed 3 or 4, 8, and 15 days post infection and analyzed as described in materials and methods. The integrity of mRNA and cDNA synthesis was controlled by the amplification of the GAPDH transcript. For GKO mice, amplification cycles were 29, 24, 34, 31, 35 and 20 for TNF-α, IL-18, IL-4, IL-10, IL-13 and GAPDH, respectively. For IL-12KO mice, we used 31, 24, 30, 34, 32, 35 and 25 cycles for TNF-α, IL-18, IFN-γ, IL-4, IL-10 and GAPDH, respectively. The data demonstrate results of individual mice and are representative for three independent experiments.

Note:- the RT-PCR analyses from the IL-12KO mice (B) were carried out in part by Schwamb B. (2008) when she was a diploma student under my supervision.

In IL-12KO mice the mRNA expression levels of both Th1 and Th2 cytokines did not follow the oocyst shedding pattern (Figure 10B). The peak of gene expression was not at the peak of infection (day 4/5), rather the expression continued to rise to peak levels at day 8, when oocyst shedding was dramatically reduced. Similar to that of GKO mice, the mRNA levels fell to basal levels after the resolution of infection (day 15).

We could not observe any differential gene expression of IL-12p40 and IL-12p35 in GKO mice; in addition, no changes were recorded in IL-5, IL-27EBI3, and IL-23p19 gene expression in both GKO and IL-12KO mice during infection (not shown).

However, using conventional RT-PCR we could only observe the trends of up regulation or down regulation of mRNA species. Therefore, quantification of changes in gene expression was highly required. The expression patterns observed by RT-PCR were used as a starting point to further confirm the differential gene expression between uninfected controls and infected animals at different time points post infection using quantitative real-time RT-PCR.

4.2. Quantitative real-time RT-PCR assay design

Determination of the absolute mRNA copy numbers of cytokine genes was performed by quantitative real-time RT-PCR on LightCycler version1.5. The procedures followed and the results obtained while designing protocols for absolute quantification of cytokine mRNAs are described as follows.

4.2.1. Cloning of PCR products and analysis of transformants

The PCR products of each cytokine gene were inserted into the multiple cloning site of pJET1/blunt vector; the recombinant plasmid DNA produced was used to transform competent JM109 *E. coli* cells. pJET1/blunt is a positive selection vector; therefore, only bacterial cells transformed by recombinant plasmid vectors grow on agar plates. Bacterial cells taking up the re-circularized vector will be killed as described by the manufacturer. However, further confirmation of grown *E. coli* colonies transformed by each cytokine gene inserts was performed by standard procedures step-wise.

Colony PCR was used to confirm the presence of cytokine gene containing plasmids in grown bacterial colonies. Figure 11A shows the amplification products of TNF-α from four single colonies transformed by TNF-α recombinant plasmids. Such confirmed single colonies were subcultured and plasmid DNA was isolated. Plasmid PCR was used to amplify the insert genes using insert specific as well as plasmid specific primers. Figure 11B presented PCR products of IFN-γ, TNF-α and IL-12p35 amplified from plasmid DNA preparations made from single colonies containing the respective genes.

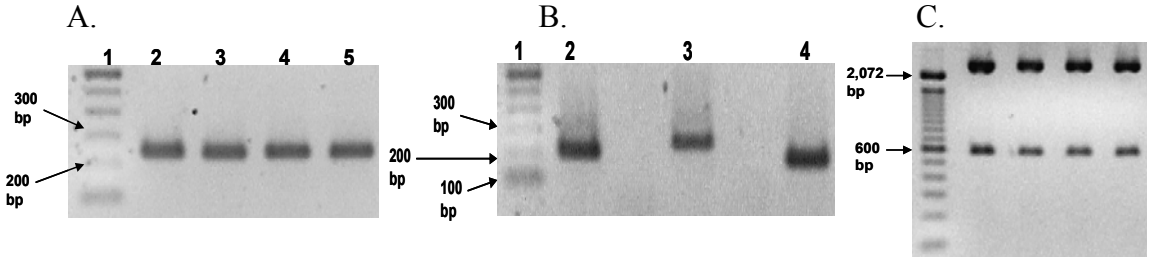

Figure 11. Analytical methods used to identify *E. coli* colonies transformed with recombinant plasmids containing cytokine gene inserts.

Competent JM109 *E. coli* strains were transformed with pJET1/blunt plasmid vectors ligated with PCR products of cytokine genes and grown overnight at 37°C. (A) Colony PCR was used to amplify TNF-α gene insert from DNA extractions of four single colonies picked from an over night culture. (B) Plasmid PCR was applied to amplify IFN-γ (Lane 2), TNF-α (Lane 3), and IL-12p35 (Lane 4) gene inserts from recombinant plasmids prepared from transformed single *E. coli* colonies. (C) Restriction digestion was performed to cut restriction sites on an insert and the plasmid. Plasmid preparations from four IFN-γ-transformed bacterial colonies were digested with PstI which produces two, 577 and 2762 bp, restriction fragments. Lane 1= 100 bp DNA marker.

Furthermore, final confirmation of the presence of the desired inserts in the transformed *E. coli* colonies was carried out using restriction digestion analysis of recombinant plasmid DNA preparations obtained from four single colonies for each insert gene. For example, digestion of IFN-γ recombinant plasmid DNAs with the restriction enzyme PstI for 1 hr at 37°C produced restriction digests of 577 and 2761 bp, as predicted from the DNA sequence (Figure 11C).

4.2.2. Designing external standard curves

Following the confirmation of recombinant plasmids containing inserts of cytokine genes, for each cytokine gene studied an external standard curve was designed using ten-fold serial dilutions of the recombinant plasmid. From the measured concentrations of plasmid DNA, the copy numbers of the serial dilutions were determined and used as the bases for the determination of the copy numbers of the cytokine gene expression in unknown samples.

As shown on figure 12D, 10-fold serial dilutions of recombinant plasmids, in this case TNF-α recombinant plasmids, from 10^2 to 10^7 copy numbers were amplified in a LightCycler together with the unknown samples. Both the plasmid standards as well as the samples were run in duplicates. The known concentrations of the plasmids were used by the Second Derivative Maximum method of LightCycler software to design a standard curve of crossing

points (CPs) versus log concentration (Figure 12E). As shown on the figure the standard curve is the linear regression line through the data points on a plot of cycle number (crossing point) versus logarithm of standard sample concentration.

A.

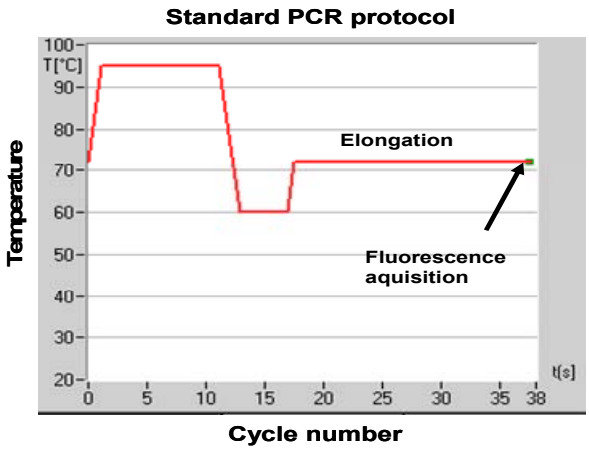

B.

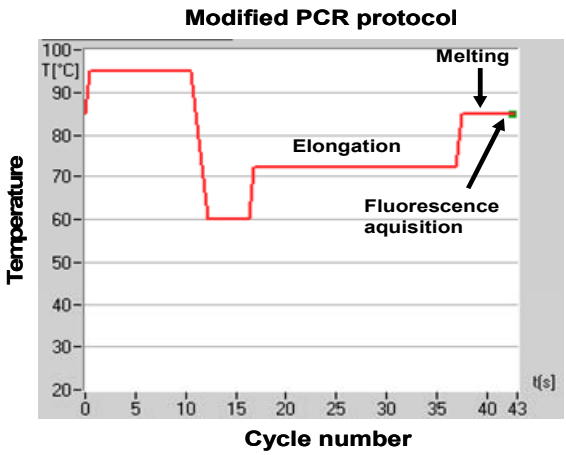

C.

1	2	3	4	5	6
	Pos...	Name	Standard	Calculate...	Crossi...
	1	pTNFa 10E7	2.500E+07	2.318E+07	14.82
	2	Repli. of pTNFa 10E7	2.500E+07	2.211E+07	14.89
	3	pTNFa 10E6	2.500E+06	2.879E+06	18.08
	4	Repli. of pTNFa 10E6	2.500E+06	2.884E+06	18.08
	5	pTNFa 10E5	2.500E+05	2.726E+05	21.78
	6	Repli. of pTNFa 10E5	2.500E+05	3.099E+05	21.58
	7	pTNFa 10E4	2.500E+04	2.428E+04	25.57
	8	Repli. of pTNFa 10E4	2.500E+04	2.421E+04	25.57
	9	pTNFa 10E3	2.500E+03	1.521E+03	29.91
	10	Repli. of pTNFa 10E3	2.500E+03	1.628E+03	29.80
	11	pTNFa 10E2	2.500E+02	4.469E+02	31.83
	12	Repli. of pTNFa 10E2	2.500E+02	2.549E+02	32.71
	13	III GKO control pool		9.125E+03	27.10
	14	Repli. of III GKO control		9.303E+03	27.07
	15	IIIA GKOday1 pool		6.616E+03	27.60
	16	Repli. of IIIA GKOday1 po		6.279E+03	27.69
	17	IIIA GKOday3 pool		9.983E+03	26.96
	18	Repli. of IIIA GKOday3 po		8.481E+03	27.22
	19	IIIA GKOday5 pool		6.087E+03	27.74
	20	Repli. of IIIA GKOday5 po		5.806E+03	27.81
	21	IIIB GKOday1 pool		3.677E+03	28.53
	22	Repli. of IIIB GKOday1 po		3.462E+03	28.62
	23	IIIB GKOday3 pool		6.283E+03	27.69
	24	Repli. of IIIB GKOday3 po		7.217E+03	27.47
	25	IIIB GKOday5 pool		8.992E+03	27.12
	26	Repli. of IIIB GKOday5 po		9.350E+03	27.06
	27	Negative control		<3.118E+01	>36.00

D.

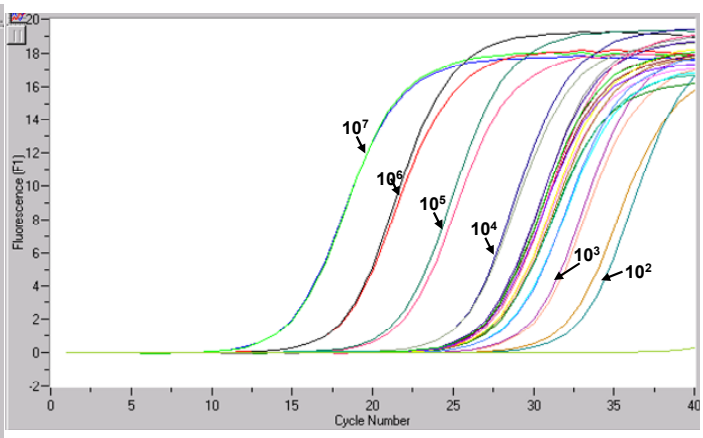

E.

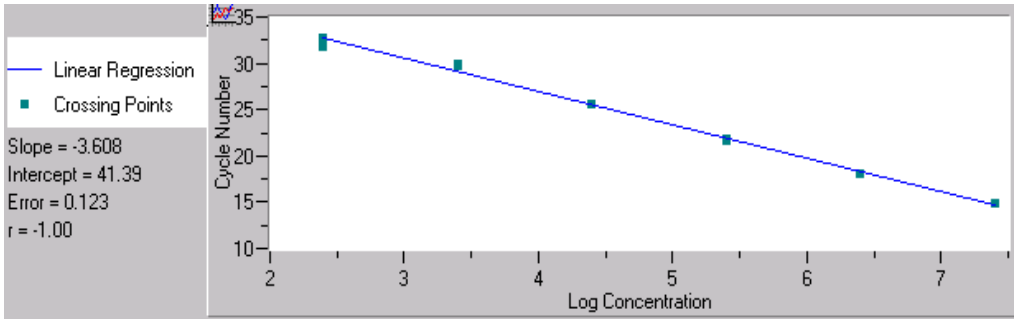

Figure 12. Quantitative PCR protocols and design of external standard curve on LightCycler.

(A) Standard PCR temperature profile (B) modified PCR temperature profile (C). For each run the quantitative analysis window of the LightCycler software displays color designation of the sample curve (1), location of the sample slot (2), sample name (3), known (4) as well as calculated (5) concentration of the standard plasmid dilutions, crossing points (6). (D) The amplification curves were displayed as fluorescence (Y-axis) and cycle number (X-axis) graph. 10^2 to 10^7 copies of the standards (D) were used to design a standard curve (E) which was used for determination of sample copy numbers (C) by the software. The standards as well as the unknown samples were run in duplicates.

4.2.3. Quantification and melting curve analysis on LightCycler

Two PCR protocols were applied depending on the specificity of the PCR reaction. In a standard PCR protocol, the SYBR Green fluorescence from amplification products accumulated at the end of every PCR cycle was measured at the end of the elongation step (72°C) of each cycle of a given PCR run (Figure 12A). Such quantification protocol was used for primer pairs that did not produce primer dimers or unspecific amplification products that could interfere with the fluorescence acquisition from the specific amplification product of the primers. The application of a modified PCR protocol was required in an attempt to quantify specific amplification products that were also accompanied by primer dimers and unspecific PCR products, since SYBR Green binds to any double stranded DNA. To avoid this primer dimers and unspecific products with melting temperatures lower than that of the specific products were melted at temperatures higher than 72°C immediately after the elongation step before fluorescence measurement from the accumulated specific product (Figure 12B). The melting temperature used was chosen after determining the melting temperature of the specific product experimentally for each cytokine gene quantified on modified PCR protocol.

To demonstrate this, two examples are given. TNF-α was among the cytokines quantified based on the standard PCR protocol. Figure 13A shows the melting curve and melting peak of

TNF-α PCR products without any primer dimers and unspecific products present. IL-4 was one of the cytokines quantified based on modified PCR protocol. Figure 13B depicted the melting peak of IL-4 PCR product (87°C) which was higher than that of unspecific bands at 84°C and primer dimers at 75°C.
Therefore, during the fluorescence acquisition step of IL-4 quantification, the PCR mixture was melted at 85°C which was high enough to melt the lower peaks but low enough to allow measurement of fluorescence from IL-4 products.

Designing of standard curves as well as calculation of unknown samples was carried out by the LightCycler software. However, after each LightCycler run, melting curve analysis was performed using the software. The analysis was an important step of quantification in order to confirm that the calculated values were based on the specific melting peaks of the desired gene depending on the protocol applied. In cases where aberrant melting curves and peaks appeared during the analysis, the reaction was repeated to solve the problem.

As a final verification step, PCR products after each light cycler run were electrophoresed on 2 % agarose gel to check the specificity of the reaction and correct size of the product (Figure 13C).

4.3. Quantitative real-time PCR analysis of Th1/Th2 cytokine gene expression changes during primary *C. parvum* infection

Using quantitative real-time RT-PCR protocols explained above, the expression patterns of both Th1 and Th2 cytokines shown on figure 10A were further confirmed to follow the oocyst shedding pattern in GKO mice as shown in figure 14A. At the start of oocyst shedding (day 3) the mRNA levels of IL-4, IL-10, IL-13, TNF-α, and IL-18 were low, comparable to the levels determined in uninfected control animals. Maximum levels were found at the peak of infection (day 8).

In IL-12KO mice, as already stated, the mRNA expression levels of both Th1 and Th2 cytokines did not follow the oocyst shedding pattern. Consequently, the peak of gene expression was not at the peak of infection, rather the expression continued to rise to peak levels at day 8 (Figure 14B). However, the peak IFN-γ mRNA level at day 8 p.i. in IL-12KO

mice (6730 copies/100 ng RNA) reached the same level as in the uninfected wild type mice (6425 copies/100 ng RNA).

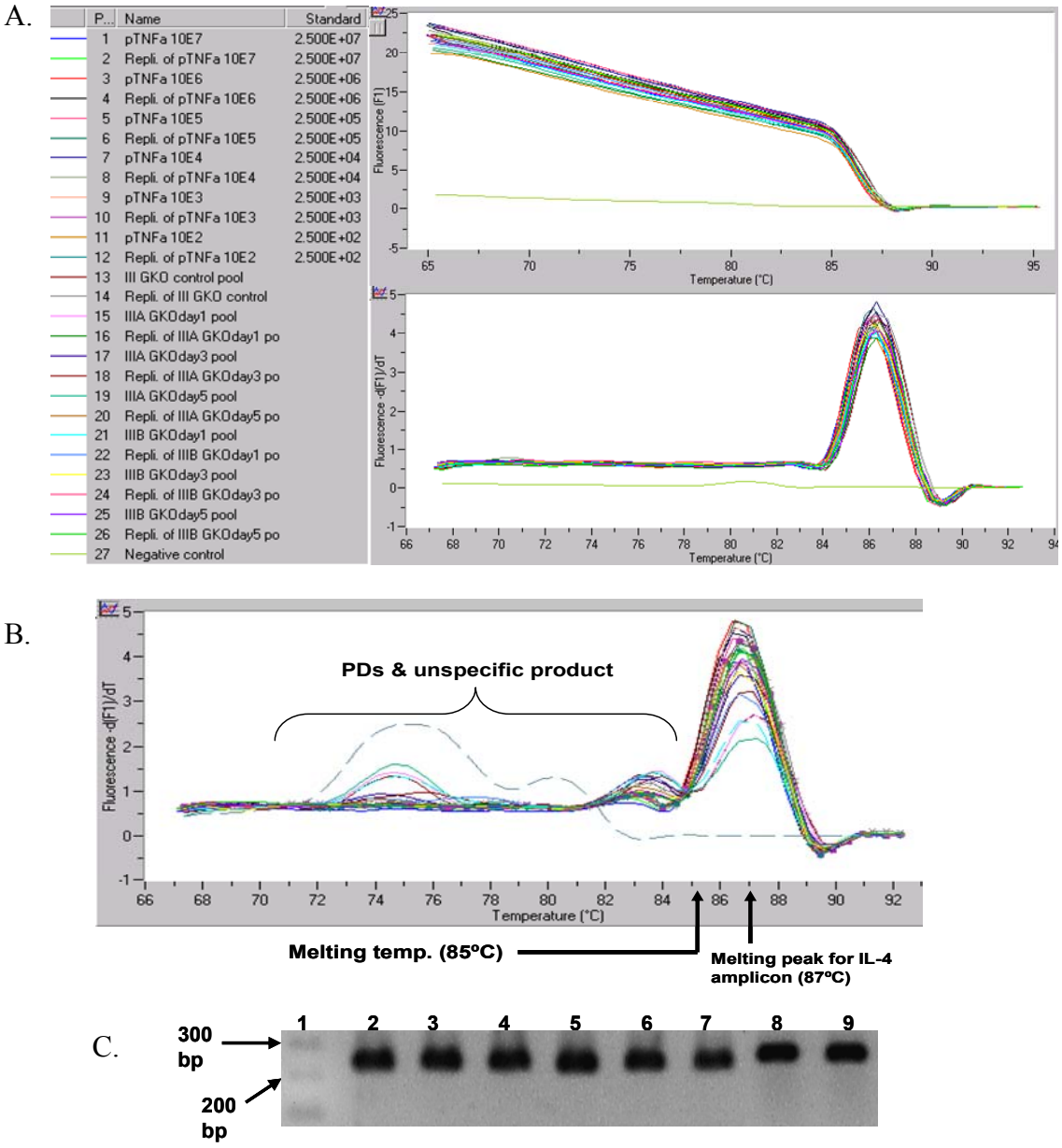

Figure 13. Melting curve analysis of PCR amplifications on LightCycler.

Melting curve analysis was applied to confirm the specificity of the PCR reaction. (A) A standard PCR protocol was applied to quantify genes where there was no interference of primer dimers and unspecifife PCR products. The melting curve and melting peak presented in this figure are from the amplification of TNF-α after a run of 40 cycles. (B) A modified PCR protocol was applied to avoid the interference of SYBR Green fluorescence from primer dimers (PDs) and unspecific products, for quantification of IL-4 amplicon which has a melting peak of 87°C. (C) The PCR reaction was run on a 2 % agarose gel to confirm the size of the specific PCR product; in this case TNF-α (248 bp product). Lane 1= 100 bp marker; lanes 2, 3, 4, 5, 6 and 7 represent 10^7, 10^6, 10^5, 10^4, 10^3, and 10^2 copies of TNF-α recombinant plasmid; lane 8 = IL-12KO Ileum day 1 p.i. cDNA; lane 9= IL-12KO Ileum day 3 p.i. cDNA.

4.4. IFN-γ plays a role during early time of infection

A previous study has shown an early induction of IFN-γ gene expression in response to *C. parvum* infection in the ileum of 3 weeks old C57BL/6 wild type mice before the onset of adaptive immunity (Leav et al., 2005). A similar role for IFN-γ in the absence of the major inducer, IL-12, has not been described yet. Therefore, we studied the possible role of IFN-γ in innate immunity in IL-12 deficient mice in order to find out the involvement of other IFN-γ inducers at this early stage. We observed that the mRNA copies of IFN-γ expression in uninfected IL-12KO mice (1×10^3 copies/ 100 ng RNA) were reduced by about 6 times as compared to wild type mice (6.43×10^3 copies/ 100 ng RNA). In addition, we showed that the mRNA expression of IFN-γ in IL-12KO mice was up-regulated within 24 hrs p.i. (Figure 14B) to the same level as in wild type mice (Table 6). The mRNA level of IFN-γ continued to rise in infected IL-12KO mice whereas there was a sharp decrease after day 1 in wild type mice (not shown).

The importance of IFN-γ during the early period of infection was further supported by the differences in oocyst shedding pattern between GKO and IL-12KO mice (Jakobi and Petry, 2008). As shown in figure 9A, IL-12KO mice resolve the infection much earlier than GKO mice. The severity of the infection in GKO mice could be due to the lack of IFN-γ response during the early time point. Further more; there were no changes in any of cytokine genes during the early period of infection in GKO mice, as shown on figure 14A. Therefore, the reduced susceptibility to infection during the early period could be attributed to the response of IFN-γ.

4.5. TNF-α may have a regulatory role for the early IFN-γ response

In order to identify further inducers of IFN-γ, other than IL-12, at this early stage, we quantified mRNAs of IL-18, TNF-α, and IL-4, which could play potential inducer roles. It was found that the mRNA expression of IL-18 started to rise later than that of IFN-γ, i.e., from day 3 onwards as shown in figure 14B. Another potential inducer of IFN-γ, TNF-α, was up-regulated in parallel with IFN-γ (Figure 14B). However, there were slightly reduced level in TNF-α mRNA at this early time in GKO mice, where there is no intact IFN-γ gene

expression (Figure 14A). Similar to IL-18, the expression of IL-4 mRNA started to rise at day 3, later than IFN-γ, ruling out its possible role as IFN-γ inducer at this early stage.

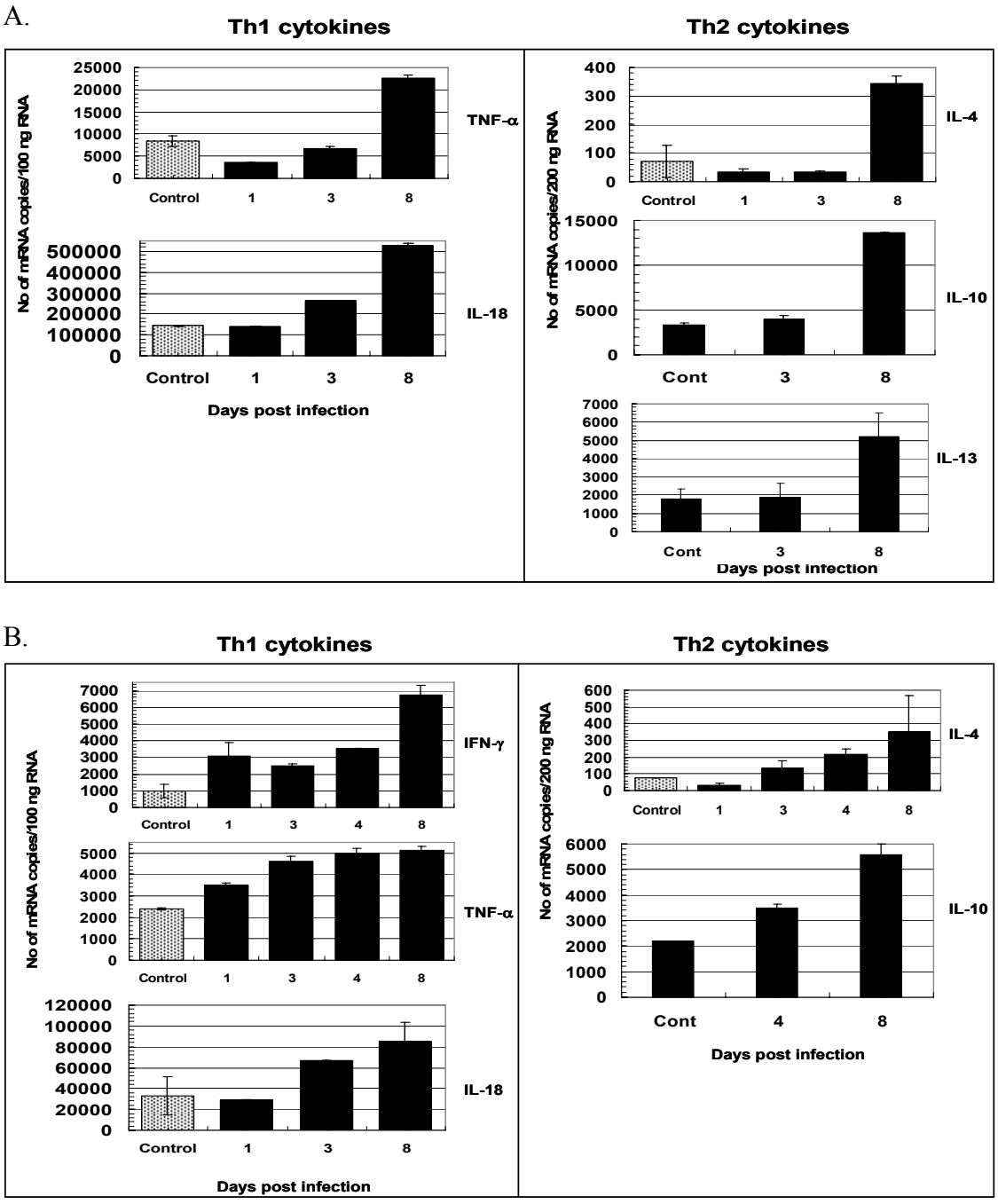

Figure 14. Quantitative real time RT-PCR analysis of Th1 and Th2 cytokine mRNA kinetics in the distal ilea of GKO (A) and IL-12KO (B) mice infected with *C. parvum*.

Total RNA was extracted from the distal ilea of mice sacrificed 1, 3, (4), and 8 days post infection. Absolute mRNA copy numbers were determined using a standard curve as described in materials and methods. The data is presented as number of mRNA copies per 100 or 200 ng RNA (1 µl cDNA being equivalent to 0.1 µg RNA) used for quantitative RT-PCR. Differences between uninfected controls and different time points post infection were compared directly. Error bars represent standard deviation.

4.6. Differential Th1 cytokine responses among mouse models

Generally, comparing cytokine mRNA levels among the mouse models we studied, infected as well as uninfected IL-12KO mice have reduced Th1 cytokine levels compared to wild type or GKO mice (Table 6). Uninfected GKO mice have only slightly higher levels of TNF-α and IL-18 than wild type mice but mount increased mRNA levels 8 days post infection. GKO mice mounted a strong Th1-type cytokine gene expression which was up-regulated with infection at levels higher than wild type mice (Table 6).

Table 6. Differential Th1 mRNA responses between GKO, IL-12KO and wild type mice infected with *C. parvum*.

Gene	Uninfected Controls	Wild type Peak p.i. day 1	Uninfected Controls	IFN-γ KO peak p.i. day 8	Uninfected Controls	IL-12KO peak p.i. day 8
TNF-α	7.01×10^3	7.97×10^3	8.4×10^3	22.5×10^3	2.4×10^3	5×10^3
IL-18	111×10^3	125×10^3	144×10^3	526×10^3	3.3×10^3	85.3×10^3
IFN-γ	6.43×10^3	11.5×10^3			1×10^3	6.73×10^3

Numbers represent mRNA copy numbers per 100 ng RNA, calculated as the mean of duplicate measurements from a cDNA sample.

4.7. Expression of Th1 and Th2 cytokines during primary infection in mesenteric lymph nodes (MLNs) and systemic lymphoid tissue (spleen) in GKO and IL-12 KO mice

Unlike that of the intestine, we did not see dramatic changes in cytokine mRNA levels in the MLNs of *C. parvum* infected GKO mice (Figure 15A and B). Overall, a similar picture was observed in the spleen (Figure 15C and D). However, an increase in expression of IL-4 in the spleen of GKO mice (at day 3 p.i.) was quantified (Figure 21A). There was a trend of increase in the expression of IL-13 mRNA in the spleen upon infection compared to uninfected GKO mice (Figure 15C), although there was variability in the band intensities among infected animals. In the spleen of IL-12KO mice increases in IL-4 and IL-13 at day 8 p.i. were

detected (Figure 15D and Figure 21B). In figure 21, IL-4 was analyzed quantitatively; whereas IL-13 was analyzed qualitatively.

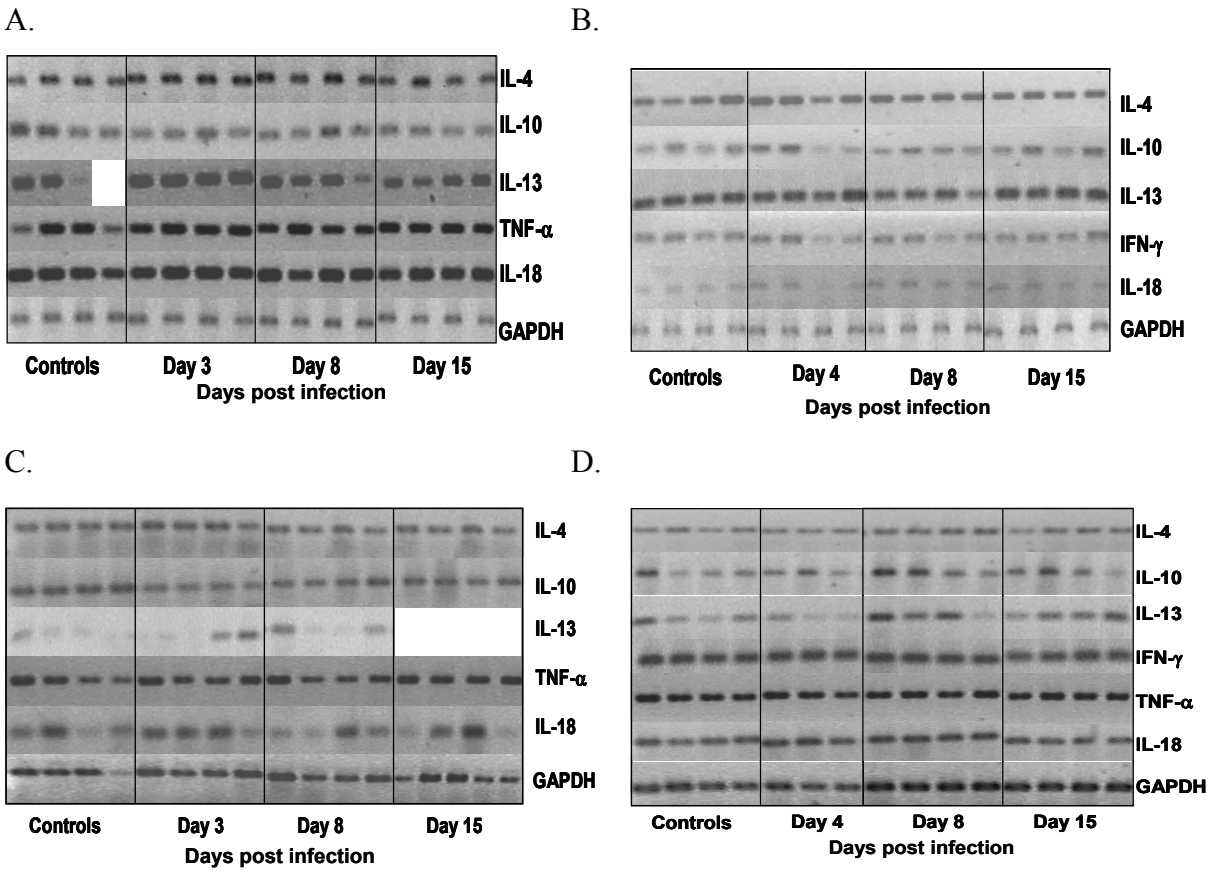

Figure 15. RT-PCR amplification of Th1 and Th2 cytokine mRNA species in MLN of GKO (A) and IL-12KO (B); and spleen of GKO (C) and IL-12KO (D) mice infected with *C. parvum*.

Total RNA was extracted from MLN and spleen of mice sacrificed 3 or 4, 8, and 15 days p.i. and analyzed as described. Amplification cycles were 32, 28, 35 and 29 for IL-4, IL-10, IL-13 and TNF-α (MLN & spleen of GKO and IL-12KO mice); 28 for IL-18 (MLN of GKO); 24 for IL-18 (MLN and spleen of IL-12KO, spleen of GKO). IFN-γ, 28 and 32 cycles from MLN and spleen of IL-12KO respectively; GAPDH at 20 & 25 cycles from GKO and IL-12KO respectively.

Note:- the RT-PCR analyses from the spleen samples (C and D)) were carried out in part by Schwamb B. (2008) when she was a diploma student under my supervision.

4.8. Gene expression of Th1 and Th2 cytokines during challenge infection of GKO and IL-12 KO mice

4.8.1. The pattern of Th1/Th2 cytokines post challenge infection in gut mucosa

The cytokines induced *in vivo* in recovered animals receiving challenge infections has not been characterized yet. As both GKO and IL-12KO mice resolve primary infection under our experimental conditions (Jakobi and Petry, 2008) we had the possibility to study the cytokine gene expression pattern upon challenge infection. We could not observe any changes in cytokine gene expression except for IL-5 and IL-13 mRNAs in GKO (Figure 16A and B) and IFN-γ in IL-12KO mice (Figure 16C and D), respectively. In GKO mice, the mRNA level of IL-5 was 2.4 times higher than in uninfected controls and 6 times higher than in mice killed at day 36 post primary infection (Figure 16B). The IL-13 level was twice higher than that of uninfected controls and 4 times higher than that of mice killed at day 36 post primary infection. In IL-12KO mice, IFN-γ mRNA was the only cytokine differentially expressed; at day 4 post challenge infection IFN-γ copy numbers were 3 times higher than those of the uninfected control mice (Figure 16D).

Generally, in both GKO and IL-12KO mice the increased cytokine levels during challenge infection were lower than the peak level reached post primary infection. Unlike that of primary infection, the increased cytokine mRNA expression during challenge infection was noticed at all time points studied, indicating the immediate mounting of cytokine gene expression and maintaining sustained levels.

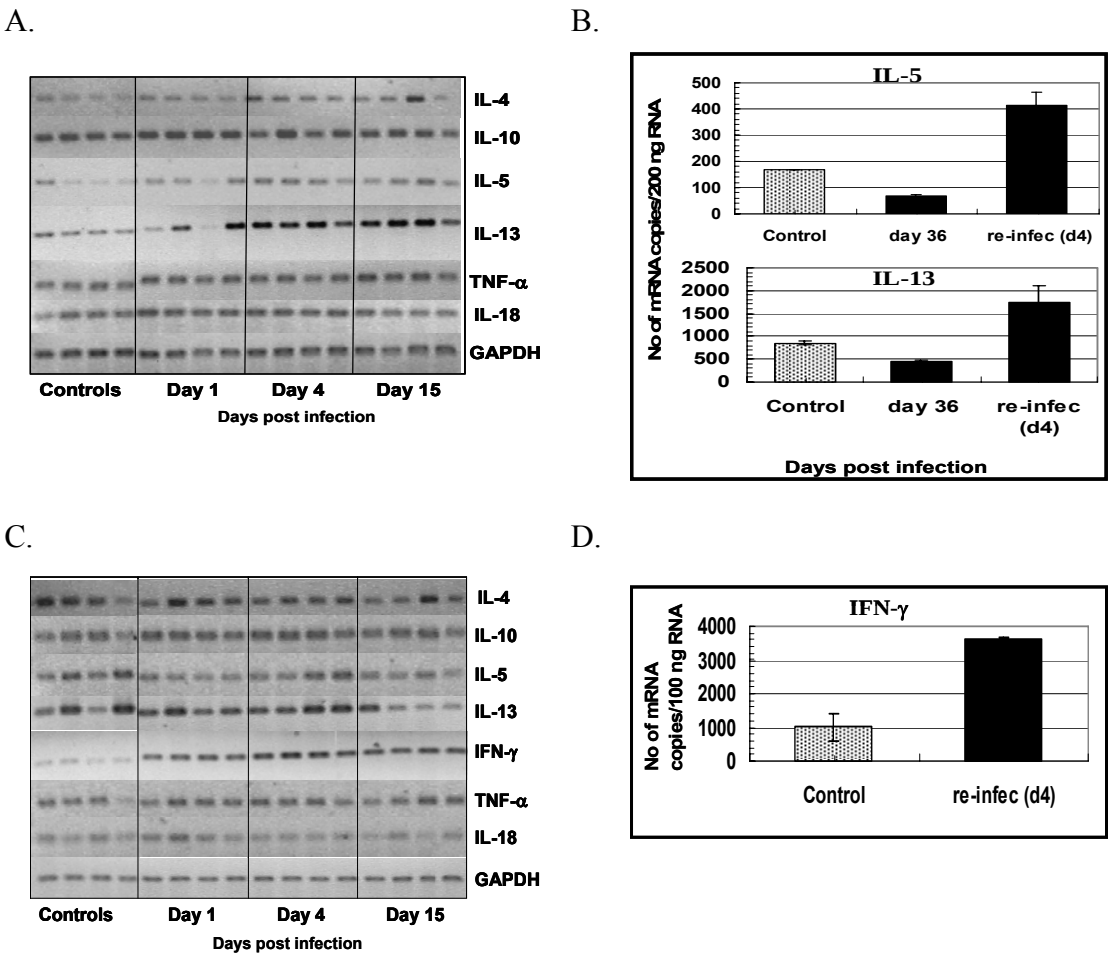

Figure 16. RT-PCR and quantitative real-time RT-PCR analysis of Th1/Th2 cytokine mRNA in the distal ilea of *C. parvum* re-infected GKO (A and B) and IL-12KO (C and D) mice.

Total RNA was extracted from the distal ilea of mice sacrificed 1, 4, and 15 days post challenge infection and analyzed as described. (A and C) For GKO mice, amplification cycles were 34, 31, 35, 35, 29, 24 and 20 for IL-4, IL-10, IL-13, IL-5, TNF-α, IL-18 and GAPDH respectively. For IL-12KO mice, we used 32, 29, 24, 34, 35, 31, 35 and 25 cycles for IFN-γ, TNF-α, IL-18, IL-4, IL-5, IL-10, IL-13 and GAPDH, respectively. The data demonstrate results of individual mice and are representative for three independent experiments. (B and D) Absolute mRNA copy numbers were determined, and the data was presented as number of mRNA copies per 100 or 200 ng RNA used for quantitative RT-PCR. Differences between uninfected controls and different time points post infection were compared directly. Error bars represent standard deviation. Uninfected mice as well as mice killed at day 36 (time of challenge infection) post primary infection were used to analyze the cytokine mRNA response post challenge infection.

4.8.2. The pattern of Th1/Th2 cytokines post challenge infection in MLN and spleen

Our attempts to further characterize the immune mechanisms involved in resistance during challenge infection were extended to study cytokine gene expression changes in MLN and spleen as was done during the primary infection. Similar to the primary infection, we did not see changes in cytokine mRNA levels in the MLN and spleen of *C. parvum* infected GKO (Figure 17A and B) as well as IL-12KO mice (Figure 17C and D).

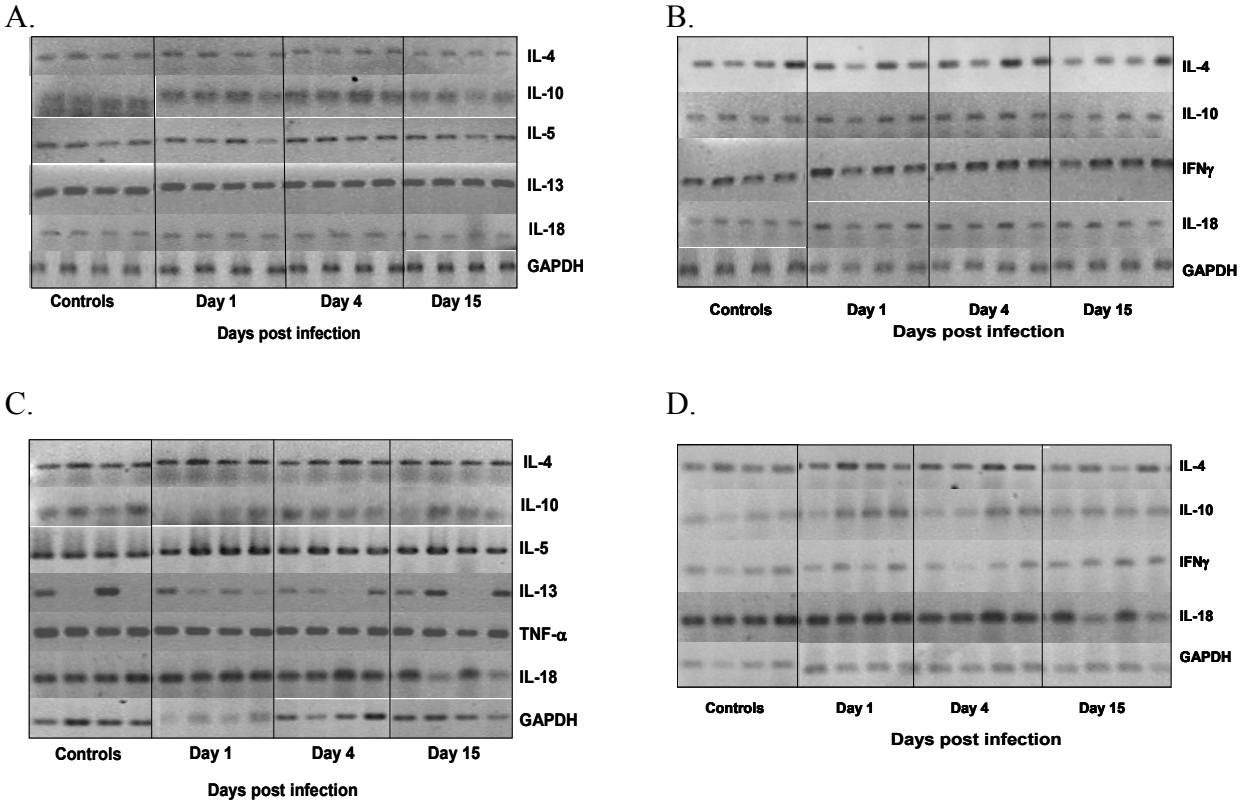

Figure 17. RT-PCR amplification of Th1 and Th2 cytokine mRNA species in MLN (A and B) and spleen (C and D) of *C. parvum* re-infected GKO (A and C) and IL-12KO (B and D) mice.

Total RNA was extracted from MLN and spleen of mice sacrificed 1, 4, and 15 days post challenge infection and analyzed as described. Uninfected mice were used as controls to analyze the cytokine mRNA response post challenge infection. Amplification cycles were 32, 28, 35, 24 and 20 for IL-4, IL-10, IL-13, IL-18 and GAPDH in both MLN and spleen of GKO and IL-12KO mice. IL-5 and TNF-α were amplified at 35 and 29 cycles respectively. IFN-γ was amplified at 32 and 28 cycles from MLN and spleen of IL-12KO respectively.

Note:- the RT-PCR analyses from the spleen samples (C and D)) were carried out in part by Schwamb B. (2008) when she was a diploma student under my supervision.

5. The role of interleukin-18 in resistance to *C. parvum* infection

Although IFN-γ plays a major role in *C. parvum* resistance, the mechanisms involved in regulation of its induction during infection require further study. When gene expression of IFN-γ was compared between non-infected wild type mice and IL-12KO mice, the expression in IL-12KO mice was lower than in the wild type mice by about 6 times (Table 6). This indicated that IL-12 is an important regulator of IFN-γ gene expression. However, as already shown in figures 10B and 14B, there was induction of IFN-γ expression in IL-12KO mice starting from 24 hrs. p.i., indicating that there were other inducers of IFN-γ in the absence of IL-12.

Interleukin-18 (IL-18) was first discovered as an IFN-γ-inducing factor (Okamura et al., 1995a; Okamura et al., 1995b), and subsequently has been shown to induce IFN-γ in other infections (Kawakami et al., 2000; Huang et al., 2002; Kinjo et al., 2002). However, IL-18 gene expression was not coincident with the early IFN-γ induction as described on section 3.5; the possible involvement of IL-18 in inducing IFN-γ expression after day 3 p.i. needs to be investigated. Furthermore, the expression of IL-18 was upregulated in GKO mice upon infection, pointing to possible functions of IL-18 in resistance to *C. parvum* infection other than inducing IFN-γ.

In order to address these two questions, the *in vivo* IL-18 protein was neutralized with a monoclonal anti-IL-18 antibody using the experimental protocol depicted on figure 18A.

A.

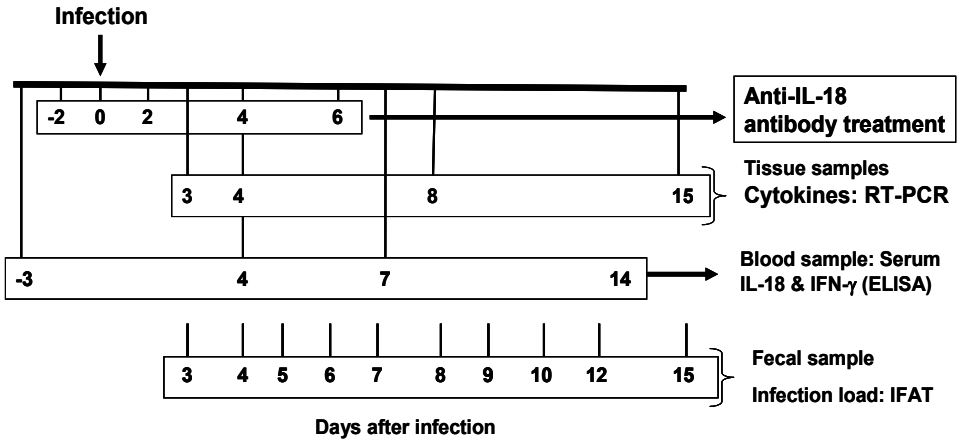

B.

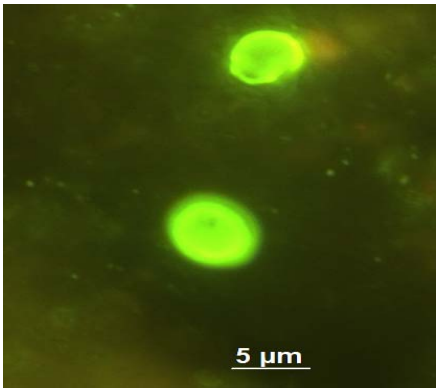

Figure 18. Experimental protocol used for *in vivo* neutralization of IL-18 using anti-IL-18 antibody and analysis of the effects.

(A) Mice were treated with anti-IL-18 antibody starting from 2 days before infection and at every 2 days until day 6. Antibody non-treated but infected mice as well as mice with no antibody treatment and infection were used as control groups. Tissues (ileum and spleen) were collected at days 3 or 4, 8 and 15 days p.i. for RNA isolation and analysis of cytokine gene expression changes. Blood samples were collected at day 3 before infection and at days 4, 7 and 14 p.i. for serum protein measurement of IL-18 and IFN-γ by ELISA. Fecal droppings were collected at days 3-10, 12 and 15 p.i. (B) The fecal shedding of oocysts by infected mice was determined using immunofluorescence test. The green oval structures are *C. parvum* oocysts.

5.1. Differential expression of IL-18 in the gut of *C. parvum* infected mice

As shown on figures 10A and B as well as 14A and B, mRNA expression of IL-18 in the ilea of mice increased upon *C. parvum* infection starting from day 3 p.i. onwards, peaking at day 8 p.i. and dropping to background levels after resolution of infection, i.e., day 15 p.i. Further more, there were differences between GKO and IL-12KO mice on their basal level of IL-18 mRNA expression. Uninfecetd GKO mice have about 4.4 times higher IL-18 mRNA levels than IL-12KO mice (Table 6). The peak mRNA level reached after infection was at day 8 p.i. in both mice; and the level in GKO mice was 6.2 times higher than in IL-12 KO mice.

Compared to the wild type mice, the basal IL-18 level in GKO mice was only slightly higher, by about 1.3 times, and upon infection it was 1.6 times higher at day 5 p.i. (Table 6). These data show that there is a reduced IL-18 basal expression level in the ilea of IL-12 KO mice compared to both wild type and GKO mice. GKO mice have a higher IL-18 basal level than both wild type and IL-12 KO mice and mount higher level upon infection.

5.2. *In vivo* neutralization of IL-18 increases the susceptibility of mice to infection

5.2.1. Systemic protein concentrations of IL-18 and IFN-γ

In order to monitor the effects of neutralizing *in vivo* IL-18 protein by antibody treatment on the systemic levels of any detectable un-neutralized IL-18 and also the consequence of the treatment on serum levels of IFN-γ blood samples were collected from mice on days 4, 7 and 14 p.i. (Figure 18A). Therefore, we could check the efficiency of the antibody on blocking the physiological compensation capacity of the animal body in producing more of IL-18 at least systemically.

Serum protein concentrations of IL-18 and IFN-γ were detected by specific ELISA in sera of IL-12KO mice at days 4, 7 and 14 p.i. and compared to pre-infection sera. The concentration of IL-18 in sera of GKO mice was measured at the same time points. Pre-infection serum was taken 3 days before infection for comparison with sera from animals infected with *C. parvum*. The IL-18 concentration in both mouse strains increased during infection peaking at day 7 and decreased by the time of resolution (Figure 19). In treated GKO mice IL-18 was totally blocked due to antibody application. In IL-12KO mice, serum IL-18 was totally blocked during treatment; however, after termination of antibody treatment (day 6) the higher level of serum protein in IL-12KO mice could not be completely neutralized as shown on day 7. IFN-γ concentrations could only be detected at day 7 p.i. in non treated mice (mean of three mice: 525 ng/ml serum). IL-12KO mice receiving antibody injection did not show any levels of IFN-γ.

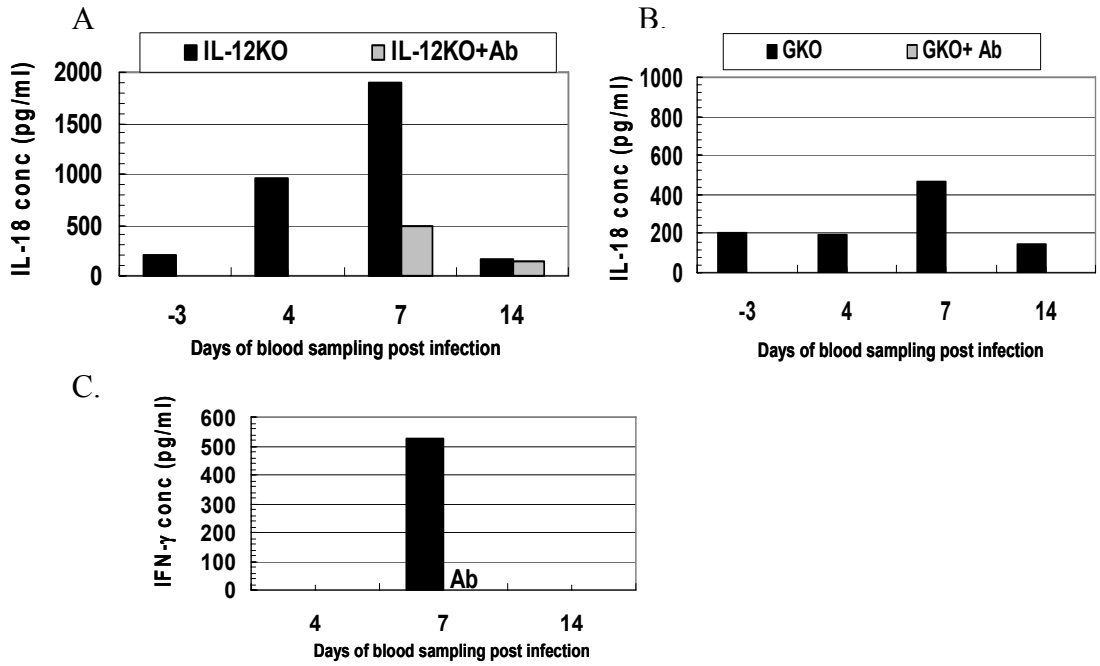

Figure 19. Protein concentrations of IL-18 and IFN-γ in sera of IL-12KO, and IL-18 in GKO mice.

Protein concentrations of IL-18 were detected by specific ELISA at days 4, 7 and 14 p.i. in sera of IL-12KO (A) and GKO mice (B). (C) The concentration of IFN-γ in sera of IL-12KO mice was determined by ELISA at days 4, 7 and 14 p.i. Pre-infection serum was taken 3 days before infection for comparison with sera of infected mice. Ab = antibody. Black bars, Ab-non-treated; Ab-treated mice are no bars (absence of measured protein) except days 7 and 14 of A (grey bars).

Note:- ELISA measurement of IL-18 and IFN-γ protein concentrations was carried out by Schwamb B. (2008) when she was a diploma student under my supervision.

5.2.2. Influence of anti-IL-18 antibody on fecal oocyst shedding of mice

In order to monitor the effect of anti-IL-18 antibody treatment on the intensity of *C. parvum* infection, feces were collected on days 3 to 10, day 12 and day 15 p.i. in both GKO and IL-12KO mice (Figure 18A).

C. parvum oocysts were detected in feces of GKO and IL-12KO mice by immunofluorescence test (IFAT) at chosen time points post infection (Figure 18B). The optimal antibody doses for injection of GKO and IL-12KO were determined in pilot studies and used in two independent injection experiments. In both strains of animals, antibody injection resulted in an overall increased oocyst shedding when compared to antibody non-treated animals; however, both antibody treated as well as non-treated mice recovered from infection within two weeks. The oocyst shedding of antibody treated GKO mice was significantly increased at days 5, 7 and 8 p.i. ($p<0.05$) (Figure 20A). Oocyst shedding of

antibody treated IL-12KO mice was significantly increased at days 5, 6, 7 and 8 of which changes at days 6 and 7 are highly significant ($p<0.001$) (Figure 20B). The IL-12KO mice were affected more than that of the GKO mice in that the antibody treatment resulted in a shift of the peak of infection in IL-12KO mice from day 4 to day 6 with increased severity of infection (Figure 20).

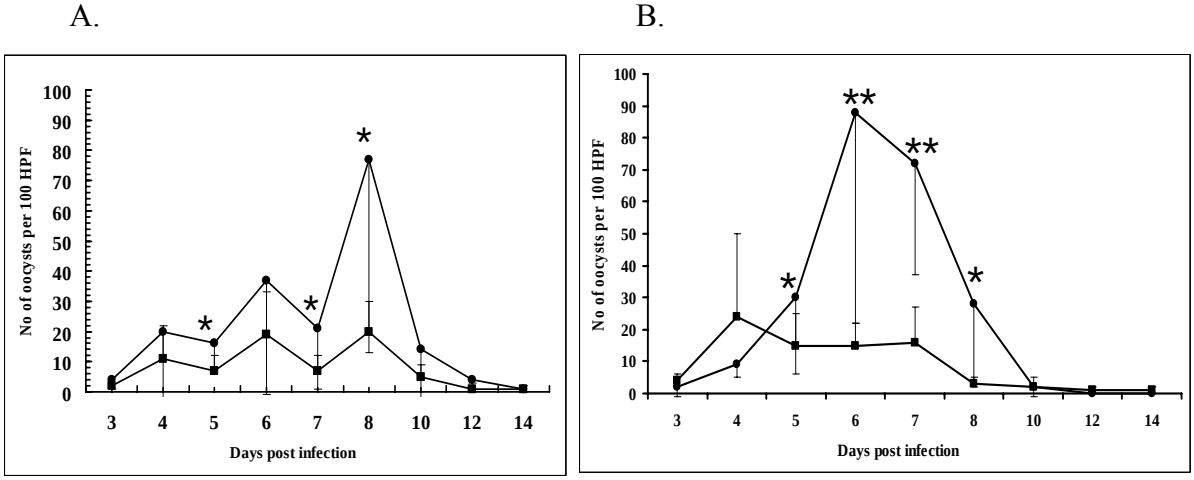

Figure 20. Influence of anti-IL-18-antibody treatment on the fecal oocyst shedding of GKO (A) and IL-12KO (B) mice.

Animals were infected with 10^6 *C. parvum* oocysts. The neutralizing antibody was injected intraperitoneally at days -2, 0, 2, 4 and 6. The fecal shedding of oocysts by infected mice was determined using immunofluorescence test (IFAT) and examined under a fluorescence microscope (×1000). The counts were expressed as number of oocysts in 100 high power optical fields (HPF). Untreated controls (■), antibody treated mice (●). Error bars represent standard deviation. Statistically significant differences are indicated by asterices (*, $p > 0.05$; **, $p > 0.001$)

Note:- analysis of the fecal oocyst shedding during infection and anti-IL-18 antibody treatment was carried out by Schwamb B. (2008) when she was a diploma student under my supervision.

5.2.3. Influence of anti-IL-18 neutralizing antibody on gene expression of cytokines

Tissues were taken at days 3, 8, and 15 for GKO and 4, 8, and 15 for IL-12KO mice (figure 18A). Gene expression profiles of cytokines IFN-γ, IL-18, TNF-α, IL-4, IL-13 as well as IL-10 were analyzed.

Antibody treatment resulted in upregulated IL-4 and IL-13 expression in the spleen of both mouse strains (Figure 21). There was no effect of treatment on gene expression of the other cytokines analyzed (Figure 22). A prominent effect of neutralization could be detected in IL-12KO mice, where IL-4 and IL-13 levels were higher at days 4 and 8 p.i. compared to non treated but infected animals (Figure 21B). Antibody injection resulted in a 6-fold increase of

IL-4 mRNA copies in spleens of IL-12 KO animals at day 4 p.i. compared to non-infected and a 4-fold increase compared to infected mice. At day 8 p.i. the neutralizing effect of the antibody was still detectable in IL-12KO although antibody treatment was terminated at day 6. In GKO mice the effect of the antibody on IL-4 gene expression could only be seen systemically at day 8 p.i.. Increased spleen IL-13 mRNA levels were observed at day 4 in addition to day 8 p.i. in GKO mice compared to non-treated animals (Figure 21A).

Unexpectedly, there were no detectable influences of anti-IL-18 treatment on the gene expression of cytokines in the gut mucosa (Figure 22A and B).

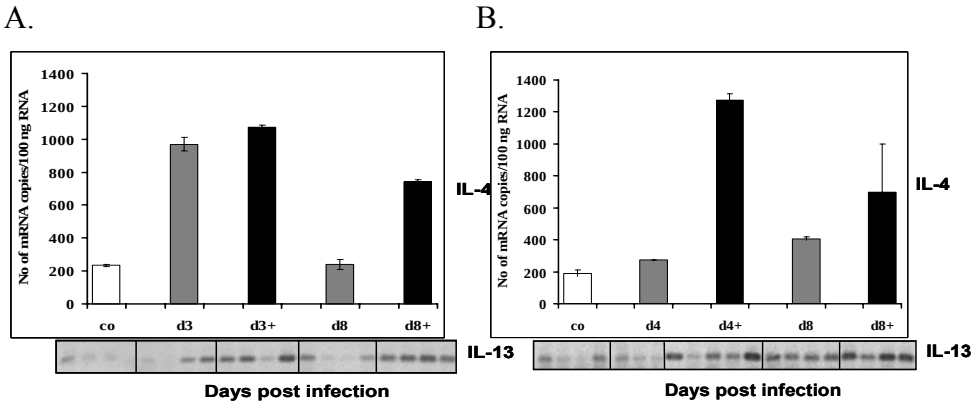

Figure 21. Influence of anti-IL-18 antibody treatment on IL-4 and IL-13 gene expression in spleen of GKO (A) and IL-12KO (B) mice.

IL-4 mRNA copy numbers were detected by quantitative real time PCR at days (d) 3 and 8 for GKO, and at days 4 and 8 for IL-12KO p.i. in spleens of Ab-treated (+), non treated (d4, d8) as well as non-treated non-infected control animals (co). IL-13 mRNA was analyzed by RT-PCR at the same time points mentioned for IL-4 using 35 amplification cycles as described. The neutralizing antibody was injected intraperitoneally at days -2, 0, 2, 4 and 6. Error bars represent standard deviation. co uninfected controls (white bars); antibody non-treated but infected animals (grey bars); +, antibody treated and infected animals (black bars).

Note:- Quantification of IL-4 mRNA in the spleen was carried out by Schwamb B. (2008) when she was a diploma student under my supervision.

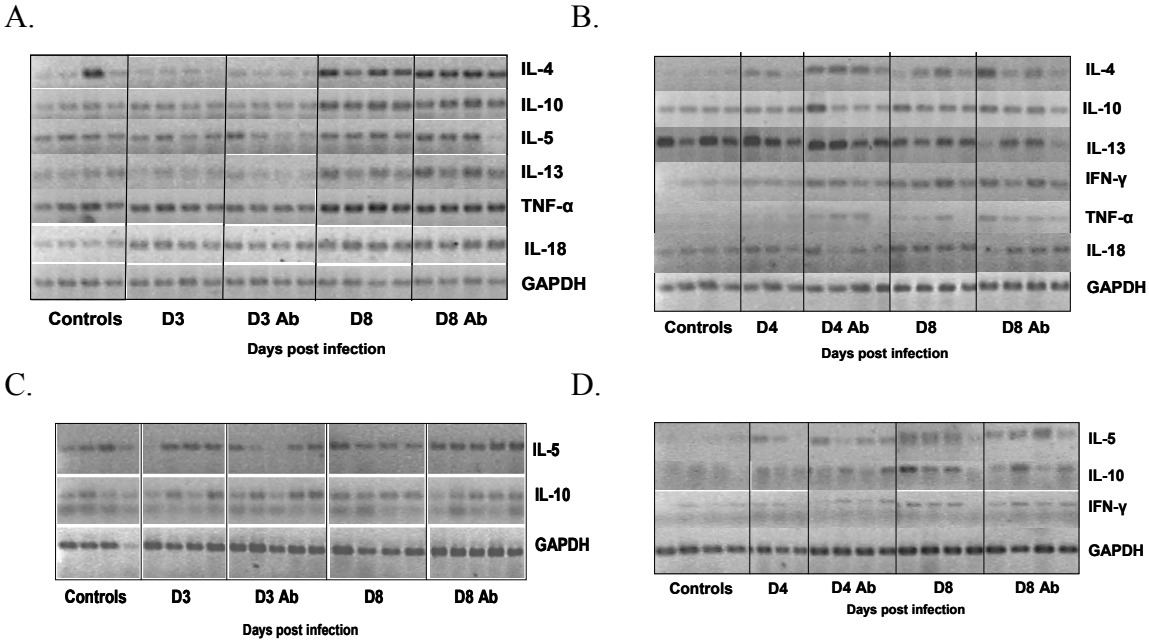

Figure 22. The effect of IL-18 neutralization on the gene expression of cytokines in the ileum and spleen during *C. parvum* infection.

The expression of cytokines in the ilea of GKO (A) and IL-12KO (B) mice; as well as in the spleen of GKO (C) and IL-12KO (D) mice treated with anti-IL-18 antibody and infected with *C. parvum*. Total RNA was extracted from the distal ilea and spleen of mice sacrificed 3 or 4, 8 and 15 days p.i. and analyzed as described. The data on day 15 were not shown. (A and B) For GKO mice, amplification cycles were 29, 34, 31, 35 and 20 for TNF-α, IL-4, IL-10, IL-13 and GAPDH respectively. For IL-12KO mice, we used 31, 32, 34, 32, 35, 35 and 25 cycles for TNF-α, IFN-γ, IL-4, IL-10, IL-13 and GAPDH, respectively. (C and D) For both GKO & IL-12KO mice 35, 31 and 25 cycles for IL-5, IL-10 and GAPDH respectively; IFN-γ was amplified at 28 cycles. Ab, antibody-treated mice.

Note:- RT-PCR analysis of cytokine mRNAs in the spleen (C and D) and ileum (B) of IL-12KO mice was carried out by Schwamb B. (2008) when she was a diploma student under my supervision.

6. Adoptive transfer of immunity from *C. parvum* infected to naive mice

In the previous sections, the roles of Th1 and Th2 cytokines during primary as well as challenge infections were presented. Th1 and Th2 cells and their corresponding cytokine products are formed from $CD4^+$ T-cells upon differentiation (Mosmann et al., 1986). Therefore, the next objective was to study the potential roles of $CD4^+$ T-cells and pan T-cells in resistance to *C. parvum* infection.

In addition to the roles of T-cells and $CD4^+$ T-cells isolated from different immunological sites, the time during patent infection when cellular immunity could be transferred to naive mice was investigated. We hypothesized that T-lymphocytes from mice recovered from primary infection, i.e. at day 15 p.i. in our experimental models, should transfer protective immunity to naive recipients. Additionally, the peak of infection was selected in both mouse models, i.e. day 5 p.i. in IL-12KO and day 8 p.i. in GKO mice, as a possible time point when resistance could be transferred through T-lymphocytes. Therefore, we isolated T-lymphocytes at the peak of infection as well as after resolution of the primary infection in both mouse models (Figure 23A).

A.

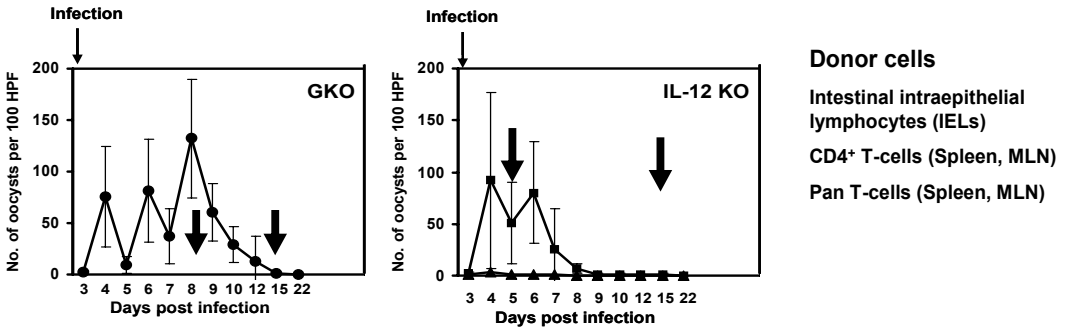

B.

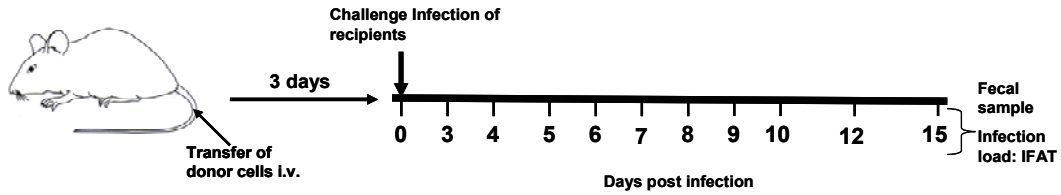

Figure 23. Experimental protocols used for adoptive transfer of donor cells to naive mice recipients. (A) Donor cells (IELs, $CD4^+$ T-cells) were prepared from donor mice at days 5 and 15 (IL-12KO mice), and at days 8 and 15 (GKO mice) p.i. of donor animals. Pan T-cells were prepared at day 15 p.i. (B) Donor cells were injected into the tail vein of naive recipient mice; at day 3 p.i. recipient mice were challenged with *C. parvum* infection. Fecal samples were collected from infected recipient mice at days 3-10, 12 and 15 p.i to monitor the infection load (by IFAT) of recipient mice as a measure of protection by transferred donor cells. IELs = intestinal intraepithelial lymphocytes. MLN = mesenteric lymph nodes. IFAT = immunofluorescence test. Thick black arrows (A), times of donor cell preparation.

Total T-lymphocyte population ($CD4^+$ and $CD8^+$) as well as only the $CD4^+$ T-lymphocyte population were isolated from the site of infection (gut/intestinal mucosa), the local lymph nodes draining the intestine (Mesenteric lymph nodes, MLN) and also the systemic immune tissue (spleen).

Lymphocytes located at different immune tissues of the animal, gut mucosa, MLN and spleen were isolated in parallel and transferred to three groups of recipient animals: IEL recipients, MLN T-cell recipients, and spleen T-cell recipients. Therefore, one could study the relative importance of T-cells located in the gut mucosa and systemic immune locations in protecting from *C. parvum* infection.

After transfer of donor cells intravenously (i.v.) to naive recipient mice, the recipient mice were challenged with *C. parvum* infection 3 days post transfer. The protection of recipient mice by the transferred cells from challenge infection was determined by monitoring the fecal oocyst shedding starting from day 3 p.i. onwards as indicated on figure 23B.

6.1. Characterization of isolated intestinal intraepithelial lymphocytes (IELs)

About 10 donor mice, which were previously infected with *C. parvum* were used for isolation of IELs for transfer to naive mice. From each mouse the whole length of small intestines (0.5 cm below stomach) was used so as to get enough number of cells to inject to four recipient mice. Assessment of the cell yield, viability and purity (composition) of the IEL preparations was performed before transferring into recipients.

The total number of IELs isolated during each time of preparation, i.e. from 10 mice was determined by counting in a hemocytometer under light microscope. Cell numbers ranged from 3.04×10^7 to 7.98×10^7 (mean= 5.07×10^7) in GKO mice and from 1.16×10^7 to 5.74×10^7 (mean= 3.2×10^7) in IL-12KO mice. Therefore, the number of IEL yield per mouse was about 5.01×10^6 in GKO mice and 3.2×10^6 in IL-12KO mice. The average viability of cells, as determined by trypan blue exclusion procedure was 89.5 % (80 – 96.3%) for GKO mice and 93.9 % (84 – 97 %) for IL-12KO mice.

Further assessment of IEL preparations were done to determine the purity of IELs in terms of $CD4^+$ and $CD8^+$ T-cell composition. This was achieved by staining cell preparations with FITC-coupled anti-CD4 and PE-coupled anti-CD8 antibodies and determining the cell populations based on the fluorescence detections of FITC and PE fluorochromes in a Beckman COULTER® EPICS® XL TM flow cytometer. Staining of cells with rat anti-mouse IgG isotype control antibodies coupled with FITC and PE was performed in parallel with each anti-CD4-CD8 antibody staining experiments to control the fluorescence specificities of the fluorochromes (Figure 24).

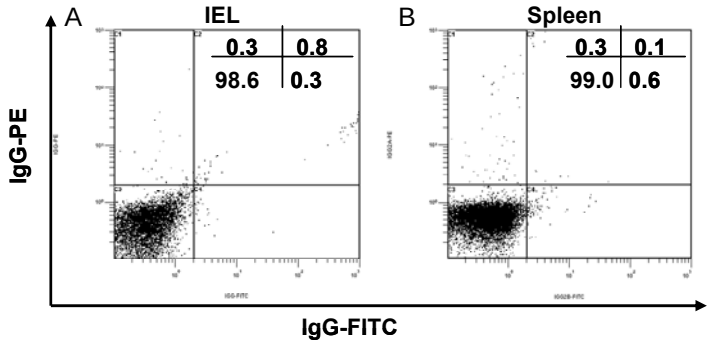

Figure 24. Flow cytometric analysis of IEL (A) and spleen cells (B) after staining with IgG-FITC and IgG-PE isotype controls.

IELs and spleen cells were isolated from mice and stained with FITC-coupled anti-IgG2b and PE-coupled anti-IgG2a antibodies as described in materials and methods. FITC and PE bound cell populations were determined in Beckman COULTER® EPICS® XL TM flow cytometer. The numbers indicate the percentage of cells in the four quadrants of the FACS histogram as analyzed by ExpoTM32 ADC Software.

6.1.1. Differential migration of $CD4^+$ T-cells to the gut mucosa between GKO and IL-12 KO mice at peak versus resolution of primary infection

The different T-cell populations in the IEL preparations were determined with flow cytometry. Accordingly, the total population of T-cells in the IELs was about 85 % and 58 % in uninfected GKO and IL-12KO control mice (Table 7). Upon infection of GKO mice, there was a slightly higher total T-cell population at the peak of infection (day 8) (69 %) than at the resolution of infection (day 15) (60 %) (Table 7). The major difference was noticed in the $CD4^+$ T-cell proportion which was 10 % at day 8, as twice as day 15 (5 %); however, this difference was not statistically significant ($P>0.05$). The proportion of $CD4^+$ T-cells at day 15 p.i. was closer to that of the uninfected control mice (4.7 %), indicating that the was infiltration of $CD4^+$ T-cells to the site of infection, the intestine, of the GKO mice at the peak of infection (Table 7 and figure 25A).

In contrast to the situation in GKO mice, there was no significant difference on the $CD4^+$ T-cell population among uninfected IL-12KO mice, and IL-12KO mice at days 5 and 15 p.i. (Table 7 and figure 25B).The total T-cell population in IL-12KO mice at day 15p.i. was higher than uninfected mice by about 9 % and this was due to the increased proportion of the $CD8^+$ T-cells at day 15 by about 19 %, i.e. from 52 % in uninfected controls to 62 % in mice at day 15p.i. (Table 7).

Table 7. Proportion of $CD4^+$ and $CD8^+$ T-cells in the IEL isolations and the effect of *C. parvum* infection on cell proportions.

	Proportions of cells in IEL preparation [mean % value (± SD)]				
Status of infection	Total T-cells	$CD4^+$	$CD8^+$	$CD4^+CD8^+$	$CD4^-CD8^-$
GKO mice					
Uninfected	84.8*	4.7	72.5	2.8	19.9
Day 8	69.2 (3.7)	10 (2.9)	57.7 (3)	1.53 (0.12)	30.7 (3.7)
Day 15	59.7 (3.8)	5 (0.6)	52.8 (4.9)	1.85 (0.5)	40.45 (3.9)
IL-12KO mice					
Uninfected	57.8*	4.5	52	1.3	42.2
Day 5	61.6 (0.14)	4.1 (1)	56.1 (1)	1.4 (0.14)	38.4 (0.14)
Day 15	67.1 (4.9)	4.2 (1.2)	61.6 (4.7)	1.33 (0.5)	30.9 (4.9)

Numbers indicate mean cell numbers determined from three independent experiments. SD = standard deviation.
* = the experiment was performed only once.

6.1.2. Population of $CD4^+$ and $CD8^+$ intestinal intraepithelial lymphocytes transferred to naive recipients

The number of IELs transferred to GKO as well as IL-12KO recipient mice was 2×10^6. Referring to section 6.1.1., the proportion of $CD4^+$ and $CD8^+$ T-cells as well as the total T-cells in transferred IEL preparation of the two mouse models was calculated and presented in table 8. $CD4^+CD8^+$ cells (double positives) were also added to the T-cell population, although they constitute a small number.

When we looked at the T-cell and subsets of T-cell population between the GKO day 8 p.i. and IL-12 day 5 p.i. donor IELs, there were only slightly more T-cells in IELs of GKO than that of IL-12KO mice by about 7 %; but there was a marked difference on the proportion of $CD4^+$ T-cells between GKO (10 %) and IL-12KO (4 %) mice. This indicates that at the peak of infection in GKO mice there was a higher number of $CD4^+$ T-cells trafficking to the IEL population, but there was no such migration evident for IL-12KO mice. When we looked at the transferred cell population (2×10^6 IELs), the total T-cell population in GKO mice and IL-12KO mice were about 1.4×10^6 and 1.2×10^6, showing that the difference was about 200,000 cells higher in GKO. The number of $CD4^+$ T-cells was twice higher in GKO than in IL-12KO mice, 2×10^5 versus 1×10^5.

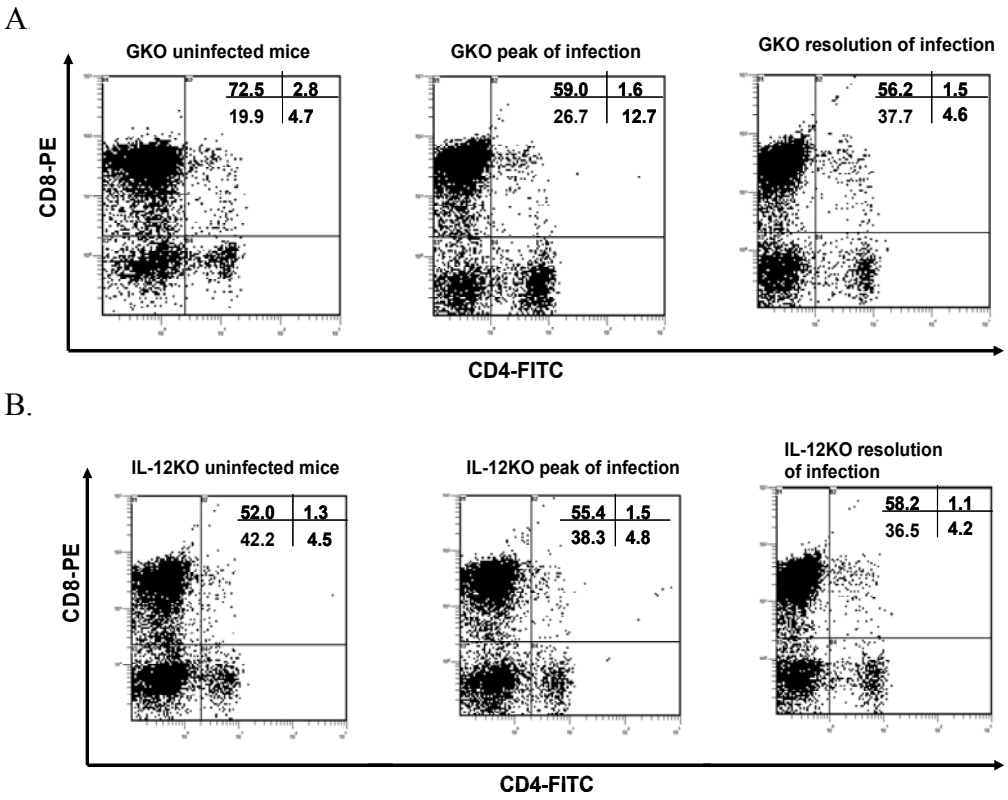

Figure 25. Flow cytometric analysis of purity and T-cell populations of IELs isolated from GKO (A) and IL-12KO (B) donor mice.

IELs were isolated from the intestine of uninfected mice, as well as from mice at peak and resolution of infection. Cells were stained with FITC-coupled anti-CD4 and PE-coupled anti-CD8 antibodies as described in materials and methods. T-cell populations were determined based on the fluorescence detections of FITC and PE fluorochromes in Beckman COULTER® EPICS® XL TM flow cytometer. The numbers indicate the percentage of cells in the four quadrants of the FACS histogram as analyzed by ExpoTM32 ADC Software.

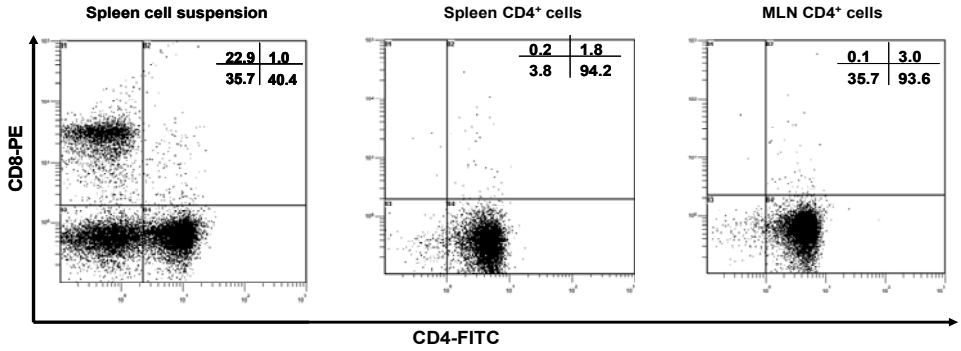

Figure 26. Flow cytometric analysis of the purity of $CD4^+$ T-cells separated by MACS technology.
Cell suspensions were prepared from MLN and spleen of mice and $CD4^+$ T-cells were positively selected using MACS technology. Separated $CD4^+$ T-cells were stained with FITC-coupled anti-CD4 and PE-coupled anti-CD8 antibodies as described. T-cell populations were determined based on the fluorescence detections of FITC and PE fluorochromes in Beckman COULTER® EPICS® XL TM flow cytometer. The numbers indicate the percentage of cells in the four quadrants of the FACS histogram as analyzed by ExpoTM32 ADC Software. Double sequential MACS columns were applied to achieve a higher $CD4^+$ cellular purity.

Table 8. Proportion of $CD4^+$ and $CD8^+$ T-cells in the IEL donors of GKO and IL-12KO mice.

		Number of T-cell composition in IELs ($\times 10^6$)			
Mouse	IELs transferred	Total T-cells	$CD4^+$	$CD8^+$	$CD4^+CD8^+$
GKO mice					
Day 8	2×10^6	1.39	0.2	1.15	0.03
Day 15	2×10^6	1.19	0.1	1.05	0.04
IL-12KO mice					
Day 5	2×10^6	1.54	0.1	1.1	0.03
Day 15	2×10^6	1.34	0.1	1.2	0.03

Numbers indicate mean cell numbers determined from three independent experiments.

6.2. Homing of adoptively transferred IELs to gut mucosal and systemic immune tissues

In order to determine the efficiency for trafficking of transferred IELs to the gut mucosa (homing) we used naive as well as primed (day 15 p.i. of IL-12KO mice) male donor cells and female recipient mice. After day 3 post transfer of male donor cells to female recipients, the intestine, spleen, MLN and Peyer's patches were collected from the recipients. IELs were

isolated from the intestine. From these tissues and IELs of recipient mice genomic DNA was prepared and used as a template to amplify a male chromosome (Y) restricted gene (*tdy*). Male DNA from naive IELs was not detected from IELs and PPs of recipients, but there was scant amplification of male DNA from MLN of recipients (Figure 27A). As shown on the same figure, upon re-amplification of previous PCR products, there was detection of male DNA from IEL, MLN as well as PPs of female recipients. In contrast, transferred primed IELs reached at tissues of recipients by day 3 post transfer. Primed IELs preferentially home to the intestine as there was higher amplification product of the male chromosome restricted gene from the IEL preparations than from other tissues of the female recipients (Figure 27B). As was shown on the same figure, there were still some cells remaining in the systemic tissue (spleen) indicated by a faint amplification product from the male chromosomal gene.

On the other hand, it was not possible to detect male chromosomal restricted gene amplification product from MLN and PPs. Assuming that the absence of amplification product from PPs and MLN could be due to the very small number of cells trafficking to these lymphoid tissues, re-amplification using 5 µl of the previous PCR product as a template was performed in order to detect any male DNA that could be present in MLN and PPs, but there was no product detected (Figure 27B). Using the same protocol, re-amplification of previous PCR product from IEL and spleen genomic DNA produced a strong amplification product (Figure 27B). In order to determine the frequency of IELs that traffic to tissues of the recipient mice, a standard was designed using amplification of the *tdy* gene using 10-fold serially diluted male chromosomal genomic DNA starting from 100ng. Using this standard, the PCR product amplified from IELs was equivalent to the PCR product of 1:1000 to 1:10,000 dilution of the standard on the basis of band intensity. Therefore, the frequency of the donor IELs that traffic to the recipient intestine was about 1 donor cell to 1,000 to 10,000 recipient IEL populations. The frequency of donor IELs that are present in the spleen were much lower (Figure 27 B).

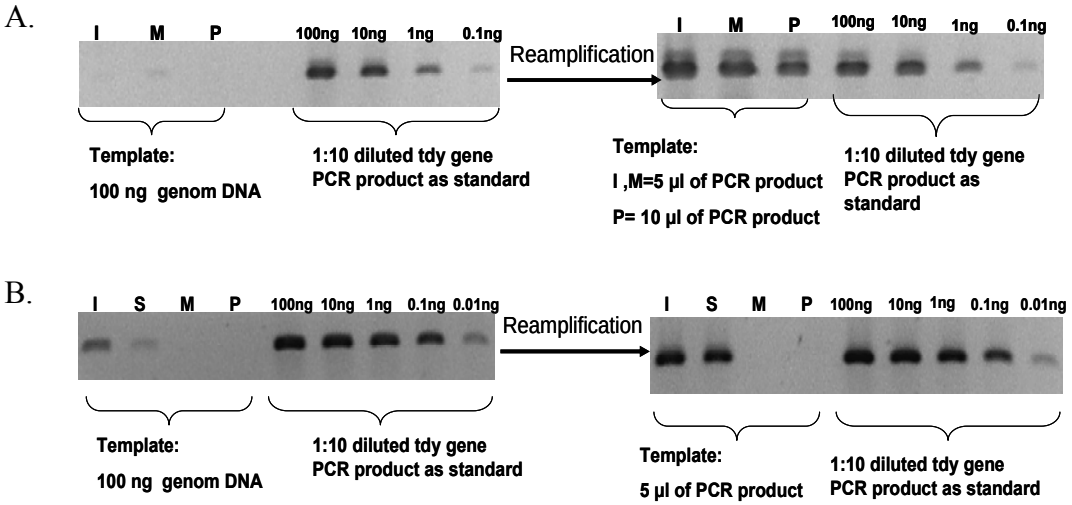

Figure 27. Homing of transferred male donor naive (A) and primed (B) IELs to tissues of female recipient mice.

Male donor IELs were transferred i.v. to female recipient mice. Genomic DNA was isolated from intraepithelial lymphocytes (I), spleen (S), MLN (M) and Peyer's patches (P) of female recipients 3 days post transfer. The male chromosome-restricted *tdy* gene was amplified by PCR from 100 ng of female genomic DNA preparations. *Tdy* gene was amplified from 100, 10, 1, 0.1 and 0.01 ng of male genomic DNAs and used as standard to determine the frequency of male donor cells that traffic to female tissues. Re-amplification of the PCR product was performed to detect any male DNA present from MLN and PPs.

6.3. Adoptive transfer of primed IELs provided protection to naive recipient mice from *C. parvum* infection

6.3.1. Protection of naive GKO recipient mice from *C. parvum* infection was conferred by day 15 p.i. donor IELs but not by day 8 p.i. donor IELs prepared from GKO mice

In order to address this objective, we chose two important time points during primary infection of GKO donor mice, i.e., the peak of infection (day 8 p.i.) and the resolution of infection (day 15 p.i.) as a possible time when protective immune cells could be transferred to naive mice.

From each time point, day 8 or day 15, IELs were isolated from the intestine of donor animals, and 2×10^6 IELs were injected intravenously (i.v.) to each of the recipient mice. After 3 days post transfer of the cells, the recipient mice were infected with *C. parvum* oocyst (Figure 23B). In parallel, animals which did not get donor cells were infected with *C. parvum* to serve as a control group to compare the fecal oocyst shedding with the animals that got

primed donor cells. For the analysis of oocyst shedding as a measure of protection we looked at the shedding profile at days 4, 6, and 8 p.i. since it has been shown that the oocyst shedding by GKO mice was very low at days 5, 7 and after day 8 and these days are not important for comparison between recipients and non-recipients.

Accordingly, IELs transferred from GKO donor mice at day 8 p.i. conferred minimal protection to *C. parvum* infection. This was shown by a variable reduced oocyst shedding by the recipients at days 4, 6 and 8 p.i. compared to non-recipient control animals (Figure 28A). On the other hand, IELs transferred from GKO donor mice at day 15 p.i., when the infection had resolved, conferred protection to *C. parvum* infection. This was shown by a significantly reduced oocyst shedding at days 4, 6 and 8 p.i. compared to non-recipient control animals (Figure 28C).

At both time points of donor cell transfer, day 8 and day 15, the adoptive transfer experiments were performed three times. For further analysis of the significance of the protection conferred by the transferred cells, the ooycst shedding profiles of the three experiments were converted to percent protection so that they can be compared among themselves. For the calculation of percent protection, the mean of oocyst shedding by the control animals was taken as 100 %, which means 0 % protection. The reduction of oocyst shedding as a result of transfer of cells from donor animals was calculated as percent of oocyst reduction from that of the control animlas.

The percent protection was calculated for each important time point post challenge infection of recipient animals, i.e. days 4, 6, and 8 p.i. The percent of protection from the repetitive experiments was found to be 22 – 37 at days 4, 6 and 8 p.i. (Figure 28B). Using the average percent of protection from the repetitive experiments there was no statistically significant difference ($p>0.05$) in protection between day 8 IEL recipients and non-recipient control animals (Figure 28B). This may indicate the low number of established protective cells in the intestine of GKO mice by the time of the peak of infection.

However, at day 15 p.i. IELs provided about 70 – 80 % protection from infection at days 4, 6 and 8 p.i. (Figure 28D), and this protection was statistically significant ($p<0.05$) at all of the days considered.

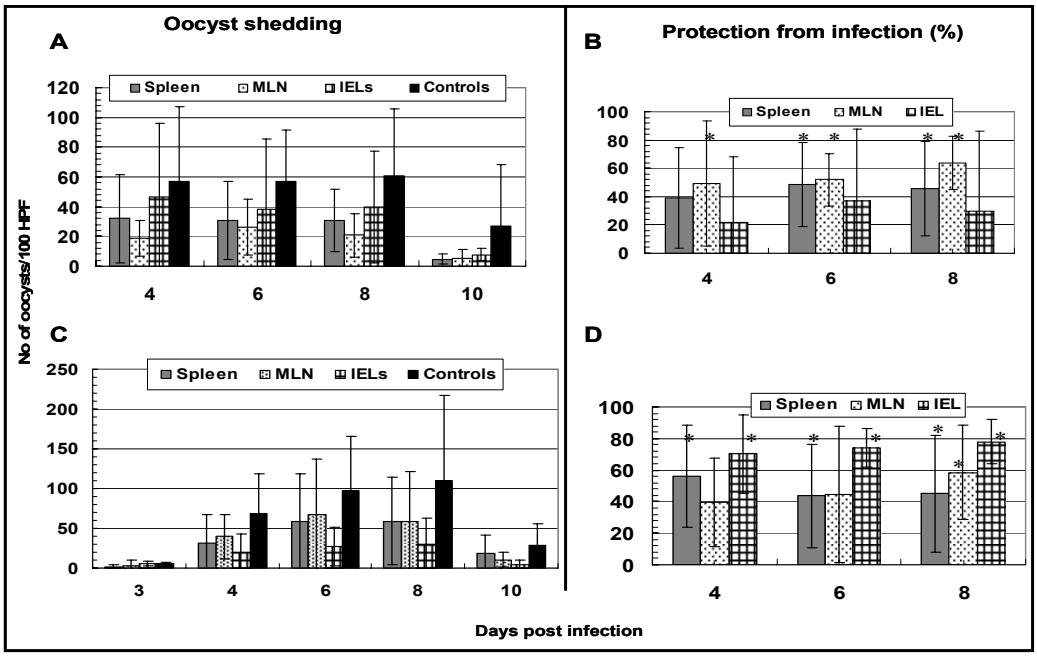

Figure 28. Protection of naive GKO mice from *C. parvum* infection by adoptive transfer of primed IELs and CD4$^+$ T-cells.

Recipient animals as well as non-recipient controls were infected with 10^6 *C. parvum* oocysts 3 days after transfer of donor cells. Fecal oocyst shedding by recipients of day 8 p.i. (A), day 15 p.i. (C) donor cells (IELs, spleen, MLN) as well as non-recipient controls at days 3 or 4, 6, 8 and 10 p.i. was determined by IFAT and examined under fluorescence microscope (×1000). The counts were expressed as number of oocysts in 100 high power optical fields (HPF). (B and D) Protection rates conferred by transferred cells at days 4, 6 and 8 p.i.; B, day 8 p.i. donor cell recipients; D, day 15p.i. donor cell recipients. Error bars represent standard deviations (SDs) of the mean of 3 different experiments (total of 12 animals). Black bars, non-recipient controls; grey bars, spleen CD4$^+$ T-cell recipients; dotted (spotted) bars, MLN CD4$^+$ T-cells recipients; squared bars, IEL recipients. MLN= mesenteric lymph nodes; IEL= intestinal intraepithelial lymphocytes; HPF= high power optical fields. Statistically significant differences are indicated by asterices (*, $p < 0.05$).

6.3.2. Protection of naive IL-12KO recipient mice from *C. parvum* infection was conferred by donor IELs as early as 5 days p.i.

One advantage of the IL-12KO mouse model over that of the GKO mouse is that one can study the importance of IFN-γ during infection. It has been shown in sections 4.1 and 4.3 that IFN-γ was upregulated at the site of infection (intestine) within 24 hrs and reached at peak level at day 8 p.i. (Figures 10B and 14B). IL-12KO mice clear the infection by this time, and the peak of infection is earlier, day 5. It has been shown that IELs contribute to the source

IFN-γ in the intestine during infection (Leav et al., 2005). Therefore, we aimed to transfer protective IELs from IL-12KO donors at the peak of infection (day 5 p.i.) and the resolution of infection (day 15 p.i.) to naive mice. By doing so we transferred cells that produce IFN-γ in response to challenge infection that could lead to different status of protection compared to GKO donor cells.

From each time point, day 5 or day 15, IELs were isolated from the intestine of donor animals, and 2×10^6 IELs were injected intravenously (i.v.) to each of the recipient mice. After 3 days post transfer of the cells, the recipient mice were infected with *C. parvum*. For the analysis of oocysts shedding as a measure of protection we looked at the shedding profile at days 3, 4, 5, 6 p.i. since it has been shown that the oocyst shedding by IL-12KO mice falls down by day 8.

Accordingly, IELs transferred from IL-12KO donor mice at day 5 p.i conferred significant protection to challenge *C. parvum* infection. This was shown by a highly reduced fecal oocyst shedding of the recipients at days 3, 4, 5 and 6 p.i. compared to non-recipient control animals (Figure 29A). Similarly, IELs transferred from IL-12KO donor mice at day 15 p.i., when the infection resolved, conferred significant protection to challenge *C. parvum* infection. This was also shown by a significantly reduced oocyst shedding at days 3, 4, 5 and 6 p.i. compared to non-recipient control animals (Figure 29C).

In a similar way as that of GKO mice, at both time points of donor cell transfer, day 5 and day 15, the adoptive transfer experiments were performed three times and the results were analyzed as described for GKO recipients. Accordingly, the percent protection at days 4, 5 and 6 provided by day 5 p.i. donor IELs was 74 – 79 % (Figure 29B). This protection rate was statistically significant ($p<0.05$) at all days post challenge infection. Similarly, at day 15 p.i. donor IELs provided an increased percent protection, 87 – 93 % from infection at days 4, 5 and 6 p.i. (Figure 29D), and this was statistically significant ($p<0.05$) at all time points considered.

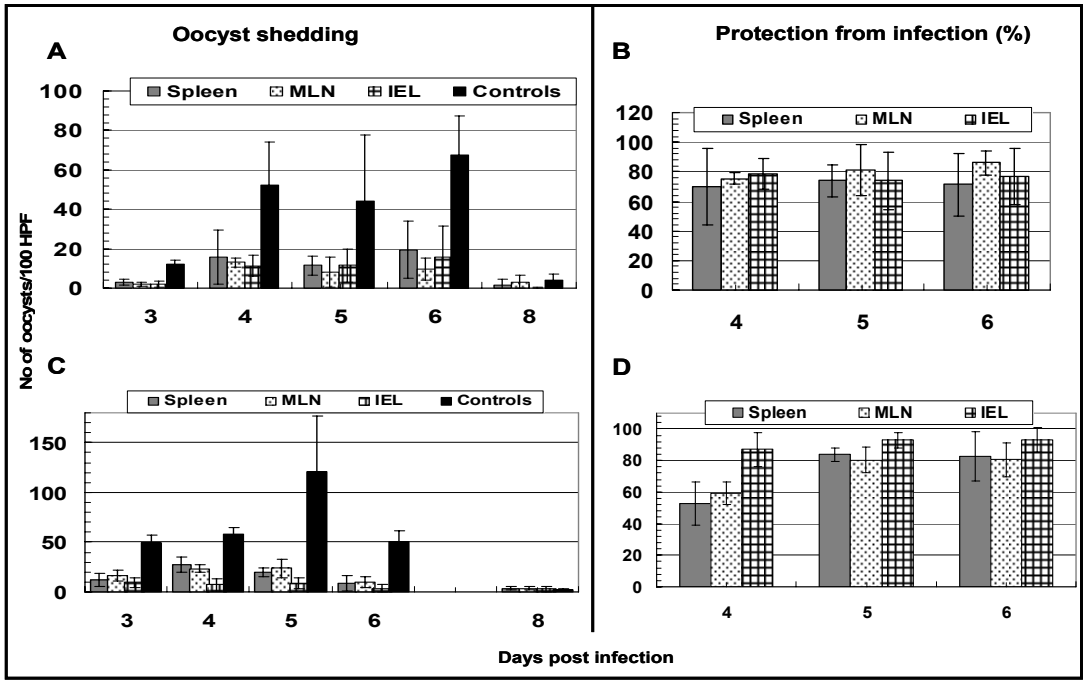

Figure 29. Protection of naive IL-12KO mice from *C. parvum* infection by adoptive transfer of primed IELs and CD4$^+$ T-cells.

Recipient animals as well as non-recipient controls were infected with 10^6 *C. parvum* oocysts 3 days after transfer of donor cells. Fecal oocyst shedding by recipients of day 5 p.i. (A), day 15 p.i. (C) donor cells (IELs, spleen, MLN) as well as non-recipients controls at days 3, 4, 5, 6 and 8 p.i. was determined by IFAT as described. (B and D) Protection rates conferred by transferred cells at days 4, 5 and 6 p.i.; B, day 5 p.i. donor cell recipients; D, day 15p.i. donor cell recipients. Error bars represent standard deviations (SDs) of the means of individual mice in a single representative experiment (A and C). Black bars, non-recipient controls; grey bars, spleen CD4$^+$ T-cell recipients; dotted (spotted) bars, MLN CD4$^+$ T-cells recipients; squared bars, IEL recipients. MLN= mesenteric lymph nodes; IEL= intestinal intraepithelial lymphocytes; HPF= high power optical fields. $P<0.05$, statistically significant differences in protection between recipients and non-recipients were calculated at all time points.

6.4. Adoptive transfer of primed CD4$^+$ T-cells provided protection to naive recipient mice from *C. parvum* infection

6.4.1. Protection of naive GKO recipient mice from *C. parvum* infection was conferred by 8 and 15 days p.i. CD4$^+$ T-cells prepared from tissues of GKO donor mice

Although highly susceptible to *C. parvum* infection, GKO mice resolve the infection in 15 days (Jakobi and Petry, 2008), indicating that IFN-γ independent factors resolve an established infection. CD4$^+$ T-cells play the dominant part of the cellular immune response to

the parasite; they are also contributors of IFN-γ production. Therefore, we studied the contribution of primed $CD4^+$ T-cells isolated from previously infected donor mice to transfer immunity to naive recipient mice by adoptive transfer followed by infection of the recipients. In order to achieve this objective $CD4^+$ T-cells were separated from MLN and spleen of donor mice by MACS technology. The purity of $CD4^+$ T-cells after MACS separation over two successive columns was reached about ≥ 94 % as confirmed by flow cytometry measurement using FITC-coupled acti-CD4 antibody.

At both time points of transfer from GKO mice, days 8 and 15 p.i., 2×10^6 primed $CD4^+$ T-cells were injected i.v. to each naive GKO recipient mouse and the recipients were infected with *C. parvum*. The subsequent data collection on oocyst shedding and analysis of the protection status of recipients were performed as described on previous section (6.3.).
Accordingly, $CD4^+$ T-cells transferred from GKO donor mice at day 8 p.i. conferred protection to *C. parvum* infection. This was shown by a reduced fecal oocyst shedding by the recipients at days 4, 6 and 8 p.i. compared to non-recipient control animals (Figure 28A). Similarly, $CD4^+$ T-cells transferred from GKO donor mice at day 15 p.i. conferred protection to challenge *C. parvum* infection as indicated by a significantly reduced oocyst shedding at days 4, 6 and 8 p.i. compared to non-recipient control animals (Figure 28C).

The average rate of protection from three repetitive experiments was calculated and used to test the statistical significance of protection conferred from challenge infection. Accordingly, the percent protection at days 4, 6 and 8 provided by day 8 MLN $CD4^+$ T-cell recipients was 49 – 64 (Figure 28B). This protection was statistically significant ($p<0.05$) at days 4, 6 and 8 post challenge infection. The protection at days 4, 6 and 8 provided by day 8 spleen $CD4^+$ T-cell recipients was 39 – 46 (Figure 28B); the protection conferred by spleen $CD4^+$ T-cells was statistically significant at days 6 and 8 p.i.

Similar to the day 8 p.i. recipients, the oocyst shedding from recipients of day 15 p.i. $CD4^+$ T-cells was reduced compared to non-recipient control animals (Figure 28C). Day 15 p.i. $CD4^+$ T-cell donors provide similar protection to day 8 cell donors; however, the significance of protection provided by MLN and spleen cells was different between day 8 and day 15 donors. The protection rate provided by spleen $CD4^+$ T-cell recipients ranged from 44 – 56 %, with statistically significant protection from infection at days 4, 6 and 8 p.i. of recipient mice (Figure 28D). MLN $CD4^+$ T-cell donors provided percent protection of 40 – 59 % at days 4, 6

and 8 p.i. However, the protection was statistically significant ($p<0.05$) only at day 8 p.i. (Figure 28D).

6.4.2. Protection of naive IL-12KO recipient mice from *C. parvum* infection was conferred by 5 and 15 days p.i. $CD4^+$ T-cells prepared from tissues of IL-12KO mice

Additionally, the role of $CD4^+$ T-cells with intact IFN-γ gene expression in transferring resistance to naive recipient mice was studied. In order to address this objective, primed $CD4^+$ T-cells were isolated from MLN and spleen of previously infected IL-12KO donor mice as described above and transferred to naive recipient mice followed by infection of the recipients. The time points used for transfer from IL-12KO mice were days 5 and 15 p.i., and the same number of donor $CD4^+$ T-cells (2×10^6) were injected i.v. to each naive IL-12KO recipient mouse.

Accordingly, recipients of both MLN and spleen donor $CD4^+$ T-cells had very much reduced fecal oocyst shedding compared to non-recipient control animals (Figures 29A and C). The protection rate provided by day 5 p.i. spleen $CD4^+$ T-cell recipients ranged from 70 – 73 % at days 4, 5 and 6 p.i. (Figure 29D); as shown at the same figure, MLN $CD4^+$ T-cell donors provided 76 – 86 % of protection at days 4, 5 and 6 p.i. The protection of naive recipients of both spleen and MLN donor cells from infection was statistically significant at all days p.i. (Figure 29D). These protection rates conferred by both spleen and MLN cells were statistically significant ($p<0.05$) at all days post infection (Figure 29B).

Similarly, the protection rate provided by day 15 p.i. spleen $CD4^+$ T-cell recipients ranged from 53 – 83 % (Figure 29D); as shown at the same figure, MLN $CD4^+$ T-cell donors provided 59 – 80 % of protection at days 4, 5 and 6 p.i. The protection of naive recipients of both spleen and MLN donor cells was statistically significant ($p<0.05$) from infection at all days analyzed (Figure 29D).

In conclusion, donor $CD4^+$ T-cells transferred from IL-12KO donor mice at both days 5 and 15 p.i. conferred significant protection to naive recipients from *C. parvum* infection.

6.5. Naive CD4$^+$ T-cells and IELs do not provide protection to naive recipient mice

Further more, we attempted to show the importance of *C. parvum* infection in donor mice for transfer of cellular resistance, i.e. priming of donor cells with *C. parvum* antigens *in vivo* in order to transfer protective immunity by CD4$^+$ T-cells and IELs. This was addressed by transferring similar number of cells as above from naive (uninfected) GKO donor mice to naive recipients using the same experimental protocol.

As depicted on figure 30A, there were similar levels of the fecal oocyst shedding between naive donor cell recipients (spleen and MLN CD4$^+$ T-cells as well as IELs) and non-recipients control animals post infection. Although the recipients of naive IELs had a slightly lower oocyst shedding at days 6 and 8 p.i., there was no statistically significant protection conferred by IELs at these time points (Figure 30B). Therefore, priming of donor cells, as has been shown in the previous sections, was a prerequisite to transfer resistance to recipient mice through donor cells.

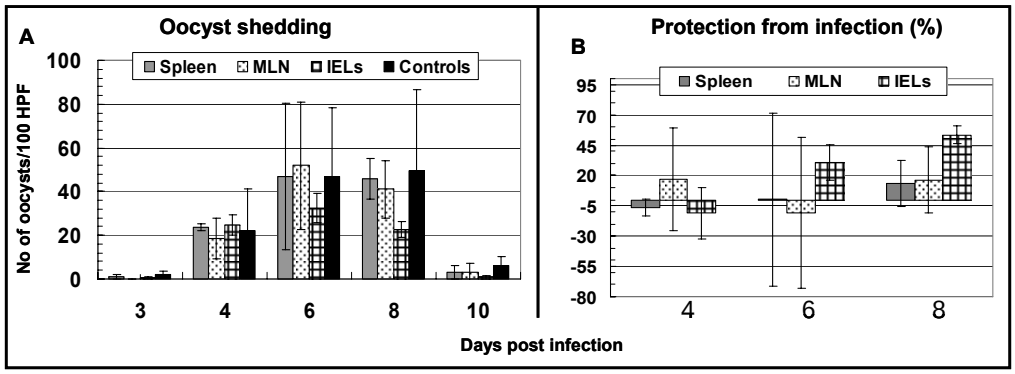

Figure 30. Adoptive transfer of naive IELs and CD4$^+$ T-cells to naive GKO recipient mice.
Recipient animals as well as non-recipient controls were infecetd with 10^6 *C. parvum* oocysts 3 days after transfer of donor cells. (A) Fecal oocyst shedding by recipients of naive donor cells (IELs, spleen, MLN) as well as non-recipient controls at days 3, 4, 6, 8 and 10 p.i. was determined by IFAT as described. (B) Protection rates conferred by transferred cells at days 4, 6 and 8 p.i. Error bars represent standard deviations (SDs) of the mean of 4 recipient animals. Black bars, non-recipient controls; grey bars, spleen CD4$^+$ T-cell recipients; dotted (spotted) bars, MLN CD4$^+$ T-cells recipients; squared bars, IEL recipients. MLN= mesenteric lymph nodes; IEL= intestinal intraepithelial lymphocytes.

6.6. Adoptive transfer of pan T-cells provided equivallent level of protection with that of $CD4^+$ T-cells

6.6.1. Rationale for the experiment and separation of donor cells

Although $CD4^+$ T-cells were the dominant players in resistance to *C. parvum* infection, there could also be a minor contribution by $CD8^+$ T-cells as suggested by some studies (Perryman et al., 1994; McDonald and Bancroft, 1994), but there are no conclusive results to date. As shown in section 6.3., primed $CD4^+$ T-cells contributed significantly in protecting naive recipients from infection, but the oocyst shedding of the naive recipients was not completely cleared showing that the transferred cells did not prevent establishment of infection by the recipients. Therefore, a further question was forwarded to address if there is any involvement of $CD8^+$ T-cells in increasing the protection efficiency of the donor cells.

In order to address this question, pan T-cells, i.e. $CD4^+$ and $CD8^+$ T-cells, were prepared in parallel with $CD4^+$ T-cells from the same MLN and spleen cell suspensions of the same donor mice at day 15 p.i.

The purity of T-cells separated by MACS was assessed by flow cytometry (Figure 31). We also tested the possibility of increasing the purity of total T-cells separated by using two successive MACS separations of the same cell suspension. However, the purity of the T-cells as well as the proportion of $CD4^+$ and $CD8^+$ T-cells in the preparation was similar from one column and second column (Table 9). Therefore, for the subsequent experiments of pan T-cell isolation only one MACS column was used for a given tissue cell suspension, i.e. spleen or MLN.

Figure 31 presented the purity of T-cells isolated from spleen and MLN of IL-12KO mice was about 95 % and 97 %, respectively. From this total T-cell population, $CD4^+$ T-cells represented the majority, about 57 % in the spleen and 57.8 % in the MLN; the remaining cell population was $CD8^+$ T-cells, 37.9 % in the spleen and 39.6 % in MLN. Isolated cells were transferred to two groups of naive recipients: one group receiving 2×10^6 pan T-cells and the other group receiving 2×10^6 primed $CD4^+$ T-cells. Therefore, from 2×10^6 pan T-cells transferred to naive recipients, the number of $CD4^+$ T-cells was 1.15×10^6 and 1.16×10^6 in the preparations of spleen and MLN respectively; whereas, the number of $CD8^+$ T-cells was

7.58×10^5 and 7.92×10^5 in the preparations of spleen and MLN. The $CD4^+$ T-cell population transferred in pan T-cells is lower than that of pure $CD4^+$ T-cells transferred by about 42 %.

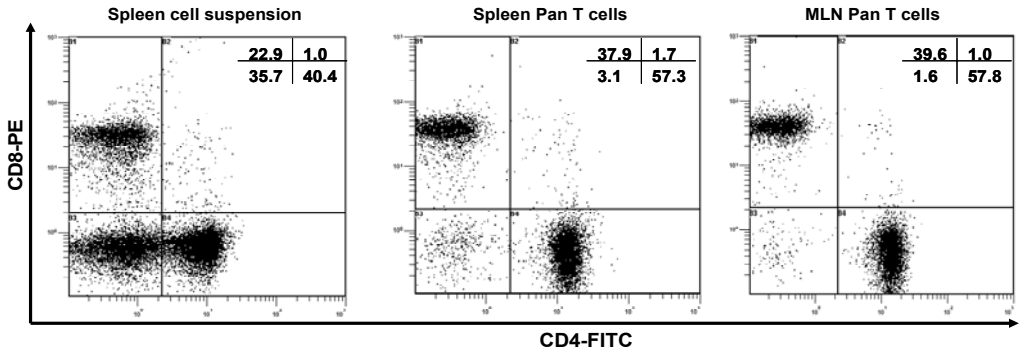

Figure 31. Flow cytometric analysis of the purity and cell populations of pan T-cells separated by MACS technology.

Cell suspensions were prepared from MLN and spleen of mice; pan T-cells were negatively selected using MACS technology. Un-separated spleen cell suspensions as well as separated pan T-cells were stained with FITC-coupled anti-CD4 and PE-coupled anti-CD8 antibodies as described. T-cell populations were determined based on the fluorescence detections of FITC and PE fluorochromes in Beckman COULTER® EPICS® XL TM flow cytometer. The numbers indicate the percentage of cells in the four quadrants of the FACS histogram.

Table 9. Flow cytometry analysis of pan T-cell preparation of IL-12KO mice separated through a single MACS column versus subsequent two MACS columns.

Tissue	Pan T-cell (%)	$CD4^+$ T-cell (%)	$CD8^+$ T-cell (%)
Spleen One column	93.3	55.0	38.3
Two columns	94.4	56.0	38.4
MLN One column	96.5	55.4	41.1
Two columns	97	55.9	41.1

Numbers indicate percentages of cell populations in a preparation, and are taken from a single experiment.

6.6.2. Protection of naive IL-12KO recipient mice from *C. parvum* infection was equally conferred by $CD4^+$ T-cell and pan T-cell donors

Figure 32A presented the fecal oocyst shedding pattern by recipients of pan T-cells versus $CD4^+$ T-cells in parallel compared to that of non-recipient controls. The levels of fecal oocyst shedding by pan T-cell and $CD4^+$ T-cell recipients were similar. In IL-12KO mice, the protection conferred by spleen pan T-cells was 61 – 92 % at days 4, 5 and 6 p.i. Similarly, the

protection conferred by spleen $CD4^+$ T-cells was 75 – 96 % at days 4, 5 and 6 p.i. There was no statistically significant difference in protection rates between recipients of spleen pan T-cells and spleen $CD4^+$ T-cell (P>0.05) (Figure 32B). Similarly, MLN pan T cells provided 72 – 86 % protection at days 4, 5 and 6 p.i.; MLN $CD4^+$ T-cells provided 80 – 96 % protection at days 4, 5 and 6 p.i.. There were no statistically significant differences in protection rates between recipients of spleen pan T cells and spleen $CD4^+$ T-cell donors from spleen as well as MLN (P>0.05) (Figure 32C).

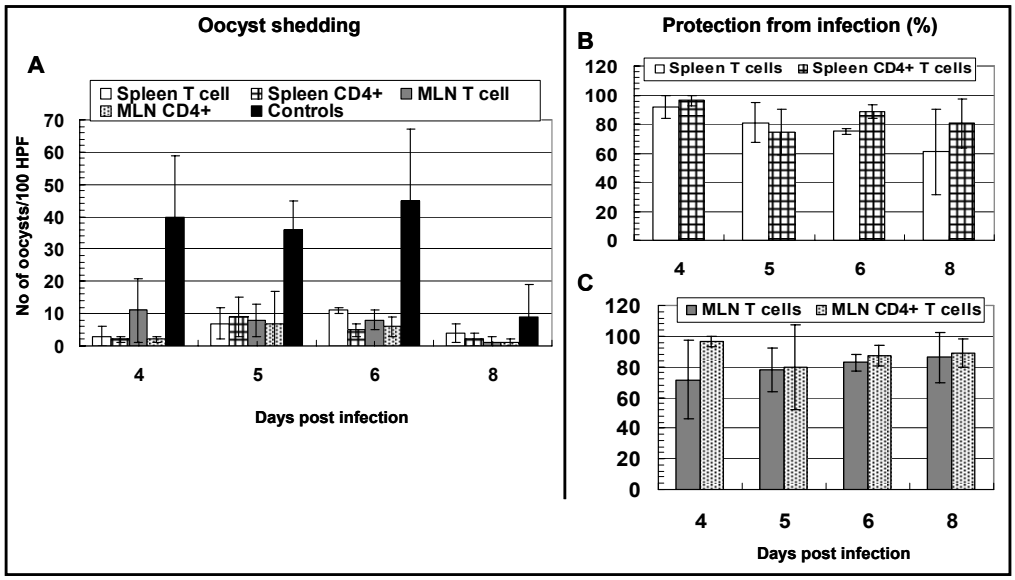

Figure 32. Protection of naive IL-12KO mice from *C. parvum* infection by adoptive transfer of primed pan T-cells and $CD4^+$ T-cells.

Recipient animals as well as non-recipient controls were infected with 10^6 *C. parvum* oocysts 3 days after transfer of donor cells. (A) Fecal oocyst shedding by recipients of day 15 p.i. donor cells (pan T-cells and $CD4^+$ T-cells) as well as non-recipient controls at days 4, 5, 6 and 8 p.i. was determined by IFAT as described. Protection rates conferred by spleen cells (B) and MLN cells (C) at days 4, 5, 6 and 8 p.i. Error bars represent standard deviations (SDs) of the mean of 4 recipient animals. Black bars, non-recipient controls; horizontally-lined bars, spleen pan T-cell recipients; grey slant-lined bars, spleen $CD4^+$ T-cell recipients; dotted bars, MLN pan T-cells; squared bars, MLN $CD4^+$ T-cell recipients. MLN= mesenteric lymph nodes. $P < 0.05$, statistically significant differences in protection between recipients and non-recipients.

6.7. Increasing the number of donor IELs did not affect the level of protection transferred to naive recipients

The role of IELs in transferring resistance to naive recipient mice has been described in section 6.3. In both GKO and IL-12KO recipients, however, there was no complete protection from challenge infection with *C. parvum*. Although there could be many reasons for this, one

potential factor could be the requirement for larger number of cells than used in this study (2×10^6) for complete protection. In order to test this, donor IELs were isolated from IL-12KO mice at day 15 p.i. and transferred to two different groups of mice, each group consisting of 4 mice. One group received 2×10^6 cells and the second group received a double dose, 4×10^6 cells.

As shown on figure 34A, the level of fecal oocyst shedding by the two groups of recipient mice was similar. The protection conferred by 2×10^6 IELs was 81 – 88 % at days 4, 5 and 6 p.i. (Figure 34B). Similarly, the protection conferred by 4×10^6 IELs was 75 – 84 % at days 4, 5 and 6 p.i. There was no statistically significant difference in percent protection between recipients of 2×10^6 and 4×10^6 IELs 8 ($p>0.3$). However, compared to non-recipient control animals both 2×10^6 as well as 4×10^6 IELs provided statistically significant percent protection upon challenge infection ($p<0.05$). This was similar to the results described on section 6.3.2.

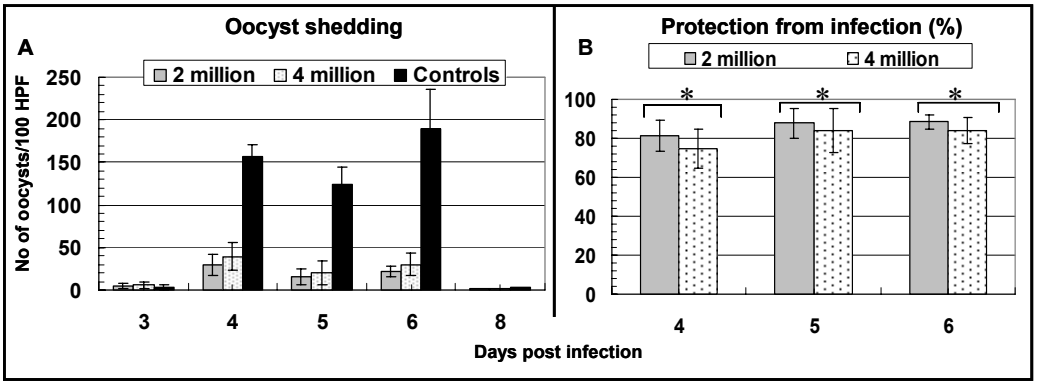

Figure 34. The effect of increasing the number of donor IELs on the level of protection transferred to naive recipients.

One group of mice was injected with 2 million and another with 4 million day 15 p.i. donor IELs. Recipient animals as well as non-recipient controls were infected with 10^6 *C. parvum* oocysts 3 days after transfer of donor cells. (A) Fecal oocyst shedding by recipients at days 3, 4, 5, 6, and 10 p.i. was determined by IFAT as described. (B) Protection rates conferred by transferred cells at days 4, 5 and 6 p.i. Error bars represent standard deviations (SDs) of the means of 4 animals. Black bars, non-recipient controls; grey bars, spleen 2 million IEL recipients; dotted bars, 4 million IEL recipients. Asterices (*, $P > 0.3$) indicate no statistically significant differences.

6.8. $CD4^+$ T-cells from wild type mice 15 days p.i. did not transfer protection to susceptible GKO mice

It has been shown that adult wild type mice are resistance to *C. parvum* infection and shed very negligible oocysts upon infection. As described on the previous sections, primed donor

$CD4^+$ T-cells prepared from infected animals transferred protective immunity to naive recipients, both in GKO and IL-12KO mice. On the contrary, naive $CD4^+$ T-cells did not confer protection of recipients from *C. parvum* infection. Taken together, the results suggested that infection of donor mice was an important criterion for transfer of cellular protective immunity. In order to strengthen these findings, we asked if $CD4^+$ T-cells from the resistant wild type mice could transfer immunity to the susceptible naive GKO mice. This question was addressed by transferring $CD4^+$ T-cells from wild type donor mice at day 15 p.i. to naive GKO mice and challenging the recipient with *C. parvum* infection. However, transferring wild type $CD4^+$ T-cells means also transferring IFN-γ secreting cells to IFN-γ deficient mice (GKO) that could lead to resistance independent of the transferrable cellular immunity. In order to avoid this problem, recipient GKO mice were divided into two groups of antibody treatment. One group was treated with anti-IFN-γ antibody (XMG) at days -2, 0, 2, 4, and 6 in reference to the time of infection (day 0); therefore, any IFN-γ secretion by the donor cells would be neutralized and these mice are basically identical to the GKO mice. This group received wild type donor cells at 3 days before infection, and the remaining procedures were identical to the previous experiments. The other group of GKO mice was treated with control IgG in addition to transfer of wild type donor cells, i.e., they will have IFN-γ secreting donor cells before infection.

Accordingly, there was no difference in oocyst shedding pattern between non-recipient controls and naive GKO recipients with XMG as well as IgG treatments at days 3, 4, 6, 8 and 10 p.i. (Figure 35A). As shown on figure 35B, there was no statistically significant difference in protection rates among the animal groups ($p>0.05$).

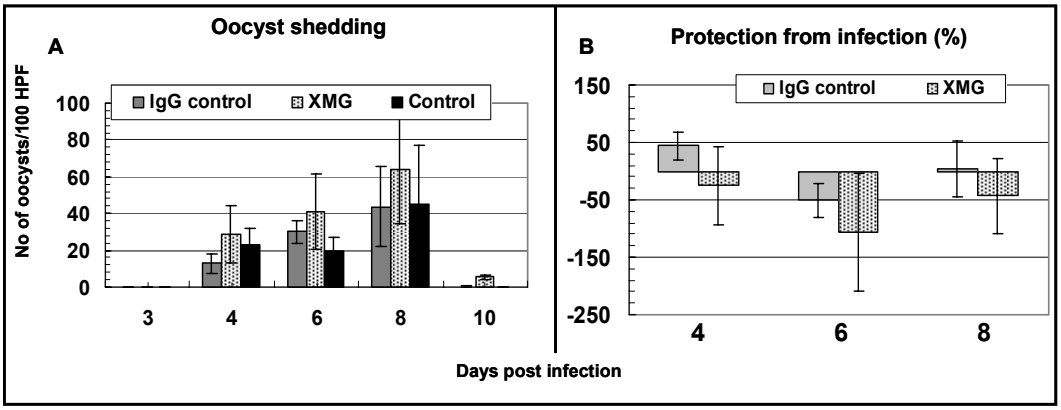

Figure 35. Adoptive transfer of CD4$^+$ T-cells from wild type mice at 15 days p.i. to GKO mice.

Spleen CD4$^+$ T-cells were prepared from infected wild type donors and transferred to two groups of naive GKO recipients as described. One group was injected with anti-IFN-γ antibody (XMG) at days -2, 0, 2, 4, and 6 in reference to the day of infection (0); the second group was injected with control IgG at the same days used for XMG. Recipient animals as well as non-recipient controls were challenged with 10^6 *C. parvum* oocysts 3 days after transfer of donor cells. (A) Fecal oocyst shedding by GKO recipients at days 3, 4, 6, 8 and 10 p.i. was determined by IFAT as described. (B) Protection rates conferred by transferred cells at days 4, 6 and 8 p.i.. Error bars represent standard deviations (SDs) of the mean of 4 animals. Black bars, non-recipient controls; grey bars, IgG control injected; dotted (spotted) bars, XMG injected.

IV. DISCUSSION

7. Dynamics of Th1/Th2 cytokines in interferon-gamma KO (GKO) and interleukin-12p40 KO (IL-12KO) mice during primary and challenge *Cryptosporidium parvum* infections

7.1. Gene expression of Th1 and Th2 cytokines during primary infection in the gut mucosa of GKO and IL-12KO mice

7.1.1. IFN-γ plays a prominent role during early stage of infection

In this study we present data that strengthen the role of IFN-γ during the early innate immune response to *C. parvum* infection, in agreement with Leav *et al* (2005) and Kapel *et al* (1996). However, Ehigiator *et al*. (2005) detected only marginal increased levels of IFN-γ mRNA at day 3 in IL-12KO mice.

IFN-γ is a significant player in the innate immune response against *C. parvum* as shown in nude mice (lacking thymus and T-cells) and SCID mice (lacking both T and B cells). However, the cellular source of the early/innate IFN-γ response to the pathogen, especially in the intestine, has not been clearly identified yet. Production of IFN-γ by a non-T-cell was shown in a study done on adult mice where anti-CD4 treated animals given anti-IFN-γ treatment have an increase infection compared to anti-CD4 treated ones (Ungar et al., 1991). This was further supported by the relative resistance of adult SCID mice to *C. parvum* infection, although deficient in T and B lymphocytes. The resistance of these mice to *C. parvum* infection is IFN-γ-dependent, as shown by IFN-γ-neutralization (Chen et al., 1993b; McDonald and Bancroft, 1994).

In vitro cryptosporidial sporozoites activated splenic NK cells from SCID mice in the presence of macrophages to produce IFN-γ through IL-12 and TNF-α (McDonald and Bancroft, 1998). NK cells from the peripheral blood of humans were activated through IL-15, which is up regulated during *C. parvum* infection (Dann et al., 2005). A T-cell independent source of IFN-γ has also been shown in infections of other intracellular pathogens; the source of IFN-γ in such conditions is NK cells (Bancroft et al., 1991; Hunter et al., 1994).

Nevertheless, evidence that NK cells in the intestine are the source of IFN-γ in T-cell-independent mechanism of immunity is lacking. No effect on reproduction of *C. parvum* in SCID mice treated with anti-asialo-GM1 antibodies, which effectively deplete NK cell numbers *in vivo*, has been observed (Rohlman et al., 1993). In addition stimulation of NK activity by injection of IL-2 did not affect the pattern of infection in SCID mice (McDonald and Bancroft, 1994). It is possible that, in these studies, anti-asialo-GM1 antibodies or exogenous IL-2 was less effective in the gastrointestinal tract than in other organs. Alternatively, another cell type in addition to T-cells and NK cells in the mucosa can produce IFN-γ. SCID mice which retain elements of innate immune system including NK cells and phagocytes were shown to activate macrophages through NK cell secreted IFN-γ in response to a variety of pathogens including *C. parvum* (Bancroft and Kelly, 1994). Recently, the role of macrophages and neutrophils in host resistance during acute *C. parvum* infection has been shown (Takeuchi et al., 2008). Therefore, the early IFN-γ response may also originate from a sub-population of antigen-presenting cells such as macrophages and dendritic cells (Frucht et al., 2001; Das et al., 2001). It has to be determined if there is preferential activation of some types of innate immune cells, i.e. NK cells, macrophages or dendritic cells to produce IFN-γ in response to *C. parvum* infection compared to other infections. Leav *et al* (2005) associated the early increase in IFN-γ response to the IELs of infected mice; particularly the $CD8\alpha^+$ $TCR\alpha\beta^+$ subsets of the IELs. This rapid activation of $CD8^+$ T-cells was described as pathogen unspecific, i.e., not part of the adaptive immune response.

There is a possibility that different cell types of the gut mucosa contribute to the innate immune response by IFN-γ production in a redundant way. However, the exact nature of these cells and their relative contribution to the response remains to be addressed. This can also be done in comparison to the innate cellular players in the resistant wild type mice. As our result indicated, wild type mice were resistant to maintaining *C. parvum* infection, as shown by negligible oocyst shedding, they were infectable but the parasite could not complete the life cycle of the overall. These mice, however, have a slight increase in IFN-γ response at 24 hrs p.i. and, thereafter, the response falls down to uninfected control levels. Identifying the immune cell types involving in this response in wild type versus in IL-12KO mice, and the progression of the response in IL-12KO mice as compared to the cessation of the response in wild type mice may assist in identifying immune mechanisms important for resistance to *C. parvum* infection.

7.1.2. TNF-α may have a regulatory role for the early IFN-γ response

Urban *et al*. (1996) showed that IL-12 confers resistance to *C. parvum* in SCID mice through IFN-γ production, and the role of IL-12 was blocked by administration of anti-IFN-γ. The data in the present study indicated that in the absence of the major inducer, i.e. IL-12 (in IL-12KO mice), there is involvement of IL-12–independent IFN-γ inducer pathways.

The concomitant increase of TNF-α gene expression with that of IFN-γ suggests the involvement of TNF-α as a possible alternative IFN-γ inducer at this early stage. In support of this Lean *et al.* (2006) showed a reduced IFN-γ response in TNF-α-/- mice at the peak of *C. parvum* infection. The absence of any changes in TNF-α in GKO mice during early period in this study indicates that TNF-α was induced in association with IFN-γ response to *C. parvum* infection, as shown in IL-12KO mice, and there may not be other immune mechanisms carried out by TNF-α at least during the early stages of infection.

In summary, the data strengthens the possibility that TNF-α may be a potential regulator of the early IFN-γ response in the absence of IL-12. However, this shows that under normal conditions where IL-12 expression is intact, TNF-α may have simply a redundant function that can be taken over by other factors. This is in agreement with previous reports based on different experimental approaches that showed variable results concerning the role of TNF-α in *C. parvum* infection. Neutralization of TNF-α by anti-TNF-α antibodies showed no effect on infection (Chen et al., 1993a; McDonald and Bancroft, 1994); as well as TNF-α deficient mice controlled infection as effectively as wild type mice (Lean et al., 2006). In contrast, increased expression of TNF-α was reported in *C. parvum* infection *in vitro* and *in vivo* experiments (Seydel et al., 1998; Maillot et al., 2000; Lacroix et al., 2001; Robinson et al., 2001a). Lean *et al*. (2006) showed that TNF-α inhibits *C. parvum* sporozoite invasion of intestinal epitehlial cells *in vitro*.

When we looked at additional potential inducers of IFN-γ, we found that IL-18 did not play a regulatory role in the early IFN-γ response, similar to a previous observation (Lacroix et al., 2001). Lacroix *et al* (2001) reached a similar conclusion using a different approach, where injection of caspase 1 inhibitor in neonates did not modify the IFN-γ response to infection. Caspase 1 is a protease that cleaves pro-IL-18 protein inside cells to release the mature IL-18

form. Furthermore, the present study supplied no evidence for IL-4 as an IFN-γ inducer in the early phase of infection, in contrast to a study by McDonald *et al* (2004) where IL-4 was suggested as a potential inducer of IFN-γ during early period of *C. parvum* infection in BALB/c mice. BALB/c mice, unlike the C57BL/6 mice that we used, preferentially develop Th2 responses (Chatelain et al., 1992; Wakeham et al., 2000) and are less dependent on IFN-γ to control *C. parvum* infection (Mead and You, 1998).

7.2. The pattern of cytokine gene expression in the gut mucosa during a patent primary *C. parvum* infection

In addition to the cytokine response at 24 hrs p.i. discussed above, we studied the dynamics of Th1 and Th2 cytokines at the later key time points selected during the patent infection in the intestine (the site of infection), MLN, and spleen. The results indicated the involvement of both Th1 (IFN-γ, TNF-α, and IL-18) and Th2 (IL-4, IL-10, and IL-13) cytokines in the host's immune response to infection in both GKO as well as IL-12KO mice. The increased cytokine response seen at the peak of infection in GKO was similar with the work of Lacroix *et al*. (2001) who demonstrated most pronounced changes in IL-4 and IL-10 at day 9 p.i. in both neonate and adult groups of GKO mice. The group also showed peak levels of Th1 (IFN-γ, TNF-α, IL-12p40) and Th2 (IL-4, IL-10) cytokines in wild type neonates at the same time point p.i. The present work addresses the pattern of cytokines at a further time point, i.e. at the time of resolution of infection (2 weeks post primary infection) and also at a much further time point, 5 weeks post infection (time of challenge infection). Although data was not presented on this manuscript showing all the cytokines at the time of challenge infection, it has been shown for the expression level of IL-5 and IL-13 to compare the expression levels with that of uninfected controls and post challenge infection. Therefore, in summary, after reaching the peak level of gene expression at the peak of oocyt shedding (GKO) or later (IL-12KO), the expression of cytokines fall down to uninfected control levels.

The logical explanation for this pattern would be that both Th1 and Th2 cytokine mediated immune mechanisms involved during infection coincide with the infection load in the intestine of GKO mice. However, the importance of these responses may reduce once the infection is cleared. Alternatively, the level of cytokine expression may be a mere indication of the number of inflammatory immune cells, phagocytes (notably macrophages neutrophils, and mast cells) and T-lymphocytes, which infiltrate to the infected gut at different time points post infection.

Thus, all of the cytokine responses of the cellular infilitrates may have no relevance to the resolution of infection.

On the other hand, the above explanation may not explain the situation in IL-12KO mice, since the peak of cytokine gene expression was days after the infection load in the intestine was reduced. The data from this model may indicate us that both Th1 and Th2 cytokine mediated immune mechanisms are involved in resolution of infection from the gut.

If there is a similar explanation to be given for the cytokine pattern observed in both mouse models, it may be that the changes in cytokine gene expression may correspond to the time required for the *C. parvum* antigen specific $CD4^+$ T-cells to differentiate and produce cytokines. Based on this scenario, once naive $CD4^+$ T-cells are stimulated with *C. parvum* antigen, the cells undergo expansion by cell division. The progeny $CD4^+$ T-cells produced during this process respond by cytokine expression on the basis of Th1 and Th2 lineage. The peak cytokine gene expression at day 8 may, therefore, indicate the highest number of Th1 and Th2 cells differentiated as effector cells to produce Th1 and Th2 cytokines. During the differentiation process into Th1 and Th2 lineage, there will also be production of effector and memory cells for both lineages. The effector cells produce cytokines and die. The memory cells can survive for long period of time to respond against the second encounter of the antigen. Therefore, after day 8 p.i. in both mouse models there may be a higher proportion of dying effector cells than cytokine producing effector cells.

The early IFN-γ response discussed above continued to rise until reaching peak levels at day 8 and fell down afterwards. Therefore, our results support the importance of this cytokine for prevention the start of infection (wild type mice) as well as decreasing the severity of infection (IL-12KO mice), compared to the high susceptibility of GKO mice. This is in agreement with previous established reports that indicate the importance of IFN-γ in resistance to *C. parvum* infection using various approaches: using IFN-γ neutralizing antibody or GKO mice (Chen et al., 1993b; McDonald et al., 1994; Urban, Jr. et al., 1996; Theodos et al., 1997), increased gene expression in infected mice (Lacroix et al., 2001; Ehigiator et al., 2005; Singh et al., 2005) and increased gene expression in infected calves (Wyatt et al., 1997; Pasquali et al., 1997; Canals et al., 1998; Wyatt et al., 2001). On the contrary, it was suggested that IFN-γ may not have a major role in controlling primary infection in humans (White et al., 2000).

In contrast to the cytokine response to *C. parvum* in the mouse models, the situation in calves and humans, which are natural hosts of the pathogen, is discussed as follows.

In calves at 3 days p.i. expression of IL-10 by gut mucosal lymphocytes was associated with advancement of infection, whereas IL-10 was not expressed in any uninfected control calves (Wyatt et al., 2002). In studies to examine mucosal responses later in the course of infection, during peak clinical disease, naive calves were terminated 6 – 9 days following experimental infection at 3 days of age. In these studies, mucosal T-cells secret increased levels of IFN-γ and IL-12, but no IL-2, IL-4, or IL-10 (Wyatt et al., 1997; Pasquali et al., 1997; Canals et al., 1998). Characterization of the mucosal immune response in ileum of calves infected at 4 days of age and terminated at 13 days of age suggested that a Th1-like response was associated with recovery, as indicated by increased IFN-γ expression by gut mucosal lymphocytes (Wyatt et al., 2001).

Similarly, severe *Cryptosporidium*-associated diarrhea has been described for an HIV-negative individual with IFN-γ deficiency (Gomez Morales et al., 1995). After *in vitro* restimulation, lymphocytes from immunocompetent persons who had recovered from *Cryptosporidium* infection produced IFN-γ (Gomez Morales et al., 1995; Gomez-Morales et al., 1999), whereas lymphocytes from HIV-infected individuals with active cryptosporidiosis, i.e., primary *C. parvum* infection, did not produce IFN-γ (Gomez-Morales et al., 1999). In other studies, IFN-γ was not detected in stools (of infected as well as non-infected subjects) or stimulated PBMC obtained at the time of acute infection (Gomez-Morales et al., 1999; Kirkpatrick et al., 2002; Kirkpatrick et al., 2006b). Stool samples may not be the appropriate specimen to study cytokine protein levels. Generally, the study in human intestine is difficult to conduct since it is not as simple as in mice and calves to get intestinal samples. Even in those cases where studies were done on biopsies taken from HIV/AIDS patients it may be difficult to reach at a conclusion. This is because there is a marked reduction in the number of $CD4^+$ T-cells in such patients and there may be also other opportunistic diseases that co-infect such patients together with *C. parvum*. Therefore, in such cases studying *C. parvum* specific cytokine responses in the gut will face logical problems. Therefore, it may not be realistic to exclude IFN-γ from playing a role in human cryptosporidiosis based on the data obtained from peripheral blood lymphocytes (PBMCs) which may not have *C. parvum* specific T-cell populations or are at low number to release IFN-γ or other cytokine sufficient enough to be detected by ELISA.

A recent review by Pantenburg *et al*. (2008) discussed the importance of IFN-γ-independent mechanisms in resolution of acute infection in humans. Increased expression of IL-15 was noted in the jejunal mucosa of symptomatic individuals without prior sensitization to *Cryptosporidium* (Robinson et al., 2001b). IL-15 expression was inversely correlated with parasite burden. Thus, IL-15 seems to be part of the human innate immune response to *Cryptosporidium*. In *in vitro* studies, IL-15 was shown to activate natural killer cells to eliminate intestinal *Cryptosporidium*-infected epithelial cells (Dann et al., 2005), but there is no independent study for comparison. Neither IFN-γ nor IL-15 were detected in the intestinal mucosa of AIDS patients with chronic uncontrolled cryptosporidiosis (Okhuysen et al., 2001).

The role of IL-12 in the absence of IFN-γ is still unclear because there is no change in its mRNA expression upon infection in GKO mice (not shown). Furthermore, Th2 cytokines were induced *in vivo* at the same level as in IL-12KO mice, showing that IL-12 did not play an inhibitory role on the regulation of Th2 cytokines in *C. parvum* infection. Therefore, the suppression of Th2 cell differentiation by IL-12 may not be an important function in *C. parvum* infection. In IL-12KO mice, the peak of cytokine expression (day 8) was later than the peak of infection (day 4/5), in partial agreement with that of Ehigiator *et al.* (2005).

Moreover, IL-12KO mice showed reduced basal Th1 cytokine levels compared to wild type and even GKO mice which underlines the importance of IL-12 in the development of a Th1 response. In GKO mice, dramatically increased TNF-α and IL-18 levels could not compensate for the loss of IFN-γ in conferring resistance. Therefore, the Th1 response appears to be not effective in the absence of IFN-γ.

According to the traditional Th1/Th2 hypothesis (Mosmann et al., 1986), Th1 cells secrete the Th1 cytokines that promote cytotoxic ($CD8^+$ T-cells) to protect against intracellular infections, whereas Th2 cells secrete Th2 cytokines which activate B-cells to up-regulate antibody production, target parasitic organisms (worms), and also involve in allergy. *C. parvum* infects intestinal epithelial cells and all the developmental stages take place intracellularly, a location difficult to be attacked by antibody-mediated (Th2) immune mechanisms. Although cytotoxic T-cells kill host cells infected with intracellular pathogens, including the *Cryptosporidium*-related *Toxoplasma*, $CD8^+$ T-cells were shown to play only minor or no roles in resistance to *C. parvum*, where as $CD4^+$ T-cells were shown to play predominantly in mouse models.

C. parvum infection is accompanied by an antibody-mediated Th2 response in infected individuals with production of parasite-specific immunoglobulin (Ig) of all major classes (Williams and Burden, 1987; Hill et al., 1990; Peeters et al., 1992). In a recent report from our lab, immunodeficient mice infected with the parasite mounted parasite specific systemic as well as mucosal IgA and IgG responses (Jakobi and Petry, 2008). However, the protective role of antibodies is questionable as high titers of parasite-specific IgG/IgA and mucosal IgA can be found in AIDS patients with chronic cryptosporidiosis (Ungar et al., 1986; Reperant et al., 1994; Cozon et al., 1994). Furthermore, studies employing gene-targeted B-cell-deficient mice indicate that B-cells are not essential for resistance to and recovery from *C. parvum* infections in mice (Chen et al., 2003).
In this regard the role of the Th2 cytokines in resolving an established *C. parvum* infection is not clear. They could induce antibody responses, which have been shown to be non-protective.

The other phenomenon which is not clear is the existence of both Th1 and Th2 cytokine responses during the same period of infection in the adaptive immune response. A key feature of the Th1/Th2 hypothesis is that Th1 and Th2 cells can antagonize each other's actions, either by blocking polarized maturation of the opposite cell type or by blocking its receptor functions (Lafaille, 1998). This is in contrast to the cytokine response against *C. parvum* infection presented in this work. It is clear that the effective immune response to the parasite is IFN-γ and IL-12 based Th1 cytokine mediated.

The major question during the adaptive immune response to the pathogen is what would be the role of the Th2 cytokines, as shown in our study and others. One potential explanation could be that the Th2 cytokines may be induced to keep in balance of the Th1 cytokine response, especially the IFN-γ and TNF-α, from causing exaggerated inflammatory reaction that would worsen the infection. In support of this argument, the protective immune response against *T. gondii*, an Apicomplexan related to *C. parvum*, is mediated by a Th1 response. However, overproduction of Th1 cytokines such as IL-12 and IFN-γ can be detrimental to the host and cause severe pathology that can be lethal. Consequently, oral infection of C57BL/6 mice with *T. gondii* results in acute intestinal inflammation, which has been attributed to IFN-γ production (Liesenfeld et al., 1999) that is dependent on CD40/CD40L interactions (Li et al., 2002). In this condition Th2 cytokines are important to limit the pathology induced by hyper Th1 cytokine response (Nickdel et al., 2001). The Th2 cytokine response in *C. parvum* infection could have similar effects. Therefore, protection could be a result of delicate balance between the

production of Th1, (also pro-inflammatory) cytokines needed to control parasite growth and Th2 (can also be assigned as regulatory) cytokines needed to limit pathology.

In addition to the Th2 cytokine species described in previous publications, the present work demonstrates the importance of IL-13 in *C. parvum* infection for the first time. IL-13 has similar functions as IL-4 such as in Ig-class switching and eosinophil activation. However, the inability of IL-13 to regulate T-cell differentiation and the distinct role of IL-13 in nematode infections demonstrate that IL-4 and IL-13 are not redundant (Chomarat and Banchereau, 1998; McKenzie et al., 1998; Barner et al., 1998; Urban, Jr. et al., 1998).

However, the experimental mouse strain used has a great influence on the immune response to the parasite. In this regard, BALB/c IFN-γKO mice resolved the infection within 15 days whereas C57BL/6 IFN-γKO mice were severely affected and eventually die of infection as shown by other workers (Smith et al., 2000; Lacroix et al., 2001). However, C57BL/6 IFN-γKO mice resolved the infection within 2 weeks at our laboratory conditions (Jakobi and Petry, 2008), allowing us to study the cytokine response of these mice at the time of resolution of the infection. These studies indicate that in BALB/c IFN-γKO mice described elsewhere and C57BL/6 IFN-γKO mice used under our conditions, IFN-γ independent mechanisms can lead to protection. Studies on BALB/c mice indicated that the Th2 cytokines play an important role, such that, IL-4KO mice were susceptible to infection, IL-4 was upregulated at early time point during infection (24 hrs) (McDonald et al., 2004) and was suggested as inducing IFN-γ response in such conditions. The role of IL-4 in C57BL/6 mice is contradictory, since IL-4KO mice had increased levels of oocyst shedding, but only during the recovery phase of infection (Aguirre et al., 1998), but under our lab conditions the C57BL/6 IL-4KO mice were resistant to infection (unpublished data). Also, Campbell *et al.* (2002) demonstrated the refractory of C57BL/6 IL-4KO and IL-10KO mice to *C. parvum* infection, whereas IL-12KO mice were susceptible to infection.

These contradictory findings are directed to the differences in the genetic background of experimental mice used. Therefore, we and others that used mice under the C57BL/6 could not detect an early IL-4 or other Th2 cytokine response.

7.3. Expression of Th1 and Th2 cytokines during primary infection in MLN and systemic lymphoid tissue (spleen)

In contrast to the situation in the ileum we were unable to detect dramatic changes in cytokine mRNA levels in the MLN and spleen, except for IFN-γ, IL-4 and IL-13 in some cases. However, studies from various groups have detected various cytokines after *in vitro* stimulation of splenocytes or MLN lymphocytes with parasite lysate or recombinant protein (Harp et al., 1994; Theodos et al., 1997; You and Mead, 1998; Smith et al., 2000; Ehigiator et al., 2005; Wyatt et al., 2005). The discrepancy may be due to low number of parasite-specific lymphocytes that populate MLN and spleen which may be too small to give clear changes at tissue mRNA level. Furthermore, the data suggest that *C. parvum* is a minimally invasive mucosal surface pathogen. Therefore, an effective clearance of the pathogen may be provided sufficiently by the response to the site of infection, i.e. the gut as shown by the prominent intestinal cytokine responses.

Systemic responses have also been studied in calves. *C. parvum* oocyst antigen extracts were shown to elicit antigen-specific IFN-γ production in peripheral blood mononuclear cells (PBMCs) cultures, specifically on $CD4^+$ T-cells, from calves 5 weeks following experimental infection (de Graaf et al., 1998).

In contrast to the cytokine response, infection is generally accompanied by increased levels of local and systemic antibody levels, although the response was not protective.

7.4. The pattern of Th1 /Th2 cytokine gene expression during challenge infection

The present study further indicates different mechanisms of immune resistance between primary and challenge infections; as well as between GKO and IL-12KO mice upon challenge infection. IL-5 and IL-13 responses were increased in GKO mice, whereas the IFN-γ response was increased in IL-12KO mice. The data in IL-12KO mice correlate with results from humans infected with *C. parvum* where expression of IFN-γ in the jejunum is associated with prior sensitization (White et al., 2000). In 13 of 26 immunocompetent patients, mucosal IFN-γ expression was detected after experimental challenge, a finding similar to previous observations that PBMC from immunocompetent recovered patients express IFN-γ when stimulated *in vitro* (reviewed in Riggs, 2002). All IFN-γ+ cells in mucosal biopsies were confined to the lamina

propria (LP). Most (nine of 13) IFN-γ+ patients were also seropositive to *C. parvum* prior to experimental challenge, indicating previous exposure. Further, most (six of nine) IFN-γ+, seropositive patients did not excrete oocysts after challenge. In contrast, most seronegative individuals did not express mucosal IFN-γ following experimental challenge. It was suggested that mucosal IFN-γ production may be an important part of the memory response and resistance to re-infection in previously exposed immunocompetent individuals (White et al., 2000).

Therefore, in infected hosts with intact IFN-γ response this cytokine may be relevant in mediating resistance during challenge infections. However, in hosts who suffer from immunodeficiency such as in AIDS patients the production of IFN-γ from T-cells may be impaired and sustained levels of IFN-γ by innate immunity in such conditions may be impossible. In such states of immunodeficiency, a Th2 response mediated by IL-5 and IL-13 may be involved although the protection from infection may not be as efficient as IFN-γ-mediated mechanisms as shown in mouse studies (Jakobi and Petry, 2008). However, the absence of differential gene expression of IL-4 and IL-10 during challenge infection unlike that of the primary infection may indicate the lesser importance of IL-4 and IL-10 mediated Th2 responses for resistance after challenge infections. Interestingly, as mentioned before, studies done in IL-4KO and stat6KO mice suggested IL-4-independent roles of IL-13 in host immunity (Barner et al., 1998; Urban, Jr. et al., 1998). One possible function of IL-5 and IL-13 may be through mucosal immune responses such as immunoglobulin A (IgA) production. Our previous report (Jakobi and Petry, 2008) showed a booster IgG and secretory IgA (sIgA) antibody response upon secondary parasite challenge at much higher levels in GKO than in IL-12KO mice. A marked increase in *C. parvum* antigen-specific IgA secretion from intestinal mucosa during challenge infection was also shown by others (Huang et al., 1996; Guk et al., 2003; Guk and Chai, 2007). Mucosally secreted *C. parvum* surface antigen-specific IgA may be an important means of coating the parasite surface and preventing from adhering to the intestinal epithelial cells thus limiting infection. However, as discussed earlier the importance of antibody responses to protect from *C. parvum* infection is doubtful.

In human volunteers, IL-4, like IFN-γ, was found to be expressed by lymphocytes in the gut of infected individuals and was associated with memory immune responses; however, this expression did not correlate with oocyst shedding. Besides, IL-4 was expressed only in a subset of individuals who also produced IFN-γ, so its importance in humans remains unclear (Robinson et al., 2001b).

The gene expression of cytokines in MLN and spleen post challenge infection is generally similar to that of the primary infection in that there were no evident changes and can be attributed to the minimal invasive nature of the pathogen. Furthermore, the immediate induction of cytokine response post challenge infection in the gut in a sustained manner, but not in MLN and spleen, may indicate the importance of immune mechanisms carried out by *C. parvum* primed cells (may also be ascribed as memory cells) at the site of infection rather than at other locations. One can not rule out the presence of *C. parvum* primed cells in other sites, but, can be ascribed to the lower cellular population of these cells in MLN and spleen.

Generally, IFN-γ has been shown to be an important part of both the innate and adaptive immune responses to *C. parvum*; however, the mechanisms of resistance mediated by the cytokine alone are not completely understood. IFN-γ has diverse effects in cell-mediated immune responses. GKO mice have defects on multiple immune cellular functions (Dalton et al., 1993); IFN-γ involves in diverse functions against viruses and microbes (Shtrichman and Samuel, 2001). The cytokine has recently been shown to directly induce resistance to *C. parvum* in human intestinal adenocarcinoma cells (Pollok et al., 2001). Mechanisms suggested for IFN-γ-mediated enterocyte resistance include reduced host cell permissiveness to parasite invasion and/or modification of intracellular Fe^{2+} concentrations, possibly leading to decreased intracellular development (Pollok et al., 2001). Similarly, IFN-γ reduced the intracellular iron pools within *Salmonella* infected macrophages, thus restricting the acquisition of iron by engulfed bacteria while strengthening macrophage immune response functions. (Nairz et al., 2008). Activation of macrophages with IFN-γ not only upregulates antimicrobial effector mechanisms but also modulates iron regulatory proteins such as ferroportin to reduce intracellular iron availability (Collins, 2008).

IFN-γ is also important in the production of several immune components essential for the control of *C. parvum*, such as NO (Leitch and He, 1999) and TNF-α (Lacroix et al., 2001). The activation of tumour necrosis factor-α (TNF-α) expression via up regulation of its transcription factor NF-κB by IFN-γ has been suggested as one potential mechanism of IFN-γ action in *C. parvum* infection (Lean et al., 2002). Additionally, IFN-γ may confer protection against *C. parvum* through recruitment of effector T-cells and macrophages to sites of infection via the production of the non-ELR (Glutamic acid-Leucine) C-X-C chemokines and the MIP-1β (Macrophage inflammatory protein-1β) and RANTES (Regulated upon activation, normal T-

cell expressed and secreted) C-C chemokines (Lacroix-Lamande et al., 2002) that attract the inflammatory cells to the site of infection.

8. The role of interleukin-18 in resistance to *C. parvum* infection

In this study, IL-12 has been identified as an important regulator of IFN-γ gene expression when gene expression of IFN-γ was compared between non-infected wild type mice and IL-12KO. However, the presence of other inducers was evident in IL-12KO mice upon infection.
Interleukin-18 (IL-18) was first discovered as IFN-γ-inducing factor; subsequently, the cytokine was shown to enhance IFN-γ production by a variety of cells (Okamura et al., 1995b; Okamura et al., 1998; Dinarello, 1999). The cytokine has also been shown as an important inducer of IFN-γ during infection with fungi and bacteria (Kawakami et al., 2000; Huang et al., 2002; Kinjo et al., 2002).

The increase in IL-18 mRNA in IL-12KO was seen only after the start of oocyst shedding (day 3); mice deficient in IL-18 have also been shown to be susceptible to *C. parvum* infection (Ehigiator et al., 2007). Therefore, it was logical to address the possible involvement of IL-18 in inducing IFN-γ expression in this part of the infection.
The anti-IL-18 neutralization studies indicated a divergence on the effects between mRNA and protein levels of IFN-γ. Serum IFN-γ level was detected only at the peak of infection (day 7) in mice not treated with antibody, indicating a potential role of IL-18 in IFN-γ induction at least systemically, which was not shown at the mRNA level from the spleen as well as intestine.

In support of the results in this work, IL-18 neutralization reduces or eliminates IFN-γ release from spleen cells of mice (Mastroeni et al., 1999). *In vivo* neutralization of IL-18 causes a reduction in circulating IFN-γ levels. Similar results obtained with the *Cryptococcus neoformans* and *Yersinia enterocolitica* mouse models showed that *in vivo* neutralization of IL-18 impairs host resistance to infection (Kawakami et al., 1997; Zhang et al., 1997; Bohn et al., 1998).

8.1. Differential expression of IL-18 in the gut of *C. parvum* infected mice

As shown in the present work, mRNA expression of IL-18 in the ilea of mice increased upon *C. parvum* infection starting from day 3 p.i. onwards, peaking at day 8 p.i. and dropping to

background levels after resolution of infection. This suggests that IL-18 plays a role in the adaptive immune response to *C. parvum* infection, and the main site of function could be the intestine. Absence of changes in gene expression during the challenge infection suggests that IL-18 is associated with resistance to primary infection but not against second encounter of the pathogen.

In addition, the differential IL-18 gene expression in the intestine of GKO, IL-12KO and wild type mice is interesting. The data show that there is a reduced IL-18 basal expression level in IL-12KO mice compared to both wild type and GKO mice; and the GKO mice have a higher IL-18 basal level than both wild type and IL-12KO mice and mount higher level upon infection. Taken together, one may draw the importance of IL-12 in the basal expression of intestinal IL-18 as well as in IL-18 response to *C. parvum* infection. The data may also indicate the involvement of IL-18 in compensating for related functions to that of IFN-γ, although such possible roles are not clear yet. One possible function that could be shared by both IFN-γ and IL-18 is inhibition of the development of *C. parvum* in infected intestinal epithelial cells, although the molecular mechanisms of actions could be different for IL-18 and IFN-γ. In an *in vitro* experiment, exogenous IFN-γ directly inhibited the development of *C. parvum* in cultured enterocytes, where inhibition of parasite invasion and depletion of intracellular iron were identified as possible mechanisms of action (Pollok et al., 2001). McDonald *et al*. (2006) showed that one potential protective role of IL-18 could be through inhibition of intracellular development of the parasite through IL-18 mediated expression of antimicrobial peptides.

Therefore, the previous studies combined with the present data indicate that there may be potential collaborative and/or independent actions of IFN-γ and IL-18 at the level of infected intestinal epithelial cells. It is established that intestinal epithelial cells are important producers of IL-18 under normal physiological conditions and the constitutive expression of IL-18 by IECs may have an important role in mucosal immunity (Takeuchi et al., 1997). However, the status of IL-18 production during infection by the infected cells themselves compared to the neighboring uninfected cells is unknown. Additionally, the possible intracellular interaction between the developing *C. parvum* stages and their antigens and the subsequent induction of host immune genes by the infected cells themselves as well as the healthy nearby epithelial cells is not clear yet. It is possible that the induction of IL-18 expression may be modulated by the developing parasite during the initial days p.i. This is supported by the start in rise of the IL-18 mRNA from day 3 p.i. on wards (the time of start in oocyst shedding) in both GKO as well as

IL-12 KO mice. The parasite has already finished one replication cycle within 3 days p.i. and then the IL-18 mRNA starts to rise.

Therefore, in future one important area of investigation would be studying the molecular interactions between the developing parasite inside epithelial cells, and the epithelial cell gene modulation during this early period of infection as well as throughout the patent infection. The possible involvement of IL-18 in apoptosis of infected versus non-infected intestinal epithelial cells is very interesting to study. It is known that *C. parvum* modulated the host cell apoptosis pathway. Thus, the parasite may possibly modulate the expression of IL-18 in intestinal epithelial cells for its own advantage.

8.2. Effect of *in vivo* neutralization of IL-18 during *C. parvum* infection

8.2.1. *In vivo* neutralization of IL-18 increases the susceptibility of mice to infection

Neutralization of serum IL-18 protein with monoclonal anti-IL-18 antibody showed an increased susceptibility of both GKO and IL-12KO mice to *C. parvum* infection, IL-12KO being highly affected. However, both mice resolved the infection within 2 weeks the same as mice with unblocked serum levels of IL-18, indicating that IL-18 plays an import role in decreasing the severity of infection but does not affect immune mechanisms that resolve the infection.

The neutralizing efficiency of the antibody used was remarkable. In GKO mice, serum IL-18 was completely neutralized; in IL-12KO mice it could only be detected around the peak of infection. However, the GKO mice were injected with a dose twice that of IL-12KO mice. This was optimized in preliminary experiments using the oocyst shedding pattern as a measure of the effective dose to use for an experiment. The use of higher dose of anti-IL-18 was acceptable considering the higher intestinal basal IL-18 mRNA in GKO mice than that of IL-12KO mice. However, when we compare the serum levels of IL-18 protein between these two mice, one can see interesting differences. Uninfected mice have similar serum levels of IL-18; in contrast upon infection IL-12KO mice mounted a much higher level starting from day 4 p.i. and the peak level was greater than three times higher than the peak levels of GKO mice. This is in sharp contrast to the intestinal gene expression pattern of IL-18 mRNA.

One further point to forward is the effect of the antibody on neutralizing intestinal IL-18 protein content. Considering the high IL-18 production by the intestinal epithelial cells, and also the increase in the gut during infection, neutralizing IL-18 in the gut microenvironment would be very important. The access of the gut IL-18 content to the neutralizing antibody was not determined in this study; however, it's an ongoing objective of the laboratory to procure appropriate methods to study the protein content of IL-18 and IFN-γ in the gut, the neutralizing effect of intraperitoneal (i.p.) injected antibody on gut IL-18 and IFN-γ proteins, etc.

Our result is the first report on the role of IL-18 in *C. parvum* infection using a neutralizing antibody. Similar roles for IL-18 were reported in other infections. A study using *in vivo* neutralization of IL-18 showed that IL-18 is required for the control of bacterial growth in mice infected intravenously with a virulent *Salmonella* (Mastroeni et al., 1999); similar study was done in *Yersinia* (Bohn et al., 1998) where IL-18 was shown to mediate resistance in an IFN-γ-dependent as well as IFN-γ-independent mechanisms. Further *in vivo* studies have shown the importance of IL-18 in the protective immune response to a number of bacterial and fungal infections including *Chlamydiae* (Lu et al., 2000), *Shigella* (Sansonetti et al., 2000), and *Cryptococcus* (Kawakami et al., 1997; Zhang et al., 1997).

8.2.2 Influence of anti-IL-18 neutralizing antibody on gene expression of cytokines

The fact that in GKO mice, IL-18 gene expression was increased during infection and also anti-IL-18 treatment leads to increased parasite shedding suggests a role of IL-18 besides the induction of IFN-γ. The present data suggest a potential role of IL-18 in *C. parvum* infection as regulator of Th2 cytokines so as to balance Th1/Th2 responses to infection. This was shown by increased splenic IL-4 and IL-13 (also locally) mRNAs in anti-IL-18-treated and infected IL-12KO mice which were the most affected by antibody-treatment. Slight increment of IL-4 and IL-13 was also seen in GKO mice with IL-18 neutralization. This regulatory role of IL-18 seems to be restricted to IL-4 and IL-13 since there was no dysregulation of other Th2 cytokines studied (data not shown). This was in agreement with the situation with intestinal nematode infection where IL-18 was demonstrated to work as a direct regulator of Th2 cytokines but not as an IFN-γ-inducing cytokine (Helmby et al., 2001; Liu et al., 2006).
The anti-IL-18 neutralization studies indicated a divergence between local and systemic effects on Th2 responses.

This new role of IL-18 in *C. parvum* resistance is very likely, because in IL-12KO mice there is no IL-12 which can inhibit the expression of Th2 cytokines and IL-18 seems to compensate this function of IL-12. On the other hand, the data also indicate that over expression of Th2 cytokines is very detrimental to the host during *C. parvum* infection as shown by the increased infection load when Th2 cytokines are over expressed. Therefore, a delicate balance between the Th1/Th2 cytokines is crucial for clearance of the infection. The reason that GKO mice, where IL-12 gene is intact but unresponsive to infection, are also affected by IL-18 neutralization may indicate the involvement of both IL-18 and IL-12 in inhibiting the Th2 cytokines to keep the Th1/Th2 balance, but the basal expression level of IL-18 may be sufficient together with IL-12 for this function.

IL-18 is a multi-functional cytokine (Nakanishi et al., 2001). Therefore, there could be more immunological functions of IL-18 in *C. parvum* resistance to be revealed. Recently, it has been demonstrated in an *in vitro* model that IL-18 leads to an increased expression of the antimicrobial peptides cathelicidin LL-37 and α-defensin-2 in intestinal epithelial cells leading to a reduction of *C. parvum* replication (McDonald et al., 2006). Furthermore, IL-18 produced by epithelial cells activates intraepithelial lymphocytes (Okazawa et al., 2004).

From these interesting observations one can conclude that IL-18 may have different immunological functions in the gut mucosa and systemically in the context of resistance to *C. parvum* infection. In the gut mucosa, IL-18 may have multifaceted roles targeted towards the parasite-epithelial cell interaction, possibly through antimicrobial peptides or in some yet unknown mechanisms. The systemic immune functions of IL-18 may be somewhat different; regulating serum IFN-γ level, Th1/Th2 cytokine balance are functions clearly shown in this study. The systemic functions of IL-18 may be similar to that of IL-12 since the IL-12KO mice were highly affected by anti-IL-18 treatment, as well as serum level of IL-18 is much higher in IL-12KO mice upon infection. Therefore, IL-18 may compensate some functions of IL-12 systemically. Since the spleen mRNA level does not reflect the effect on serum IFN-γ level, IL-18 may regulate post-transcriptional mechanisms of IFN-γ synthesis systemically.

9. Adoptive Transfer of immunity from *C. parvum* infected to naive mice

Transfer of immunity from *Cryptosporidium* primed mice to naive mice, mostly SCID mice, has been carried out to address certain immunological questions. As mentioned earlier, adoptive transfer was used to show the importance of T-cells and $CD4^+$ T-cells in resistance to the pathogen (Mead et al., 1991a; McDonald et al., 1992; Chen et al., 1993a; McDonald and Bancroft, 1994; Perryman et al., 1994).

The present study aimed to investigate the possibility of transferring protective cellular immunity to naive animals with intact cellular immunity, except lacking IFN-γ or IL-12. Besides, the time of development of this transferrable cellular immunity in reference to the patent *C. parvum* infection was studied. The relative contribution of T-cells of the gut mucosal versus systemic immune compartments in resistance to *C. parvum* was investigated. The importance of prior infection of donors (priming) was stressed as an important criterion in success of transferring immunity. Addressing these questions will likely forward our understanding of the host immune response to the pathogen, points out further questions to be addressed and, therefore, paves the way for immunological approaches to control and prevent infection in susceptible hosts.

9.1. Isolation of intestinal intraepithelial lymphocytes (IELs) from the mouse small intestine

A number of strategies have been developed for obtaining enriched preparations of IELs from mouse small intestine (Davies and Parrott, 1981; Shires et al., 2001; Wang et al., 2004; Montufar-Solis and Klein, 2006). In choosing among the different IEL isolation protocols, one has to consider factors such as the purity and viability of IELs, time of preparation, adequacy of IEL yield (for evaluating on light microscope, flow cytometry, and transfer to four recipient animals that we used). In this regard, although some workers obtained highly pure IELs using MACS sorting (Shires et al., 2001; Wang et al., 2004) or double Percoll step gradient (Montufar-Solis and Klein, 2006), such approaches may be impractical on daily basis and may produce low overall cell yield.

The methodology applied for isolation of IELs in this work was based on Davies *et al*. (1981) and Lefrancois and Lycke (2003) with some modifications such as use of filtration of the cell

suspension over gauze and Nylon wool column before the step of Percoll step gradient centrifugation, aimed at removing dead cells and debris but enriching the T-lymphocyte cell population. Nylon wool filtration has been applied by many workers to separate T-lymphocytes from B-lymphocytes and other adhering cellular components of lymphoid tissues (macrophages and dendritic cells) (Trizio and Cudkowicz, 1974; Handwerger and Schwartz, 1974). The combined use of Nylon wool and Percoll gradient centrifugation has been applied by other workers as well (Montufar-Solis and Klein, 2006). Whereas, some have used Nylon wool filtration followed by purification of IELs over a density separation medium such as Lymphocyte-M (Lyscom and Brueton, 1982). The average IEL yield and viability of cells obtained in this work was similar to other workers (Lyscom and Brueton, 1982; Adjei et al., 2000).

9.2. Isolation of $CD4^+$ and Pan T-lymphocytes from spleen and MLN

Lymphocytes located at different immune tissues of the animal, gut mucosa, MLN and spleen were isolated and transferred to recipients in parallel. Therefore, one could study the relative importance of T-cells located in the gut mucosa and systemic immune locations in protecting from *C. parvum* infection.

This may have further implications such as in designing immunotherapeutic or vaccination strategies to prevent *C. parvum* infection; it is desirable to know the importance of the gut mucosal versus the systemic immune systems in clearing the parasite from the body. *C. parvum* is a gut mucosal pathogen infecting intestinal epithelial cells and the whole intracellular developmental process occurs in gut epithelial layer. Furthermore, there is no any report of crossing of *C. parvum* from the gut mucosal surface to the underlying intestinal layers where there are blood vessels that could carry the parasite to the systemic circulation. Therefore, it was desirable to study the importance of the gut mucosal versus the systemic immune systems during resolution of *C. parvum* infection. Conventional vaccines that aim to elicit systemic antibody production against *C. parvum* antigenic structures may not get access to the gut mucosal location of *C. parvum* to kill the parasite. Since the parasite is also not migrating to the blood circulation the antibodies elicited by conventional vaccines may not be fruitful and to date such attempts have failed. On the other hand, it may be possible that *C. parvum* specific T-cells could migrate from the gut mucosa to the systemic location such as in the spleen, because lymphocytes are migrating cells (Millan et al., 2006).

9.3. Differential migration of $CD4^+$ T-cells to the gut mucosa between GKO and IL-12KO mice during infection

In this study, we demonstrate differences between the two mouse models in the phenotypic distribution of mucosal T-cells (IELs) at the peak versus at the resolution of infection. The data show that there were no marked changes in the mucosal IEL population in IL-12KO mice at the peak as well as resolution of infection compared to uninfected controls, except a slight increase in the $CD8^+$ T-cell population at the resolution of infection. However, there was increased migration of $CD4^+$ T-cells in the IEL compartment of GKO mice at the peak of infection compared to the resolution of infection and uninfected controls; the increase was 100 %. The reason that we did not see changes in cell number in IL-12KO mice could be because of the minimal mucosal inflammation in these mice that did not lead to clear changes in cell number infiltrates to the mucosa. The present result was in partial agreement to previous reports on mouse studies. In immunocompetent ICR neonatal mice, there was an increase of $CD4^+$ IEL by day 7 p.i. and an increase in $CD8^+$ IEL by day 16 p.i. (Chai et al., 1999). In contrast, Guk ***et .al.*** (2003) reported an increase in the $CD8^+$ IELs in the gut of neonatal wild type mice infected with *C. parvum*.

Redistribution of local $CD4^+$ and $CD8^+$ T-lymphocytes normally dispersed throughout intestinal mucosa towards the epithelial surface can occur within 24 h in response to *C. parvum* infection, as demonstrated by experimental inoculation of bovine ileal explants with oocysts (Wyatt et al., 1999). The phenotype of ileal IELs from calves 3 days p.i., prior to onset of clinical disease, showed no significant differences from un-infected controls in $CD4^+$ IELs, but showed an early trend towards increased expression of CD8 and γδTCR (Wyatt et al., 2002).

During peak clinical disease, 5 – 8 days p.i., in calves ileal IEL were populated with significantly increased numbers of $CD8^+$ αβ+ T-cells and activated (CD25+/IL-2Rα+) $CD4^+$ T-cells compared to age-matched uninfected controls (Wyatt et al., 1997; Pasquali et al., 1997). Upon complete recovery of infection, 13 – 19 days p.i. of calves, both $CD4^+$ and $CD8^+$ T-cells in ileal mucosa had reverted to the normal phenotype, being similar to those in uninfected age-matched controls (Wyatt et al., 1997; Abrahamsen et al., 1997). These findings suggest that $CD8^+$ T-cells, in addition to $CD4^+$ T-cells, may have a key role in protection of calves, unlike the case in rodent models.

The T-cells in the IEL population have been shown to be activated specifically by infection with mucosal pathogens (McDonald, 1999). An increase in the CD8αβ+ T-cells of the gut IELs have been reported in a number of intracellular infections (viruses, bacteria and protozoa), such as reovirus (Cuff et al., 1993), lymphocytic choriomeningitis virus (LCMV) (Sydora et al., 1996), simian immunodeficiency virus (SIV) (Couedel-Court et al., 1997; Mattapallil et al., 1998), *Listeria* (Emoto et al., 1996) and *Toxoplasma* (Chardes et al., 1994). After intracellular infection of the mucosa, isolated IELs might exhibit antigen-specific MHC class I restricted lysis of either infected cells or cells modified to express antigens of the infectious agent. An increase of combinations of IEL subsets at various periods post infection were also observed in other pathogens such as *Eimeria* (Findly et al., 1993) and *Encephalitozoon* (Moretto et al., 2004).

An increase in the $CD8^+$ T-cells and also cytotoxic killing of infected cells by activated IELs in many intracellular pathogens is in sharp contrast to the situation in *C. parvum* infection, except probably in calves where cytotoxicity have to be vividly demonstrated.

9.4. Homing of adoptively transferred IELs to gut mucosal and systemic immune tissues

As one of the prerequisites for successful transfer of cellular immunity to recipients, trafficking of the transferred donor cells to the immune tissues of the recipients was determined. After i.v. injection of the donor cells types, donor cells could settle easily in the spleen of recipients passively through blood circulation, however, IELs have to traffic (or, migrate) actively to the intestine epithelium. Therefore; only homing of IELs was studied. Accordingly, we confirmed that i.v. transferred *C. parvum* primed donor IELs were identified in the gut of recipients within 3 days post transfer. Based on the PCR assay, the relative concentration of donor cell DNA within the recipient IEL population was approximately 1 ng donor cell DNA in 10,000 ng recipient cell DNA. Although the donor IELs preferentially traffic to the gut, some cells were identified in the spleen too. However, none of primed IEL DNAs was identified from other mucosal immune compartments, MLN and PPs. This indicates the lower frequency of primed donor IELs trafficking to these sites, which could not be detected by the PCR assay applied. Previously, Buzoni-Gatel *et al* (1999) studied homing of *Toxoplasma* primed IELs using radioactive isotope labelling and fluorescence assay with 5-and-6-fluorescein diacetate, succimidyl ester (CFSE). In this study, antigen-primed IEL home to the intestine and other host

organs. Two hours after the i.v. injection of ^{51}Cr-labeled primed IEL, 22 % of the total radioactivity was detected in the small intestine of the recipient mice. Increased radioisotope activity was also observed in spleen (15 %) other tissues but 2 % or less in other gut immune compartments, Peyer's patches (<1 %), MLNs (2 %). In comparison, Ag-primed splenocytes traffic preferentially to the spleen rather than the intestine since following splenocyte transfer, most of the radioactivity was recovered in either the spleen (37 %) or the lungs (35 %); whereas only 5 % of the splenocyte radioactivity was detected in the intestine. One day after transfer 17 % and 20 % of *Toxoplasma* primed IELs were detected in PPs and MLNs respectively.

This is in contrast to the lower detection of *C. parvum* primed IELs in MLN and PPs. The differences could be due to the time differences after transfer, 1 day versus 3 days, which may indicate a continuous migration of transferred cells among the lymphoid tissues. Therefore, the actual proportion of cells captured at a given time point post transfer may not be the same picture at another time. The other possibility could be due to differences in the pathogenesis of the two pathogens, *C. parvum* and *Toxoplasma*, both of which start with infecting the gut epithelial cells, but after that *Toxoplama* is also known to disseminate to other organs of the body. Such kind of trespassing of the intestinal mucosa is not reported for *C. parvum*. This difference could lead to the concentration of *C. parvum* primed IELs in the gut, where they are relevant, whereas *Toxoplasma* primed IELs could be required in other sites too.

However, in the present study naive IELs trafficked to the intestine at almost similar frequency to that of MLN and PPs. This is in partial agreement with the report of Buzoni-Gatel *et al* (1999) who demonstrated 20 % of the primed IELs in the intestine, whereas <10 % of the unprimed IEL traffic to this organ, and 1 % and 30 % of naive IELs primed to PPs and MLN, respectively.

9.5. Adoptive transfer of primed IELs provided protection to naive recipient mice from *C. parvum* challenge infection

The present work addressed two important concepts on adaptive mucosal cellular immunity to *C. parvum*. 1) The requirement for IFN-γ mediated effector functions of gut mucosal IELs in resistance to the pathogen during the acute phase, i.e. at the peak, of infection.
2) The sufficiency of IFN-γ-independent effector functions of IELs for the resolution of the infection.

The first issue was addressed in two types of transfer experiments. First, transferring IELs from GKO day 8 p.i. donors to naive GKO recipients did not protect recipients from infection. This may indicate the absence of established protective cells in the intestine of GKO mice by the time of peak of infection, which could be due to the requirement for IFN-γ mediated functions of the transferred cells.

Second, transferring IELs from IL-12KO day 5 p.i. donors to naive IL-12KO recipients markedly reduces the fecal oocyst shedding and conferred significant protection upon infection. This may indicate the presence of established protective IELs in the intestine of IL-12KO mice by the time of peak of infection. This could indicate the importance of IFN-γ-mediated functions of IELs in protection against *C. parvum* during this part of the primary infection.

In summary, although numerically a relatively higher number of T-cells and specifically $CD4^+$ T-cells were transferred to GKO day 8 p.i. recipients than the IL-12KO day 5 p.i. recipients (Figures 25), the protective quality of the cells was insignificant in GKO day 8 recipients. This indicates a factor absent in GKO mice, but present in IL-12KO mice, and that is IFN-γ. Therefore, T-cells in the gut mucosa, i.e., IELs, contribute to resistance to *C. parvum* infection during the adaptive immune response through IFN-γ production.

Referring back to the intestinal cytokine gene expression pattern during infection, there was a peak Th1/Th2 cytokine mRNA expression in the intestine of GKO mice at day 8, but these increased cytokine levels are not shown to be protective by the adoptive transfer experiments. This may indicate that the high number of $CD4^+$ T-cells that infiltrate the infected intestine may be producing cytokines that promote pathology rather than protection; or these cytokine responses are not sufficient to confer protection by themselves. The cytokine environment in GKO mice at day 8 p.i. did not promote protective mechanisms. Therefore, the presence of IFN-γ on the side of Th1 cytokine response is critical for resistance.

In order to further substantiate the present findings, supportive experiments could be done by using the IL-12 day 5 p.i. donor cells and treating recipient mice with anti-IFN-γ antibody (XMG) to neutralize the IFN-γ component of these cells. Such experiments are expected to produce similar results as GKO day 8 p.i. recipients where there would be no protection upon challenge infection.

Similarly, the second issue was addressed in two types of transfer experiments. Donor IELs were used to transfer cellular immunity from both GKO and IL-12KO mice at the resolution (recovery) of infection, i.e. day 15 p.i., to naive GKO and IL-12KO recipients. Unlike the cells transferred from the peak of infection, cells transferred from recovered animals (both GKO and IL-12KO) conferred cellular immunity to naive mice. The recipients had a markedly reduced fecal oocyst shedding and significant protection from challenge infection. These results suggest that there are immune mechanisms mediated by gut mucosal T-cells (IELs) that resolve infection in the absence of IFN-γ as shown by the protection of GKO day 15p.i. recipients. IFN-γ, which was critical component of cellular immunity during the peak of infection, may not be an absolute requirement for resolution of infection although it can play some minor roles, as shown by the higher percent of protection of the IL-12KO day 15 p.i. recipients.

Therefore, we can conclude that the role of IFN-γ in the gut mucosal immune response to *C. parvum* is during the innate immune response, shown by early gene expression of the cytokine; as well as during the adaptive immune response which is contributed by the T-cells of the gut mucosa (IELs). However, the cytokine may not be required for resolution of infection as shown by the resolution of the infection in the GKO mice as well as the transfer of protective cellular immunity (T-cells) from the recovered GKO mice to naive mice.

Generally, in both GKO and IL-12KO donor IELs at both time points of transfer, there was a substantial proportion of the $CD8^+$ T-cell component, but we did not perform experiments associating the role of this large $CD8^+$ T-cell population to the transferrable cellular immunity. Although the $CD4^+$ T-cell population is relatively smaller in number they are expected to contribute to the observed protective immunity. First of all, the changes in number of $CD4^+$ T-cells at the peak of infection in GKO were not observed in $CD8^+$ T-cells in both mice. This change was a 100 % increase of $CD4^+$ T-cells from uninfected controls and also compared to recovered mice. There was no such influx of $CD8^+$ T-cells during the infection. Although this influx did not protect the recipients that is because of the lack expression of an important factor in the cells, but simply shows us that during active infection these cells are drawn to the site of infection.

However, the important factor for protection is the quality of the cells, i.e. the presence of *C. parvum* antigen specific cells in the IELs. These cells would not be huge in number but their

response could be robust. Normally, IEL preparation from a naive mouse is composed of higher proportion of $CD8^+$ T-cells than that of $CD4^+$ T-cells. This was also evident in the present work. Therefore, considering these argument it is not possible to associate the higher percentage of $CD8^+$ T-cells in IEL preparations to the transferred protection. It is only a small number of the transferred cells that are specific to the pathogen which respond upon challenge infection.

Earlier experiments conducted could also support the role for $CD4^+$ IELs. McDonald *et al.* (1996) used the gastric parasite *C. muris*, to show that immunity could be adoptively transferred to immunocompromised SCID mice using small intestinal IEL donors from animals recovered from infection. The protection obtained was predominantly associated with the donor $CD4^+$ T-cell population, as removal of these cells before transfer abrogated immunity. Adjei *et al.* (2000) also showed protection of SCID recipient mice from challenge *C. parvum* infection by adoptive transfer of primed IELs from BALB/c mice 60 days p.i.

For comparison, studies by Buzoni-Gatel *et al.* (1997) showed that immunity against *Toxoplasma* infection could be transferred between immunocompetent mice using $CD8^+$ donor IELs from infected mice.

9.6. Adoptive transfer of primed $CD4^+$ T-cells provided protection to naive recipient mice from *C. parvum* challenge infection

The dominant contribution of $CD4^+$ T-cells to the cellular immune response against *C. parvum* has been addressed in different approaches (Chen et al., 1993a; McDonald and Bancroft, 1994; Perryman et al., 1994; Harp et al., 1994; Aguirre et al., 1994).

The challenge in transferring gut mucosal $CD4^+$ T-cells is the difficulty in getting enough cells to transfer to a group of recipient mice. $CD4^+$ T-cells constitute only a small proportion of the IELs, about 4 to 10 % was the yield obtained in this study. Therefore, another tissue source, spleen and MLN, were considered to obtain enough number of pure $CD4^+$ T-cell preparations.

The present data demonstrate the importance of primed $CD4^+$ T-cells from mucosal (MLN) and systemic (spleen) sites in transferring protective cellular immunity to naive mice. Unlike the gut mucosal IELs, $CD4^+$ T-cells transferred from GKO donor mice at day 8 p.i conferred protection to challenge *C. parvum* infection. These findings show the presence of IFN-γ independent

factors that contribute to resistance against infection within mucosal and systemic $CD4^+$ T-cells by the peak of infection, a phenomenon not seen in the IELs.

The significance of protection conferred by MLN and spleen cells was reciprocal at day 8 p.i. and day 15 p.i. (Figure 28A and C). Day 8 p.i. MLN cells provide significant protection to GKO recipients at all days post infection; whereas day 15 p.i. spleen cells provide significant protection to GKO recipients at all days post infection. Therefore, there may be variable importance of MLN and spleen tissues in orchestrating protective immune response against *C. parvum* infection at different time points post infection. During the peak of infection the MLN that drain the intestine provided statistically significant protection at all time points post challenge infection of recipients. However, spleen donor cells were much important when transferred by the time of resolution of infection as shown by statistically significant percent protection at all days post challenge infection of recipients.

This may indicate the relative abundance of *C. parvum* specific $CD4^+$ T-cells in the spleen after resolution of infection but not at the peak of infection. This could be logical since cells have to migrate from the site of infection through the blood circulation or lymph vessels to reach different lymphoid tissues such as spleen, located relatively farther anatomically from the gut. MLN collects lymph from the intestine, and can easily access to the cellular immune reactions that are actively going on in the gut.

In comparison, the reason why we did not get protection from IELs at the peak of infection in GKO mice could be various. The small number of relevant $CD4^+$ T-cells, i.e. antigen specific ones that are produced by the proliferation of naive $CD4^+$ T-cells during the infection process, could be a potential reason. While the cytokine production by these $CD4^+$ T-cells in the gut was at the peak level by day 8 p.i., the type of antigen specific $CD4^+$ T-cells that release cytokines could be different from the $CD4^+$ T-cells transferred and survive in the recipients' intestine. During an encounter of an antigen naive $CD4^+$ T-cells differentiate into two cell populations-effector and memory cells (LaRosa and Orange, 2008). The effector cells could be Th1 or Th2 and secrete Th1 and Th2 cytokines in response to infection and die shortly. The memory $CD4^+$ T-cells are long living cells that respond more quickly and vigorously on the second encounter of the same antigen. The effector $CD4^+$ T-cells have also the potential to develop into long-lived memory $CD4^+$ T-cells (Dutton et al., 1999). The process of differentiating to a full effector state takes 4 – 5 days *in vitro* (Swain et al., 1996; Rogers et al., 1998) and a day or so

longer *in vivo* after introduction of either protein in adjuvant (Bradley et al., 1991) or to infection with influenza virus (Roman et al., 2002). The kinetics of effector and memory $CD4^+$ T-cell formation has not been determined for *C. parvum*; however, the cells that are transferred from the peak of infection may be a combination of cytokine producing effector cells and memory cells at an unknown proportion.

The protective capacity of IL-12KO $CD4^+$ donor cells from both MLN and spleen was similar (Figure 29A and C) and very much higher than that of GKO donor cells in terms of significance of protection conferred to the recipients. The results also show that there was equivalent level of protection conferred between IL-12KO IELs and $CD4^+$ T-cell donors at both the peak and resolution of infection. From this observation it could be deduced that even if the $CD4^+$ T-cells possess IFN-γ independent protective mechanisms, $CD4^+$ T-cells with intact IFN-γ gene are very much efficient in transferring cellular immunity.

It is interesting to compare the protective capacity of primed $CD4^+$ T-cells from MLN and spleen to the gene expression of cytokines in these tissues during *C. parvum* infection. The reason for absence of clear changes in these tissues, unlike that of the gut, was argued on the basis of small number of antigen specific cells among a large population of lymphoid cells that could not be detected on basis of mRNA analysis. In line with this, the data presented here on the basis of adoptive transfer of $CD4^+$ T-cells show that indeed there are *C. parvum* specific cells populating the MLN and spleen since their transfer conferred protection. This is an *in vivo* confirmation of the findings of previous workers who showed an *in vitro* proliferation and cytokine secretion of MLN and spleen $CD4^+$ T-cells in response to *C. parvum* surface antigens (Harp et al., 1994; Theodos et al., 1997; You and Mead, 1998; Smith et al., 2000; Ehigiator et al., 2005; Wyatt et al., 2005).

Although the number of *C. parvum* antigen-specific $CD4^+$ T-cells could be small within the transferred cells, these cells can undergo a quick response by proliferating in the recipients upon contact with the parasite and confer cellular immune reactions against the organism. In support of this, memory cells derived after adoptive transfer from *in vitro* stimulated effectors acquire the capacity to initiate rapid cell division and cytokine secretion in response to antigenic stimulation. This capacity may be linked to the fact that memory cells are less dependent on costimulation, thus bypassing the lag phase needed for antigen-presenting cells (APCs) to upregulate costimulatory molecules (Dooms and Abbas, 2006).

In contrast to previous adoptive transfer experiments performed to show the importance of $CD4^+$ T-cells, we used animals with intact cellular immunity as recipients. Therefore, the transferred cells will have to compete with the naive $CD4^+$ T-cells within the recipients for exposure to antigen stimulation, cytokine microenvironments for growth and differentiation, etc. The transferred cells are primed, therefore, are expected to have a quick response to infection.

Furthermore, the present study indicates the possible time during infection when memory to *C. parvum* antigens could be formed. Therefore, the protection conferred by transferred cells in the present study can be associated with *C. parvum* specific memory $CD4^+$ T-cells. These memory cells could be generated at least starting from the peak of infection onwards; however, it is possible that memory cells also form at earlier period than we studied. In contrast, McDonald et al. (1994) showed that adoptive immunity occurred only when the donor animals had developed resistance to *C. muris*; cells transferred soon after the peak of oocyst production were no more protective than unprimed lymphoid cells. The difference in the pathogens, *C. parvum* versus *C. muris*, or the differences in the immune status of recipients, partial immunocompetent versus SCID, may account to the different results between our study and that of McDonald et. al. (1994). Further studies are required to understand the kinetics of *C. parvum* specific memory $CD4^+$ T-cell generation and their distribution in different immune compartments, as well as, the importance of such memory cells for protective cellular immunity against the pathogen.

9.7. Adoptive transfer of pan T-cells provided equivalent level of protection with that of $CD4^+$ T-cells

Although $CD4^+$ T-cells were the dominant players in resistance to *C. parvum* infection, there could also be a minor contribution by $CD8^+$ T-cells as suggested by some studies (Perryman et al., 1994; McDonald and Bancroft, 1994). However, there are no conclusive results to date. The present results show that the oocyst shedding by $CD4^+$ T-cell recipients was not completely cleared, showing that the transferred cells did not prevent establishment of infection.

According to the present data, there were no additional roles of $CD8^+$ T-cells over that of $CD4^+$ T-cells. The protective efficiency of pan T-cells is not different from that of $CD4^+$ T-cells, i.e., neither of the preparations could prevent establishment of infection. Overall, the same

protection rate between pan T-cells and $CD4^+$ T-cell recipients from infection could indicate that $CD8^+$ T cell may not play protective role in resistance to *C. parvum* infection. Moreover, the data indicate that $CD4^+$ T-cells provide similar level of protection when used at a dose of 2×10^6 or at a dose of 42 % lesser per mouse.

9.8. Priming of donor mice with *C. parvum* infection is the pre-requisite for transfer of cellular immunity

The importance of *C. parvum* infection in donor mice for transfer of cellular immunity, i.e. priming of donor cells with *C. parvum* antigens, was indicated in two separate approaches: using naive cells from non-infected animals and cells isolated from infected wild type mice.

9.8.1. Naive $CD4^+$ T-cells and IELs do not provide protection to naive recipient mice

The data in this study show that priming of cell donor animals is required for transferring protective cellular immunity. Thus, unlike the primed cells, naive cells from uninfected GKO and IL-12KO mice were not able to transfer immunity to naive recipients. This was in partial agreement to most of previous reports (McDonald and Bancroft, 1994; McDonald et al., 1996; Adjei et al., 2000) who transferred protective cellular immunity using primed immnuocompetent cells to SCID mice. However, these workers also showed protection of SCID recipients by unprimed cells, in contrast to the present study. SCID mice are deficient in specific cellular immune cells so that they could get any protection by the transferred unprimed cells that could populate the lymphoid tissues of the recipients and proliferate. However, the protection takes longer in that the unprimed cells need time for establishing a specific immunity. In contrast, we used generally immunocompetent mice that possess lymphocytes in their lymphoid tissues and can resolve the infection without any transfer of donor cells. Therefore, transferring unprimed (naive) cells in our model mice is not any different from the cells they possess in respect to *C. parvum* antigens. Similar to the present work, Buzoni-Gatel *et al* (1997) used immunocompetent recipients where unprimed IELs did not protect recipients against *Toxoplasma* challenge.

9.8.2. $CD4^+$ T-cells from wild type mice 15 days p.i. did not transfer protection to susceptible GKO mice

It has been shown that adult wild type mice are resistant to *C. parvum* infection and shed very negligible numbers of oocysts upon infection. As described in the previous sections, primed donor $CD4^+$ T-cells, but not naive cells, prepared from infected animals transferred protective immunity to naive recipients. Taken together, the results suggest that infection of donor mice was an important criterion for transfer of cellular protective immunity.
This was further substantiated by showing that adoptive transfer of spleen $CD4^+$ T-cells from wild type donor mice day 15 p.i. to naive GKO mice did not protect recipients from challenge infection. The transfer of IFN-γ production into the GKO mice was neutralized by anti-IFN-γ treatment so that the outcomes would not be complicated by the IFN-γ produced by donor cells. However, wild type spleen donor cells without neutralization of IFN-γ could also not protect from infection, showing that the IFN-γ producing cells were not sufficient enough or spleen cells could not traffic to the gut where the IFN-γ response to infection was noticed unlike that of the spleen. If the latter is true, the study may show that IFN-γ production at the gut mucosa may be more relevant than in the systemic tissue. Further experiments are required to find out the relative contribution of intestinal versus systemic IFN-γ production for resistance to the pathogen. Homing of spleen and MLN $CD4^+$ T-cells to the intestine should also be studied. Additionally, production of IFN-γ by the transferred wild type $CD4^+$ T-cells in the intestine versus in the spleen should be verified.

Our result is in contrast to previous reports by McDonald *et al.* (1996) on *C. muris*, a murine gastric pathogen, and Adjei *et al.* (2000) on *C. parvum*. They transferred protective cellular immunity using primed immnuocompetent cells to SCID mice; therefore, the discrepancy could be due to the immunological differences of the recipients used between the current experiment and previous reports.

In an early experiment (Harp and Whitmire, 1991) it was not possible to transfer resistance to *C. parvum* infection using lymphoid cells from previously infected adult immunocompetent to newborn mice of the same strain. Adult wild type mice are resistant to *C. parvum* infection; therefore, there could be no sufficiently primed cells obtained from such donors. The use of immunocompetent recipients has been considered as a factor that could hinder the transfer of

cellular resistance as shown by McDonald *et al.* (1994) who could not transfer resistance to *C. muris* to immunologically intact mice.

In conclusion, according to the results of the present work, priming of donors with infection, i.e., the presence of established infection and the generation of sufficient *C. parvum* antigen specific cells are important components of the transferrable cellular immunity.

9.9. Number of transferred cells does not change the level of transferred protective cellular immunity

Similar to the $CD4^+$ T-cells IELs did not prevent establishment of infection in the recipient mice though they provided significant protection. Therefore, the possibility of achieving higher efficiency of protection was further tested by transferring two different IEL cell numbers, the normal dose (2 million) and a double dose (4 million). Transferring twice higher number of IELs could not produce better protection than the usual cell number, i.e., 2 million. This is similar to the findings with $CD4^+$ T-cells, where we showed that using 2 million $CD4^+$T-cells or a 42 % lower $CD4^+$ cell number (within pan T-cell preparation) produced similar protection efficiency.

The lowest possible cell number that transfers protective immunity was not addressed in this work. McDonald *et al* (1994) showed that adoptive immunity against *C. muris* was routinely obtained with 1.5×10^7 primed spleen or MLN cells injected intraperitoneally from wild type mice to SCID mice. Protection of SCID mice was also observed by using as few as 2.5×10^5 donor spleen cells when injected i.v.

In conclusion, protective cellular immunity to *C. parvum* was successfully transferred via primed IELs as well as intestinal and systemic $CD4^+$ T-cells, indicating the importance of the adaptive immune response against *C. parvum*. Identifying the role of primed $CD4^+$ T-cell donors in *C. parvum* infection in animals having $CD4^+$ T-cells further strengthens the prominent role of pathogen specific $CD4^+$ T-cells as a major factor in resistance to the pathogen.

Furthermore, some other immunologically important inferences may be made from the present work. Such important future outcomes may be:

1. The use of *C. parvum* antigen specific $CD4^+$ T-cells in immunotherapeutic or prophylactic approaches to control cryptosporidiosis in immunocompromised patients. The application of such intervention has been shown to be effective for treatment of some viral and cancer diseases (Leen et al., 2007), where there are no alternative chemotherapeutic options similar to that of Cryptosporidiosis.

There are some prerequisites to apply this approach in Cryptosporidiosis: identifying immunodominant *C. parvum* antigens, in addition to the already known ones; designing working protocols for in vitro generation of *C. parvum* peptide specific $CD4^+$ T-cell lines, studying the immune homeostasis of such cells *in vivo* and their relevance to protect infection. The approach could be taken as an alternative means if there is a failure in designing protective vaccines of other forms, or therapeutic agents, which are still not available.

2. Identifying novel $CD4^+$ T-cell-mediated immune effector mechanisms. Classically, $CD4^+$ T-cells have been shown to be helpers to other effector mechanisms that clear infections. The lack of evidences for cytotoxic killing of *C. parvum* infected intestinal epithelial cells, and the demonstration of $CD4^+$ T-cells as major immune cells to the infection leads to the difficult question how $CD4^+$ T-cells eradicate *C. parvum* infected host cells. Any possible experiment solving this question may contribute not only to understand resistance to *C. parvum* but also may be a novel immunological effector mechanism that could contribute to other areas too.

10. T-cell killing of *C. parvum* infected cells: does it exist?

Traditionally, two kinds of immune response have been described against invading pathogens: antibody mediated-immune response to clear extracellular pathogens and parasites and cell-mediated immune response (mainly by $CD8^+$ T-cells) to clear intracellular infections. *C. parvum* is an intracellular pathogen and all of the developmental stages take place inside infected intestinal epithelial cells. However, the immune response to this pathogen has been described as $CD4^+$ T-cell and Th1 cytokine mediated although Th2 cytokines are also elicited upon infection. Cytotoxic ($CD8^+$ T-cells) have a negligible or no role as shown by many studies.

This is an exception to the general accepted immunological phenomenon to date. In summary, the immune mechanisms that clear *C. parvum* infected cells are still not clear.

10.1. Why do $CD8^+$ T-cells (cytotoxic T-cells) not kill *C. parvum* infected host cells?

This is a very difficult issue to discuss. There are described mechanisms that are applied by intracellular pathogens to evade the host's immune system. Although similar mechanisms could also be applied by *C. parvum* infection, none has ever been characterized yet. At which points during infection can *C. parvum* evade the host's immune response to avoid cytotoxic clearance by $CD8^+$ T-cells? Possible scenarios from other intracellular pathogens could be raised to indicate the existence of immune evasion mechanisms from $CD8^+$ T-cell-mediated cytotoxicity.

Lysosomal degradation of the intracellular developmental stages of *C. parvum* would be required for recognition of *C. parvum* infecetd host cells by $CD8^+$ T-cells. Autophagy of intracellular pathogens contributes to the effective elimination of viruses, bacteria and parasites (Vyas et al., 2008). However, many pathogens strive to escape the autophagy machinery, for example, herpes simplex virus type 1 (Orvedahl et al., 2007) and *Shigella* (Vyas et al., 2008; Crotzer and Blum, 2008) use proteins to antagonize autophagy. The ability of pathogens to escape autophagy might allow survival within host cells and, therefore, represent a new mechanism for immune evasion.

In this regard, the unique location of *C. parvum* inside infected cells is worth mentioning. All stages of *C. parvum* are located in a parasitophorous vacuole, formed extracytoplasmically but intracellularly within infected cells. The structure could hinder lysosomal degradation of *C. parvum* proteins that could be presented through the MHC-I pathway. Lack of MHC-I presented *C. parvum* proteins may be the possible reason why $CD8^+$ T-cells do not kill infected cells.

After degradation of antigens from intracellular pathogens, peptides from the degraded antigen bind to MHC-I molecule to be presented on the infected cell surface for recognition by $CD8^+$ T-cells. Aguirre *et al* (1994) showed that MHC-II (important for $CD4^+$ T-cells) deficient mice are more susceptible to *C. parvum* infection than MHC-I deficient mice (important for function of $CD8^+$ T-cells). Therefore, one possible question could be raised: does *C. parvum* modulate the MHC-I Ag presentation pathway so that there is no presentation of the pathogen's antigen on the surface of infected epithelial cells to be recognized by $CD8^+$ T-cells?
The use of such immune evasion strategies has been described by some viruses, such as adenovirus, human cytomegalovirus, human herpes vurus and Epstein Barr virus (EBV) (Hewitt, 2003; Rowe et al., 2007).

10.2. Unknown mechanism: $CD4^+$ T-cell-mediated killing of *C. parvum* infected cells

It is widely accepted that $CD4^+$ T-cells provide helper functions for $CD8^+$ T-cell mediated cytotoxicity of infected cells. However, quite recently interesting novel functions of $CD4^+$ T-cells are emerging that indicate $CD4^+$ T-cell mediated killing of viral-infected cells. Studies of mouse γ-herpesvirus 68 (MHV-68) have shown that $CD4^+$ T-cells can control a herpesvirus infection and its malignant consequences *in vivo*, independent of $CD8^+$ T-cells and B-cells (Heller et al., 2006). EBV-specific cells were among the first $CD4^+$ cytolytic T-lymphocytes (CTLs) to be isolated using EBV-transformed B-cells (Nikiforow et al., 2003). Subsequently, in mice infected with the murine choriomeningitis virus (LCMV), LCMV-specific $CD4^+$ T-cell cytotoxicity, partly due to FasL-induced apoptosis, was reported (Jellison et al., 2005). Cytotoxic $CD4^+$ T-cells positive for the cytotoxic effector molecules perforin and granzyme were also identified in human blood (Appay et al., 2002). Perforin-mediated cytolytic $CD4^+$ T-cells were shown to play a role in controlling influenza infection, in addition to antibody mediated responses promoted by the same cells (Brown et al., 2006). $CD4^+$ T-cells were also shown to provide both helper and cytotoxic functions during Epstein-Barr virus infection (MacArthur et al., 2007).

Therefore, novel $CD4^+$ T-cell mediated immune functions are emerging. The presence of $CD4^+$ T-cell mediated cytotoxicity of *C. parvum* infected host cells should be an interesting issue to be addressed. Identification of such novel immune effector mechanisms may provide a solution to the puzzle on the clearance of *C. parvum* infected epithelial cells.

11. SUMMARY

Cryptosporidium parvum is an intracellular protozoan pathogen causing enteritis which can become life-threatening in the immunocompromised host. $CD4^+$ T-cells and interferon (IFN)-γ play dominant roles in host immune response to infection. However, $CD4^+$ T-cell mediated effector immune mechanisms that lead to resistance are poorly understood. The major obstacle to study the complete immune response to the pathogen has been the lack of proper animal infection model, i.e., adult immunocompetent animals. In this study, we approached this problem by analyzing the immune response of mice deficient in IFN-γ or interleukin (IL)-12 in parallel to wild type mice.

Dynamics of Th1 and Th2 cytokine genes in interferon-γ KO (GKO) and interleukin-12 KO (IL-12KO) mice during primary and challenge *C. parvum* infections

In this study the gene expression of Th1 and Th2 cytokines at local and systemic immune tissues was investigated during primary as well as challenge infection with *C. parvum*. Analysis of cytokine mRNA changes was performed by qualitative RT-PCR as well as quantitative real-time RT-PCR. Our results identified IFN-γ as the key cytokine in the innate as well as adaptive immunity during primary and challenge *C. parvum* infection. However, the gene expression of the other Th1 (TNF-α, IL-18) and Th2 cytokines (IL-4, IL-10, IL-13) increased during infection reaching peak levels at or after the peak of infection and return to background levels after the infection is resolved. This indicates that both Th1 and Th2 cytokines may be involved in resolving the infection the former being dominant over the latter. The continuous rise of cytokine genes to peak levels after cessation of fecal oocyst shedding in IL-12KO mouse model indicates that the increases in gene expression of cytokines during *C. parvum* infection did not necessarily coincide with the infection load in the intestine. Therefore, the time for peak of cytokine gene expression was the same (day 8 p.i.) in both interferon-γ KO (GKO) and IL-12KO mice, and this time may be indicative of the highest number of cytokine producing effector lymphocytes present in the gut during infection.

IL-12 is a very important regulator of IFN-γ; however, in the absence of IL-12 there are other inducers of IFN-γ throughout the different stages of infection. In this regard, tumor necrosis factor (TNF)-α may act as an inducer of the early IFN-γ response in IL-12KO mice. The early rise of IFN-γ could result from NK cells or antigen presenting cells which may be replaced by

the adaptive immune response at later stage of the infection. In addition, IL-12 may be an important regulator of the Th1 cytokine response to *C. parvum* infection since IL-12KO mice have a reduced Th1 cytokine gene expression compared to GKO and wild type mice of the same experimental condition, i.e. with or without infection.

The pattern of cytokine gene expression during challenge infection was different from that of the primary infection, indicating the possible involvement of different immune mechanisms during primary infection and challenge infection. A significant increase of the Th2 cytokines, IL-5 and IL-13, was observed in the absence of IFN-γ. In animals with intact IFN-γ gene, IFN-γ was the only cytokine shown to be upregulated throughout the period studied after challenge infection. In both GKO as well as IL-12KO mice, cytokine genes were upregulated with 1 day post challenge infection and the levels were maintained at a sustained level during the period of study, indicating the presence of *C. parvum* antigen specific cells that respond quickly upon second encounter of pathogen. Similar with that of the primary infection, the site of infection (intestine) showed significant changes in cytokine gene expression, most probably due to the relatively higher proportion of *C. parvum* antigen specific cytokine producing lymphocytes at the site of infection compared to MLN and spleen.

Further studies are required to understand the molecular mechanisms involved in IFNγ-mediated resistance especially during the early period of infection.

The role of IL-18 in resistance to *C. parvum* infection

The study presented data that indicate the contribution of IL-18 to resistance against *C. parvum* infection. The gene expression of IL-18 increases during the period of adaptive immune response to infection. Neutralization of the *in vivo* IL-18 protein with a monoclonal anti-IL-18 antibody leads to increased susceptibility of both GKO and IL-12KO mice to infection. Therefore, IL-18 may have multiple immune functions against *C. parvum* infection since IFN-γ deficient mice were also affected by neutralizing IL-18 protein so that induction of IFN-γ during infection may not be the only effector function of IL-18. In this study IL-18 neutralization did not modulate the gene expression of IFN-γ in the gut as well as spleen. However, IL-18 may regulate the serum IFN-γ protein level as shown in IL-12KO mice treated with anti-IL-18 antibody. The effect of IL-18 neutralization on the IFN-γ protein levels in the gut should be studied since the local IFN-γ response may be more relevant than the systemic in

resistance against the gut infection. Furthermore, IL-18, on its own or together with IL-12, may involve in regulating the Th1/Th2 cytokine balance during infection since dysregulated systemic Th2 cytokines, notably IL-4 and IL-13, were noticed upon IL-18 neutralization in both GKO and IL-12KO mice. Such homeostasis of Th1 and Th2 cytokines seems to be an important phenomenon during *C. parvum* infection, implicating that shifting of the cytokine environment to either Th1 or Th2 direction may be detrimental to the host.
In summary, IL-18 may have multiple effector immune functions during *C. parvum* infection that need to be studied in detail.

Adoptive transfer of immunity from *C. parvum* infected to naive mice

Furthermore, this study shows that the resistance (or immunity) developed during or after resolution of infection was transferrable to naive recipients with intact cellular immunity. This was achieved by transferring primed gut IELs as well as spleen and MLN $CD4^+$ T-cells. This cellular immunity conferred significant protection of recipients when transferred from the peak as well as resolution of infection of IL-12KO donor mice. In contrast, donor cells from GKO mice conferred variable significance of protection at different times post infection depending on the tissue of origin. GKO IEL donors provide significant protection after the resolution of infection, but not at the peak of infection. However, GKO $CD4^+$ T-cells from MLN and spleen provided statistically significant protection from both time points post infection. Altogether, we can conclude that IFN-γ is a critical component of the protective immunity in the gut (IELs) at the peak of infection; whereas this cytokine may not be a critical component of the immunological factors that resolve the infection. In addition, spleen and MLN derived $CD4^+$ T-cells are capable of transferring protective immunity in the presence or absence of IFN-γ. Furthermore, these results indicate the presence of *C. parvum* specific $CD4^+$ T-cells in MLN and spleen in addition to the gut mucosa although *C. parvum* is a gut mucosal surface pathogen.

Moreover, priming of the donor animals by infection with *C. parvum* was identified as an important parameter for the successful transfer of protective cellular immunity. This was proved by using naive donor cells that could not confer protection of naive recipients to infection. Additionally, donor cells from *C. parvum* inoculated wild type mice were not able to confer protection to naive recipients since wild type mice were resistant to infection and subsequently there may not be primed cells in these mice.

However, the transferred cellular immunity could not prevent the establishment of infection in naive recipients completely; even doubling the number of donor cells could not confer a better establishment as well.
Moreover, transfer of both $CD4^+$ and $CD8^+$ T-cells (pan T-cells) did not provide a better protection of naive recipients than that of $CD4^+$ T-cells alone. This may indicate the irrelevance of $CD8^+$ T-cells in protection against *C. parvum*.

In conclusion, protective cellular immunity to *C. parvum* was successfully transferred via primed IELs as well as intestinal and systemic $CD4^+$ T-cells, indicating the importance of the adaptive immune response against *C. parvum*. $CD4^+$ T-cell mediated mechanisms for clearance of *C. parvum* infected cells are not understood yet; therefore, the possibility of *C. parvum* infected cell killing by $CD4^+$ T-cells should be investigated.

12. REFERENCES

Abdo,A., Klassen,J., Urbanski,S., Raber,E., and Swain,M.G. (2003). Reversible sclerosing cholangitis secondary to cryptosporidiosis in a renal transplant patient. J. Hepatol. *38*, 688-691.

Abrahamsen,M.S., Lancto,C.A., Walcheck,B., Layton,W., and Jutila,M.A. (1997). Localization of alpha/beta and gamma/delta T lymphocytes in *Cryptosporidium parvum*-infected tissues in naive and immune calves. Infect. Immun. *65*, 2428-2433.

Abrahamsen,M.S., Templeton,T.J., Enomoto,S., Abrahante,J.E., Zhu,G., Lancto,C.A., Deng,M., Liu,C., Widmer,G., Tzipori,S., Buck,G.A., Xu,P., Bankier,A.T., Dear,P.H., Konfortov,B.A., Spriggs,H.F., Iyer,L., Anantharaman,V., Aravind,L., and Kapur,V. (2004). Complete genome sequence of the apicomplexan, *Cryptosporidium parvum*. Science *304*, 441-445.

Abubakar,I., Aliyu,S.H., Arumugam,C., Hunter,P.R., and Usman,N.K. (2007a). Prevention and treatment of cryptosporidiosis in immunocompromised patients. Cochrane Database Syst. Rev. CD004932.

Abubakar,I., Aliyu,S.H., Arumugam,C., Usman,N.K., and Hunter,P.R. (2007b). Treatment of cryptosporidiosis in immunocompromised individuals: systematic review and meta-analysis. Br. J. Clin. Pharmacol. *63*, 387-393.

Adjei,A.A., Shrestha,A.K., Castro,M., and Enriquez,F.J. (2000). Adoptive transfer of immunity with intraepithelial lymphocytes in *Cryptosporidium parvum*-infected severe combined immunodeficient mice. Am. J. Med. Sci. *320*, 304-309.

Aguirre,S.A., Mason,P.H., and Perryman,L.E. (1994). Susceptibility of major histocompatibility complex (MHC) class I- and MHC class II-deficient mice to *Cryptosporidium parvum* infection. Infect. Immun. *62*, 697-699.

Aguirre,S.A., Perryman,L.E., Davis,W.C., and McGuire,T.C. (1998). IL-4 protects adult C57BL/6 mice from prolonged *Cryptosporidium parvum* infection: analysis of CD4+alpha beta+IFN-gamma+ and CD4+alpha beta+IL-4+ lymphocytes in gut-associated lymphoid tissue during resolution of infection. J. Immunol. *161*, 1891-1900.

Aley,S.B., Zimmerman,M., Hetsko,M., Selsted,M.E., and Gillin,F.D. (1994). Killing of *Giardia lamblia* by cryptdins and cationic neutrophil peptides. Infect. Immun. *62*, 5397-5403.

anonymous (1982). Cryptosporidiosis, asessment of chemotherapy of males with acquired immune deficiency syndrome (AIDS). *Morbid. Mortal. Wkly. Rpt.* 31, 89-102.

Appay,V., Zaunders,J.J., Papagno,L., Sutton,J., Jaramillo,A., Waters,A., Easterbrook,P., Grey,P., Smith,D., McMichael,A.J., Cooper,D.A., Rowland-Jones,S.L., and Kelleher,A.D. (2002). Characterization of CD4(+) CTLs ex vivo. J. Immunol. *168*, 5954-5958.

Artis,D. and Grencis,R.K. (2008). The intestinal epithelium: sensors to effectors in nematode infection. Mucosal Immunology *1*, 252-264.

Auray,G., Lacroix-Lamande,S., Mancassola,R., mier-Poisson,I., and Laurent,F. (2007). Involvement of intestinal epithelial cells in dendritic cell recruitment during *C. parvum* infection. Microbes. Infect. *9*, 574-582.

Ayabe,T., Satchell,D.P., Wilson,C.L., Parks,W.C., Selsted,M.E., and Ouellette,A.J. (2000). Secretion of microbicidal alpha-defensins by intestinal Paneth cells in response to bacteria. Nat. Immunol. *1*, 113-118.

Ball,T.B., Plummer,F.A., and Hayglass,K.T. (2003). Improved mRNA quantitation in LightCycler RT-PCR. Int. Arch. Allergy Immunol. *130*, 82-86.

Bancroft,G.J. and Kelly,J.P. (1994). Macrophage activation and innate resistance to infection in SCID mice. Immunobiology *191*, 424-431.

Bancroft,G.J., Schreiber,R.D., and Unanue,E.R. (1991). Natural immunity: a T-cell-independent pathway of macrophage activation, defined in the scid mouse. Immunol. Rev. *124*, 5-24.

Barner,M., Mohrs,M., Brombacher,F., and Kopf,M. (1998). Differences between IL-4R alpha-deficient and IL-4-deficient mice reveal a role for IL-13 in the regulation of Th2 responses. Curr. Biol. *8*, 669-672.

Birch,D.E. (1996). Simplified hot start PCR. Nature *381*, 445-446.

Bjorneby,J.M., Leach,D.R., and Perryman,L.E. (1991). Persistent cryptosporidiosis in horses with severe combined immunodeficiency. Infect. Immun. *59*, 3823-3826.

Bohn,E., Sing,A., Zumbihl,R., Bielfeldt,C., Okamura,H., Kurimoto,M., Heesemann,J., and Autenrieth,I.B. (1998). IL-18 (IFN-gamma-inducing factor) regulates early cytokine production in, and promotes resolution of, bacterial infection in mice. J. Immunol. *160*, 299-307.

Bradley,L.M., Duncan,D.D., Tonkonogy,S., and Swain,S.L. (1991). Characterization of antigen-specific CD4+ effector T cells in vivo: immunization results in a transient population of MEL-14-, CD. J. Exp. Med. *174*, 547-559.

Brasseur,P., Lemeteil,D., and Ballet,J.J. (1988). Rat model for human cryptosporidiosis. J. Clin. Microbiol. *26*, 1037-1039.

Brown,D.M., Dilzer,A.M., Meents,D.L., and Swain,S.L. (2006). CD4 T cell-mediated protection from lethal influenza: perforin and antibody-mediated mechanisms give a one-two punch. J. Immunol. *177*, 2888-2898.

Buzoni-Gatel,D., Debbabi,H., Moretto,M., mier-Poisson,I.H., Lepage,A.C., Bout,D.T., and Kasper,L.H. (1999). Intraepithelial lymphocytes traffic to the intestine and enhance resistance to *Toxoplasma gondii* oral infection. J. Immunol. *162*, 5846-5852.

Buzoni-Gatel,D., Lepage,A.C., mier-Poisson,I.H., Bout,D.T., and Kasper,L.H. (1997). Adoptive transfer of gut intraepithelial lymphocytes protects against murine infection with *Toxoplasma gondii*. J. Immunol. *158*, 5883-5889.

Caccio,S.M. and Pozio,E. (2006). Advances in the epidemiology, diagnosis and treatment of cryptosporidiosis. Expert. Rev. Anti. Infect. Ther. *4*, 429-443.

Cama,V., Gilman,R.H., Vivar,A., Ticona,E., Ortega,Y., Bern,C., and Xiao,L. (2006). Mixed *Cryptosporidium* infections and HIV. Emerg. Infect. Dis. *12*, 1025-1028.

Campbell,L.D., Stewart,J.N., and Mead,J.R. (2002). Susceptibility to *Cryptosporidium parvum* infections in cytokine- and chemokine-receptor knockout mice. J. Parasitol. *88*, 1014-1016.

Canals,A., Pasquali,P., Zarlenga,D.S., Fayer,R., Almeria,S., and Gasbarre,L.C. (1998). Local ileal cytokine responses in cattle during a primary infection with *Cryptosporidium parvum*. J. Parasitol. *84*, 125-130.

Chai,J.Y., Guk,S.M., Han,H.K., and Yun,C.K. (1999). Role of intraepithelial lymphocytes in mucosal immune responses of mice experimentally infected with *Cryptosporidium parvum*. J. Parasitol. *85*, 234-239.

Chardes,T., Buzoni-Gatel,D., Lepage,A., Bernard,F., and Bout,D. (1994). *Toxoplasma gondii* oral infection induces specific cytotoxic CD8 alpha/beta+ Thy-1+ gut intraepithelial lymphocytes, lytic for parasite-infected enterocytes. J. Immunol. *153*, 4596-4603.

Chatelain,R., Varkila,K., and Coffman,R.L. (1992). IL-4 induces a Th2 response in *Leishmania major*-infected mice. J. Immunol. *148*, 1182-1187.

Chen,W., Harp,J.A., and Harmsen,A.G. (2003). *Cryptosporidium parvum* infection in gene-targeted B cell-deficient mice. J. Parasitol. *89*, 391-393.

Chen,W., Harp,J.A., and Harmsen,A.G. (1993a). Requirements for CD4+ cells and gamma interferon in resolution of established *Cryptosporidium parvum* infection in mice. Infect. Immun. *61*, 3928-3932.

Chen,W., Harp,J.A., Harmsen,A.G., and Havell,E.A. (1993b). Gamma interferon functions in resistance to *Cryptosporidium parvum* infection in severe combined immunodeficient mice. Infect. Immun. *61*, 3548-3551.

Chen,X.M., Keithly,J.S., Paya,C.V., and LaRusso,N.F. (2002). Cryptosporidiosis. N. Engl. J. Med. *346*, 1723-1731.

Cherwinski,H.M., Schumacher,J.H., Brown,K.D., and Mosmann,T.R. (1987). Two types of mouse helper T cell clone. III. Further differences in lymphokine synthesis between Th1 and Th2 clones revealed by RNA hybridization, functionally monospecific bioassays, and monoclonal antibodies. J. Exp. Med. *166*, 1229-1244.

Chomarat,P. and Banchereau,J. (1998). Interleukin-4 and interleukin-13: their similarities and discrepancies. Int. Rev. Immunol. *17*, 1-52.

Chou,Q., Russell,M., Birch,D.E., Raymond,J., and Bloch,W. (1992). Prevention of pre-PCR mis-priming and primer dimerization improves low-copy-number amplifications. Nucleic Acids Res. *20*, 1717-1723.

Clark,D.P. and Sears,C.L. (1996). The pathogenesis of cryptosporidiosis. Parasitol. Today *12*, 221-225.

Collins,H.L. (2008). Withholding iron as a cellular defence mechanism - friend or foe? Eur. J. Immunol. *38*, 1803-1806.

Couedel-Court, Le,G.R., Tulliez,M., Guillet,J.G., and Venet,A. (1997). Direct ex vivo simian immunodeficiency virus (SIV)-specific cytotoxic activity detected from small intestine intraepithelial lymphocytes of SIV-infected macaques at an advanced stage of infection. J. Virol. *71*, 1052-1057.

Coulliette,A.D., Huffman,D.E., Slifko,T.R., and Rose,J.B. (2006). *Cryptosporidium parvum*: Treatment effects and the rate of decline in oocyst infectivity. J. Parasitol. *92*, 58-62.

Cozon,G., Biron,F., Jeannin,M., Cannella,D., and Revillard,J.P. (1994). Secretory IgA antibodies to *Cryptosporidium parvum* in AIDS patients with chronic cryptosporidiosis. J. Infect. Dis. *169*, 696-699.

Crabb,J.H. (1998). Antibody-based immunotherapy of cryptosporidiosis. In Opportunistic protozoa in humans, S.Tzipori, ed. (San Diego: Academic Press), pp. 121-149.

Crotzer,V.L. and Blum,J.S. (2008). Cytosol to lysosome transport of intracellular antigens during immune surveillance. Traffic. *9*, 10-16.

Cuff,C.F., Cebra,C.K., Rubin,D.H., and Cebra,J.J. (1993). Developmental relationship between cytotoxic alpha/beta T cell receptor-positive intraepithelial lymphocytes and Peyer's patch lymphocytes. Eur. J. Immunol. *23*, 1333-1339.

Culshaw,R.J., Bancroft,G.J., and McDonald,V. (1997). Gut intraepithelial lymphocytes induce immunity against *Cryptosporidium* infection through a mechanism involving gamma interferon production. Infect. Immun. *65*, 3074-3079.

Dalton,D.K., Pitts-Meek,S., Keshav,S., Figari,I.S., Bradley,A., and Stewart,T.A. (1993). Multiple defects of immune cell function in mice with disrupted interferon-gamma genes. Science *259*, 1739-1742.

Dann,S.M., Wang,H.C., Gambarin,K.J., Actor,J.K., Robinson,P., Lewis,D.E., Caillat-Zucman,S., and White,A.C., Jr. (2005). Interleukin-15 activates human natural killer cells to clear the intestinal protozoan *cryptosporidium*. J. Infect. Dis. *192*, 1294-1302.

Das,G., Sheridan,S., and Janeway,C.A., Jr. (2001). The source of early IFN-gamma that plays a role in Th1 priming. J. Immunol. *167*, 2004-2010.

Davies,M.D. and Parrott,D.M. (1981). Preparation and purification of lymphocytes from the epithelium and lamina propria of murine small intestine. Gut *22*, 481-488.

de Graaf,D.C., Walravens,K., Godfroid,J., and Peeters,J.E. (1998). A *Cryptosporidium parvum* oocyst low molecular mass fraction evokes a CD4+ T-cell-dependent IFN-gamma response in bovine peripheral blood mononuclear cell cultures. Int. J. Parasitol. *28*, 1875–80.

Dinarello,C.A. (1999). IL-18: A TH1-inducing, proinflammatory cytokine and new member of the IL-1 family. J. Allergy Clin. Immunol. *103*, 11-24.

Dooms,H. and Abbas,A.K. (2006). Control of CD4+ T-cell memory by cytokines and costimulators. Immunol. Rev. *211*, 23-38.

Dutton,R.W., Swain,S.L., and Bradley,L.M. (1999). The generation and maintenance of memory T and B cells. Immunol. Today *20*, 291-293.

Ehigiator,H.N., McNair,N., and Mead,J.R. (2007). *Cryptosporidium parvum*: The contribution of Th1-inducing pathways to the resolution of infection in mice. Exp. Parasitol. *115*, 107-113.

Ehigiator,H.N., Romagnoli,P., Borgelt,K., Fernandez,M., McNair,N., Secor,W.E., and Mead,J.R. (2005). Mucosal cytokine and antigen-specific responses to *Cryptosporidium parvum* in IL-12p40 KO mice. Parasite Immunol. *27*, 17-28.

Emoto,M., Neuhaus,O., Emoto,Y., and Kaufmann,S.H. (1996). Influence of beta 2-microglobulin expression on gamma interferon secretion and target cell lysis by intraepithelial lymphocytes during intestinal *Listeria monocytogenes* infection. Infect. Immun. *64*, 569-575.

Enriquez,F.J. and Sterling,C.R. (1993). Role of CD4+ TH1- and TH2-cell-secreted cytokines in cryptosporidiosis. Folia Parasitol. Praha. *40*, 307-311.

Fayer,R. (2004). *Cryptosporidium*: A water-borne zoonotic parasite. Vet. Parasitol. *126*, 37-56.

Fayer,R., Andrews,C., Ungar,B.L., and Blagburn,B. (1989). Efficacy of hyperimmune bovine colostrum for prophylaxis of cryptosporidiosis in neonatal calves. J. Parasitol. *75*, 393-397.

Fayer,R., Speer,C.A., and Dubey,J.P. (1997). The general biology of *Cryptosporidium*. In *Cryptosporidium* and Cryptosporidiosis, R.Fayer, ed. (Boca Raton: CRC Press), pp. 1-41.

Findly,R.C., Roberts,S.J., and Hayday,A.C. (1993). Dynamic response of murine gut intraepithelial T cells after infection by the coccidian parasite *Eimeria*. Eur. J. Immunol. *23*, 2557-2564.

Flanigan,T., Whalen,C., Turner,J., Soave,R., Toerner,J., Havlir,D., and Kotler,D. (1992). *Cryptosporidium* infection and CD4 counts. Ann. Intern. Med. *116*, 840-842.

Frucht,D.M., Fukao,T., Bogdan,C., Schindler,H., O'Shea,J.J., and Koyasu,S. (2001). IFN-gamma production by antigen-presenting cells: mechanisms emerge. Trends Immunol. *22*, 556-560.

Gardner,A.L., Roche,J.K., Weikel,C.S., and Guerrant,R.L. (1991). Intestinal cryptosporidiosis: pathophysiologic alterations and specific cellular and humoral immune responses in rnu/+ and rnu/rnu (athymic) rats. Am. J. Trop. Med. Hyg. *44*, 49-62.

Gomez Morales,M.A., Ausiello,C.M., Urbani,F., and Pozio,E. (1995). Crude extract and recombinant protein of *Cryptosporidium parvum* oocysts induce proliferation of human peripheral blood mononuclear cells in vitro. J. Infect. Dis. *172*, 211-216.

Gomez Morales,M.A. and Pozio,E. (2002). Humoral and cellular immunity against *Cryptosporidium* infection. Curr. Drug Targets. Immune. Endocr. Metabol. Disord. *2*, 291-301.

Gomez-Morales,M.A., La Rosa,G., Ludovisi,A., Onori,A.M., and Pozio,E. (1999). Cytokine profile induced by *Cryptosporidium* antigen in peripheral blood mononuclear cells from immunocompetent and immunosuppressed persons with cryptosporidiosis. J. Infect. Dis. *179*, 967-973.

Gookin,J.L., Chiang,S., Allen,J., Armstrong,M.U., Stauffer,S.H., Finnegan,C., and Murtaugh,M.P. (2006). NF-kappaB-mediated expression of iNOS promotes epithelial defense against infection by *Cryptosporidium parvum* in neonatal piglets. Am. J. Physiol Gastrointest. Liver Physiol *290*, G164-G174.

Gookin,J.L., Duckett,L.L., Armstrong,M.U., Stauffer,S.H., Finnegan,C.P., Murtaugh,M.P., and Argenzio,R.A. (2004). Nitric oxide synthase stimulates prostaglandin synthesis and barrier function in *C. parvum*-infected porcine ileum. Am. J. Physiol Gastrointest. Liver Physiol *287*, G571-G581.

Gookin,J.L., Foster,D.M., Coccaro,M.R., and Stauffer,S.H. (2008). Oral delivery of L-arginine stimulates prostaglandin-dependent secretory diarrhea in *Cryptosporidium parvum*-infected neonatal piglets. J. Pediatr. Gastroenterol. Nutr. *46*, 139-146.

Guk,S.M. and Chai,J.Y. (2007). Role of murine Peyer's patch lymphocytes against primary and challenge infections with *Cryptosporidium parvum*. Korean J. Parasitol. *45*, 175-180.

Guk,S.M., Yong,T.S., and Chai,J.Y. (2003). Role of murine intestinal intraepithelial lymphocytes and lamina propria lymphocytes against primary and challenge infections with *Cryptosporidium parvum*. J. Parasitol. *89*, 270-275.

Handwerger,B.S. and Schwartz,R.H. (1974). Separation of murine lymphoid cells using nylon wool columns. Recovery of the B cell-enriched population. Transplantation *18*, 544-548.

Harp,J.A. and Whitmire,W.M. (1991). *Cryptosporidium parvum* infection in mice: inability of lymphoid cells or culture supernatants to transfer protection from resistant adults to susceptible infants. J. Parasitol. *77*, 170-172.

Harp,J.A., Whitmire,W.M., and Sacco,R. (1994). In vitro proliferation and production of gamma interferon by murine CD4+ cells in response to *Cryptosporidium parvum* antigen. J. Parasitol. *80*, 67-72.

Hayday,A., Theodoridis,E., Ramsburg,E., and Shires,J. (2001). Intraepithelial lymphocytes: exploring the Third Way in immunology. Nat. Immunol. *2*, 997-1003.

Heine,J., Moon,H.W., and Woodmansee,D.B. (1984a). Persistent *Cryptosporidium* infection in congenitally athymic (nude) mice. Infect. Immun. *43*, 856-859.

Heine,J., Pohlenz,J.F., Moon,H.W., and Woode,G.N. (1984b). Enteric lesions and diarrhea in gnotobiotic calves monoinfected with *Cryptosporidium* species. J. Infect. Dis. *150*, 768-775.

Heller,K.N., Gurer,C., and Munz,C. (2006). Virus-specific CD4+ T cells: ready for direct attack. J. Exp. Med. *203*, 805-808.

Helmby,H., Takeda,K., Akira,S., and Grencis,R.K. (2001). Interleukin (IL)-18 promotes the development of chronic gastrointestinal helminth infection by downregulating IL-13. J. Exp. Med. *194*, 355-364.

Hershberg,R.M. and Mayer,L.F. (2000). Antigen processing and presentation by intestinal epithelial cells - polarity and complexity. Immunol. Today *21*, 123-128.

Hewitt,E.W. (2003). The MHC class I antigen presentation pathway: strategies for viral immune evasion. Immunology *110*, 163-169.

Hijjawi,N.S., Meloni,B.P., Ng'anzo,M., Ryan,U.M., Olson,M.E., Cox,P.T., Monis,P.T., and Thompson,R.C. (2004). Complete development of *Cryptosporidium parvum* in host cell-free culture. Int. J. Parasitol. *34*, 769-777.

Hill,B.D., Blewett,D.A., Dawson,A.M., and Wright,S. (1990). Analysis of the kinetics, isotype and specificity of serum and coproantibody in lambs infected with *Cryptosporidium parvum*. Res. Vet. Sci. *48*, 76-81.

Hommer,V., Eichholz,J., and Petry,F. (2003). Effect of antiretroviral protease inhibitors alone, and in combination with paromomycin, on the excystation, invasion and in vitro development of *Cryptosporidium parvum*. J. Antimicrob. Chemother. *52*, 359-364.

Huang,D.S., Lopez,M.C., Wang,J.Y., Martinez,F., and Watson,R.R. (1996). Alterations of the mucosal immune system due to *Cryptosporidium parvum* infection in normal mice. Cell Immunol. *173*, 176-182.

Huang,K. and Yang,S. (2002). Inhibitory effect of selenium on *Cryptosporidium parvum* infection in vitro and in vivo. Biol. Trace Elem. Res. *90*, 261-272.

Huang,X., McClellan,S.A., Barrett,R.P., and Hazlett,L.D. (2002). IL-18 contributes to host resistance against infection with *Pseudomonas aeruginosa* through induction of IFN-gamma production. J. Immunol. *168*, 5756-5763.

Hunt,E., Fu,Q., Armstrong,M.U., Rennix,D.K., Webster,D.W., Galanko,J.A., Chen,W., Weaver,E.M., Argenzio,R.A., and Rhoads,J.M. (2002). Oral bovine serum concentrate improves cryptosporidial enteritis in calves. Pediatr. Res. *51*, 370-376.

Hunter,C.A., Subauste,C.S., Van,C., V, and Remington,J.S. (1994). Production of gamma interferon by natural killer cells from *Toxoplasma gondii*-infected SCID mice: regulation by interleukin-10, interleukin-12, and tumor necrosis factor alpha. Infect. Immun. *62*, 2818-2824.

Ivanov,I.I., McKenzie,B.S., Zhou,L., Tadokoro,C.E., Lepelley,A., Lafaille,J.J., Cua,D.J., and Littman,D.R. (2006). The orphan nuclear receptor RORgammat directs the differentiation program of proinflammatory IL-17+ T helper cells. Cell *126*, 1121-1133.

Jakobi, V. (2006). *In vivo* and *in vitro* Untersuchungen zur Immunantwort und Parasitenentwicklung bei Infektionen mit dem Darmparasiten *Cryptosporidium parvum*. Dissertation, Department of Biology, Johannes Gutenberg University, Mainz, Germany.

Jakobi,V. and Petry,F. (2006). Differential expression of *Cryptosporidium parvum* genes encoding sporozoite surface antigens in infected HCT-8 host cells. Microbes. Infect. *8*, 2186-2194.

Jakobi,V. and Petry,F. (2008). Humoral immune response in interleukin-12 and interferon-γ deficient mice after infection with *Cryptosporidium parvum*. Parasite Immunol. *30*, 151-161.

Jarry,A., Cerf-Bensussan,N., Brousse,N., Selz,F., and Guy-Grand,D. (1990). Subsets of CD3+ (T cell receptor alpha/beta or gamma/delta) and CD3- lymphocytes isolated from normal human gut epithelium display phenotypical features different from their counterparts in peripheral blood. Eur. J. Immunol. *20*, 1097-1103.

Jellison,E.R., Kim,S.K., and Welsh,R.M. (2005). Cutting edge: MHC class II-restricted killing in vivo during viral infection. J. Immunol. *174*, 614-618.

Jenkins,M.C., O'Brien,C., Trout,J., Guidry,A., and Fayer,R. (1999). Hyperimmune bovine colostrum specific for recombinant *Cryptosporidium parvum* antigen confers partial protection against cryptosporidiosis in immunosuppressed adult mice. Vaccine *17*, 2453-2460.

Kaiko,G.E., Horvat,J.C., Beagley,K.W., and Hansbro,P.M. (2008). Immunological decision-making: how does the immune system decide to mount a helper T-cell response? Immunology *123*, 326-338.

Kalia,V., Sarkar,S., Gourley,T.S., Rouse,B.T., and Ahmed,R. (2006). Differentiation of memory B and T cells. Curr. Opin. Immunol. *18*, 255-264.

Kapel,N., Benhamou,Y., Buraud,M., Magne,D., Opolon,P., and Gobert,J.G. (1996). Kinetics of mucosal ileal gamma-interferon response during cryptosporidiosis in immunocompetent neonatal mice. Parasitol. Res. *82*, 664-667.

Kawakami,K., Koguchi,Y., Qureshi,M.H., Miyazato,A., Yara,S., Kinjo,Y., Iwakura,Y., Takeda,K., Akira,S., Kurimoto,M., and Saito,A. (2000). IL-18 contributes to host resistance against infection with *Cryptococcus neoformans* in mice with defective IL-12 synthesis through induction of IFN-gamma production by NK cells. J. Immunol. *165*, 941-947.

Kawakami,K., Qureshi,M.H., Zhang,T., Okamura,H., Kurimoto,M., and Saito,A. (1997). IL-18 protects mice against pulmonary and disseminated infection with *Cryptococcus neoformans* by inducing IFN-gamma production. J. Immunol. *159*, 5528-5534.

Kellogg,D.E., Rybalkin,I., Chen,S., Mukhamedova,N., Vlasik,T., Siebert,P.D., and Chenchik,A. (1994). TaqStart Antibody: "hot start" PCR facilitated by a neutralizing monoclonal antibody directed against Taq DNA polymerase. Biotechniques *16*, 1134-1137.

Kelly,P., Jack,D.L., Naeem,A., Mandanda,B., Pollok,R.C., Klein,N.J., Turner,M.W., and Farthing,M.J. (2000). Mannose-binding lectin is a component of innate mucosal defense against *Cryptosporidium parvum* in AIDS. Gastroenterology *119*, 1236-1242.

Kelsall,B. and Strober,W. (1999). Gut-associated lymphoid tissue. In Mucosal Immunology, P.L.Ogra, J.Mestecky, M.E.Lamm, W.Strober, J.Bienenstock, and J.R.McGhee, eds. (San Diego: Academic Press), pp. 293-317.

Kinjo,Y., Kawakami,K., Uezu,K., Yara,S., Miyagi,K., Koguchi,Y., Hoshino,T., Okamoto,M., Kawase,Y., Yokota,K., Yoshino,K., Takeda,K., Akira,S., and Saito,A. (2002). Contribution of IL-18 to Th1 response and host defense against infection by *Mycobacterium tuberculosis*: a comparative study with IL-12p40. J. Immunol. *169*, 323-329.

Kirkpatrick,B.D., Daniels,M.M., Jean,S.S., Pape,J.W., Karp,C., Littenberg,B., Fitzgerald,D.W., Lederman,H.M., Nataro,J.P., and Sears,C.L. (2002). Cryptosporidiosis stimulates an inflammatory intestinal response in malnourished Haitian children. J. Infect. Dis. *186*, 94-101.

Kirkpatrick,B.D., Huston,C.D., Wagner,D., Noel,F., Rouzier,P., Pape,J.W., Bois,G., Larsson,C.J., Alston,W.K., Tenney,K., Powden,C., O'Neill,J.P., and Sears,C.L. (2006a).

Serum mannose-binding lectin deficiency is associated with cryptosporidiosis in young Haitian children. Clin. Infect. Dis. *43*, 289-294.

Kirkpatrick,B.D., Noel,F., Rouzier,P.D., Powell,J.L., Pape,J.W., Bois,G., Alston,W.K., Larsson,C.J., Tenney,K., Ventrone,C., Powden,C., Sreenivasan,M., and Sears,C.L. (2006b). Childhood cryptosporidiosis is associated with a persistent systemic inflammatory response. Clin. Infect. Dis. *43*, 604-608.

Kuhls,T.L., Greenfield,R.A., Mosier,D.A., Crawford,D.L., and Joyce,W.A. (1992). Cryptosporidiosis in adult and neonatal mice with severe combined immunodeficiency. J. Comp. Pathol. *106*, 399-410.

Kunisawa,J., Takahashi,I., and Kiyono,H. (2007). Intraepithelial lymphocytes: their shared and divergent immunological behaviors in the small and large intestine. Immunol. Rev. *215*, 136-153.

Lacroix,S., Mancassola,R., Naciri,M., and Laurent,F. (2001). *Cryptosporidium parvum*-specific mucosal immune response in C57BL/6 neonatal and gamma interferon-deficient mice: role of tumor necrosis factor alpha in protection. Infect. Immun. *69*, 1635-1642.

Lacroix-Lamande,S., Mancassola,R., Naciri,M., and Laurent,F. (2002). Role of gamma interferon in chemokine expression in the ileum of mice and in a murine intestinal epithelial cell line after *Cryptosporidium parvum* infection. Infect. Immun. *70*, 2090-2099.

Lafaille,J.J. (1998). The role of helper T cell subsets in autoimmune diseases. Cytokine Growth Factor Rev. *9*, 139-151.

LaRosa,D.F. and Orange,J.S. (2008). 1. Lymphocytes. J. Allergy Clin. Immunol. *121*, S364-S369.

Laurent,F., McCole,D., Eckmann,L., and Kagnoff,M.F. (1999). Pathogenesis of *Cryptosporidium parvum* infection. Microbes Infect. *1*, 141-148.

Lean,I.S., Lacroix-Lamande,S., Laurent,F., and McDonald,V. (2006). Role of tumor necrosis factor alpha in development of immunity against *Cryptosporidium parvum* infection. Infect. Immun. *74*, 4379-4382.

Lean,I.S., McDonald,V., and Pollok,R.C. (2002). The role of cytokines in the pathogenesis of *Cryptosporidium* infection. Curr. Opin. Infect. Dis. *15*, 229-234.

Leav,B.A., Mackay,M., and Ward,H.D. (2003). *Cryptosporidium* species: new insights and old challenges. Clin. Infect. Dis. *36*, 903-908.

Leav,B.A., Yoshida,M., Rogers,K., Cohen,S., Godiwala,N., Blumberg,R.S., and Ward,H. (2005). An early intestinal mucosal source of gamma interferon is associated with resistance to and control of *Cryptosporidium parvum* infection in mice. Infect. Immun. *73*, 8425-8428.

Leen,A.M., Rooney,C.M., and Foster,A.E. (2007). Improving T cell therapy for cancer. Annu. Rev. Immunol. *25*, 243-265.

Lefrancois,L. and Lycke,N. (2003). Isolation of mouse small intestinal intraepithelial lymphocytes, Peyer's patch, and lamina propria cells. In Current Protocols in Immunology, W.John E.Coligan, ed. John Wiley & Sons,Inc.).

Leitch,G.J. and He,Q. (1999). Reactive nitrogen and oxygen species ameliorate experimental cryptosporidiosis in the neonatal BALB/c mouse model. Infect. Immun. *67*, 5885-5891.

Leitch,G.J. and He,Q. (1994). Arginine-derived nitric oxide reduces fecal oocyst shedding in nude mice infected with *Cryptosporidium parvum*. Infect. Immun. *62*, 5173-5176.

Li,W., Buzoni-Gatel,D., Debbabi,H., Hu,M.S., Mennechet,F.J., Durell,B.G., Noelle,R.J., and Kasper,L.H. (2002). CD40/CD154 ligation is required for the development of acute ileitis following oral infection with an intracellular pathogen in mice. Gastroenterology *122*, 762-773.

Liesenfeld,O., Kang,H., Park,D., Nguyen,T.A., Parkhe,C.V., Watanabe,H., Abo,T., Sher,A., Remington,J.S., and Suzuki,Y. (1999). TNF-alpha, nitric oxide and IFN-gamma are all critical for development of necrosis in the small intestine and early mortality in genetically susceptible mice infected perorally with *Toxoplasma gondii*. Parasite Immunol. *21*, 365-376.

Liu,Q., Liu,Z., Whitmire,J., Alem,F., Hamed,H., Pesce,J., Urban,J.F., Jr., and Gause,W.C. (2006). IL-18 stimulates IL-13-mediated IFN-gamma-sensitive host resistance in vivo. Eur. J. Immunol. *36*, 1187-1198.

Lochner,M., Wagner,H., Classen,M., and Forster,I. (2002). Generation of neutralizing mouse anti-mouse IL-18 antibodies for inhibition of inflammatory responses in vivo. J. Immunol. Methods *259*, 149-157.

Loos,M. and Clas,F. (1987). Antibody-independent killing of gram-negative bacteria via the classical pathway of complement. Immunol. Lett. *14*, 203-208.

Lu,H., Yang,X., Takeda,K., Zhang,D., Fan,Y., Luo,M., Shen,C., Wang,S., Akira,S., and Brunham,R.C. (2000). *Chlamydia trachomatis* mouse pneumonitis lung infection in IL-18 and IL-12 knockout mice: IL-12 is dominant over IL-18 for protective immunity. Mol. Med. *6*, 604-612.

Lyscom,N. and Brueton,M.J. (1982). Intraepithelial, lamina propria and Peyer's patch lymphocytes of the rat small intestine: isolation and characterization in terms of immunoglobulin markers and receptors for monoclonal antibodies. Immunology *45*, 775-783.

Mac Kenzie,W.R., Hoxie,N.J., Proctor,M.E., Gradus,M.S., Blair,K.A., Peterson,D.E., Kazmierczak,J.J., Addiss,D.G., Fox,K.R., Rose,J.B., and Davis,J.P. (1994). A massive outbreak in Milwaukee of *Cryptosporidium* infection transmitted through the public water supply. N. Engl. J. Med. *331*, 161-167.

MacArthur,G.J., Wilson,A.D., Birchall,M.A., and Morgan,A.J. (2007). Primary CD4+ T-cell responses provide both helper and cytotoxic functions during Epstein-Barr virus infection and transformation of fetal cord blood B cells. J. Virol. *81*, 4766-4775.

MacMicking,J., Xie,Q.W., and Nathan,C. (1997). Nitric oxide and macrophage function. Annu. Rev. Immunol. *15*, 323-350.

Magalhaes,J.G., Tattoli,I., and Girardin,S.E. (2007). The intestinal epithelial barrier: how to distinguish between the microbial flora and pathogens. Semin. Immunol. *19*, 106-115.

Magram,J., Connaughton,S.E., Warrier,R.R., Carvajal,D.M., Wu,C.Y., Ferrante,J., Stewart,C., Sarmiento,U., Faherty,D.A., and Gately,M.K. (1996). IL-12-deficient mice are defective in IFNγ production and type 1 cytokine responses. Immunity *4*, 471-481.

Maillot,C., Gargala,G., Delaunay,A., Ducrotte,P., Brasseur,P., Ballet,J.J., and Favennec,L. (2000). *Cryptosporidium parvum* infection stimulates the secretion of TGF-beta, IL-8 and RANTES by Caco-2 cell line. Parasitol. Res. *86*, 947-949.

Mastroeni,P., Clare,S., Khan,S., Harrison,J.A., Hormaeche,C.E., Okamura,H., Kurimoto,M., and Dougan,G. (1999). Interleukin 18 contributes to host resistance and gamma interferon production in mice infected with virulent *Salmonella typhimurium*. Infect. Immun. *67*, 478-483.

Mattapallil,J.J., Smit-McBride,Z., McChesney,M., and Dandekar,S. (1998). Intestinal intraepithelial lymphocytes are primed for gamma interferon and MIP-1beta expression and display antiviral cytotoxic activity despite severe CD4(+) T-cell depletion in primary simian immunodeficiency virus infection. J. Virol. *72*, 6421-6429.

McDonald,S.A.C., O'Grady,J.E., Bajaj-Elliott,M., Notley,C.A., Alexander,J., Brombacher,F., and McDonald,V. (2004). Protection against the early acute phase of *Cryptosporidium parvum* infection conferred by interleukin-4-induced expression of T helper 1 cytokines. J. Infect. Dis. *190*, 1019-1025.

McDonald,V. (2000). Host cell-mediated responses to infection with *Cryptosporidium*. Parasite Immunol. *22*, 597-604.

McDonald,V. (1999). Gut intraepithelial lymphocytes and immunity to Coccidia. Parasitol. Today *15*, 483-487.

McDonald,V. and Bancroft,G.J. (1994). Mechanisms of innate and acquired resistance to *Cryptosporidium parvum* infection in SCID mice. Parasite Immunol. *16*, 315-320.

McDonald,V. and Bancroft,G.J. (1998). Immunological control of *Cryptosporidium* infection. In Immunology of intracellular parasitism, F.Y.Liew and F.E.G.Cox, eds. (Basel: Karger), pp. 103-123.

McDonald,V., Deer,R., Uni,S., Iseki,M., and Bancroft,G.J. (1992). Immune responses to *Cryptosporidium muris* and *Cryptosporidium parvum* in adult immunocompetent or immunocompromised (nude and SCID) mice. Infect. Immun. *60*, 3325-3331.

McDonald,V., Pollok,R.C., Dhaliwal,W., Naik,S., Farthing,M.J., and Bajaj-Elliott,M. (2006). A potential role for interleukin-18 in inhibition of the development of *Cryptosporidium parvum*. Clin. Exp. Immunol. *145*, 555-562.

McDonald,V., Robinson,H.A., Kelly,J.P., and Bancroft,G.J. (1994). *Cryptosporidium muris* in adult mice: adoptive transfer of immunity and protective roles of CD4 versus CD8 cells. Infect. Immun. *62*, 2289-2294.

McDonald,V., Robinson,H.A., Kelly,J.P., and Bancroft,G.J. (1996). Immunity to *Cryptosporidium muris* infection in mice is expressed through gut CD4+ intraepithelial lymphocytes. Infect. Immun. *64*, 2556-2562.

McKenzie,G.J., Bancroft,A., Grencis,R.K., and McKenzie,A.N. (1998). A distinct role for interleukin-13 in Th2-cell-mediated immune responses. Curr. Biol. *8*, 339-342.

Mead,J.R., Arrowood,M.J., Healey,M.C., and Sidwell,R.W. (1991a). Cryptosporidial infections in SCID mice reconstituted with human or murine lymphocytes. J. Protozool. *38*, 59S-61S.

Mead,J.R., Arrowood,M.J., Sidwell,R.W., and Healey,M.C. (1991b). Chronic *Cryptosporidium parvum* infections in congenitally immunodeficient SCID and nude mice. J. Infect. Dis. *163*, 1297-1304.

Mead,J.R. and You,X. (1998). Susceptibility differences to *Cryptosporidium parvum* infection in two strains of gamma interferon knockout mice. J. Parasitol. *84*, 1045-1048.

Meisel,J.L., Perera,D.R., Meligro,C., and Rubin,C.E. (1976). Overwhelming watery diarrhea associated with a *cryptosporidium* in an immunosuppressed patient. Gastroenterology *70*, 1156-1160.

Millan,J., Hewlett,L., Glyn,M., Toomre,D., Clark,P., and Ridley,A.J. (2006). Lymphocyte transcellular migration occurs through recruitment of endothelial ICAM-1 to caveola- and F-actin-rich domains. Nat. Cell Biol. *8*, 113-123.

Miller,J.R. (1998). Decreasing cryptosporidiosis among HIV-infected persons in New York City, 1995-1997. J. Urban. Health *75*, 601-602.

Montufar-Solis,D. and Klein,J.R. (2006). An improved method for isolating intraepithelial lymphocytes (IELs) from the murine small intestine with consistently high purity. J. Immunol. Methods *308*, 251-254.

Moretto,M., Weiss,L.M., and Khan,I.A. (2004). Induction of a rapid and strong antigen-specific intraepithelial lymphocyte response during oral *Encephalitozoon cuniculi* infection. J. Immunol. *172*, 4402-4409.

Morgan,U.M. and Thompson,R.C.A. (1998). PCR detection of *Cryptosporidium*: The way forward? Parasitol. Today *14*, 245.

Morrison,D.A., Bornstein,S., Thebo,P., Wernery,U., Kinne,J., and Mattsson,J.G. (2004). The current status of the small subunit rRNA phylogeny of the coccidia (Sporozoa). Int. J. Parasitol. *34*, 501-514.

Mosmann,T.R., Cherwinski,H., Bond,M.W., Giedlin,M.A., and Coffman,R.L. (1986). Two types of murine helper T cell clone. I. Definition according to profiles of lymphokine activities and secreted proteins. J. Immunol. *136*, 2348-2357.

Nairz,M., Fritsche,G., Brunner,P., Talasz,H., Hantke,K., and Weiss,G. (2008). Interferon-gamma limits the availability of iron for intramacrophage *Salmonella typhimurium*. Eur. J. Immunol. *38*, 1923-1936.

Nakanishi,K., Yoshimoto,T., Tsutsui,H., and Okamura,H. (2001). Interleukin-18 regulates both Th1 and Th2 responses. Annu. Rev Immunol. *19*, 423-474.

Nathan,C. and Shiloh,M.U. (2000). Reactive oxygen and nitrogen intermediates in the relationship between mammalian hosts and microbial pathogens. Proc. Natl. Acad. Sci. U. S. A *97*, 8841-8848.

Nichols,G. (2008). Epidemiology. In *Cryptosporidium* and Cryptosporidiosis, R.Fayer and L.Xiao, eds. CRC Press), pp. 79-118.

Nickdel,M.B., Roberts,F., Brombacher,F., Alexander,J., and Roberts,C.W. (2001). Counter-protective role for interleukin-5 during acute *Toxoplasma gondii* infection. Infect. Immun. *69*, 1044-1052.

Nikiforow,S., Bottomly,K., Miller,G., and Munz,C. (2003). Cytolytic CD4(+)-T-cell clones reactive to EBNA1 inhibit Epstein-Barr virus-induced B-cell proliferation. J. Virol. *77*, 12088-12104.

Nime,F.A., Burek,J.D., Page,D.L., Holscher,M.A., and Yardley,J.H. (1976). Acute enterocolitis in a human being infected with the protozoan *Cryptosporidium*. Gastroenterology *70*, 592-598.

Nurieva,R.I., Chung,Y., Hwang,D., Yang,X.O., Kang,H.S., Ma,L., Wang,Y.H., Watowich,S.S., Jetten,A.M., Tian,Q., and Dong,C. (2008). Generation of T follicular helper cells is mediated by interleukin-21 but independent of T helper 1, 2, or 17 cell lineages. Immunity. *29*, 138-149.

O'Donoghue,P.J. (1995). *Cryptosporidium* and cryptosporidiosis in man and animals. Int. J. Parasitol. *25*, 139-195.

Okamura,H., Nagata,K., Komatsu,T., Tanimoto,T., Nukata,Y., Tanabe,F., Akita,K., Torigoe,K., Okura,T., Fukuda,S., and . (1995a). A novel costimulatory factor for gamma interferon induction found in the livers of mice causes endotoxic shock. Infect. Immun. *63*, 3966-3972.

Okamura,H., Tsutsi,H., Komatsu,T., Yutsudo,M., Hakura,A., Tanimoto,T., Torigoe,K., Okura,T., Nukada,Y., Hattori,K., and . (1995b). Cloning of a new cytokine that induces IFN-gamma production by T cells. Nature *378*, 88-91.

Okamura,H., Tsutsui,H., Kashiwamura,S., Yoshimoto,T., and Nakanishi,K. (1998). Interleukin-18: a novel cytokine that augments both innate and acquired immunity. Adv. Immunol. *70*, 281-312.

Okazawa,A., Kanai,T., Nakamaru,K., Sato,T., Inoue,N., Ogata,H., Iwao,Y., Ikeda,M., Kawamura,T., Makita,S., Uraushihara,K., Okamoto,R., Yamazaki,M., Kurimoto,M., Ishii,H., Watanabe,M., and Hibi,T. (2004). Human intestinal epithelial cell-derived interleukin (IL)-18, along with IL-2, IL-7 and IL-15, is a potent synergistic factor for the proliferation of intraepithelial lymphocytes. Clin. Exp. Immunol. *136*, 269-276.

Okhuysen,P.C., Chappell,C.L., Crabb,J.H., Sterling,C.R., and DuPont,H.L. (1999). Virulence of three distinct *Cryptosporidium parvum* isolates for healthy adults. J. Infect. Dis. *180*, 1275-1281.

Okhuysen,P.C., Robinson,P., Nguyen,M.T., Nannini,E.C., Lewis,D.E., Janecki,A., Chappell,C.L., and White,A.C., Jr. (2001). Jejunal cytokine response in AIDS patients with chronic cryptosporidiosis and during immune reconstitution. AIDS *15*, 802-804.

Orvedahl,A., Alexander,D., Talloczy,Z., Sun,Q., Wei,Y., Zhang,W., Burns,D., Leib,D.A., and Levine,B. (2007). HSV-1 ICP34.5 confers neurovirulence by targeting the Beclin 1 autophagy protein. Cell Host. Microbe *1*, 23-35.

Panciera,R.J., Thomassen,R.W., and Garner,F.M. (1971). Cryptosporidial infection in a calf. Vet. Pathol. *8*, 479-484.

Pantenburg,B., Dann,S.M., Wang,H.C., Robinson,P., Castellanos-Gonzalez,A., Lewis,D.E., and White,A.C., Jr. (2008). Intestinal immune response to human *Cryptosporidium* sp. infection. Infect. Immun. *76*, 23-29.

Pasquali,P., Fayer,R., Almeria,S., Trout,J., Polidori,G.A., and Gasbarre,L.C. (1997). Lymphocyte dynamic patterns in cattle during a primary infection with *Cryptosporidium parvum*. J. Parasitol. *83*, 247-250.

Pasquali,P., Fayer,R., Zarlenga,D., Canals,A., Marez,T., Gomez Munoz,M.T., Almeria,S., and Gasbarre,L.C. (2006). Recombinant bovine interleukin-12 stimulates a gut immune response but does not provide resistance to *Cryptosporidium parvum* infection in neonatal calves. Vet. Parasitol. *135*, 259-268.

Peeters,J.E., Villacorta,I., Vanopdenbosch,E., Vandergheynst,D., Naciri,M., Ares Mazas,E., and Yvore,P. (1992). *Cryptosporidium parvum* in calves: kinetics and immunoblot analysis of specific serum and local antibody responses (immunoglobulin A [IgA], IgG, and IgM) after natural and experimental infections. Infect. Immun. *60*, 2309-2316.

Perryman,L.E., Kapil,S.J., Jones,M.L., and Hunt,E.L. (1999). Protection of calves against cryptosporidiosis with immune bovine colostrum induced by a *Cryptosporidium parvum* recombinant protein. Vaccine *17*, 2142-2149.

Perryman,L.E., Mason,P.H., and Chrisp,C.E. (1994). Effect of spleen cell populations on resolution of *Cryptosporidium parvum* infection in SCID mice. Infect. Immun. *62*, 1474-1477.

Petry,F. (2000). Laboratory diagnosis of *Cryptosporidium parvum* infection. In Cryptosporidiosis and Microsporidiosis, F.Petry, ed. (Basel: S. Karger), pp. 33-49.

Petry,F., Botto,M., Holtappels,R., Walport,M.J., and Loos,M. (2001). Reconstitution of the complement function in C1q-deficient (C1qa-/-) mice with wild-type bone marrow cells. J. Immunol. *167*, 4033-4037.

Petry,F., Jakobi,V., Wagner,S., Tessema,T.S., Thiel,S., and Loos,M. (2008). Binding and activation of human and mouse complement by *Cryptosporidium parvum* (Apicomplexa) and susceptibility of C1q- and MBL-deficient mice to infection. Mol. Immunol. *45*, 3392-3400.

Petry,F. and Loos,M. (1998). Bacteria and complement. In The human complement system in health and disease, J.E.Volanakis and M.M.Frank, eds. (New York: Marcel Dekker, Inc.), pp. 375-392.

Petry,F., Robinson,H.A., and McDonald,V. (1995). Murine infection model for maintenance and amplification of *Cryptosporidium parvum* oocysts. J. Clin. Microbiol. *33*, 1922-1924.

Pollok,R.C., Farthing,M.J., Bajaj-Elliott,M., Sanderson,I.R., and McDonald,V. (2001). Interferon gamma induces enterocyte resistance against infection by the intracellular pathogen *Cryptosporidium parvum*. Gastroenterology *120*, 99-107.

Ramirez,N.E., Ward,L.A., and Sreevatsan,S. (2004). A review of the biology and epidemiology of cryptosporidiosis in humans and animals. Microbes Infect. *6*, 773-785.

Rasmussen,K.R., Martin,E.G., Arrowood,M.J., and Healey,M.C. (1991). Effects of dexamethasone and dehydroepiandrosterone in immunosuppressed rats infected with *Cryptosporidium parvum*. J. Protozool. *38*, 157S-159S.

Rehg,J.E., Hancock,M.L., and Woodmansee,D.B. (1987). Characterization of cyclophosphamide-rat model of cryptosporidiosis. Infect. Immun. *55*, 2669-2674.

Reiner,S.L. (2007). Development in motion: helper T cells at work. Cell *129*, 33-36.

Reperant,J.M., Naciri,M., Iochmann,S., Tilley,M., and Bout,D.T. (1994). Major antigens of *Cryptosporidium parvum* recognised by serum antibodies from different infected animal species and man. Vet. Parasitol. *55*, 1-13.

Riggs,M.W. (2002). Recent advances in cryptosporidiosis: The immune response. Microbes Infect. *4*, 1067-1080.

Robertson,J.M., MacLeod,M., Marsden,V.S., Kappler,J.W., and Marrack,P. (2006). Not all CD4+ memory T cells are long lived. Immunol. Rev. *211*, 49-57.

Robertson,L.J. and Gjerde,B.K. (2007). *Cryptosporidium* oocysts: challenging adversaries? Trends Parasitol. *23*, 344-347.

Robinson,P., Okhuysen,P.C., Chappell,C.L., Lewis,D.E., Shahab,I., Janecki,A., and White,A.C., Jr. (2001a). Expression of tumor necrosis factor alpha and interleukin 1 beta in jejuna of volunteers after experimental challenge with *Cryptosporidium parvum* correlates with exposure but not with symptoms. Infect. Immun. *69*, 1172-1174.

Robinson,P., Okhuysen,P.C., Chappell,C.L., Lewis,D.E., Shahab,I., Lahoti,S., and White,A.C., Jr. (2001b). Expression of IL-15 and IL-4 in IFN-gamma-independent control of experimental human *Cryptosporidium parvum* infection. Cytokine *15*, 39-46.

Rocha,F., Musch,M.W., Lishanskiy,L., Bookstein,C., Sugi,K., Xie,Y., and Chang,E.B. (2001). IFN-gamma downregulates expression of Na(+)/H(+) exchangers NHE2 and NHE3 in rat intestine and human Caco-2/bbe cells. Am. J. Physiol Cell Physiol *280*, C1224-C1232.

Roche. Absolute Quantification with External Standards. Technical Note No. LC 11/update. 2003.

Rogers,P.R., Huston,G., and Swain,S.L. (1998). High antigen density and IL-2 are required for generation of CD4 effectors secreting Th1 rather than Th0 cytokines. J. Immunol. *161*, 3844-3852.

Rohlman,V.C., Kuhls,T.L., Mosier,D.A., Crawford,D.L., and Greenfield,R.A. (1993). *Cryptosporidium parvum* infection after abrogation of natural killer cell activity in normal and severe combined immunodeficiency mice. J. Parasitol. *79*, 295-297.

Roman,E., Miller,E., Harmsen,A., Wiley,J., Von Andrian,U.H., Huston,G., and Swain,S.L. (2002). CD4 effector T cell subsets in the response to influenza: heterogeneity, migration, and function. J. Exp. Med. *196*, 957-968.

Rose,J.B., Huffman,D.E., and Gennaccaro,A. (2002). Risk and control of waterborne cryptosporidiosis. FEMS Microbiol. Rev. *26*, 113-123.

Rowe,M., Glaunsinger,B., van,L.D., Zuo,J., Sweetman,D., Ganem,D., Middeldorp,J., Wiertz,E.J., and Ressing,M.E. (2007). Host shutoff during productive Epstein-Barr virus infection is mediated by BGLF5 and may contribute to immune evasion. Proc. Natl. Acad. Sci. U. S. A *104*, 3366-3371.

Rozen,S. and Skaletsky,H. (2000). Primer3 on the WWW for general users and for biologist programmers. In Bioinformatics Methods and Protocols: Methods in Molecular Biology. Humana Press, S.Krawetz and S.Misener, eds. (Totowa, NJ: Humana Press), pp. 365-386.

Sansonetti,P.J., Phalipon,A., Arondel,J., Thirumalai,K., Banerjee,S., Akira,S., Takeda,K., and Zychlinsky,A. (2000). Caspase-1 activation of IL-1beta and IL-18 are essential for *Shigella flexneri*-induced inflammation. Immunity. *12*, 581-590.

Schmidt,W., Wahnschaffe,U., Schafer,M., Zippel,T., Arvand,M., Meyerhans,A., Riecken,E.O., and Ullrich,R. (2001). Rapid increase of mucosal CD4 T cells followed by clearance of intestinal cryptosporidiosis in an AIDS patient receiving highly active antiretroviral therapy. Gastroenterology *120*, 984-987.

Schwamb B. (2008) Untersuchungen zur Zytokinantwort in Mäusen nach Infektion mit *Cryptosporidium parvum*. Diploma Thesis, Department of Biology, Johannes Gutenberg University, Mainz, Germany.

Sears,C.L. and Guerrant,R.L. (1994). Cryptosporidiosis: the complexity of intestinal pathophysiology. Gastroenterology *106*, 252-254.

Seydel,K.B., Zhang,T., Champion,G.A., Fichtenbaum,C., Swanson,P.E., Tzipori,S., Griffiths,J.K., and Stanley,S.L., Jr. (1998). *Cryptosporidium parvum* infection of human intestinal xenografts in SCID mice induces production of human tumor necrosis factor alpha and interleukin-8. Infect. Immun. *66*, 2379-2382.

Shen,L. and Turner,J.R. (2006). Role of epithelial cells in initiation and propagation of intestinal inflammation. Eliminating the static: tight junction dynamics exposed. Am. J. Physiol Gastrointest. Liver Physiol *290*, G577-G582.

Shires,J., Theodoridis,E., and Hayday,A.C. (2001). Biological insights into TCRgammadelta+ and TCRalphabeta+ intraepithelial lymphocytes provided by serial analysis of gene expression (SAGE). Immunity. *15*, 419-434.

Shtrichman,R. and Samuel,C.E. (2001). The role of gamma interferon in antimicrobial immunity. Curr. Opin. Microbiol. *4*, 251-259.

Singh,I., Theodos,C., Li,W., and Tzipori,S. (2005). Kinetics of *Cryptosporidium parvum*-specific cytokine responses in healing and nonhealing murine models of *C. parvum* infection. Parasitol. Res. *97*, 309-317.

Slavin,D. (1955). *Cryptosporidium meleagridis* (sp. nov.). J. Comp. Pathol. *65*, 262-266.

Smith,H.V. and Corcoran,G.D. (2004). New drugs and treatment for cryptosporidiosis. Curr. Opin. Infect. Dis. *17*, 557-564.

Smith,H.V., Nichols,R.A.B., and Grimason,A.M. (2005). *Cryptosporidium* excystation and invasion: getting to the guts of the matter. Trends Parasitol. *21*, 133-142.

Smith,L.M., Bonafonte,M.T., Campbell,L.D., and Mead,J.R. (2001). Exogenous interleukin-12 (IL-12) exacerbates *Cryptosporidium parvum* infection in gamma interferon knockout mice. Exp. Parasitol. *98*, 123-133.

Smith,L.M., Bonafonte,M.T., and Mead,J.R. (2000). Cytokine expression and specific lymphocyte proliferation in two strains of *Cryptosporidium parvum*-infected gamma-interferon knockout mice. J. Parasitol. *86*, 300-307.

Sonobe,Y., Yawata,I., Kawanokuchi,J., Takeuchi,H., Mizuno,T., and Suzumura,A. (2005). Production of IL-27 and other IL-12 family cytokines by microglia and their subpopulations. Brain Res. *1040*, 202-207.

Steinman,L. (2007). A brief history of T(H)17, the first major revision in the T(H)1/T(H)2 hypothesis of T cell-mediated tissue damage. Nat. Med. *13*, 139-145.

Stockdale,H.D., Spencer,J.A., and Blagburn,B.L. (2008). Prophylaxis and Chemotherapy. In *Cryptosporidium* and Cryptosporidiosis, R.Fayer and L.Xiao, Eds. CRC Press, Boca Raton, FL, pp. 255-287.

Sugi,K., Musch,M.W., Field,M., and Chang,E.B. (2001). Inhibition of Na+,K+-ATPase by interferon gamma down-regulates intestinal epithelial transport and barrier function. Gastroenterology *120*, 1393-1403.

Sulaiman,I.M., Xiao,L., and Lal,A.A. (1999). Evaluation of *Cryptosporidium parvum* genotyping techniques. Appl. Environ. Microbiol. *65*, 4431-4435.

Swain,S.L., Agrewala,J.N., Brown,D.M., Jelley-Gibbs,D.M., Golech,S., Huston,G., Jones,S.C., Kamperschroer,C., Lee,W.H., McKinstry,K.K., Roman,E., Strutt,T., and Weng,N.P. (2006). CD4+ T-cell memory: generation and multi-faceted roles for CD4+ T cells in protective immunity to influenza. Immunol. Rev. *211*, 8-22.

Swain,S.L., Croft,M., Dubey,C., Haynes,L., Rogers,P., Zhang,X., and Bradley,L.M. (1996). From naive to memory T cells. Immunol. Rev. *150*, 143-167.

Sydora,B.C., Jamieson,B.D., Ahmed,R., and Kronenberg,M. (1996). Intestinal intraepithelial lymphocytes respond to systemic lymphocytic choriomeningitis virus infection. Cell Immunol. *167*, 161-169.

Taghi-Kilani,R., Sekla,L., and Hayglass,K.T. (1990). The role of humoral immunity in *Cryptosporidium* spp. infection. Studies with B cell-depleted mice. J. Immunol. *145*, 1571-1576.

Takeuchi,D., Jones,V.C., Kobayashi,M., and Suzuki,F. (2008). Cooperative role of macrophages and neutrophils in host Antiprotozoan resistance in mice acutely infected with *Cryptosporidium parvum*. Infect. Immun. *76*, 3657-3663.

Takeuchi,M., Nishizaki,Y., Sano,O., Ohta,T., Ikeda,M., and Kurimoto,M. (1997). Immunohistochemical and immuno-electron-microscopic detection of interferon-gamma-inducing factor ("interleukin-18") in mouse intestinal epithelial cells. Cell Tissue Res. *289*, 499-503.

Teichgräber, V. (2004). On Memory T Lymphocytes: Heterogeneity of the immunological memory. Dissertation, Eberhard-Karls-Universität zu Tübingen, Tübingen, Germany.

Theodos,C.M., Sullivan,K.L., Griffiths,J.K., and Tzipori,S. (1997). Profiles of healing and nonhealing *Cryptosporidium parvum* infection in C57BL/6 mice with functional B and T lymphocytes: the extent of gamma interferon modulation determines the outcome of infection. Infect. Immun. *65*, 4761-4769.

Trizio,D. and Cudkowicz,G. (1974). Separation of T and B lymphocytes by nylon wool columns: evaluation of efficacy by functional assays in vivo. J. Immunol. *113*, 1093-1097.

Tzipori,S. (1988). Cryptosporidiosis in perspective. Adv. Parasitol. *27*, 63-129.

Tzipori,S. and Griffiths,J.K. (1998). Natural history and biology of *Cryptosporidium parvum*. In Opportunistic protozoa in humans, S.Tzipori, ed. (San Diego: Academic Press), pp. 6-36.

Tzipori,S. and Ward,H. (2002). Cryptosporidiosis: Biology, pathogenesis and disease. Microbes Infect. *4*, 1047-1058.

Tzipori,S. and Widmer,G. (2000). The biology of *Cryptosporidium*. In Cryptosporidiosis and Microsporidiosis, F.Petry, ed. (Basel: S. Karger), pp. 1-32.

Ungar,B.L., Burris,J.A., Quinn,C.A., and Finkelman,F.D. (1990). New mouse models for chronic *Cryptosporidium* infection in immunodeficient hosts. Infect. Immun. *58*, 961-969.

Ungar,B.L., Kao,T.C., Burris,J.A., and Finkelman,F.D. (1991). *Cryptosporidium* infection in an adult mouse model. Independent roles for IFN-gamma and CD4+ T lymphocytes in protective immunity. J. Immunol. *147*, 1014-1022.

Ungar,B.L., Soave,R., Fayer,R., and Nash,T.E. (1986). Enzyme immunoassay detection of immunoglobulin M and G antibodies to *Cryptosporidium* in immunocompetent and immunocompromised persons. J. Infect. Dis. *153*, 570-578.

Urban,J.F., Jr., Fayer,R., Chen,S.J., Gause,W.C., Gately,M.K., and Finkelman,F.D. (1996). IL-12 protects immunocompetent and immunodeficient neonatal mice against infection with *Cryptosporidium parvum*. J. Immunol. *156*, 263-268.

Urban,J.F., Jr., Noben-Trauth,N., Donaldson,D.D., Madden,K.B., Morris,S.C., Collins,M., and Finkelman,F.D. (1998). IL-13, IL-4Ralpha, and Stat6 are required for the expulsion of the gastrointestinal nematode parasite *Nippostrongylus brasiliensis*. Immunity. *8*, 255-264.

Vyas,J.M., Van,d., V, and Ploegh,H.L. (2008). The known unknowns of antigen processing and presentation. Nat. Rev. Immunol. *8*, 607-618.

Wakeham,J., Wang,J., and Xing,Z. (2000). Genetically determined disparate innate and adaptive cell-mediated immune responses to pulmonary *Mycobacterium bovis* BCG infection in C57BL/6 and BALB/c mice. Infect. Immun. *68*, 6946-6953.

Wang,H.C., Dann,S.M., Okhuysen,P.C., Lewis,D.E., Chappell,C.L., Adler,D.G., and White,A.C., Jr. (2007). High levels of CXCL10 are produced by intestinal epithelial cells in AIDS patients with active cryptosporidiosis but not after reconstitution of immunity. Infect. Immun. *75*, 481-487.

Wang,H.C., Montufar-Solis,D., Teng,B.B., and Klein,J.R. (2004). Maximum immunobioactivity of murine small intestinal intraepithelial lymphocytes resides in a subpopulation of CD43+ T cells. J. Immunol. *173*, 6294-6302.

Warren,C.A. and Guerrant,R.L. (2008). Clinical Disease and Pathology. In *Cryptosporidium* and Cryptosporidiosis, R.Fayer and L.Xiao, Eds. CRC Press, Boca Raton, FL, pp. 235-253.

White,A.C., Jr., Cron,S.G., and Chappell,C.L. (2001). Paromomycin in cryptosporidiosis. Clin. Infect. Dis. *32*, 1516-1517.

White,A.C., Robinson,P., Okhuysen,P.C., Lewis,D.E., Shahab,I., Lahoti,S., DuPont,H.L., and Chappell,C.L. (2000). Interferon-gamma expression in jejunal biopsies in experimental human cryptosporidiosis correlates with prior sensitization and control of oocyst excretion. J. Infect. Dis. *181*, 701-709.

WHO (2006). Microbial aspects. In WHO Guidelines for Drinking-water Quality First addendum to third edition, World Health Organization), pp. 121-144.

Widmer,G. (1998). Genetic heterogeneity and PCR detection of *Cryptosporidium parvum*. Adv. Parasitol. *40*, 223-239.

Williams,R.O. and Burden,D.J. (1987). Measurement of class specific antibody against *cryptosporidium* in serum and faeces from experimentally infected calves. Res. Vet. Sci. *43*, 264-265.

Wilson,C.L., Ouellette,A.J., Satchell,D.P., Ayabe,T., Lopez-Boado,Y.S., Stratman,J.L., Hultgren,S.J., Matrisian,L.M., and Parks,W.C. (1999). Regulation of intestinal alpha-defensin activation by the metalloproteinase matrilysin in innate host defense. Science *286*, 113-117.

Wyatt,C.R., Barrett,W.J., Brackett,E.J., Schaefer,D.A., and Riggs,M.W. (2002). Association of IL-10 expression by mucosal lymphocytes with increased expression of *Cryptosporidium parvum* epitopes in infected epithelium. J. Parasitol. *88*, 281-286.

Wyatt,C.R., Brackett,E.J., and Barrett,W.J. (1999). Accumulation of mucosal T lymphocytes around epithelial cells after in vitro infection with *Cryptosporidium parvum*. J. Parasitol. *85*, 765-768.

Wyatt,C.R., Brackett,E.J., Perryman,L.E., Rice Ficht,A.C., Brown,W.C., and O'Rourke,K.I. (1997). Activation of intestinal intraepithelial T lymphocytes in calves infected with *Cryptosporidium parvum*. Infect. Immun. *65*, 185-190.

Wyatt,C.R., Brackett,E.J., and Savidge,J. (2001). Evidence for the emergence of a type-1-like immune response in intestinal mucosa of calves recovering from cryptosporidiosis. J. Parasitol. *87*, 90-95.

Wyatt,C.R., Lindahl,S., Austin,K., Kapil,S., and Branch,J. (2005). Response of T lymphocytes from previously infected calves to recombinant *Cryptosporidium parvum* P23 vaccine antigen. J. Parasitol. *91*, 1239-1242.

Xiao,L. and Fayer,R. (2008). Molecular characterisation of species and genotypes of *Cryptosporidium* and *Giardia* and assessment of zoonotic transmission. Int. J. Parasitol.

Xiao,L., Fayer,R., Ryan,U., and Upton,S.J. (2004). *Cryptosporidium* Taxonomy: Recent Advances and Implications for Public Health. Clin. Microbiol. Rev. *17*, 72-97.

Xiao,L. and Feng,Y. (2008). Zoonotic cryptosporidiosis. FEMS Immunol. Med. Microbiol. *52*, 309-323.

Yassien,N.A., Khalifa,E.A., and el-Nouby,K.A. (2001). Role of anti-oxidant preparation (oxi-guard) on *Cryptosporidium parvum* infection in albino mice. J. Egypt. Soc. Parasitol. *31*, 95-106.

You,X. and Mead,J.R. (1998). Characterization of experimental *Cryptosporidium parvum* infection in IFN-gamma knockout mice. Parasitology *117*, 525-531.

Zaalouk,T.K., Bajaj-Elliott,M., George,J.T., and McDonald,V. (2004). Differential regulation of beta-defensin gene expression during *Cryptosporidium parvum* infection. Infect. Immun. *72*, 2772-2779.

Zadrozny,L.M., Stauffer,S.H., Armstrong,M.U., Jones,S.L., and Gookin,J.L. (2006). Neutrophils do not mediate the pathophysiological sequelae of *Cryptosporidium parvum* infection in neonatal piglets. Infect. Immun. *74*, 5497-5505.

Zasloff,M. (2002). Antimicrobial peptides of multicellular organisms. Nature *415*, 389-395.

Zhang,T., Kawakami,K., Qureshi,M.H., Okamura,H., Kurimoto,M., and Saito,A. (1997). Interleukin-12 (IL-12) and IL-18 synergistically induce the fungicidal activity of murine peritoneal exudate cells against *Cryptococcus neoformans* through production of gamma interferon by natural killer cells. Infect. Immun. *65*, 3594-3599.

Publications, Abstracts, Posters and Talks

Publications

Tessema T.S., Jakobi V., Petry F. Adoptive transfer of protective cellular immunity against *Cryptosporidium parvum* from infected to naive mice through intestinal intraepithelial lymphocytes (IELs) and $CD4^+$ T-cells. (Manuscript in preparation).

Tessema T.S., Schwamb B., Lochner M., Förster I., Jakobi V., Petry F. Dynamics of gut mucosal and systemic Th1/Th2 cytokine responses in interferon-gamma and interleukin-12p40 knock out mice during primary and secondary *Cryptosporidium parvum* infections. (Manuscript submitted for publication)

Petry F., Jakobi V., Wagner S., Tessema T.S., Thiel S., Loos M. (2008). Binding and activation of human and mouse complement by *Cryptosporidium parvum* (Apicomplexa) and susceptibility of C1q- and MBL-deficient mice to infection. *Mol Immunol.* 2008;45(12):3392-400.

Poster presentation

Tessema T.S., Schwamb B., Jakobi V., Petry F. (2008). Dynamics of gut mucosal & systemic Th1/Th2 Cytokine responses in IFN-gamma and IL-12p40KO mice during *C. parvum* Infection. 23rd Meeting of the German Society for Parasitology, March 5 – 7th 2008, Hamburg, Germany.

Schwamb B., Tessema T.S., Lochner M., Förster I., Petry F. (2008). Influence of IL-18 on the systemic and local immune response to *Cryptosporidium parvum* infection in IFN-γKO and IL-12KO mice. 23rd Meeting of the German Society for Parasitology, March 5 – 7th 2008, Hamburg, Germany.

Jakobi V., Stumm C., Tessema T.S., Petry F. (2007). Differential expression of *Cryptosporidium parvum* genes *in vitro* and *in vivo*. 1st Three Countries Joint Meeting-Living Together. Physiopathology of intracellular parasitic diseases, June 14 – 16th 2007, Strasbourg, France.

Jakobi V, Tessema TS, Kneib I & Petry F (2006). Evaluation of interferon-gamma and interleukin-12 knockout mice as models for the development of vaccination strategies against cryptosporidiosis. 3. Annual Workshop of the COST Action 857, March 17 – 20th 2006, Dresden, Germany.

Oral presentation

Tessema T.S., Schwamb B., Jakobi V., Petry F. (2008). Dynamics of gut mucosal and systemic Th1/Th2 cytokine responses in IFN-γ and IL-12KO mice during *Cryptosporidium parvum* infection and challenge infection. 11th German Meeting on Th1/Th2 Research, German society of Immunology, June 18 – 19th 2008, Marburg, Germany.

Tessema T.S., Jakobi V., Petry F., (2007). Cytokine responses of mice after primary infection and re-challenge with *Cryptosporidium parvum*. Statusworkshop of the German Society of Hygiene and Microbiology (DGHM)-Fachgruppe "Eukaryotic Pathogens", February 23 – 24th 2007, Stuttgart, Germany.

CURRICULUM VITAE

Tesfaye Sisay Tessema
Alfred-Mumbächer Str.67a
D-55128 Mainz, Germany
E-mail: Tesfu74@yahoo.com
Born on 14/03/1974 in Dessie, Ethiopia.
Married and two children.
Nationality: Ethiopian

EDUCATION

2006 – present. PhD study, Institute of Medical Microbiology and Hygiene, Johannes Gutenberg-University of Mainz, in the group of Prof. Dr. F. Petry.

2000, Sept – 2002, Sept. Master of Science, Molecular Biology, Catholic University of Leuven, Leuven, Belgium.

1997, July. Doctor of Veterinary Medicine (D.V.M.), Addis Ababa University, Faculty of Veterinary Medicine, Debre-Zeit, Ethiopia.

1981 – 1991. Elementary and Secondary education, Dessie, Ethiopia.

WORK AND RESEARCH EXPERIENCE

2006, March – present. Doctoral thesis research, Institute of Medical Microbiology and Hygiene, Johannes Gutenberg University of Mainz, Mainz, Germany.

2004, Nov – 2006, March. Molecular Mechanisms of inflammatory diarrhea using IL-10KO mouse model of chronic intestinal inflammation, in the group of Prof. U. Seidler, Institute of Gastroenterology and Hepatology, Hannover Medical School, Hannover, Germany.

2002 – 2004, Nov. Lecturer, Faculty of Veterinary Medicine, Addis Ababa University, Debre-Zeit, Ethiopia.

2001 – 2002. Masters thesis research.

1998 – 2000. Assistant lecturer, Faculty of Veterinary Medicine, Addis Ababa University, Debre-Zeit, Ethiopia. Research on bacterial flora of the respiratory tract in small ruminants.

1996 – 1997. Undergraduate thesis research.

Erklärung

Hiermit versichere ich, das ich die vorliegende Dissertation eigenständig verfasst und keine enderen als die angegebenen Hilfsmittel verwendet habe.

Die Dissertation habe ich weder als Arbeit für eine staatliche oder andere wissenschaftliche Prüfung eingereicht noch ist sie oder ein Teil dieser als Dissertation bei einer anderen Fakultät oder einem anderen Fachbereich eingereicht worden.

Declaration

Herewith, I confirm that I have written the present PhD thesis myself and independently, and that I have not submitted it at any other university worldwide.

Mainz, September 2008

_____

Tesfaye Sisay Tessema